

Gedruckt mit Unterstützung des Deutschen Akademischen Austauschdienstes

Development and Biopharmaceutical Evaluation of Microemulsions for Targeted Delivery of Ceramides and other Stratum Corneum Lipids into the Stratum Corneum

Dissertation

zur Erlangung des akademischen Grades
doctor rerum naturalium (Dr. rer. nat.)

vorgelegt der
Naturwissenschaftlichen Fakultät I
Biowissenschaften
der Martin-Luther-Universität Halle-Wittenberg

von

MSc. Pharm. Fitsum Feleke Sahle
geboren am 30. August 1980 in Wolliso

Gutachter:

1. Prof. Dr. Dr. h.c. Reinhard Neubert
2. Prof. Dr. Johannes Wohlrab
3. Prof. Dr. Gerald Brezesinski

Halle (Saale), 09.03. 2012

To Vulnerable Children of the Mother Nature who are devoid of Love and Care

Abbreviations and Symbols

AA:	arachidonic acid
ABC:	area between the curves
AD:	atopic dermatitis
a_N :	hyperfine splitting constant/ isotropic hyperfine coupling constant
AUC:	area under the curve
BA:	behenic acid
BC:	bicontinuous
CER [AP]:	ceramide AP
CER [EOS]:	ceramide EOS
CER [NP:]	ceramide NP
CER:	ceramide
CHOL:	cholesterol
co-SAA:	co-surfactant
D_{app} :	apparent diffusion coefficient
DLS:	Dynamic light scattering
DMSO:	dimethyl sulfoxide
DSC:	Differential scanning calorimetry
FFA:	free fatty acid
HAC:	acetic acid
HD-PMI:	^{14}N HD-PMI (2-heptadecyl-2, 3, 4, 5, 5-pentamethyl-imidazoline-1-oxyl)
HeG:	hexylene glycol
HLB:	hydrophilic-lipophilic balance
HPGCH4:	HYDRIOL [®] PGCH.4 (polyglyceryl-4-caprate)
HPGMO4:	HYDRIOL [®] PGMO.4 (polyglyceryl-4-oleate)
IF:	line shape factor
IPM:	isopropyl myristate
IPP:	isopropyl palmitate
IS:	irritation score
LA:	lignoceric acid
Lin A:	linoleic acid
LPP:	long periodicity phase
LW:	line width factor
MDT:	mean dissolution time
ME:	microemulsion
miglyol:	Miglyol [®] 812
min:	minute

Mo:	total percentage of dose released and penetrated
Mon:	month
ON:	over night
PA:	palmitic acid
PAPEOSME:	lecithin-based optimised CER [EOS] ME
PAPOME:	lecithin-based optimised CER [AP] ME
PCS:	photon correlation spectroscopy
PeG:	1, 2 pentandiol
PEG:	polyethylene glycol
PG:	propylene glycol
Phosal :	Phosal [®] 75 SA
PNPOME:	lecithin-based optimised CER [NP] ME
PT-PD:	pseudo-ternary phase diagram
RSD:	relative standard deviation
RT:	room temperature
SA:	stearic acid
SAA:	surfactant (surface active agents)
SB:	stratum basale
SC:	stratum corneum
SD:	standard deviation
SG:	stratum granulosum
SIM:	selected ion monitoring
SLS:	sodium lauryl sulphate
SPP:	short periodicity phase
SS:	stratum spinosum
Tagat:	Tagat [®] O 2 V (PEG-20 glyceryl oleate)
TAPEOSME:	TEGO [®] CARE PL 4 based optimised CER [EOS] ME
TAPOME:	TEGO [®] CARE PL 4 based optimised CER [AP] ME
τ_c :	rotational correlation time
TCPL4:	TEGO [®] CARE PL 4 (polyglycerol-4-laurate)
TEWL:	transepidermal water loss
TNPOME:	TEGO [®] CARE PL 4 based optimised CER [NP] ME
tris:	tris (hydroxymethyl) aminomethane
Tween 80:	Tween [®] 80 (Polyoxyethylen-80-sorbitanmonooleat)

Contents

Abbreviations and Symbols	i
List of Tables	vi
List of Figures	vii
1. Introduction.....	1
1.1. Ceramides and the Stratum Corneum	1
1.1.1. The Skin	1
1.1.2. The Epidermis	2
1.1.3. The Stratum Corneum	3
1.1.3.1. Compositions of SC Lipid Lamella in Healthy Skin	4
1.1.3.2. Lamellar Organization and Lateral Packing of Lipids in the SC.....	6
1.1.3.2.1. Lamellar Organization of Lipids in SC.....	6
1.1.3.2.2. Lateral Packing of Lipids in the SC.....	9
1.1.3.3. Alterations of SC Lipid Composition and Organization in Affected Skin .	10
1.1.3.4. SC Lipid Replenishment Therapy: Strategies, Challenges and Attempts ..	11
1.1.4. Summary	12
1.2. Microemulsions (MEs).....	12
1.2.1. Morphologies/Nanostructures of MEs	13
1.2.2. Theories of ME Formation.....	14
1.2.3. Why MEs?.....	14
1.2.4. Formulation of MEs	15
1.2.4.1. Formulation Considerations.....	15
1.2.4.2. Preparation of MEs	18
1.2.5. Characterization of MEs	18
1.2.6. Factors Governing the Nanostructures and other Physicochemical Properties of MEs	19
1.2.7. Applications of MEs	20
1.2.8. MEs in Dermal and Transdermal Drug Delivery.....	20
1.2.9. Limitations of MEs	21
1.3. Objective of the Research	21
2. Preparation and Characterisation of MEs Containing CERs and other SC Lipids	23
2.1. Introduction	23
2.2. Materials and Methods	24
2.2.1. Materials.....	24
2.2.2. Methods.....	24
2.2.2.1. LC/ESI-MS	24
2.2.2.2. Solubility Determination.....	25
2.2.2.3. ME Preparation	25
2.2.2.4. Construction of Pseudo-ternary Phase Diagram.....	25
2.2.2.5. Cross-Polarised Light Microscopy	26
2.2.2.6. Electrical Conductivity	26
2.2.2.7. Differential Scanning Calorimetry (DSC)	26
2.2.2.8. Refractive Index.....	27
2.2.2.9. Viscosity	27
2.2.2.10. Dynamic Light Scattering (DLS).....	27

2.2.2.11. Electron Paramagnetic Resonance (EPR).....	28
2.2.2.12. Thermodynamic Stability	28
2.3. Results and Discussion.....	28
2.3.1. Formulation and Characterisation of SC Lipids MEs	28
2.3.1.1. Formulation and Characterisation of CER [AP] MEs	29
2.3.1.1.1. Determination of the Solubility of CER [AP] in Various Solvents and Co-solvents	29
2.3.1.1.2. Selection of Appropriate ME Components.....	30
2.3.1.1.3. Formulation and Characterisation of TCPL4-based CER [AP] MEs	32
2.3.1.1.4. Formulation and Characterisation of Lecithin-based CER [AP] MEs	51
2.3.1.2. Formulation and Characterisation of CER [EOS] MEs Containing other SC Lipids	60
2.3.1.2.1. Formulation and Characterisation of TCPL4-based CER [EOS] and other SC Lipids MEs	61
2.3.1.2.2. Formulation and Characterisation of Lecithin-based CER [EOS] MEs with other SC Lipids.....	63
2.3.1.3. Formulation and Characterisation of CER [NP] MEs Containing other SC Lipids	65
2.3.1.3.1. Formulation and Characterisation of TCPL4-based CER [NP] and other SC Lipids MEs	65
2.3.1.3.2. Formulation and Characterisation of Lecithin-based CER [NP] and other SC Lipids MEs	67
2.4. Conclusion.....	69
3. Skin Irritation/Corrosion Study	71
3.1. Introduction	71
3.2. Materials and Methods	71
3.2.1. Materials.....	71
3.2.2. Method	71
3.3. Results and Discussion.....	72
3.4. Conclusion.....	73
4. <i>In Vitro</i> Release and Penetration Study	74
4.1. Introduction	74
4.2. Materials and Methods	74
4.2.1. Materials.....	74
4.2.2. Methods.....	74
4.2.2.1. Solubility Study	74
4.2.2.2. Model Membrane Preparation	75
4.2.2.3. <i>In Vitro</i> release and Penetration Study	75
4.2.2.4. Automated Multiple Development (AMD)-HPTLC	76
4.3. Results and Discussion.....	77
4.3.1.1. Solubility of CER [AP] in Dodecanol and Dodecanol Containing Solvent Mixtures	77
4.3.1.2. <i>In Vitro</i> Release and Penetration Studies.....	77
4.4. Conclusion.....	82
5. <i>Ex Vivo</i> Skin Permeability Study.....	83

5.1.	Introduction	83
5.2.	Material and Methods	84
5.2.1.	Materials.....	84
5.2.2.	Methods.....	84
5.2.2.1.	Synthesis of CER [NP]-D3-18 (Deuterated CER [NP]).....	84
5.2.2.2.	Column Chromatography	85
5.2.2.3.	Thin Layer Chromatography	85
5.2.2.3.1.	LC/ESI-MS Method Development	86
5.2.2.4.	LC/ESI-MS Method Validation.....	86
5.2.2.5.	Preparation of MEs and ME Gels	87
5.2.2.6.	<i>Ex Vivo</i> Permeability Experiment.....	87
5.3.	Results and Discussion.....	88
5.3.1.	Method Development and Validation	88
5.3.2.	<i>Ex Vivo</i> Permeability Study	92
5.4.	Conclusion.....	95
6.	Summary and Perspectives	96
6.1.	English version.....	96
6.2.	German version	100
7.	References.....	106
8.	Appendixes	114
	Appendix A: Selection of appropriate ME Ingredients	114
	Appendix B: Development of CER [AP] MEs.....	121
	Appendix C: Development of CER [EOS] MEs containing other SC lipids	126
	Appendix D: Development of CER [NP] MEs containing other SC Lipids	140
	Appendix E: Investigation the Partitioning behaviour of HD-PMI in ME phases....	155

List of Tables

Table 1.1: Common skin diseases and associated change in SC lipid composition and organisation.....	11
Table 2.1: Solubility of CER [AP] in various solvents and co-solvents at RT (21-23°C) and 32°C (N=3).....	29
Table 2.2: Compositions and stabilities of optimised TCPL4-based CER [AP] MEs. ..	33
Table 2.3: Viscosity, refractive index, droplet diameter and nanostructure of optimised TCPL4-based CER [AP] MEs.	45
Table 2.4: KV/K _B values of HD-PMI calculated in selected ME components.	49
Table 2.5: Viscosities, microviscosities and relative micropolarities, of selected TCPL4-based MEs at 25°C and their proposed nanostructures.....	50
Table 2.6: Compositions and stabilities of optimised lecithin-based CER [AP] MEs. ..	52
Table 2.7: Viscosity, refractive index, droplet diameter and nanostructure of optimised lecithin-based CER [AP] MEs.....	58
Table 2.8: Viscosities, microviscosities and relative a_N values of selected TCPL4 and lecithin-based MEs at 25°C along with their proposed nanostructures.	59
Table 2.9: Compositions and stabilities of optimised TCPL4-based CER [EOS] MEs.	62
Table 2.10: Viscosity, refractive index, pseudo-droplet diameter, and nanostructures of optimised TCPL4-based CER [EOS] MEs.....	63
Table 2.11: Compositions and stabilities of optimised lecithin-based CER [EOS] MEs.	64
Table 2.12: Viscosity, refractive index, pseudo-droplet diameter and nanostructure of optimised lecithin-based CER [EOS] MEs.....	65
Table 2.13: Compositions and stabilities of optimized TCPL4-based CER [NP] MEs.	66
Table 2.14: Viscosity, refractive index, droplet diameter, and nanostructures of optimised TCPL4-based CER [NP] MEs.	67
Table 2.15: Compositions and stabilities of optimized TCPL4-based CER [NP] MEs.	68
Table 2.16: Viscosity, refractive index, droplet diameter and nanostructure of lecithin-based CER [AP] MEs.	69
Table 3.1: Compositions and ISs of selected TCPL4 and lecithin-based MEs (n=6). ...	72
Table 4.1: Solubility of CER [AP] in dodecanol and other dodecanol containing mixtures at 32°C (N=3).....	77
Table 4.2: Characteristics of TCPL4 and lecithin-based CER [AP] MEs chosen for release and penetration study.....	77
Table 4.3: Compositions of a conventional hydrophilic cream (DAC) used as reference formulation during release and penetration studies of CER [AP] from MEs.....	78
Table 4.4: <i>In vitro</i> pharmacokinetic parameters obtained from release and penetration study of CER [AP] from selected dosage forms (n=5).....	81
Table 5.1: Values depicting the precision and accuracy of the LC/ESI-MS method for quantification of exogenous deuterated CER [NP] in SC and other layers of the skin. .	92
Table 5.2: Compositions of MEs and ME gels selected for <i>ex vivo</i> permeability study.	93
Table 5.3: Viscosity, refractive index, droplet diameter, and nanostructure of lecithin and TCPL4-based CER [NP] MEs selected for permeability study.....	93
Table 6.1: Compositions and stabilities of TCPL4 and lecithin-based MEs of SC lipids developed.	97
Table 6.2: Zusammensetzungen und Stabilitäten von Lecithin- und TCPL4-basierten SC-Lipid-MEs.....	101

List of Figures

Figure 1.1: Cross-sectional schematic of the human skin, adopted from [9].	2
Figure 1.2: Chemical structures of the various CER classes identified in human SC.	5
Figure 1.3: Arrangement of SC lipids in the LPP as proposed by Baustra et al. (2000), adopted from [44]	7
Figure 1.4: The flip-flop transition of CERs from fully extended state (a) to hair pin state (b) explaining the arrangement adjacent lamellae as described by Kiselev et al. (2005), adopted from [46].	8
Figure 2.1: The PT-PDs of various TCPL4-based ME systems (II= 2 phase region; ME= ME region; LC= liquid crystal region; O/W= O/W ME region; W/O= W/O ME region; BC= BC ME region).	35
Figure 2.2: Electrical conductivity curves of some ME systems: conductivity of SAA-oil (R: %, m/m) drawn as a function of percent hydrophilic phase; a) TCPL4:(IPP-Lin A, 4:1); b) TCPL4:(IPP-Lin A, 9:1); c) (TCPL4-HPGMO4, 1:1):(IPP-Lin A,9:1); d) (TCPL4-HPGMO4,1:1):(IPP-Lin A, 9:1) (N=3).	36
Figure 2.3: DSC thermograms of TCPL4-based MEs obtained along the 65:35 dilution lines diluted with low (A) and high (B) ratios of PeG in the hydrophilic phase.	38
Figure 2.4: The chemical structure of HD-PMI.	40
Figure 2.5: Change in EPR parameters of TCPL4-based MEs containing IPP-Lin A (9:1) as oily phase and TCPL4-HPGMO4 (1:1) as SAA mixture at 25°C as a function of percent hydrophilic phase (water-PeG equals 1:9 (left), 3:7 (middle) and 1:1 (right)).	41
Figure 2.6: Change in EPR parameters of TCPL4-based MEs containing IPP-Lin A (9:1) as oily phase and TCPL4-HPGMO4 (1:1) as SAA mixture at 40°C as a function of percent hydrophilic phase (water-PeG equals 1:9 (left), 3:7 (middle) and 5:5 (right)).	42
Figure 2.7: A linear curve describing the relationship between τ_c of HD-PMI and η in PeG over a range of temperature.	49
Figure 2.8: Effect of temperature on microviscosities of selected optimized TCPL4-based MEs.	51
Figure 2.9: PT-PDs of lecithin-based MEs at different water-PeG ratios: a, 1:1; b, 2:3; c, 3.5:6.5; d, 1:3; e 1.5:8.5 and f, 1:9. II= 2 phase region; ME= ME region; O/W= O/W ME region; W/O= W/O ME region; BC= BC ME region, the blue band on the ME region=region of stable CER [AP] MEs.	53
Figure 2.10: Electrical conductivity of lecithin-based MEs as a function of Wt% of the hydrophilic phase (water-PeG 1:9-3.5:6.5). R= phosal-miglyol (% m/m) (N=3).	54
Figure 2.11: DSC thermograms of lecithin-based MEs obtained along the 40 % SAA (a) and R=65:35 (b) dilution lines diluted with water-PeG 3.5:6.5 and 1:9, respectively.	56
Figure 2.12: Change in EPR parameters of lecithin-based MEs at 40% phosal dilution line at 25°C (a) and 40°C (b) as a function of percentage hydrophilic components containing 1.5:8.5 (left) and 1:1 (right) water-PeG.	57
Figure 2.13: Effect of temperature on microviscosities of selected lecithin-based MEs.	60
Figure 4.1: Schematic representation of a multi-layer membrane model described by Neubert et al (1991) adopted from [184].	76
Figure 4.2: Rate of CER [AP] released and penetrated into the deeper layers of the multi-layer membrane model comprised of 4 membranes (N=5).	79

Figure 4.3: Overall release and penetration profile of CER [AP] from various formulations into membranes of multi-layer membrane model (N=5).....	81
Figure 5.1: Schematic representation of the mechanism by which phytosphingosine couples with octadecanoic-18, 18, 18-D3 acid to form deuterated CER [NP].....	89
Figure 5.2: LC/ESI-MS chromatograms and spectrum of deuterated CER [NP] and SC extracts obtained in negative ionization mode.....	91
Figure 5.3: Percentage deuterated CER [NP] permeated into the different layers of the skin from various formulations.....	94

1. Introduction

Ceramides (CERs) are sphingolipid metabolites that are the major constituents of the stratum corneum (SC) along with free fatty acids (FFAs) and cholesterol (CHOL) [1]. To date, 12 classes of CERs have been identified in human SC [1], which play a major role in the water-retaining properties of the epidermis and are claimed to dramatically increase skin's hydration level, repair the cutaneous barrier, prevent vital moisture loss, and contribute to reducing dry flaky skin and aged appearance [2]. They can also be used against some skin diseases such as atopic dermatitis (AD) [2] and psoriasis [3-4]. Beside their structural role, CERs also play an important role in intracellular signalling and regulates several biological processes, such as proliferation, differentiation, apoptosis, inflammation and immune responses [5]. Hence, CERs and their derivatives have drawn attention as active components in both pharmaceutical and cosmetic industries [2]. However, the effectiveness of these compounds is limited due to their inherent hydrophobicity and potential precipitation as fine lipid micellar suspensions when administered in hydrophilic formulations. Moreover, from conventional dosage forms, they cannot penetrate the SC to reach the site where they exert their biological activity [6-7]. Therefore, to realise the therapeutic benefits of these lipids, an appropriate drug delivery system that can enhance their solubility and SC permeability should be developed.

1.1. Ceramides and the Stratum Corneum

1.1.1. The Skin

Epidermis, dermis and hypodermis (subcutaneous tissue) form the three major layers of the skin from outside to inside [8], Fig 1.1. Hypodermis is a fatty subcutaneous layer of the skin, whereas, dermis (3-5 mm thick) is a layer of connective tissue that contains primarily fibroblasts embedded in acellular collagen/elastin matrix that accounts for the majority of skin thickness. The overlying epidermis, the stratified avascular layer, is responsible for the formation and maintenance of the skin barrier to both desiccation and penetration of xenobiotics [4].

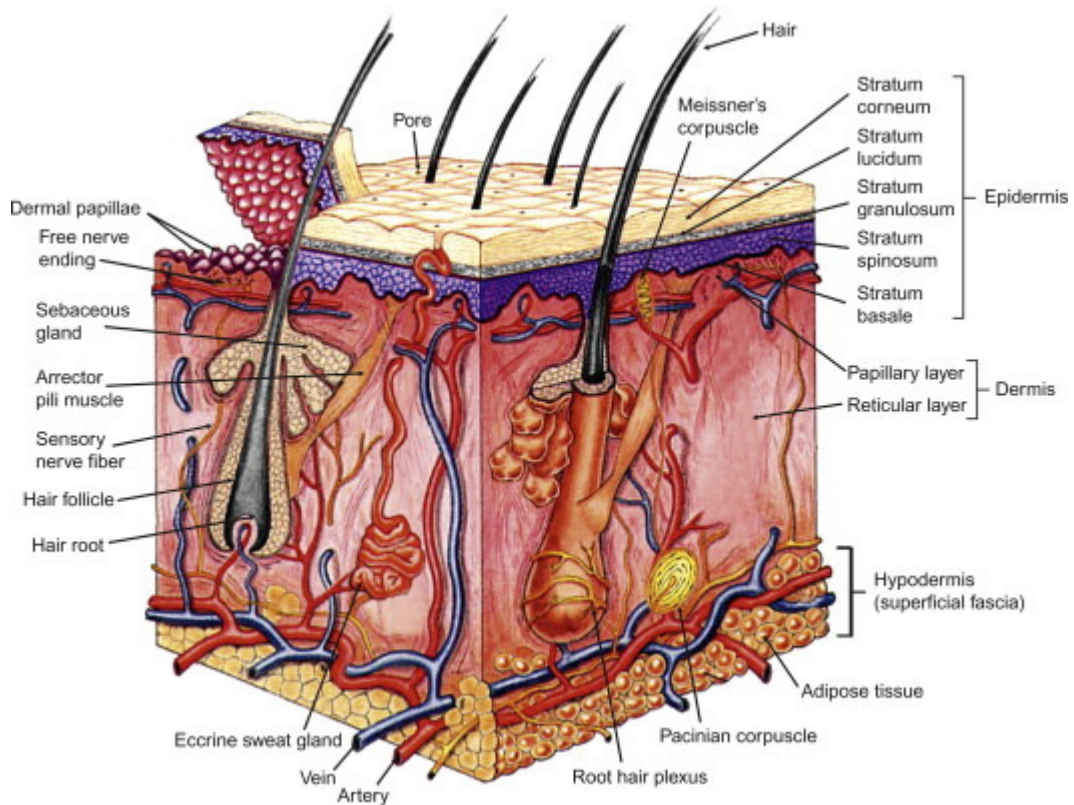


Figure 1.1: Cross-sectional schematic of the human skin, adopted from [9].

1.1.2. The Epidermis

Epidermis (50–100 μm) comprises four different layers of cells namely the stratum basale (SB), the stratum spinosum (SS), the stratum granulosum (SG) and the SC, from inside to outside [10-11], Fig 1.1. It is a dynamic, constantly self-renewing tissue, in which desquamation on the SC is balanced by cell growth in the lower layers of the epidermis [11-12]. The epidermal cells at the basal layer, Keratinocytes, proliferate and upon leaving the layer they start to differentiate and migrate towards the surface of the skin. The terminal differentiation occurs at the SG–SC interface during, which the viable keratinocytes are transformed into corneocytes (flattened dead cells filled with keratin filaments and water) [3, 11].

Epidermis is a highly active site of SC lipids synthesis, which is also responsive to alterations in barrier status. Injury to the skin initiates a recovery response that leads to restoration of the barrier function within hrs to days, depending on species, age, and severity of the injury [13].

Keratinocytes, the most abundant cells of the epidermis, synthesise the lipids and other structural proteins of the SC in a controlled and regulated manner both in time and in space [11, 14]. During migration from the basal layer to the SG they undergo a number

of changes in both structure and composition [11], that is, they synthesise precursor lipids in the SB, SS, and SG; they assemble the precursor lipids in the lamellar bodies (carriers of SC lipid precursors) in SS and SG; and they release the contents of the lamellar bodies at the SG-SC intercellular interface by the process of exocytosis [11, 14-16].

The lamellar bodies are enriched mainly in polar lipids mainly glycosphingolipids, free sterols and phospholipids and catabolic enzymes [11, 14]. At the SG-SC interface the released polar lipids undergo considerable metabolic changes and convert enzymatically into the nonpolar products: phospholipids are degraded into glycerol and FFAs whereas the glucosylsphingolipids degrade into CERs and assemble into lamellar structures surrounding the corneocytes [11, 14-16].

Besides the usual polar and neutral lipids found in epithelial tissues of the body, the viable epidermis contains certain unique phospholipids and glycosphingolipids. Therefore, the transformation of the SG into the SC is accompanied by depletion of phospholipids and generation of large amounts of sphingolipids composed of longer chain, more saturated FFAs than are present in lipids in the subjacent viable epidermis [12].

1.1.3. The Stratum Corneum

The SC (10 to 20 μm thick [10]) protects the body against loss of physiologically important components as well as entry of harmful environmental insults [17]. It contains about 15 layers of corneocytes separated by a unique and complex mixture of highly ordered multi-lamellar lipid sheets [14, 17-21], which is often referred to as a brick wall-like structure [19].

The corneocytes, flat dead cells filled with keratin filaments and water, are surrounded by a densely cross-linked protein envelope, the so-called cornified envelope, to which a lipid monolayer (the cornified lipid envelope) is further covalently attached [3, 11]. The cornified lipid envelope is formed from CERs with ω -hydroxy groups, which are capable of covalently binding to the cornified envelope proteins, especially involucrin. The lipid envelope serves as an interface between the hydrophilic corneocytes and the lipophilic multi-lamellar lipid sheets that are surrounding the corneocytes [22]. The corneocytes are interconnected by other proteins called corneodesmosomes, which are important for the SC cohesion [11].

The whole SC contains about (5-15) % lipids, (75-80) % proteins, and (5-10) % unknown materials on dry weight basis [20]. The small percentage of intercellular lipids in the SC, the only continuous tortuous path through the SC, defines the pathway through which molecules can diffuse across the SC and plays the major role in the selective permeability and skin barrier functions [11, 17-18, 20-21, 23-24]. The very dense corneocyte envelope is impermeable to most diffusing substances so that the main penetration pathway through the SC remains the intercellular lipid lamella [24], which also plays the prominent role in dermal and transdermal drug delivery [25].

1.1.3.1. Compositions of SC Lipid Lamella in Healthy Skin

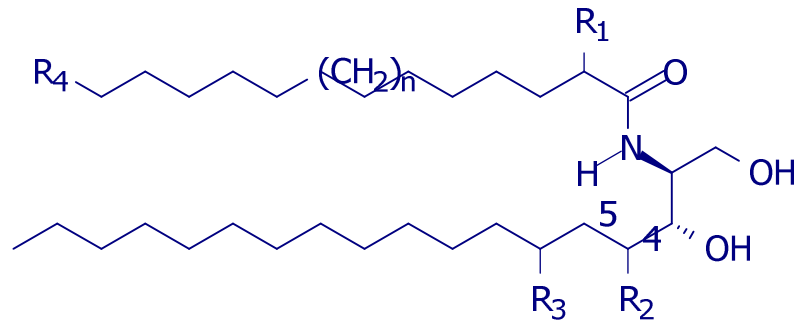
The multi-lamellar lipid lamellae of the SC are made of a unique complex mixture of polar and non-polar lipids that, unlike biological membranes, is almost devoid of phospholipids [3, 19-20, 26]. Their main components are CERs, CHOL, and FFAs (predominantly long-chain and saturated), which exist nearly in equimolar amounts: on weight basis, they contribute about (40–50) %, (20–33) % and (7–13) %, respectively [4, 17, 27]. The other lipids in the lamellar sheets include cholesterol-3-sulphate (0–7 wt %) and cholesteryl esters (0–20 wt %) [18, 27-28]. Nevertheless, these lipids vary with location and depth of the skin; age, sex, and pathological state of the individual; between individuals; between races and season of the year [14, 18, 29]. The amount of FFAs is higher at the upper layer of the SC and decreases towards the inner layer of the SC [30].

a) Ceramides

CERs are critical for the formation of the highly ordered intercellular multi-membrane lipid lamellae together with CHOL and the long chain FFAs [4, 22]. They are mainly originated from the deglycosylation of glucosylated CER precursors catalyzed by the β -glucocerebrosidase or through hydrolysis of sphingomyelin by means of the acid sphingomyelinase [3]. Unlike other tissue CERs, SC CERs are extremely complex [11].

They contain a sphingoid moiety (which can be sphingosine (S), dihydrosphingosine (D), phytosphingosine (P), or 6-hydroxy-sphingosine (H)), linked with a long chain FFA moiety (which can be nonhydroxy (N), α -hydroxy (A), or ester-linked ω -hydroxy (EO)) through an amide bond [3, 31]. To date, 12 different types of free CERs have been identified in human SC, which are named as “Ceramide XY” where “X” represents the type of FFA moiety and Y represents the type of sphingoid base [1, 22], Fig 1.2. The acyl-CERs (CER [EOS], CER [EOP], CER [EOD] and CER [EOH]) have

a unique structure of linoleic acid (Lin A) linked to the ω -hydroxy fatty acid moiety [1, 22]. In essential fatty acid deficiency, oleate substitutes for linoleate as the predominant ω -esterified species in CER [EOS] and CER [EOP] causing a profound barrier abnormality [13].



	R1	R2	R3	R4		R1	R2	R3	R4	
CER [AS]	OH	H	H	H	4,5-double bond	CER [AP]	OH	OH	H	H
CER [NS]	H	H	H	H	4,5-double bond	CER [NP]	H	OH	H	H
CER [EOS]	H	H	H	OH	4,5-double bond	CER [EOP]	H	OH	H	OH
CER [AH]	OH	H	OH	H	4,5-double bond	CER [ADS]	OH	H	H	H
CER [NH]	H	H	OH	H	4,5-double bond	CER [NDS]	H	H	H	H
CER [EOH]	H	H	OH	OH	4,5-double bond	CER [EODS]	H	H	H	OH

The ω OH group (R4) is mostly esterified with Lin A; generally $n=2-22$ (May also refer to unsaturated FFAs) [21, 32-33] but $n=12-14$ is the most abundant [11, 19] and mostly $n=18-22$ with the ω esterified CERs [21].

Figure 1.2: Chemical structures of the various CER classes identified in human SC.

CER [NS] is expressed ubiquitously in mammalian tissues [22]. The relative percentage of each CER class proposed by various authors is different but CER [NP] and CER [NS] are present at higher percentages in contrast to CER [AP] and CER [EOS] [3, 34-35].

Apart from structural roles, CERs also have physiological roles in signal transduction and cell regulation relevant to apoptosis, cell differentiation, cell growth arrest, senescence, and immune responses [31].

b) Free Fatty Acids

Unlike their precursor membrane lipids, SC lamellar membranes contain mostly saturated FFAs of significantly longer chain length, which varies between C16 and C26. The main FFAs in SC include palmitic acid (PA) (C16:0), stearic acid (SA: C18:0), behenic acid (BA) (C22:0), lignoceric acid (LA) (C24:0) and hexacosanoic acid (C26:0), which contribute approximately 10, 10, 15, 25 and 10 % (m/m), respectively,

of the total SC FFAs [24]. Other FFAs include oleic acid (C18:1, n-9) eicosapentaenoic acid (C20:5, n-3), docosahexaenoic acid (C 22:6, n-3), Lin A (C18:2, n-6), the most abundant polyunsaturated fatty acid, and its derivatives (α -linolenic acid (C18:3, n-3), γ -linolenic acid (C18:3, n-6), dihomogamma-Lin A, (C20:3, n-6)) and arachidonic acid (AA) (C20:4, n-6) [36-37]. Some odd chain FFAs have also been identified in human SC [33-34]. Among the different FFAs, the C 18 unsaturated and the C22 and C24 saturated are present in relatively large amount [24, 38]. All the FFAs can be synthesised in the body from glucose and acetate-carbon sources. However, the body is incapable of inserting double bonds beyond the *n*-9 position [39-40] and cannot synthesise the two essential FFAs, Lin A and AA. Lin A may be converted into AA in keratinocytes in the extreme essential FFA deficiency state [39].

c) Acid Mantle of the SC

Apart from the structural lipids in the SC, there are lipids secreted by sebaceous glands and exist widespread on the surface of the skin to provide the skin 'self-sterilising' properties [41]. It mainly consists of triglycerides, wax/sterol esters, squalene and some FFAs [11, 14, 18, 28]. *cis*-6-Hexadecenoic acid is the most abundant and ubiquitous lipid in human skin and has been suggested to be the most active antimicrobial lipid in skin surface lipids [41]. These lipids may also alter the endogenous lipid structure by increasing alkyl chain mobility [11].

1.1.3.2. Lamellar Organization and Lateral Packing of Lipids in the SC

SC lipids matrix displays a refined spatial organisation of the lipids into lipid lamellae that are oriented approximately parallel to the surface of the corneocytes. The uniqueness of the organisation is strongly dependent on SC lipid composition [15] and governs the permeability and barrier properties of the SC [27, 42].

1.1.3.2.1. Lamellar Organization of Lipids in the SC

Understanding of the lipid matrix in the SC began through observation of the lipid lamellae under an electron microscope [43]. Further information were obtained on the lamellar organisation and lateral packing of the lipids in the lipid lamellae using the results of small angle and wide angle x-ray scattering techniques, respectively [44-45]. Later on, the result of neutron scattering was applied in an attempt to elucidate the lamellar organisation of the matrix [46]. However, the illustration of the lamellar organisation of the lipids in the lamellae is not yet fully agreed upon and various models describing the organisation have been proposed by different authors. Some of the

models are briefly discussed. Small angle X-ray diffraction results of the human SC showed the existence two phases called the short and long periodicity phases (SPP and LPPs) that approximately are 60 and 130 Å, respectively, [21, 23, 26, 46-48] and some of the models took this into consideration.

The Domain Mosaic Model

The domain mosaic model described by Forslind et al. (1994) [45] contains a multi-lamellar two-phase system in which a discontinuous lamellar crystalline structure is embedded in a continuous liquid crystalline structure, which is referred as grain border and is assumed to be the path for the permeation of both hydrophilic and hydrophilic compounds.

The Sandwich Model

Bouwstra et al. (2000) [44] postulated a sandwich model based on the results of small angle X-ray diffraction and other findings. In this model, the lamellar phase contains a narrow liquid sub-lattice (30 Å) sandwiched between two wide lipid crystalline layers (50 Å), representing the LPP of 130 Å. According to the authors, the wide lipid layers comprise CERs with longer chain FFAs (C-24 to C-26), the ω -esterified CER and CHOL forming a crystalline sub-lattice, while, the central, narrow fluid lipid monolayer comprises the ω -esterified unsaturated FFA of the ω -esterified CER, CHOL and CER with a short FFA chain (C-16) in hairpin conformation, Fig 1.3. The formation of fluid sub-lattice is mainly attributed to the relatively immobile unsaturated FFA. The authors also suggested that CER [EOS], which forms the crystalline sub-lattice and extends all the way to the narrow fluid sub-lattice, plays a significant role in forming the LPP.

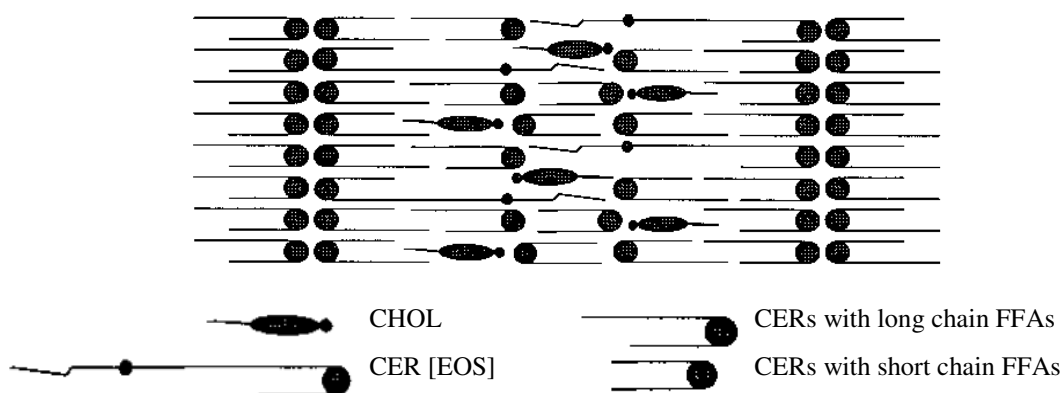


Figure 1.3: Arrangement of SC lipids in the LPP as proposed by Bouwstra et al. (2000), adopted from [44]

The Single Gel Phase Model

Following the above models, in 2001 Norlén (2001) [49] came up with a different model called the “Single gel phase model”. Unlike the above models, in this model, the lipids in lipid lamellae exist as a single and coherent gel phase, where, gel, according to the author is defined as “a crystalline lamellar lipid structure that usually has a hexagonal hydrocarbon chain packing with rotational disorder along the lipid chain axes and usually contains some water between the lamellae”. However, although no phase boundaries exist, the single gel phase may be regarded as crystal in the CHOL-deficient areas and as extremely tightly packed liquid crystal in CHOL-rich areas.

The Armature Reinforcement Model

Kiselev et al. (2005) [46], as was later supported by Kiselev (2007) [50], Kessner et al. (2008) [32] and Schröter et al. (2009) [48], applied neutron scattering technique to reveal the arrangement of lipids in the SC lipid lamellae. Unlike the sandwich model proposed by Bouwstra et al. (2000) [44] in which all CERs exist as hair pins (Fig 1.3) in this model CER [AP] exists as fully extended state at partial hydration of the skin, so that it penetrates the other layers and reinforces the adhesion between the lamellae. However, in fully hydrated state the CER undergoes flip-flop transition and exist as one sided, Fig 1.4, explaining the structural alteration of the lamellae under hydration by excess water: in highly hydrated systems water may exist between adjacent layers, whose thickness is dependent on the degree of humidity.

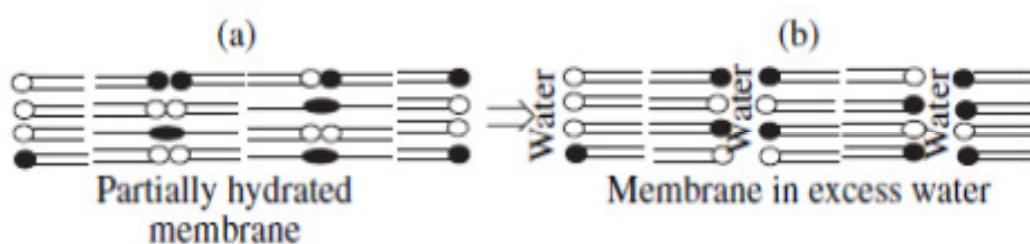


Figure 1.4: The flip-flop transition of CERs from fully extended state (a) to hair pin state (b) explaining the arrangement adjacent lamellae as described by Kiselev et al. (2005), adopted from [46]

The Asymmetry Model

Recently, Norlén (2011) came up with the “asymmetry model” describing the lamellar organisation of SC lipids in the SC [51]. The author hypothesised that CER [NP], which he believe plays the key role, exists as fully extended conformation forming a 45 and 65

Å bilayer: the 45 Å bilayer consists of the short chain of CER [NP] (having 18 C atoms) and cholesterol, whereas, the 65 Å bilayer consists of the long chain of CER [NP] (having 24 C atoms) as the main fraction and lignoceric and behenic acid as main free fatty acids.

Therefore, according to the models described above CERs, especially CER [EOS], CER [AP], and CER [NP] are vital for the formation of tough SC lipid lamellae.

1.1.3.2.2. Lateral Packing of Lipids in the SC

Besides the lamellar organisation the lateral packing of lipids in SC determines the barrier function of the SC [11]. Depending on the distance between the hydrocarbon chains of the lipids in the lamellae, three crystalline phases are possible: the disordered phase (liquid crystalline phase) and the ordered phases (hexagonal and orthorhombic phases) [11, 25, 52]. In the liquid crystalline phase the distances between the hydrocarbon chains is not very well defined, with a lattice constant of 0.46 nm, and exhibit a high degree of permeability. The hexagonal packing has equally distributed hydrocarbon chains with a lattice constant of 0.41 nm and has medium permeability. Whereas, the orthorhombic phase has a very densely packed hydrocarbon chains, which are not equally distributed in the lattice with lattice constants of 0.41 nm and 0.37 nm and hence exhibit very low permeability. Various techniques have shown that the LPP of the SC exhibits mainly an orthorhombic arrangement [47], which converts into hexagonal organisation at around 40 °C [53].

All the major three classes of SC lipid are important for the formation of the orthorhombic lateral packing [11, 23, 54-55]. The architecture of the CER head group also affects the lipid lateral packing of the lipids. The head groups of the phytosphingosine based CERs, like CER [AP], have the highest number of hydroxyl groups, which affects formation of hydrogen bonds in the head group region and increases the stability of the orthorhombic phase [54, 56]. Optimum amount of FFAs is also required for the formation of the orthorhombic phase in the LPP phase. Investigation of the arrangement using model membranes showed that in the absence of FFAs no orthorhombic phase was obtained [14, 19, 23-24, 26, 32, 42], but as the level of FFAs increased then SPP predominated [26, 55]. A study by Norlen et al. (1999) indicated that as one goes deeper into the SC layers, the amount of FFA decreased, which resulted in an increase in transepidermal water loss (TEWL) [30]. Longer chain FFAs have stronger Van der Waals interactions promoting the orthorhombic lateral packing [11, 21, 54]. In addition, a certain degree of heterogeneity in the lipid mixture is

important for the formation of the orthorhombic phase [54]. A study by Caussin et al. (2008) showed that, porcine skin has lower percentage of phytosphingosine based CERs than humans and relatively shorter chain FFAs that resulted in mainly hexagonal lateral packing [54]. In contrast, cholesterol-3-sulphate may lead to reduction of the lattice density and, consequently, to an increase in the SC permeability [11].

1.1.3.3. Alterations of SC Lipid Composition and Organization in Affected Skin

Diseased skin is often associated with an altered SC lipid composition and organisation that leads to reduced barrier function [11]. Various environmental and physical factors such as soap, dry air and age play a significant role in initiating depletion of the skin barrier [57]. As a result, the skin loses water and becomes dry, cracked and fissured and allows the entrance of allergens, toxins and microorganisms that can cause the skin to become inflamed and irritated. It may also lead to other skin conditions such as severe dryness, itching and scratching that can further lead to secondary skin infections such as herpes, molluscum, warts, staphylococcus, streptococcus, pseudomonas, fungus, yeast and tuberculosis. Depleted SC lipids may also be associated with eczema, common dry skin, excessively washed skin, and other dry and sensitive skin situations like chapped lips, hand and leg eczemas [57].

It has been shown that a number of skin disorders, such as psoriasis, AD, ichthyosis or xerosis are correlated with changes in lipid composition [28, 58]. Deficiency of n-6 essential FFAs, such as Lin A, γ -linolenic acid and AA, may also lead to inflammatory skin conditions, which can be reversed by either systemic or topical administration of n-6 essential FFAs [13]. The summary of the common pathogenesis changes in the SC in various skin diseases and the associated change in SC lipid composition and organisation is shown in Table 1.1.

As a consequence of alterations of the barrier function allergens and irritants may easily enter the skin causing allergic inflammation. In return, the inflammation may further degrade the barrier function closing the vicious circle. Therefore, replenishing the missing SC lipids and restoring the barrier function may relieve the symptoms, prevent aggravation of the disease with minimum side effects and may decrease the use of some anti-inflammatory drugs such as corticoids [59].

Table 1.1: Common skin diseases and associated change in SC lipid composition and organisation.

No.	Skin condition	Change in lipid composition and organisation	Pathogenesis
1	AD	Reduced level of CERs [59-60] but mainly CER [EOS] [13] and CER [NP] [61]; reduced <i>cis</i> -6-Hexadecenoic acid [41]; reduced level of CHOL in old age [57]. Increased hexagonal lateral packing as well as reduced LPP and increased SPP [11]	Up-regulation of sphingomyelin deacylase and impaired conversion of Lin A to γ -Lin A [13, 16]
2	Lamellar ichthyosis	Small change in CER composition and FFA level strongly reduced. Increased hexagonal lateral packing [11]	-
3	Type 2 Gaucher disease	increased level of glucosylceramides and altered lipid organisation [11]	The level of glucocerebrosidase is strongly reduced [11]
4	Psoriasis	Reduced level of CERs [3-4]	-
5	Essential FFA deficiency	CER [EOS]-ol increased and the presence of the liquid phase is increases [11]	Replacement of Lin A with oleic acid [11]
6	Sjögren-Larsson syndrome	Significant reduced level of CER [EOS], CER [NP] and CER [AP] and increased level of FFAs [60]	-

1.1.3.4. SC Lipid Replenishment Therapy: Strategies, Challenges and Attempts

In a study application of SC lipid mixture reduced the severity of stubborn-to-recalcitrant childhood AD and normalised TEWL rates and replenished the lamellar membrane bilayers [13]. In another study the use of a CER containing cream showed a significant improvement of erythema, pruritus, and fissuring compared to controls [13]. Schröter et al. (2009) showed that CER AP, the short-chain phytosphingosine with a high polarity founded on four OH-groups, induces the formation of a super-stable lamellae [48]. It has also been shown to be antiproliferative and proapoptotic in numerous cancer cell types *in vitro*, with the potential to act as anti cancer agent [7]. However, these lipids to be mingled into the SC should cross the SC layer and reach the SC-SG interface where the lipids are arranged into meaningful lamellae [11, 14-16]. Alternatively, it should penetrate into the deep layers of the epidermis whereby the uptake of lipids by nucleated epidermal cell layers takes place followed by release of the lipid mixture into nascent lamellar bilayers in the SC interstices [13]. Accordingly, there are some formulations containing CERs in the market (E.g. CeraVe, TriCeram, Atopiclair, Mimyx Cream).

1.1.4. Summary

Various models describing the organisation of SC lipids have been proposed but not yet fully agreed upon. However, it is shown that the tight and less permeable orthorhombic lateral packing dominates the SC with the hexagonal packing increasing in affected skin. All the three main SC lipids, CERs, FFAs and CHOL are vital for the provision of the barrier function of the skin. However phytosphingosine and long chain saturated FFAs (C22-C24) are important for the formation tight lateral packing (the orthorhombic phase) which are capable of forming strong hydrogen bonding. Several studies attribute the barrier function of the skin to the LPP, which needs the acyl-CERs, mainly CER [EOS], which act as rivets. In addition, the acyl CERs are vital for the formation of the strong covalent interaction between the SC lipid lamellae and the cornified protein envelope of the corneocytes. Essential FFAs are needed for the biosynthesis of the acyl CERs.

Several skin diseases conditions such as AD, Sjögren-Larsson syndrome, psoriasis and type 2 Gaucher disease are associated with reduced level of CERs within the SC. Whereas, some skin diseases like lamellar ichthyosis are associated with depletion of long chain FFAs of the SC. Thus, replenishment of phytosphingosine based CERs (e.g. CER [AP] and CER [NP]) acyl chain CERs (e.g. CER [EOS]) long chain FFAs (e.g. BA and LA) and essential FFAs (e.g. Lin A: which has anti-cancer effect and may also be converted into AA) may help restore the barrier function in aged and/or affected skin. However, appropriate drug delivery systems, such as colloidal drug delivery vesicles, should be employed to enable penetration of the lipids into deeper layers of the epidermis, where the lipids are arranged into the lipid lamellae. In addition, to date no penetration study involving CERs into the SC is reported and hence appropriate analytical method should be developed and the penetration of the lipids into the SC should be studied.

1.2. Microemulsions (MEs)

MEs are transparent, low viscous, optically isotropic and thermodynamically stable colloidal dispersions of oil and water, which are stabilised by an interfacial film of a surfactant (SAA), in most cases in combination with a co-surfactant (co-SAA) [62-66]. They have dynamic nanostructures and were first introduced by Hoar and Schulman in 1943, describing a transparent system obtained by titrating normal emulsions with hexanol [67].

1.2.1. Morphologies/Nanostructures of MEs

The bioavailability of drugs from MEs is dependent on the nanostructure of the MEs [68], which contain a diverse colloidal phase that varies from spherical droplet to bicontinuous (BC) and solution type [69-70]. The droplet type MEs could be oil in water (O/W) MEs, which consist of oil droplets contained in extended micelle like structures that are homogeneously dispersed in an aqueous continuous phase, or water-in-oil (W/O) MEs, which consist of water droplets contained in reversed extended micelles, which are homogeneously dispersed in an oil continuous phase. The droplets, in most cases, are not spherical [71]. BC MEs contain randomly oriented continuous channels of oil and water intertwined in a dynamic extended network separated by amphiphilic film [62, 71-75]. They appear as sponge-like structures when observed under electron microscope [71]. The solution-type MEs are simple molecular dispersions of all ME components [70]. The droplet and BC MEs are dynamic systems in which the interface is continuously and spontaneously fluctuating [62, 71-77].

Generally, droplet MEs have diameter ranging 10-100 nm [78-79]. However, MEs less than 5 nm [68, 80-81] or greater than 150 nm [82-83] have been reported. Their transparent nature accounts to the small diameter of the dispersed droplets, which is below the wavelength of visible light [64, 67, 84].

The nanostructure of MEs is mainly dependent on the concentrations and natures of the amphiphilic, oily and hydrophilic components of the ME as well as some physical factors like temperature [64]. In general, the relationship between the composition and the phase behavior of a mixture can be captured using a phase diagram, commonly a pseudo-ternary phase diagram (PT-PD) [77, 85]. The relative areas of the different zones are dependent on the physicochemical factors mentioned. A PT-PD obtained by Pestana et al. (2008) showed no BC region [86] whereas PT-PD obtained by Cheng et al. (2008) gave only W/O kind of ME [68].

In an area just outside of the ME region but close to the oil-water binary axis there is insufficient SAA concentration to facilitate the formation of a single ME phase. In this area, as was described by Winsor, MEs can exist in equilibrium with excess water and/or oil phases [87]. Type I MEs contain O/W ME in equilibrium with the free oil phase, while, Type II MEs contain W/O ME in equilibrium with the aqueous phase. Type III MEs exist as three-phase systems in which the middle ME phase is in equilibrium with both excess oil and excess aqueous phases [87-88]. The one phase MEs that are generally explored as drug delivery systems are classified as Winsor IV

systems [72, 77, 87]. In various studies of the phase behavior of ternary systems, phases with BC structures were located in the one-phase region that is very close to the three-phase body [71].

1.2.2. Theories of ME Formation

Formation of MEs is accompanied by creation of enormous surface area, which tends to increase the surface free energy of the system, which is given by Eqn. 1.1 [89].

$$\Delta G_f = \gamma\Delta A - T\Delta S \dots\dots\dots\text{Eqn. 1.1}$$

Where; ΔG_f is the free energy of formation, γ is the surface tension of the oil–water interface, ΔA is the change in interfacial area upon microemulsification, ΔS is the change in entropy of the system, and T is the absolute temperature.

However, MEs are thermodynamically stable systems, which form spontaneously suggesting a negative surface free energy of formation which is achieved by a significant reduction in interfacial tension accompanied by significant entropic changes [77].

1.2.3. Why MEs?

In comparison to many other colloidal systems, MEs possess large solubilisation capacity due to their immense interfacial area and various microdomains of different polarity within the same single-phase system, which can accommodate water-soluble, oil-soluble, amphiphilic and large molecules [64, 67, 77, 84, 90]. Apart from their high solubilisation capacity, MEs significantly enhance penetration of hydrophilic, lipophilic, and amphiphilic substances into and through biological membranes compared to conventional vehicles [75, 77, 91-94]. The small droplets have increased chance to adhere to biomembranes and to transport bioactive molecules in a more controlled fashion [95].

Besides, they are easy to formulate [64, 67, 77, 84], thermodynamically stable, optically clear [64, 77, 84], have relatively low viscosity due to low droplet interaction [64, 67, 96], have self-preserving property [97] and can be administered orally, topically, or nasally, as aerosol for direct entry into the lungs [95]. MEs can be considered as protecting medium for the entrapped drugs where they may protect some drugs from degradation and/or prevent their irritation effect on the body and may also provide a prolonged release of the drug [95].

MEs viscosity can be tailored for topical application through formulation changes or incorporation of specific gelling agents such as carbomers, xanthan gum, carrageenan or gelatin [64, 67, 96, 98-100]. In ME gels the SAAs and in some cases the oil phase (e.g. Limonene, oleic acid) may act as penetration enhancers [77, 91, 101] and hence skin permeation rate of active compounds from MEs can be controlled by the type and ratio of the ME components used [84].

1.2.4. Formulation of MEs

1.2.4.1. Formulation Considerations

Formation of stable ME involves adsorption of the SAA(s) between the oil-water interface forming an interfacial film with adequate fluidity and optimum curvature. The type of co-SAA used determines the fluidity of the film, whereas, the degree of penetration of the oil into the formed film determines the degree of curvature [102]. Thus, preparation of thermodynamically stable MEs demands appropriate choice of the SAA, co-SAA and oil. Bellow is given a short account on these major ME components.

a) Oils

Long chain triglycerides (i.e. vegetable oils), medium chain triglycerides and fatty acid esters (liquid waxes) are the most commonly used oils to develop pharmaceutical MEs [72]. Some other oils such as castor oil [94], ethyl oleate [93, 103], cyclic oils like peppermint oil [104] have also been used for the preparation of pharmaceutical MEs. Generally, small oils such as medium chain triglycerides and fatty acid esters can better penetrate the interfacial film and provide optimal film curvature [65] making them easy to microemulsify and give a wider homogeneous region [65, 97]. On the contrary, the solubilisation capacity of the lipophilic moieties usually increases with the chain length of the oily phase. Thus, the choice of the oily phase is often a compromise between its solubilisation capacity and its ability to form MEs of desired characteristics. In some cases, a mixture of oils is used to have a good balance between drug loading and emulsification [97].

b) Surfactants

SAAs should be innocuous, favour microemulsification and possess a good solubilising potential for the drug. Thus, generally, SAAs of natural origin like phospholipids are preferred over synthetic SAAs and their concentration in MEs should be maintained as low as possible irrespective of their nature, origin and type [97]. Choice of SAA(s) is

also governed by the type of the ME envisaged. Generally, SAAs with low hydrophilic-lipophilic balance (HLB) are preferred for the preparation of W/O MEs, whereas, high HLB SAAs are preferred for the preparation of O/W MEs [97]. However, only HLB of the SAA does not explicitly account for conformation and interfacial behaviour of the SAA molecule [88]. In general, combinations of various types of SAAs can be very effective for increasing the ME region [77, 85, 97], through provision of additional degree of freedom, which enables adjustment of phase behavior [104]. The commonly used SAAs for the preparation of pharmaceutical MEs include alkyl polyglycosides (sugar based SAAs: e.g. Plantacares 818, 2000) [105], polymeric SAAs like (Poloxamers/Pluronics) polyoxyethylene glycerol alcohols (e.g. SynperonicTM PE/L 101) [106], sorbitan esters (e.g. Spans 20, 80 and 85 and Tweens 20, 80 and 85) [72, 77, 84, 91, 98, 103, 107], polyglycerol fatty acid esters (Tego[®] Care PL 4 (TCPL4: polyglycerol-4-laurate) and HYDRIOL[®] PGCH.4 (HPGCH4: polyglyceryl-4-caprate) lecithin's (e.g. phosphatidilcholine) [92, 94] and polyoxyethylene glycerol fatty acid esters (e.g. Tagat) [106, 108].

Sorbitan esters have long been used for oral or parenteral use [84]. Lecithin's are natural, biodegradable and biocompatible SAAs and are, generally, regarded as green solvents [87]. Alkyl polyglycosides are also biodegradable and have good skin and eye tolerance [67], but they are pH sensitive [109]. Polyglycerol fatty acid esters and alkyl glycosides sugar based SAAs are safe and environmental friendly [105]. Other commonly used SAAs include, Brij 97 [84], Labrasol [68, 93, 107, 110-111], glyceryl oleate [110], sucrose laurate [112], ethoxylated mono-di-glyceride [104, 112], Plurol Oleique [93], Transcutol[®] [72], caprylic acid [92] and Cremophor[®] EL [99-100]. Generally, neutral and polyethylene glycol (PEG) free SAAs are relatively safe but some very mild amphoteric SAAs like Tego[®] Betain 810 (Capryl/Capramidopropyl betain) can also be used. Some ionic SAAs like (CTAB) cetyl trimethyl-ammonium-chloride (CTAC), myristyl-trimethyl-ammonium bromide (MTAB), didodecyl dimethyl lammonium bromide (DDAB), and sodium dodecyl-sulphate (SDS) [73] were also used.

c) Co-Surfactants

In most cases a SAA alone cannot sufficiently lower the oil-water interfacial tension to yield a ME and, hence, addition of co-SAAs is necessary [97]. Co-SAAs are substances that are capable of partitioning into the SAA film and interact with the SAA monolayer affecting its packing. They render the SAA film more fluid, preventing formation of liquid crystalline phases that are characterized by rigid films. In addition, adsorption of

the co-SAAs at the interface causes a further decrease in interfacial tension [85, 97]. They also distribute themselves between the aqueous and oily phase, thereby altering the chemical composition and the relative polarities of the phases [97]. In MEs stabilized by ionic SAAs, co-SAAs reduce the repulsive interactions between charged head groups [77].

Co-SAAs need not necessarily form association structures in their own [85] and hence a wide variety of molecules such as non-ionic SAAs, medium chain length alcohols, alkanolic acids, alkanediols and alkyl amines [85] can be used as co-SAAs. However, medium chain alcohols, short chain amines and alkanolic acids tend to possess unacceptable toxicity/irritation profiles and, hence, in general, alcohol free MEs are promoted [92, 113]. Alkanediols, such as propylene glycol (PG) [98, 112] and pentylene glycol (1,2-pentandiol) (PeG) [114] and alkanetriols, like glycerol are nontoxic co-SAAs but they have to be used at high concentrations to produce MEs, which is attributed to their extreme hydrophilic nature [97]. Interest in using nonionic SAAs both as a SAA and as a co-SAA is increasing owing to their improved stability, low toxicity, low irritancy and biodegradability of many nonionic SAAs [65]. The use of too lipophilic (e.g. sorbitan mono-oleate [92]) and too hydrophilic (e.g. hexyl-polyglucoside [92]) amphiphilic molecules, that segregate near the oil-water interface only from one side of the interface, in place of the common co-SAAs are also reported [74-75, 92]. In addition, the use of co-SAAs can be neglected in some twin tailed SAAs like AOT and DDAB, which are capable of forming MEs without addition of co-SAAs [77].

d) Co-Solvents

Co-solvents are often included in MEs to improve drug solubility through co-solvency and hence they help to stabilize the colloidal phase. In addition, co-solvents reduce the dielectric constant of water and render the environment more hydrophobic to increase the amount of molecularly dispersed SAA in the aqueous phase, which aids drug solubilisation by creating pockets of hydrophobic regions [85]. In other cases, co-solvents can be used to obtain MEs at relatively low SAA concentration [109].

Apart from the above major constituents, MEs could also contain other ingredients like penetration enhancer (e.g. as N-methylpyrrolidone, terpenes and glycolipids) and some solubilisers (e.g. β -cyclodextrin) [115].

1.2.4.2. Preparation of MEs

Although MEs are thermodynamically stable there may be kinetic barriers to their formation. Therefore, rapid formation of MEs usually requires a very low energy input in the form of heat or mechanical agitation and the order of component addition may also impact on the ease of MEs preparation [77]. Incorporation of drugs into MEs can be achieved through simple agitation or by the phase inversion temperature method, which involves mixing the drug solution with MEs and applying heat to form transparent drug loaded systems [85].

1.2.5. Characterization of MEs

In a PT-PD, MEs and LCs can be separated from emulsions or two-phase systems based on their clarity and transparent/translucent nature when observed visually or under an optical microscope [103, 110]. While, low viscosity and lack of birefringence, when observed under cross-polarised light microscopy, distinguish MEs from LCs [72, 93, 103, 116-117]. Gels and LCs can also be distinguished from MEs by virtue of their high viscosity and, in most cases, a non-Newtonian kind of flow [103].

Since the bioavailability of drugs from MEs is fairly dependent on the nanostructure and other characteristics of the MEs [77] characterisation of MEs is of paramount importance. However, unlike their preparation, characterization of MEs is a very complicated process and in most cases combinations techniques are used [62-63, 77].

Combination of methods like electrical conductivity (sharp change in conductivity following change in nanostructure) [72, 84, 104, 112, 117], differential scanning calorimetric (DSC) (DSC peaks of the continues phase is shown on the thermogram) [72], small-angle X-ray scattering [112], viscosity measurement along dilution lines [93], diffusion-ordered nuclear magnetic resonance spectroscopy [72] and/or diffusion coefficient measurement using pulse gradient spin-echo nuclear magnetic resonance (the diffusion coefficient of the retained phase decreases significantly) [104] are used to reveal MEs nanostructure. Commonly dynamic light scattering (DLS)/Photon correlation spectrometer (PCS) technique is used to measure the droplet size and size distribution of MEs [110, 118-121]. Droplet diameter measurement using electrophoretic light-scattering spectrophotometer was also reported [111]. However, other methods like small-angle X-ray scattering and small angle neutron scattering [108, 117-118] techniques can also be used. EPR method was employed to measure micropolarity and microviscosity of MEs [122]. Electron microscopic techniques,

mainly freeze-fracture transmission electron microscopy [68, 71, 123-124] and cryo-scanning electron microscopy [125-126] were used to study morphologies of MEs. Freeze-fracture transmission electron microscopy as a method of visualising MEs nanostructures was also reported by several authors [82, 98, 100, 110-111, 127]. The thermodynamic stability of MEs can be assessed by visual inspection, control of droplet size over time or through centrifugation [93].

1.2.6. Factors Governing the Nanostructures and other Physicochemical Properties of MEs

The phase behaviour, nanostructure, stability and other properties of MEs are highly dependent on the molecular structure of the SAA and co-SAA and molecular weight of the oil, which penetrate into the interface, and their concentration [66, 93, 128]. In most cases MEs undergo phase transition upon dilution and/or evaporation of any volatile constituents [82, 103, 121]. These properties may also be affected by the addition of drugs and other additives that have surface active properties [75]. In a study done by Pestana et al. (2008) addition of Amphotericin B to a lecithin-based ME increased the droplet diameter 3 fold [86]. Preservatives like methyl paraben and propyl paraben are known to form complexes with SAAs like polysorbates and may as well influence properties of MEs [97]. In some cases small concentration of electrolyte may decrease the ME phase areas as well as the diameter of the emulsified droplets through dehydration of the hydrophilic group of the SAA [84, 129]. The impact of electrolytes is more pronounced in case of MEs formed by ionic SAAs [85].

The physicochemical properties of MEs are also dependent on temperature [128]. Generally, MEs of non-ionic SAAs, especially those based on polyoxyethylene, alkylamine-*N*-oxides and the sugar SAAs are very susceptible to temperature due to the dehydration of the hydrophilic groups, which render the SAAs more lipophilic at higher temperatures [77, 129]. In case of ionic SAAs, the dissociation of the ionic group increased with temperature and they become more hydrophilic at elevated temperatures [130].

Another important factor, which may have considerable influence on the phase behaviour of the MEs is pH. In lecithin-based MEs to minimize hydrolysis of the phospholipids and the triglycerides to fatty acids, the pH should be adjusted at 7–8 [97]. However, pH has less effect on the phase behaviours of MEs prepared by non ionic SAAs [84]

1.2.7. Applications of MEs

MEs have wide variety of applications and are gaining interest in several areas due to their unique physical properties. Apart from drug delivery systems, they have been used in oil recovery, ground water remediation, soil cleanup, food products, catalysis and enzymatic reactions [73, 87, 131] environment decontamination [71], transcriptive syntheses and membrane recognition phenomena, new cosmetic formulations and nanotechnologies [71, 119, 132] and as microreactors in synthesis of organic compounds [119, 133-135] and polymerization [136-137].

The wide pharmaceutical applications of MEs are mentioned under section 1.2.3. Besides, recent findings in the areas of drug delivery showed that MEs have improved the oral absorption of peptides and proteins [68-69, 110, 138]. They have also evolved as a novel drug delivery vehicles for parenteral administration of hydrophobic drugs such as amphotericin B, paclitaxel and arthemter, [97] and lorazepam [83]. They can also serve as templates for the formation of nanoparticles, through interfacial polymerisation [69-70, 139-143] and hollow silica spheres [144]. According to Graf et al. (2008) [70], the combined strategy of nanoparticles dispersed in a W/O ME improved the intragastric delivery of insulin in diabetic rats.

1.2.8. MEs in Dermal and Transdermal Drug Delivery

Dermal and transdermal delivery of drugs have many advantages, which include reduced gastrointestinal side effects, pre-systemic disposition and improvement of patient compliance [72, 103]. However, the poor permeability of the SC often limits the administration of most novel drugs through the skin [91, 103]. There are various chemical and physical methods employed to promote dermal and transdermal permeation of drugs through the skin, which include the use of chemical penetration enhancers (e.g. lemonene, α -terpineol, oleic acid, ethanol and dimethyl sulfoxide (DMSO)) [91, 101], preparation of supersaturated drug delivery systems, iontophoresis, physically disrupting the skin barrier by electroporation or sonophoresis [91, 103]. However, most of these methods are not without limitations, mainly disrupting the barrier function of the skin [103]. In addition, sometimes the chemical enhancers, such as solvents or SAAs, tend to produce allergic reactions, skin irritation, and sensitization [75].

In recent years, MEs have emerged as promising vehicles for dermal and transdermal delivery of drugs [72, 75, 79, 91, 99, 103, 145]. They are found to significantly improve

the permeability of drugs through the skin compared to the conventional skin preparations like aqueous solutions, gels, creams or emulsions, and liposomes [67, 72, 74, 92-93, 145], which might be attributed to the reduction of the diffusion barrier of the SC due to interaction of the MEs components with the SC (SAAs and some oils like oleic acid may increase the fluidity of lipid portion of the SC [67, 72, 74, 79]), increased concentration and thermodynamic activity of the drug within the MEs, and the hydration effect of the MEs on the SC [79, 99, 107, 127]. They also have additional advantage of high solubilisation capacity for both lipophilic and hydrophilic drugs [67, 93]. However, the mechanism by which MEs penetrate deep into the skin is not well understood. Recently Hathout et al. (2011) hypothesized that the ME droplets are not traversing intact [145]. Each component of the ME is diffusing all along the SC, which further brings about a change in SC lipid order that allows the dermal and transdermal penetration of the drug.

1.2.9. Limitations of MEs

Despite a large number of SAAs are approved for oral and topical applications, the high percentage of SAA in MEs may lead to potential toxic effects [130]. In addition, sometimes MEs may undergo phase transitions and drug precipitation upon coming in contact with body fluids [85]. As has been studied by Prira et al. (2008) an ME was transformed into LC phase after application to the skin due to variation in ME water content where the drug diffusion coefficient in comparison with other MEs was decreased by a factor of 100 [109]. In addition, it is not an appropriate vehicle for drugs, which are insoluble or sparingly soluble in water and most pharmaceutical liquids or for drugs that are susceptible for hydrolysis. However, currently, Moniruzzaman et al. (2010) claimed that MEs of pharmaceutically acceptable ionic liquids can replace water because of their physicochemical characteristics that suit many drugs [146].

1.3. Objective of the Research

General Objective:

The general objective of this research is to develop colloidal drug delivery systems, preferably MEs, to load sufficient amounts of CER [AP], CER [EOS], CER [NP], FFAs and CHOL into the SC and evaluate their safety and bioavailability.

Specific Objectives:

The specific objectives of this research include:

- Formulation of stable CER [AP] MEs;
- Characterisation of the formulated CER [AP] MEs;
- *Ex vivo* skin toxicity investigation on the formulated MEs;
- Conduct *in vitro* release and SC penetration studies from the optimised CER [AP] MEs;
- Formulation and characterisation of stable CER [EOS] MEs;
- Formulation and characterisation of stable CER [NP] MEs;
- Formulation and characterisation of MEs of combined SC lipids;
- *Ex vivo* skin permeability investigation of SC lipids from the formulated MEs using deuterated CER [NP] as a labelled standard.

2. Preparation and Characterisation of MEs Containing CERs and other SC Lipids

2.1. Introduction

The barrier function of the skin mainly lies on the lipid matrix of the SC, which is primarily formed from CERs, FFAs and CHOL [16]. Maintaining the right composition and organisation of these lipids in the lipid matrix is of paramount importance for the skin to retain its barrier function. Disturbance in SC lipid composition might result in altered and porous SC lipid organisation [28, 58]. Studies showed that several skin disease conditions such as psoriasis [147], AD [13, 16, 148] and irritant/allergic contact dermatitis [148] are associated with depletion or disturbance of SC lipid composition. Any altered lipid organisation may in return allow the passage of exogenous substances that could induce inflammatory reactions, which results in further perturbation of the barrier function, potentially establishing a vicious cycle that may severely damage the barrier [16].

To date about 12 types of CERs have been identified in human SC, which are essential for normal functioning of the skin [1]. CER [AP] induces the formation of a super stable membrane [48], which is attributed to its four hydroxyl groups on its head structure. CER [EOS] plays a profound structural role in barrier function of the skin [13, 22]. Many disease conditions like AD, psoriasis and type 2 Gaucher's disease are associated with reduced percentage of CER [EOS] [13]. A study done by Macheleidt et al. (2002) showed that there is a significant reduction of SC lipids especially CER [NP], along with CER [EOH], in AD [149]. Some skin diseases, like lamellar ichthyosis, are associated with the depletion of long chain FFAs of the SC [11].

Studied showed that CERs are known to repair the cutaneous barrier function and have excellent curing effects on some skin diseases [2]. Besides, they play a major role in the water-retaining properties of the epidermis preventing dry flaky skin and aged appearance. Apart from structural roles, CERs play an important role in intracellular signalling and regulate a variety of biological processes, including cell proliferation, differentiation, apoptosis, inflammation and immune responses [5][7].

Thus, introduction or replenishment of the missing SC lipids may help to treat some skin disease conditions that are associated with altered SC lipid composition, terminate

the vicious cycle, which is associated with inflammation of the skin due to permeation of xenobiotics, that may cause further damage to the skin [16, 59] and strengthen the barrier function in affected and aged skin. However, the effectiveness of these compounds is limited due to their poor penetration into deep layers of the SC, which is further associated to their inherent hydrophobicity and potential precipitation as fine lipid micelle suspensions in conventional dosage forms [6-7]. On the other hand, studies showed that drugs incorporated into MEs can efficiently penetrate the SC [150-151]. Moreover, several studies demonstrated that these vesicles have high drug loading capacities for both hydrophilic and lipophilic drugs. Therefore, an attempt was made to develop colloidal drug delivery systems, particularly MEs containing sufficient amounts of CER [AP], CER [EOS], CER [NP] and/or other SC lipids to facilitate their permeation into the SC.

2.2. Materials and Methods

2.2.1. Materials

CER [AP], CER [EOS], CER [NP], and TCPL4, Evonik-Goldschmidt GmbH, Essen, Germany; HYDRIOL[®] PGMO.4 (polyglyceryl-4-oleate) (HPGMO4), Hydrior AG massgeschneiderte Tenside, Wettingen, Germany; PeG, Symrise GmbH & Co KG, Holzminden, Germany; Lin A, PA, SA, BA, LA and CHOL, Sigma-Aldrich Chemie GmbH, Taufkirchen, Germany; isopropyl palmitate (IPP) and Miglyol[®] 812 (miglyol), Caesar & Loretz GmbH, Hilden, Germany; Phosal[®] 75 SA (phosal), Phospholipid GmbH, Köln, Germany; ¹⁴N HD-PMI (2-heptadecyl-2,3,4,5,5-pentamethyl-imidazoline-1-oxyl:HD-PMI), Institute of Chemical Kinetics and Combustion, Novosibirsk, Russia, were the major materials used for the study. Double distilled water was used throughout the experiment. Other ingredients used were of pharmaceutical grades.

2.2.2. Methods

2.2.2.1. LC/ESI-MS

A validated LC/ESI-MS method [152] was used during solubility studies. For the study an HPLC system (Finnigan, San Jose, CA, USA) coupled with a Finnigan SSQ 710C MS (Finnigan, San Jose, CA, USA) was used. A reversed phase Nucleosil[®] C-18 HPLC column, 125 mm x 2 mm, 120-3 (Macherey-Nagel, Düren, Germany) fitted with a C-18 precolumn was used as a stationary phase and methanol/THF (97:3, v/v) was used as

a mobile phase. The flow rate and the injection volume were set at 0.2 ml/min and 10 μ l, respectively. The injection samples were prepared in methanol and all the solvents and co-solvents employed had different retention times than CER [AP], which was essential to avoid matrix effect.

2.2.2.2. Solubility Determination

The solubility of CER [AP] in various solvents and co-solvents was determined using the shake flask method. An excess amount of CER [AP] was added into a test tube containing 2 ml of the solvent or co-solvent of interest and the test tube was kept in a thermostatic water bath and was shaken continuously for 48 hrs. Then the excess CER [AP] was removed by filtration through a 0.45 μ m hydrophilic or hydrophobic PERFECT-flow[®] PTFE membrane filter (WICOM Germany, Heppenheim, Germany), selection of which was made based on the polarity of the solvent, and the filtrate was immediately transferred into a large volume of methanol-chloroform (1:1, v/v). The injection volumes were prepared in methanol and the CER [AP] dissolved was quantified using the LC/ESI-MS method described under 2.2.2.1. The solubility was determined at room temperature (RT: 22-23°C) and 32°C (temperature of the skin) and each experiment was conducted in triplicate and the average and standard deviation (SD) were obtained.

2.2.2.3. ME Preparation

Even though MEs form spontaneously, since CER [AP] was poorly soluble in all of the solvents used and its solubility increased with temperature, during ME preparation the ME mixtures were sonicated for 1hr at 50°C. Alternatively, the MEs could be prepared at 80°C without sonication in less than 5 min.

2.2.2.4. Construction of Pseudo-ternary Phase Diagram

The PT-PDs of the different ME systems were constructed at RT through titration of 2 g of different oil-SAA mixtures (10:90, 20:80, 30:70, 40:60, 50:50, 60:40, 70:30, 80:20 and 90:10, w/w) by adding 10 μ l of the hydrophilic phase followed by magnetic stirring. However, prior to titration, to have a general map, selected percentages the ME components (36 data points, which are evenly distributed all over the PT-PD and containing all the possible combinations of (10-90) % of each ME components) were obtained and observed. Appearance of cloudiness was taken as end point detector.

2.2.2.5. Cross-Polarised Light Microscopy

The isotropic nature of the homogeneous and cloudy phases in the PT-PD was verified using cross-polarised light microscope (Zeiss Axiolab Pol, Carl Zeiss MicroImaging GmbH, Jena, Germany). A drop of the clear and cloudy samples of the 36 mixtures under 2.2.2.4 was put on a slide and was covered by a slide cover and was observed under the microscope. MEs, as an isotropic component, appeared as dark background unlike the anisotropic LC phases, which appeared as coloured background [72, 117]. The cloudy phases appeared as stable coarse emulsions or LCs. Additional mixtures were also prepared to roughly identify the border line that divide MEs and LCs and or coarse stable emulsions.

2.2.2.6. Electrical Conductivity

The electrical conductivity of the MEs at various SAA(s)-oil(s) dilution lines (20:80, 30:70, 50:50, 65:35, 80:20 and/or 95:5) was measured at 25°C (± 0.2) by adding an increasing amount of the hydrophilic component using a conductometer (Cyberscan con 11 conductivity/TDS/ $^{\circ}$ C meter, EUTECH Instruments, Singapore). Following each addition of the hydrophilic phase, the system was subjected to magnetic stirring for about 1 min and was waited until the temperature equilibrates and conductivity readings stabilize. In case of TCPL4-based MEs, since the conductivity of the MEs was too low, 0.0025 M NaCl solution was used in place of distilled water. Conductivity readings were conducted in triplicates and the average and SD were calculated.

2.2.2.7. Differential Scanning Calorimetry (DSC)

The DSC thermogram of the MEs was obtained using a DSC (DSC 200, Netzsch-Gerätebau GmbH, Selb, Germany) equipped with an automatic liquid N₂ cooling unit. Prior to DSC measurements, about 10 mg of the sample was filled in an aluminium pan and was pressure sealed. Another empty pressure sealed aluminium pan was used as a reference pan. The DSC thermograms were obtained in a heating mode over -60 to 25°C. During measurement, the sample was allowed to equilibrate at -60°C and then the temperature was raised constantly at a rate of 5°C min⁻¹. N₂ gas was used as a purging gas at flow rate of 10 ml/min.

2.2.2.8. Refractive Index

The refractive index of stable MEs was obtained using an Abbe refractometer (Carl-Zeiss, Jena, Germany) at $25 \pm 2^\circ\text{C}$. Readings were made in triplicate and the average and the RSD were calculated.

2.2.2.9. Viscosity

Viscosity of stable MEs was measured at $25 \pm 0.2^\circ\text{C}$ using a rotational viscometer (Anton Paar GmbH, Graz, Austria) at 16 varying shear rates ($0.1\text{-}100\text{s}^{-1}$) and, since all MEs exhibited Newtonian flow, the average and the RSD values were calculated.

2.2.2.10. Dynamic Light Scattering (DLS)

The light scattering hardware set-up, consisting of commercially available equipment for simultaneous static and dynamic experiments from ALV-Laser, Langen, Germany was used for the determination of droplet diameter of the MEs. A green Nd: YAG DPSS-200 laser (532 nm, Coherent, Auburn, USA) with an output of 200 mW was used as a light source. The sample cell was placed on a motor-driven precision goniometer ($\pm 0.01^\circ$), which enabled the photomultiplier detector to be moved from 20° to 150° scattering angles, and was allowed 10 min for temperature equilibration. The second order intensity time correlation functions (g^2) was recorded with an ALV-5000E Multiple Tau Digital Correlator with fast option, with a sampling time of 60 s. Cylindrical sample cells made of Suprasil[®] quartz glass (10 mm dm: Hellma, Mühlheim, Germany) were used as sample holder. The measurements were made at 25°C at $30, 50, 70, 90, 110$ and 130° and analysis of the results were made using ALV-5000 Multiple Tau Digital Correlator (ALV-Laser Vertriebsgesellschaft M-B.H., Langen, Germany) for MEs whose droplet size was independent of the angle measured and for those MEs whose PCS results were dependent on the angle, analysis of the results were made manually employing the appropriate equations and principles.

2.2.2.11. Electron Paramagnetic Resonance (EPR)

EPR spectra were recorded at constant temperatures using a Miniscope MS 200 X-Band spectrometer (Magnettech Berlin, Germany) operating at X band (9.4 GHz). Pyrex capillary tubes (~1 mm) were used as sample containers. The sample temperature was controlled using N₂ gas flow through the Dewar vessel (Magnettech Berlin, Germany), by allowing the sample to equilibrate for 10 min. The spectra were recorded for 24 h after sample preparation. HD-PMI was used as a spin probe at a concentration of 0.5 mM. The EPR setup include modulation amplitude of 0.02 mT, microwave frequency of 9.4 GHz/microwave power of 20 mW, centre magnetic field of 334.9 mT, sweep time 600S, sweep width of 4.95 mT and time constant of 40.96 ms. Fitting of the EPR spectra was performed using a Nitroxide spectra simulation software V. 4.99 (Biophysical laboratory EPR centre, Josef Stefan Institute, Ljubljana, Slovenia) and the rotational correlation time (τ_c), hyperfine splitting constant/ isotropic hyperfine coupling constant (a_N) the line shape factor (IF) and the line width factor (LW) were determined along with the corresponding errors from curve fitting. Finally, analysis of the results was made based on the EPR parameters obtained.

2.2.2.12. Thermodynamic Stability

The physical stability of MEs was routinely evaluated at ambient conditions by visual inspection of the samples over a period of time. Stable MEs were also challenged through centrifugation (MLW T62, VEB MLW Medizintechnik, Leipzig, Germany) at 3500 rpm for 30 min after 1 week of preparation. Any physical change, such as, turbidity, phase separation, flocculation of the droplets and/or precipitation dispersed lipids was taken as indicator of instability.

2.3. Results and Discussion

2.3.1. Formulation and Characterisation of SC Lipids MEs

Several skin disease conditions are correlated with depletion or perturbation of SC lipids, which mainly are CERs, FFAs and CHOL [11]. Formulation of MEs containing these lipids may prevent and treat some of these skin diseases. Therefore attempt was made to formulate MEs of various SC lipids.

2.3.1.1. Formulation and Characterisation of CER [AP] MEs

CERs are one of the major SC lipids, which are responsible for the barrier function of the skin. They should be present in adequate amounts and be properly organised along with the other SC lipids in order to provide the tough barrier [48]. The functional group at the polar end of the CERs governs the tightness of the formed layer [48]. Among the various CERs identified so far, CER [AP] is believed to form a very tight and super stable membrane owing to its four OH groups located on the hydrophilic head group [48]. Therefore, attempt was made to prepare stable MEs containing CER [AP].

2.3.1.1.1. Determination of the Solubility of CER [AP] in Various Solvents and Co-solvents

Development of pharmaceutical dosage forms is usually preceded by preformulation studies. Therefore, before development of MEs of CER [AP], its solubility in various solvents, oils and co-solvents was determined at RT (21-23°C) and 32°C, Table 2.1. The results in the table showed that solubility of CER [AP] increased significantly as the temperature increases. However, according to solubility classification, except in PeG and octanol, it was practically insoluble in all the solvents and the co-solvents investigated at both RT and 32°C.

Table 2.1: Solubility of CER [AP] in various solvents and co-solvents at RT (21-23°C) and 32°C (N=3).

No.	Solvent	Solubility (\pm SD) at RT ($\mu\text{g/ml}$)	Solubility (\pm SD) at 32°C ($\mu\text{g/ml}$)	Solubility classification
1	Water	n.q	n.q	Insoluble
2	Lin A	77.5 (1.82)	93.3(7.55)	Practically insoluble
3	Miglyol	86.7 (0.19)	168.4(7.52)	Practically insoluble
4	IPP	40.2 (4.47)	45.2(5.99)	Practically insoluble
5	Isopropyl myristate (IPM)	21.2 (3.27)	36.8(3.10)	Practically insoluble
6	PG	14.7 (3.32)	35.9(2.44)	Practically insoluble
7	PeG	680.0 (5.98)	898.0(2.53)	Very slightly soluble
8	Octanol	1252.2 (16.1)	3453.7(24.4)	Very slightly soluble

n.q=amount dissolved was bellow method's LOD

2.3.1.1.2. Selection of Appropriate ME Components

Development of SC lipids MEs started with formulation of stable CER [AP] MEs. Although MEs have higher solubilisation capacity than many other conventional dosage forms [64, 67, 77, 84, 90] due to the poor solubility of CER [AP] in both hydrophilic and oily phases, Table 2.1, it was necessary to choose appropriate ME components that can give stable CER [AP] MEs. In addition, since it is preferable to solubilise lipophilic compounds in O/W MEs [150-151] and CER [AP] is better soluble in oils than in water, an attempt was made to choose appropriate ME components that can give stable O/W CER [AP] MEs.

A) Selection of SAA (s)

Formulation of MEs usually needs higher concentration of SAA(s), which could irritate the skin [92]. Hence, during selection of SAA (s), due emphasis was given to safety. Accordingly, the use of ionic SAAs, most of which are irritant to the skin when used at higher concentrations [74], was intentionally secluded and eleven known skin friendly non ionic and zwitter ionic SAAs that belong to six SAA groups (lecithin's, polyglyceryl esters, alkyl glycosides, sorbitan esters, glycerol esters and poloxamers) and have different HLB values (3-16) were tested (see detail in Appendix A). Among the SAAs tested, TCPL4 and phosal gave relatively stable MEs of CER [AP]. Both SAAs are PEG free and compatible with the skin [153-154]. Generally, phosal based MEs showed better stability and loading capacity than TCPL4-based MEs, but had to be used at higher concentrations. The SAAs chosen are bulky SAAs and studies showed that MEs prepared using bulky SAAs are more stable against rupture [84]. Both SAAs, that gave stable O/W MEs, have moderate HLB values and it substantiate the conclusion that there is no direct correlation between HLB value of SAAs and their ME forming abilities [84].

B) Selection of Oil (s)

Although CER [AP] has better solubility in miglyol than the other oils investigated, Table 2.1, studies showed that the oil in which the active is most soluble may not give MEs with highest solubilisation capacity [77]. Hence, selection of appropriate oily phase was necessary and oleic acid, IPM, IPP and miglyol were tested as potential oily phases using phosal and TCPL4 as SAAs. According the results obtained, miglyol gave

relatively stable ME with phosal; whereas, IPP gave stable ME with TCPL4 (see detail in Appendix A). IPP gave more stable MEs with TCPL4 than miglyol, which may be attributed to its co-SAA activity due to the penetration of the hydrophobic group of the oil into the hydrophobic group of the SAA monolayer [77]. In addition, Lin A (an essential FFA required for the normal barrier function of the skin [13] and has inhibitory effect on the promotion of carcinogenesis process in the skin [36, 40]) when used in combination with IPP, improved the stability and loading capacity of CER [AP] and expanded the ME region extensively, Fig 2.1. Although it was possible to obtain stable TCPL4-based MEs with Lin A, it was decided to use as part of IPP since high concentration of Lin A could be irritant to the skin [155]. Since phosal contains safflower oil, which contains reasonable percentage of Lin A, it was not necessary to replace part of miglyol with Lin A.

C) Selection of Co-solvent (s)

With the SAA and oily phases chosen in A and B, the effect of co-solvents on stability of CER [AP] MEs was investigated (see detail in Appendix A). Since alcohols are irritant to the skin [74] only the effects alkanediols and alkanetriols on stability of CER [AP] MEs was investigated. Initial investigations were made using PeG as a co-solvent, as it is an excellent moisturiser and has better antimicrobial activity than the commonly used pharmaceutical co-solvent, PG [156]. Besides, it was shown that CER [AP] has better solubility in PeG than in PG, Table 2.1. The results showed that PeG enhanced the stability and loading capacity of CER [AP] MEs tremendously. Further investigations made using PG, hexylene glycol (HeG) and glycerol showed that PeG was superior. PG gave the worst system when used alone or in combination with PeG, which might be attributed to its lower degree of partitioning into the interface than PeG owing to its increased polarity. A similar effect was observed by Chaiyana et al. (2010) between ethanol and hexanol [84]. Glycerol gave a relatively clear and stable system, but appeared as gel. Therefore, PeG was chosen as a co-solvent. Heuschkel et al. also showed that PeG is preferred over PG to minimise the penetration of the active into deeper layer of the skin, facilitating localisation of SC lipids within the SC [114]. The higher the percentage of PeG in the hydrophilic phase (comprises of PeG and water); the better was the stability of the MEs. Generally, phosal based MEs needed higher percentage of PeG than TCPL4-based MEs.

D) Selection of Co-SAA (s)

Usually combination of SAAs decreases the irritant effect of a SAA and may give MEs with better characteristics [77, 85, 97]. Accordingly, the effects of different lipophilic (Plurol[®] Isostearique, Hydriol[®] PGO, Span[®] 80, HPGMO4, Span[®] 20, phosal and Synperonic[®] PE/L 101) and hydrophilic (Tween[®] 80 (Tween 80: Polyoxyethylen-80-sorbitanmonooleat), Tagat[®] O 2 V (Tagat: PEG-20-glyceryl-oleate) and Hydriol[®] PGC3) SAAs was investigated at SAA-co-SAA 4:1, 2:1 and 1:1 (see detail in Appendix A). However, most of the SAAs showed no considerable synergism except HPGMO4 (HLB=8), which showed synergism when used together with TCPL4.

Concluding, MEs prepared using lecithin were the most stable but had to be prepared at a relatively higher percentages of the SAA and PeG. Therefore, it was decided to formulate two sets of MEs, one that contains phosal, miglyol and PeG/water as amphiphilic, oily and hydrophilic components, respectively, which afterwards be referred as lecithin-based MEs and another containing, TCPL4 alone or in combination with HPGMO4, IPP alone or in combination with Lin A and water-PeG, as amphiphilic, oily and hydrophilic components, respectively, which afterwards be referred as TCPL4-based MEs.

2.3.1.1.3. Formulation and Characterisation of TCPL4-based CER [AP] MEs

A) Formulation

IPP alone or in combination with Lin A, TCPL4 alone or in combination with HPGMO4 and water-PeG mixture were used as oil, amphiphilic and hydrophilic components, respectively, for the preparation of TCPL4-based CER [AP] MEs. The effects of the percentage composition of the three ME components, as well as the effects of Lin A, HPGMO4 and ratio of PeG in the hydrophilic phase on the stability of CER [AP] MEs was thoroughly investigated in region that potentially gives O/W ME (lower percentage of oil, (5-15) %) (see detail in Appendix B).

Overall, preparation of stable TCPL4-based CER [AP] MEs demanded higher ratio of PeG in the hydrophilic phase. Replacing part of IPP with Lin A and combination of TCPL4 with HPGMO4 (TCPL4-HPGMO4, 1:1) significantly improved stability of the CER [AP] MEs. However, the level of Lin A had to be maintained low as it might be

irritant to the skin when used at higher percentages [155]. Moreover, as the percent Lin A increases, the percent PeG in the hydrophilic phase had to be proportionally increased. Interestingly, as has been shown in Fig 2.1, increasing the ratio of PeG in the hydrophilic phase, using HPGMO4 as a co-SAA and replacing part of IPP with Lin A expanded the ME region tremendously. Nonetheless, even within the ME region, the results also showed that for maximum stability the right percentage of the ME components had to be chosen. Most of the stable MEs obtained were O/W types. Accordingly, 10 stable TCPL4-based CER [AP] MEs were selected for further characterisation, Table 2.2.

Table 2.2: Compositions and stabilities of optimised TCPL4-based CER [AP] MEs.

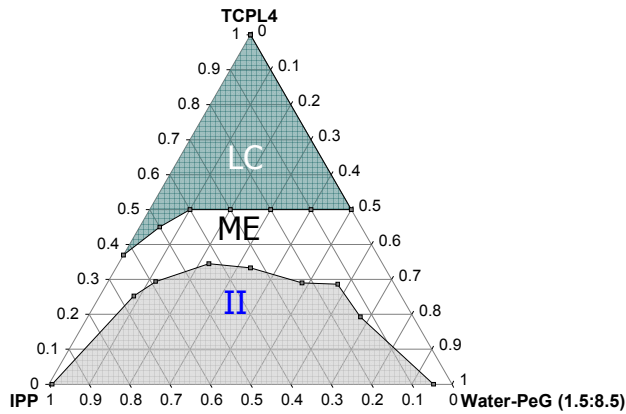
No	ME	IPP-Lin A (9:1) %	IPP-Lin A (5:2) %	TC PL 4 %	HPG MO 4 %	Water -PeG (1:9) %	Water -PeG (1.5:8.5) %	CER [AP] ^a %	Stability (± SD) (Mon)
1	TAPOME1	-	10	25	-	-	65	0.4	>24
2	TAPOME2	-	15	30	-	-	55	0.4	11 (2)
3	TAPOME3	15	-	25	-	-	60	0.4	13.5 (1.5)
4	TAPOME4	15	-	25	-	60	-	0.4	>24
5	TAPOME5	10	-	40	-	50	-	0.4	10.5 (0.5)
6	TAPOME6	5	-	40	-	55	-	0.4	10 (0.5)
7	TAPOME7	15	-	12.5	12.5	60	-	0.4	13.5 (2.5)
8	TAPOME8	5	-	15	15	65	-	0.4	> 24
9	TAPOME9	10	-	17.5	17.5	55	-	0.4	12 (0.5)
10	TAPOME10	5	-	17.5	17.5	60	-	0.4	11.5 (3.5)

^a percent per total mass of the MEs

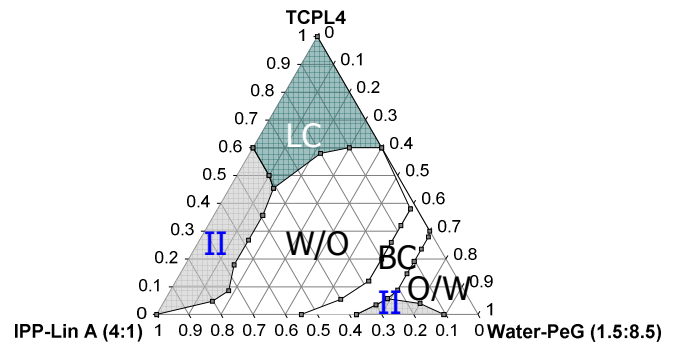
B) Characterisation

▪ Pseudo-ternary Phase Diagram

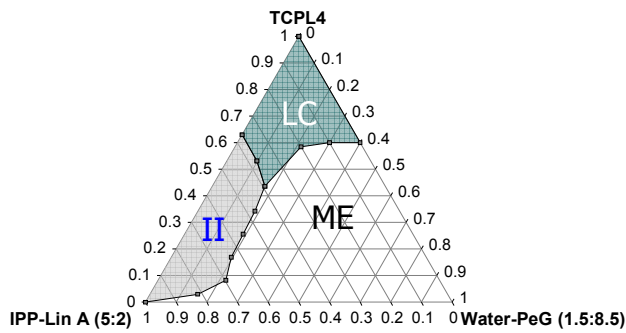
PT-PD of TCPL4-based MEs are shown in Fig 2.1. The two-phase and coarse emulsion regions in the phase diagrams was distinguished from one phase systems through visual and/or microscopic observations. In addition, unlike MEs, LC systems exhibited birefringence when observed under cross-polarised light microscope [72, 93, 103, 116-117].



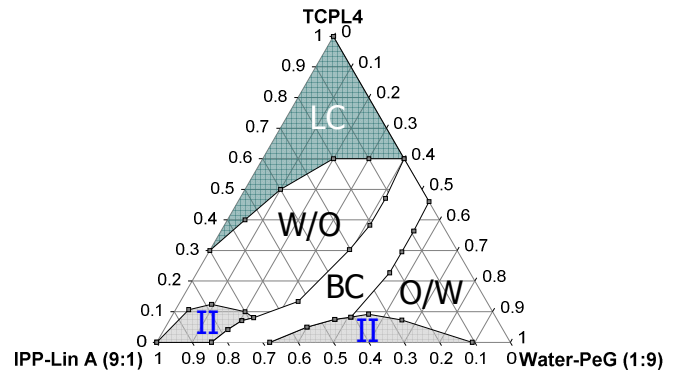
a) PT-PD of IPP, TCPL4 and water-PeG (1.5:8.5)



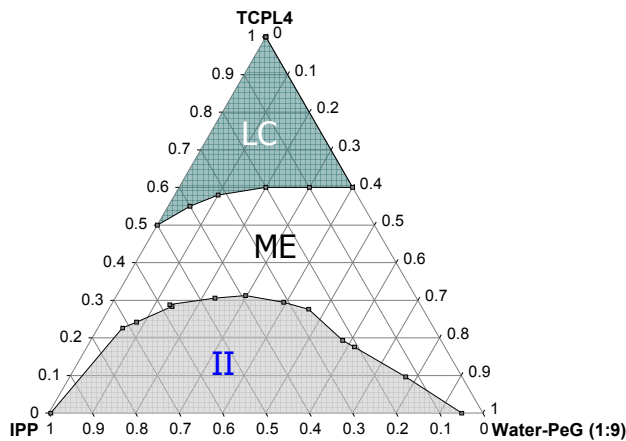
b) PT-PD of IPP-Lin A (4:1), TCPL4 and water-PeG (1.5:8.5)



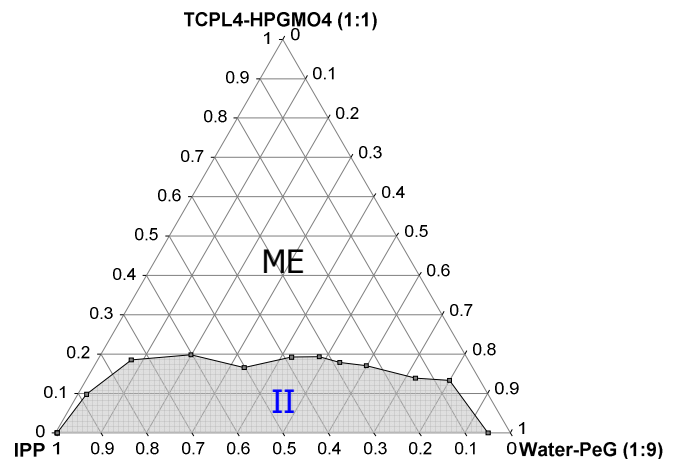
c) PT-PD of IPP-Lin A (5:2), TCPL4 and water-PeG (1.5:8.5).



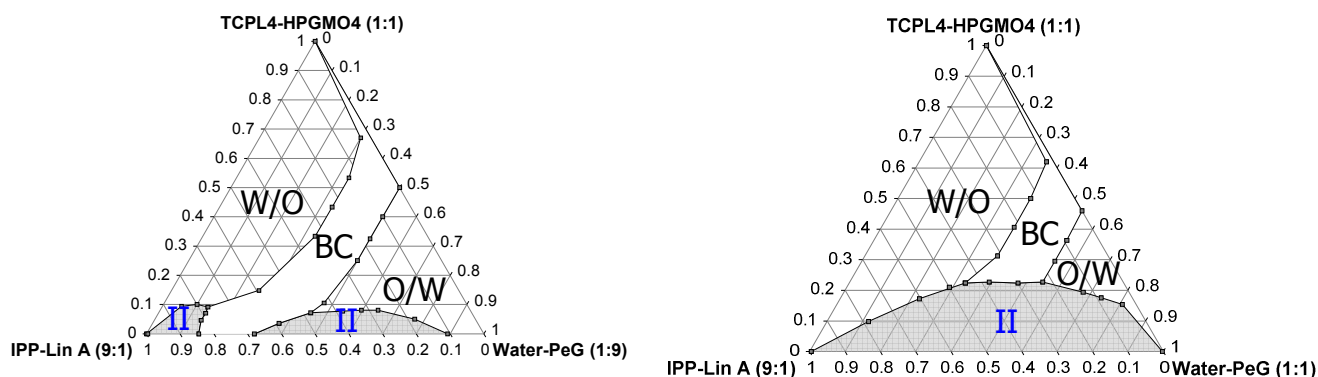
d) PT-PD of IPP-Lin A (9:1), TCPL4 and water-PeG (1:9).



e) PT-PD of IPP, TCPL4 and water-PeG (1:9).



f) PT-PD of IPP, TCPL4-HPGMO4 (1:1) and water-PeG (1:9).



- g) PT-PD of IPP-Lin A (9:1), TCPL4-HPGMO4 (1:1) and water-PeG (1:9).
 h) PT-PD of IPP-Lin A (9:1), TCPL4-HPGMO4 (1:1) and water-PeG (1:1).

Figure 2.1: The PT-PDs of various TCPL4-based ME systems (II= 2 phase region; ME= ME region; LC= liquid crystal region; O/W= O/W ME region; W/O= W/O ME region; BC= BC ME region).

As can be seen in Figs 2.1 a-c, as the ratio of Lin A in the oil component increases the two-phase region contracted tremendously and vanished at IPP-Lin A (5:2). However, another two-phase region arose at the oil-SAA side and expanded as the ratio of Lin A in the oil increases. The LC region also contracted as the ratio of Lin A in the oil increases. As can be seen in Figs 2.1a and e, as the ratio of PeG in the hydrophilic phase increases, both the two-phase and LC regions contracted extensively. The significant contraction of the two-phase region was also evident as can be seen in Figs 2.1 g and h. Interestingly, as has been depicted in Figs 2.1 e vs. f; Figs 2.1 d vs. g, using HPGMO4 as a co-SAA (TCPL4:HPGMO4, 1:1), the LC region vanished completely and the two-phase region contracted significantly. Thus, upon increasing the ratio of Lin A in the oily phase, increasing the ratio of PeG in the hydrophilic phase, and using HPGMO as a co-SAA expanded the ME region tremendously, by contracting the two-phase and liquid crystalline regions.

ME Nanostructure

Unlike formulation, characterisation of MEs is a difficult task and usually conclusive results can only be obtained using complementary techniques [72]. Consequently, an attempt was made to determine the nanostructure of TCPL4-based MEs using results of electrical conductivity, DSC and EPR techniques.

Electrical Conductivity

Electrical conductivity is the simplest but one of the most important and frequently used method for the determination of ME nanostructures [72, 84, 93]. Usually, MEs electrical conductivity changes as their nanostructure changes in PT-PDs [72, 93, 130]. The electrical conductivity curves of some TCPL4-based ME systems at various dilution lines are shown in Fig 2.2.

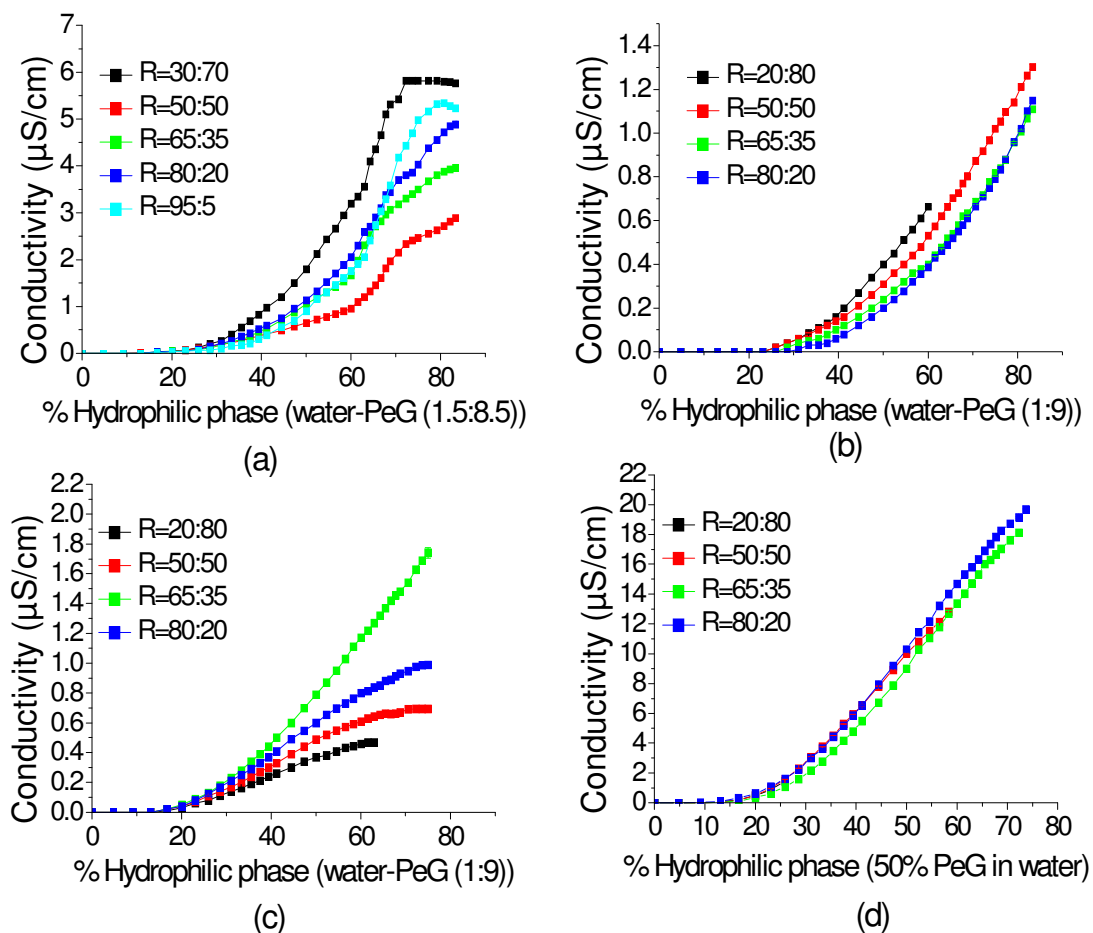


Figure 2.2: Electrical conductivity curves of some ME systems: conductivity of SAA-oil (R: %, m/m) drawn as a function of percent hydrophilic phase; a) TCPL4:(IPP-Lin A, 4:1); b) TCPL4:(IPP-Lin A, 9:1); c) (TCPL4-HPGMO4, 1:1):(IPP-Lin A, 9:1); d) (TCPL4-HPGMO4, 1:1):(IPP-Lin A, 9:1) (N=3).

Before conducting the experiment, in order to enhance the electrical conductivity of the MEs, in place of distilled water 0.0025 M NaCl aqueous solution was used, which was assumed to be too low to cause any structural change in the MEs. Previous studies also

showed that up to 0.01M NaCl was used without causing any change in MEs nanostructure [84, 104, 117].

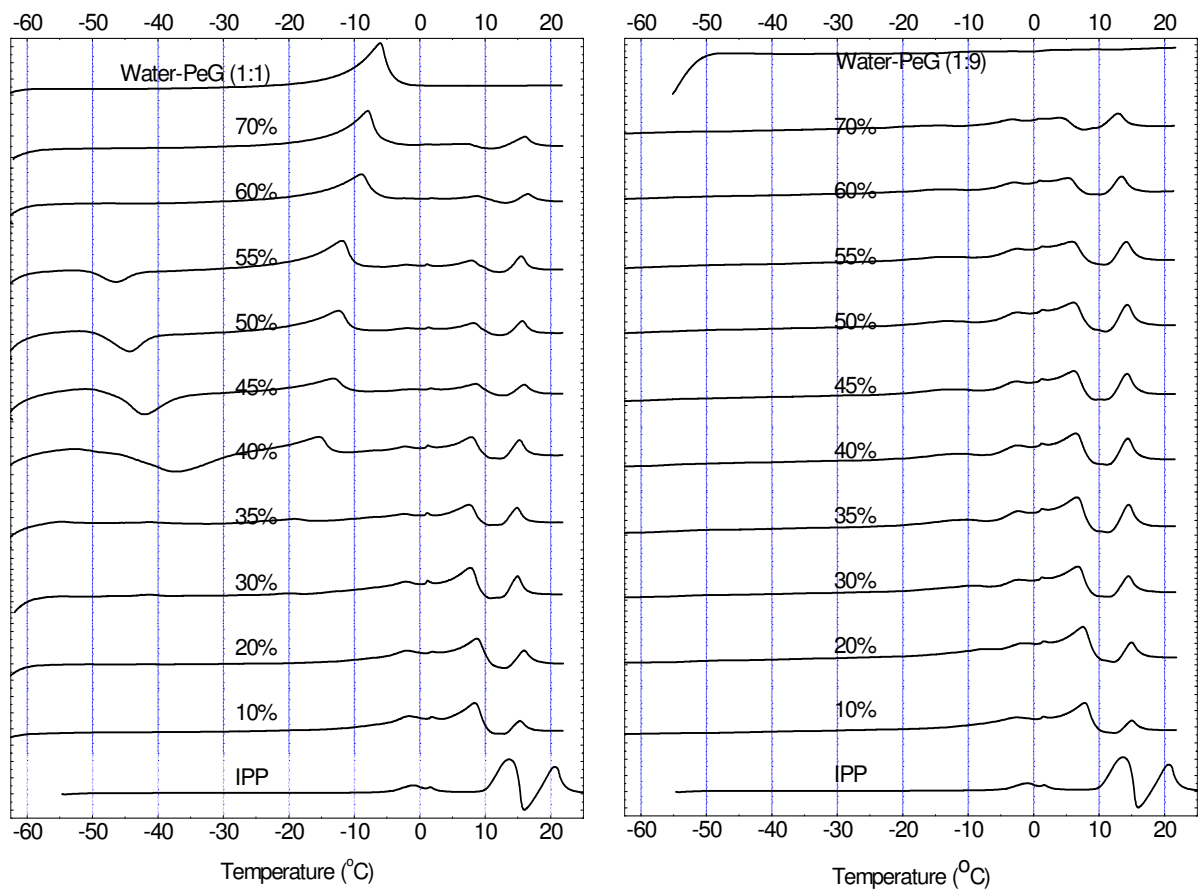
As has been shown in Fig 2.2, the MEs were not conductive at lower percentage of the hydrophilic component, which is attributed to the entrapment of the hydrophilic phase as dispersed phase in the W/O ME [72]. At this stage the concentration of the water droplets was below the critical volume fraction (percolation threshold (ϕ_p)) to undergo percolation in the oil continuous phase, which acted as an insulator [72, 93, 125]. However, upon increasing the percentage of the hydrophilic phase, the electrical conductivity increased slowly due to percolation (progressive and droplet-droplet interaction, which leads to transient cluster formation) of droplets, owing to their bigger diameter and increased concentration (above ϕ_p) to form a conductive domain. Following the slow increase, the conductivity increased sharply suggesting a change in nanostructure, which most likely is changing of W/O ME to BC ME. Finally, a slow increase in electrical conductivity was observed suggesting a change in nanostructure, which can be associated with change of BC ME into O/W ME. Same phenomenon was observed by several other authors [69, 88, 93, 157]. Accordingly, the boundaries at which the ME changes nanostructure were determined and the corresponding areas are shown in Figs 2.1 b, d, g and h. The results in Fig 2.1 showed that the nanostructure is responsive to change in ME composition.

Differential Scanning Calorimetry

Although electrical conductivity gives valuable information about nanostructure of MEs, the results obtained may not be conclusive and need to be supported by other techniques such as DSC and diffusion coefficient measurement using PGSE-NMR [72, 104]. Thus, in our case, DSC and EPR results were used to corroborate the results of electrical conductivity.

The DSC thermograms of two TCPL4-based ME systems obtained using TCPL4-HPGMO4 (1:1) as a SAA and IPP-Lin A (9:1) as an oil at a dilution line of R=65:35 are given in Fig 2.3. As can be seen in Fig 2.3 a, obtained using water-PeG (1:1) as a hydrophilic phase, the oil phase underwent phase transition at about +13.6°C while the hydrophilic phase underwent phase transition at -6.1°C. The components have moved to lower temperatures in MEs and further down as the level of entrapment increases. The same effect was also reported by Hathout et al. [72]. Paramount importance is, however,

as has been depicted in the picture no hydrophilic phase peak was obtained for MEs containing a hydrophilic component (0-35) % and no oil peak was observed above 60 % of the hydrophilic component, suggesting the existence of W/O and O/W MEs, respectively. In both instances the corresponding phases were contained within droplets to be detected by the DSC [72]. However, at (40-55) % of the hydrophilic phase, both oily and hydrophilic phase peaks appeared, which can be attributed to BC type MEs. Additional characteristic exothermic peak was also arisen at lower temperatures, which might be attributed to the bound water to the interface in the BC ME. Same effect was observed by Hathout et al. (2010) [72].



A) 65 % (TCPL4/HPGMO4 (1:1)) and 35 % (IPP/Lin A (9:1)) diluted with water-PeG (1:1).

B) 65 % (TCPL4/HPGMO4 (1:1)) and 35 % (IPP/Lin A (9:1)) diluted with water-PeG (1:9).

Figure 2.3: DSC thermograms of TCPL4-based MEs obtained along the 65:35 dilution lines diluted with low (A) and high (B) ratios of PeG in the hydrophilic phase.

The electrical conductivity result on the same dilution line suggested change in nanostructures at 33 and 54 % of the hydrophilic phase, Fig 2.1 h. Thus, the results

obtained corroborate the conductivity results except the slight shift of the BC region to the right, which can be attributed to the very low phase transition temperature in DSC.

Unlike, Fig 2.3 a, in Fig 2.3 b (obtained using water-PeG (1:9, v/v) as hydrophilic phase) no peak representing the hydrophilic component was observed, which is due to the low ratio of water in the hydrophilic phase. In addition, the exothermic peaks observed in Fig 2.3a at lower temperatures in BC MEs were not observed in 2.3 b, supporting the idea that the peaks are associated with the bound water. However, more or less the same trend in the oil peaks strength and location was observed partially corroborating the results of electrical conductivity.

Electron Paramagnetic Resonance (EPR)

EPR spectroscopy is a widely used tool to understand the aggregation behaviour of various self-assembled systems such as SAAs and polymers assemblies in solutions as well as in biological membranes [158-159]. It may also be used to investigate the effect of various solubilisates on aggregation behaviour and dynamics of micellisation processes [160]. It is a very sensitive method that requires a minimum amount of the spin probe, which causes minimal distortion of the system [159]. Nitroxide spin probes are commonly employed spin probes and the four EPR parameters obtained from typical EPR spectra include τ_c , a_N , IF and LW, see details under (see Appendix F).

A typical nitroxide EPR spectrum has three EPR lines (upper (-1), middle (0) and lower (+1) field EPR lines) and τ_c can be estimated from the spectra of the probe using Eqn. 2.1 [161].

$$\tau_c = 6.51 \times 10^{-10} \left[\left(\frac{h_o}{h_{+1}} \right)^{1/2} + \left(\frac{h_o}{h_{-1}} \right)^{1/2} - 2 \right] \Delta H_o \dots\dots\dots \text{Eqn. 2.1}$$

Where h_i is the peak amplitude and ΔH_o is the peak-to-peak line width of the centre peak.

It is noted that Eqn. 2.1 is used for the relatively fast motion of small spin probes, which undergo isotropic spectra with $\tau_c < 3$ ns, but not for the slower motion of various aliphatic spin probes, which undergo anisotropy [161-162]. a_N of nitroxide free radicals, defined as the distance between the low and high field EPR lines, is dependent on the electron density around the N nuclei, which is further dependent on the polarity of the

environment in which the spin probe resides [160, 163-165]. The LW, the peak-to-peak width of the central EPR spectral line, is a measure of spin-spin interaction as well as rotational motion of a probe. It broadens as the probe concentration increases through either spin-spin exchange or magnetic dipole interactions [166]. LW of hydrophobic spin probes increases significantly in SAA solutions as a consequence of spin probe partitioning into micelles that leads to strong spin-spin interaction [166]. IF is dependent on the interaction of probe within the surrounding environment as well as the level of spin probe entrapment [159, 167].

Although EPR parameters are commonly used to study microenvironments, to date, their potential use as a means of identifying MEs nanostructure has not been explored. Some EPR parameters, especially IF and τ_c , are highly responsive to the level of EPR probe entrapment [159, 165], which is dependent on the mobility of the media surrounding the spin probe. The mobility of the three ME components, namely the oily, hydrophilic and amphiphilic components, is dependent on the ME nanostructure. Hence, the hypothesis formulated was, highly hydrophilic and lipophilic spin probes will partition more or less completely to the hydrophilic and the lipophilic phases of the MEs, respectively, and will give information about the degree of entrapment of the phases. Consequently, HD-PMI (Fig 2.4), a lipophilic spin probe that partitions more or less in the oily phase ($\log P > 6$) [165], was used to investigate the nanostructure of the MEs. Based on our hypothesis, HD-PMI, as a lipophilic spin probe gives information about the level of entrapment of the oily phase: a high level of entrapment is expected in O/W ME and little or no entrapment is expected in W/O ME while medium level of entrapment is expected in the BC region. Therefore, as the nanostructure changes a sharp change in the EPR parameters, mainly τ_c and IF, is expected. Hence, the EPR spectrograms of the MEs along the 25 % SAA dilution line were obtained at 25 and 40°C and the EPR parameters IF, LW, τ_c were drawn as a function of percent hydrophilic phase, Figs 2.5 and 2.6. As has been shown in the figures, the effect of the ratio of PeG in the hydrophilic component was also investigated.

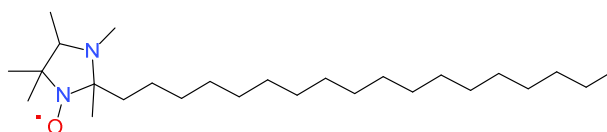


Figure 2.4: The chemical structure of HD-PMI.

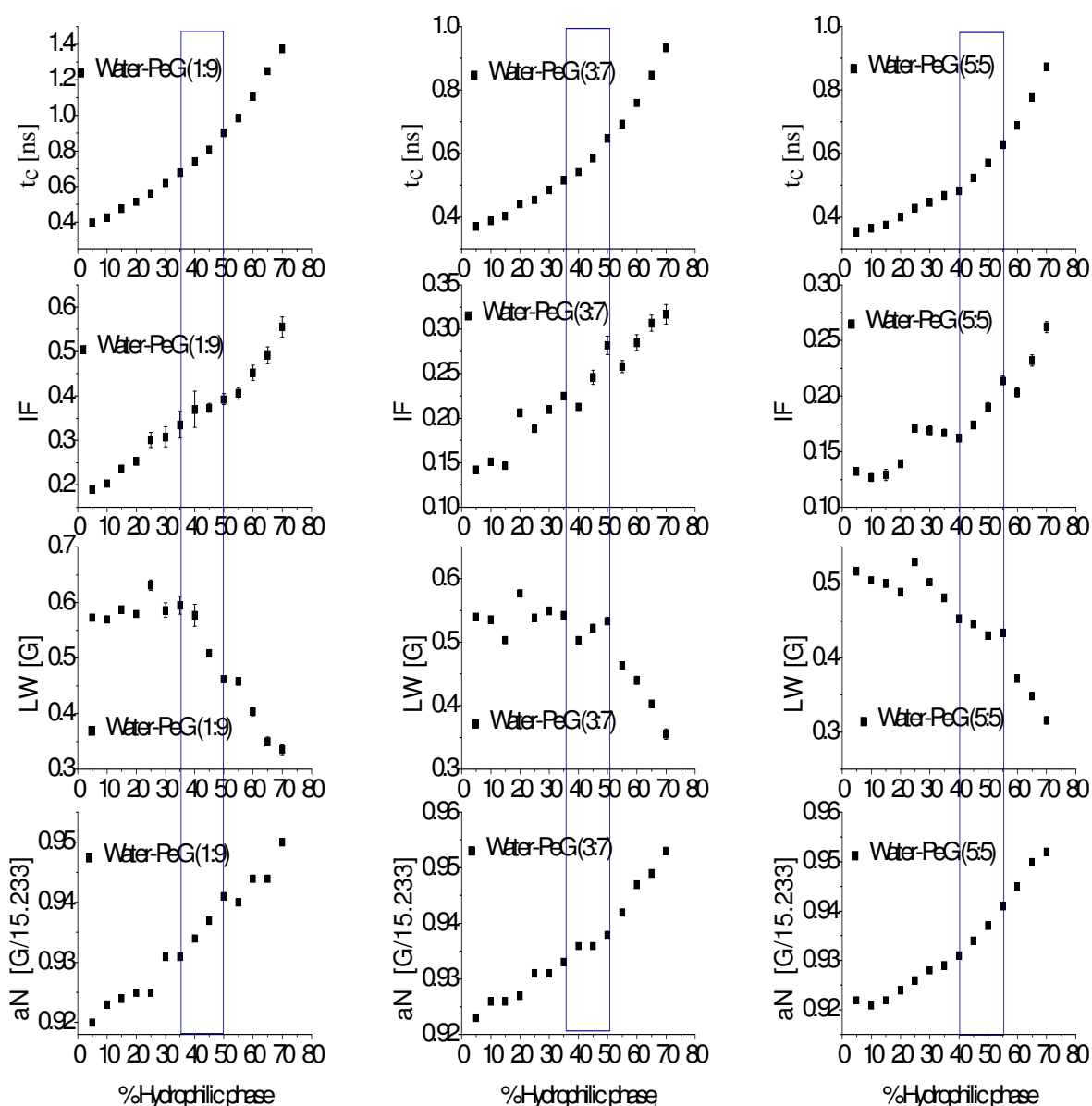


Figure 2.5: Change in EPR parameters of TCPL4-based MEs containing IPP-Lin A (9:1) as oily phase and TCPL4-HPGMO4 (1:1) as SAA mixture at 25°C as a function of percent hydrophilic phase (water-PeG equals 1:9 (left), 3:7 (middle) and 1:1 (right)).

During ME preparation and construction of PT-PD, for the sake of simplicity, the whole water-PeG mixture was considered as a hydrophilic phase. However, part of the PeG, as a co-solvent, partitions into the oily phase. Thus, along the dilution line as the amount of the Water-PeG mixture increases, which is accompanied by a decrease in the oily component, the percentage of PeG in the oily phase is constantly increasing. Consequently, since PeG has higher viscosity and polarity than the oil, T_c and a_N values increase. It was evidenced by the results of preliminary studies (see Appendix F) that

show the change in the EPR parameters of the oil at various PeG percent. The results also showed that LW decreased and IF increased smoothly as the level of PeG in the oily phase increases. The same trend was observed with the MEs investigated. Additionally, abrupt changes in the EPR parameters were also observed, which are associated with change in nanostructures, Figs 2.5 and 2.6.

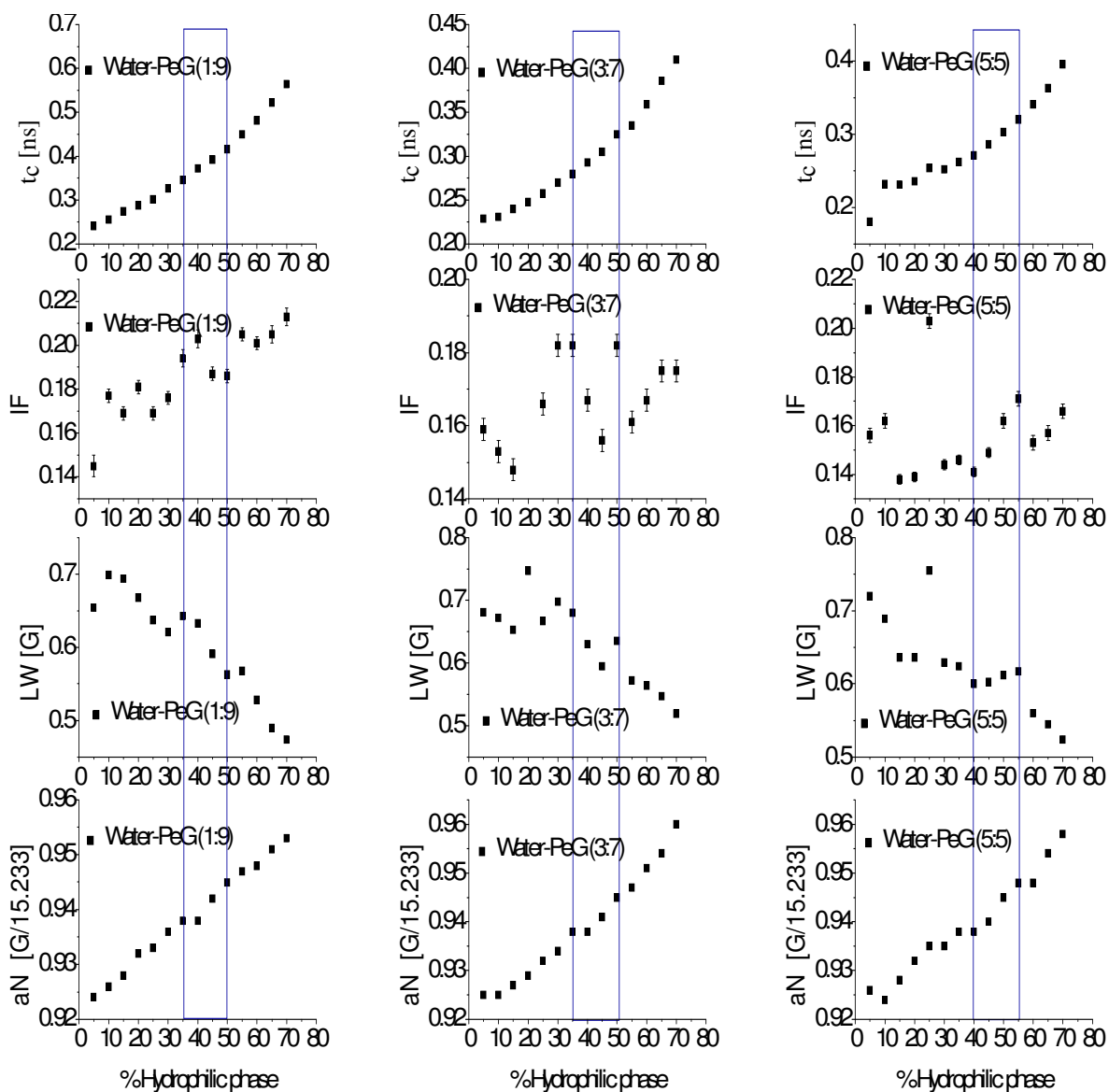


Figure 2.6: Change in EPR parameters of TCPL4-based MEs containing IPP-Lin A (9:1) as oily phase and TCPL4-HPGMO4 (1:1) as SAA mixture at 40°C as a function of percent hydrophilic phase (water-PeG equals 1:9 (left), 3:7 (middle) and 5:5 (right)).

Theoretically, as the hydrophilic component increases, the W/O ME changes to BC and then to O/W MEs. Consequently, the change in ME nanostructure will be accompanied

by a change in the level of the entrapment of the oil and the spin probe, which is dissolved more or less in the oil (see detail in Appendix F). Hence T_c is expected to increase abruptly as the W/O ME change into BC and O/W MEs. The results obtained, Figs 2.5 and 2.6, are in agreement with this hypothesis and the ME regions were accordingly categorised.

HD-PMI is a lipophilic spin probe, which has a long lipophilic chain attached with a hydrophilic group, Fig 2.4. Thus, as an amphiphilic molecule, in MEs the hydrophilic group of the spin probe may arrange on the interface close to the hydrophilic phase. Having this in mind, IF is dependent on probe entrapment and interaction with the surrounding molecules. As droplets in W/O ME join to form channels in BC ME the interfacial area decreases tremendously and again when the channels in BC ME change into droplets of O/W ME the interfacial area increases tremendously. This further affects the distribution of the spin probe in the system and their interaction. In addition, due to confinement of the oil soluble spin probe in the oily phase, the level of probe entrapment increases as the W/O ME changes into BC ME and O/W MEs. Therefore, as the ME nanostructure changes, change in IF is expected due to a change in the level of probe entrapment and probe distribution. The same result was observed and change in ME nanostructure was expressed by an abrupt change in IF values, Figs 2.5 and 2.6. The result was in agreement with the changes observed by T_c .

As has been indicated in Appendix F, as the percentage of PeG in the oily phase increases LW decreased and a_N increased smoothly. However, as can be seen in the figures, abrupt changes in both LW and a_N were observed overlapping with the abrupt changes observed by T_c and IF. These changes can again be associated with the change in interfacial area, which modifies the arrangement of spin probes within the system. As has been mentioned, when the W/O ME changes to BC ME the interfacial area decreases tremendously resulting in an increased probe-probe interaction, and so the LW. In addition, as the interfacial area decreases the number of polar groups of the spin probe coming into the surface decreases and hence a_N decreases. As the BC region changes to O/W ME, the opposite happens. Thus, all the four EPR parameters showed abrupt changes as the ME nanostructure changes and EPR results were in agreement with electrical conductivity and DSC results.

Unlike the DSC results, it was also possible to investigate the effect of temperature on ME nanostructure and the result showed that temperature has no significant effect on

the nanostructure, Figs 2.5 and 2.6. It was shown that MEs formed by non ionic SAAs are less affected by temperature [112]. In addition, as has been revealed by electrical conductivity results, the EPR results also showed the effect of the ratio of PeG in the hydrophilic phase on ME nanostructure. As can be seen in Figs 2.5 and 2.6, as the level of PeG in the hydrophilic phase decreases, the BC region moved towards the O/W ME region expanding the W/O ME. This might be due to the increase in polarity of the hydrophilic phase, which in effect favours the formation of W/O ME as the SAAs used have relatively low HLB values (equivalent HLB=9.5) to form O/W MEs.

Thus determination of MEs nanostructures using EPR had an added advantage over the DSC methods. It was possible to determine ME nanostructure at various temperatures as well as lower amount of water in the hydrophilic phase. In addition, usually stable MEs contain spectral of ingredients and hence complex DSC peaks might be obtained, which makes analysis of the results difficult.

Therefore, combining electrical conductivity, DSC and EPR results the nanostructure of the MEs was determined, Fig 2.1. As can be seen in the figure, as the ratio of Lin A in the oily phase increases the BC region moved to right, expanding the W/O ME region and contracting the O/W ME region. HPGMO4 as a co-SAA and the percentage of PeG in the hydrophilic phase increases expanded the BC and O/W ME regions and contracted the W/O ME region.

Concluding, higher ratio of PeG in the hydrophilic phase and Lin A contracted the two-phase and LC ME regions and significantly enhanced the stability of CER [AP] MEs. Higher PeG expanded the O/W ME region and contracted the W/O ME region and the opposite happened with Lin A. Using HPGMO4 as a co-SAA, vanished the LC phase, contracted the two-phase region and expanded the O/W and BC ME regions and tremendously increased stability of CER [AP] MEs. It may also significantly minimize the irritation potential of the formulation as the level of TCPL4 would be reduced. Therefore, to obtain MEs with optimum stability and desired nanostructure, the right amount of PeG in the hydrophilic phase, Lin A in oily phase and HPGMO4 should be used.

▪ Viscosity, Refractive Index and Droplet Size

The viscosity, refractive index, droplet diameter and MEs nanostructure of the 10 selected optimised TCPL4-based CER [AP] MEs are shown in Table 2.3. MEs with higher percentage of SAA(s) had higher viscosities. However, all the MEs have relatively lower viscosities and exhibited Newtonian kind of flow, which is characteristics of MEs [110, 117].

Table 2.3: Viscosity, refractive index, droplet diameter and nanostructure of optimised TCPL4-based CER [AP] MEs.

No.	ME	Viscosity (± RSD) (mPa.s)	Refractive Index (± RSD)	Droplet diameter (± RSD) (nm)	Nanost ructure
1	TAPOME1	61.8 (0.46)	1.439 (0.001)	344.8 (55.08)	BC ^c
2	TAPOME2	85.9 (1.02)	1.441 (0.002)	234.4 (84.83) ^b	W/O ^c
3	TAPOME3	69.5 (0.83)	1.440 (0.001)	256.4 (78.96) ^b	O/W ^c
4	TAPOME4	67.5 (0.44)	1.445 (0.001)	235.4 (48.92) ^b	O/W
5	TAPOME5	138.1 (1.09)	1.445 (0.000)	444.2 (18.61)	BC
6	TAPOME6	141.5 (0.73)	1.442 (0.000)	347 (48.97) ^b	O/W
7	TAPOME7	68.6 (0.52)	1.444 (0.002)	272.6 (59.62) ^b	O/W
8	TAPOME8	87.3 (0.77)	1.445 (0.001)	244.0 (110.12) ^b	O/W
9	TAPOME9	105.8 (0.66)	1.445 (0.001)	231.8 (100.24) ^b	O/W
10	TAPOME10	103.9 (0.77)	1.442 (0.001)	208.8 (79.55) ^b	O/W

^a exhibited Newtonian type of flow; ^b apparent RSD; ^c determined based on trend observed

Customarily determination of MEs droplet size and size distribution is done using PCS, which involves the measurement of the diffusion coefficient (D) of the droplets and calculation of the corresponding diameter using Stokes-Einstein Eqn. [112, 168]. The equation is applicable only for spherical droplets that do not interact in the dispersion media [168-169]. Nonetheless, studies suggested that in some cases MEs are not spherical in shape [71] and due to the large concentration of dispersed droplets it is difficult to avoid droplet-droplet interactions in MEs [169]. Although it was reported that MEs remain stable for a couple of hrs after dilution [113], studies showed that dilution of MEs results in abrupt change in ME diameter and/or nanostructure [82, 103, 121, 169]. In association to asymmetry in MEs droplets shape, the degree of light scattering and, hence, the estimated particle diameter of non-spherical particles at various angles will be different [170]. Interestingly, BC MEs were found to scatter light, which can most likely attributed to the dynamics of the continuously and spontaneously fluctuating oil and water continues channels. In addition, in most cases it is

controversial obtaining the viscosity and refractive indexes of the actual continues phase, as several physical process like partitioning and aggregation are taking place between the ME components. However, with all the above factors specified and adjusted, it might be possible to estimate the droplet size of MEs.

In our case, since the results of electrical conductivity, DSC and EPR data showed change in nanostructure upon dilution of MEs, measurement of droplet diameter was carried out without dilution of the MEs. During determination of droplet diameter, the second order intensity autocorrelation function of the MEs ($g^2(q; T)$: q is wave vector (momentum transfer) and T is delay time) was obtained at various angles (30, 50, 70, 90, 110, 130°) and the first order (field) autocorrelation function ($g^1(q; T)$) was calculated using Siegert Eqn., Eqn. 2.2 [118, 168].

$$g^2(q; T) = 1 + \beta |g^1(q; T)|^2 \dots\dots\dots \text{Eqn. 2.2}$$

Where; β is the coherence factor of the experiment.

Assuming a mono-dispersed population, $g^1(q; T)$ can be treated as a single exponential decay, Eqn. 2.3 [108] [121].

$$g^1(q; T) = \exp(-\Gamma T) \dots\dots\dots \text{Eqn. 2.3}$$

Where Γ is the decay rate

The $g^1(q; T)$ vs. T curve fitting was made to determine the decay half time ($t_{1/2}$) and Γ was calculated as $1/(t_{1/2})$. The apparent diffusion coefficient of the droplets (D_{app}) can be calculated at a given angle using Eqn. 2.4 [108, 168].

$$\Gamma = q^2 D \dots\dots\dots \text{Eqn. 2.4}$$

where, q is the absolute value of the scattering vector and is given by Eqn. 2.5 [170]:

$$q = \frac{4\pi n}{\lambda} \sin\left(\frac{\theta}{2}\right) \dots\dots\dots \text{Eqn. 2.5}$$

Where, λ is the incident laser wavelength, n is the refractive index of the sample and θ is angle at which the detector is located with respect to the sample cell.

The results obtained showed that the D_{app} values obtained at various angles were not the same suggesting that the dispersed droplets are not spherical in shape. The extent of shape irregularity was reflected by the apparent RSD values (Table 2.3), which were calculated from the pseudo-diameters calculated using D_{app} at various angles, using Eqn. 2.6. Thus, the apparent RSD values are more of indicators of droplets shape asymmetry, where high RSD refers to higher droplet shape asymmetry.

Therefore, due to angular dependence of the D values, the D values were calculated as the intercept of the plot of Γ/q^2 vs. q^2 [170] and the corresponding droplet diameters were calculated using Stokes-Einstein Eqn., Eqn. 2.6 [108, 112, 168]. The corresponding results are depicted in Table 2.3. However, for BC MEs the results were angular dependent and no linearity was observed when Γ/q^2 was plotted against q^2 and hence the average of the values was put as a pseudo-droplet diameter. Unlike the case of droplet MEs, a very high pseudo-droplet diameter and diameter deviation was observed, which can be attributed to the dynamics and structural alterations of the BC channels rather than diffusion of droplets. Interestingly, this might be used as a means of identifying MEs nanostructures and the results obtained were in agreement with the results of the PT-PD. In some MEs, which are located close to the borders of two different nanostructures, change in nanostructure was observed, which is most likely brought by the CER itself, which acts as an amphiphilic component. Thus, the nanostructure of the 10 optimised TCPL4-based MEs are shown in Table 2.3.

$$D = \frac{K_B T}{6\pi\eta r} \dots\dots\dots \text{Eqn. 2.6}$$

Where; K_B is Boltzmann's constant, T is the absolute temperature, η is viscosity of the medium and r is the radius of the droplet.

As can be seen in Table 2.3, the hydrodynamic radius of the MEs is relatively bigger than the usually reported MEs droplet diameter (10-100 nm [78, 127]). However, stable MEs with bigger diameters were also reported previously [82-83, 113]. In addition, generally, droplet diameters of MEs containing low level of oil and high SAA level were smaller and less asymmetric. Same results were reported by Shrikhande et al. (2010) [119] and Lin et al. (2009) [113]. In addition, incorporation of HPGMO4 as a co-SAA and high proportion of PeG in the hydrophilic phase resulted in MEs with

reduced droplet diameter. Pakpayat et al. (2009) also reported that combination of SAAs resulted in MEs with reduced droplet diameters [67].

▪ **Micropolarity and Microviscosity**

EPR technique is widely employed for the determination of microenvironments in lipid bilayers and nanostructures [122, 160, 163-164]. Hence, it was used to determine the micropolarity and microviscosity of TCPL4-based CER [AP] MEs. a_N of nitroxide free radicals is dependent on the electron density around the N nuclei, which is further dependent on the polarity of the surrounding environment and can be used as a measure of micropolarity in nanostructures at which the spin probe is situated [160, 163-164]. τ_c provides information about the microviscosity of the microenvironment at which the spin probe is located. In the absence of spin-spin interactions, an increase in τ_c indicates a decrease in the spin probe mobility, which is related to high microviscosity of the environment in which the spin probe is located [159, 162]. Although it might be affected by spin probe entrapment [171] in nanostructures the modified Stokes-Einstein-Debye Eqn., Eqn. 2.7, can be used to describe the relationship between τ_c and microviscosity of the surrounding media [172].

$$\tau_c = \left(\frac{\eta V}{K_B T} \right) k + \tau_o \dots \dots \dots \text{Eqn. 2.7}$$

Where; k_B = Boltzmann's constant; T = absolute temperature; μ = viscosity of the medium; V is the molecular volume of the spin probe; K is probe media interaction factor

Thus, the absolute values of microviscosity can be obtained following calibration of the EPR spectra of the spin probe in solvent systems with known viscosity [173]. In our case PeG, the co-solvent with known viscosity over a range of temperature [174] and is one of the major ME components, was used. The τ_c (ns) vs. (η/T) graph was linear ($R^2=0.9995$) for $\tau_c \leq 1.2$ ns, Fig 2.7, and the equation describing the relationship between τ_c and η in PeG is given by Eqn. 2.8.

$$\tau_c = 9.2907 \left(\frac{\eta}{T} \right) + 0.0021 \dots \dots \dots \text{Eqn. 2.8}$$

Eqn. 2.8 can be used to obtain η when HD-PMI is used as a spin probe provided that the K value (Eqn. 2.7), which depends on the nature of the vehicle in which HD-PMI is dissolved, is determined. The K values (K_V/K_B) in different vehicles with known viscosities [175] were calculated at specific temperatures, Table 2.4.

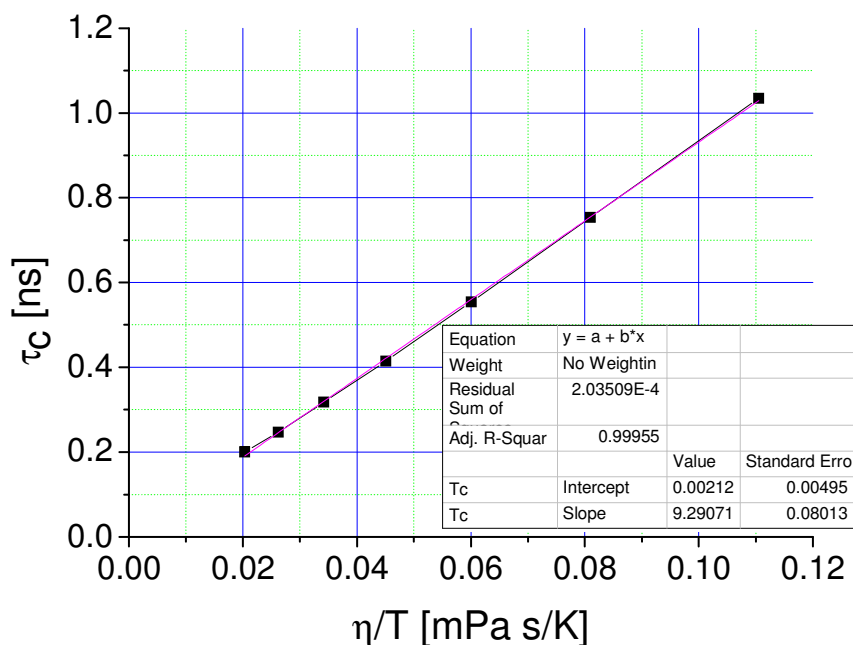


Figure 2.7: A linear curve describing the relationship between τ_c of HD-PMI and η in PeG over a range of temperature.

Table 2.4: K_V/K_B values of HD-PMI calculated in selected ME components.

No.	Component	Temp (K)	Viscosity (mPa.s)	τ_c	K_V/K_B
1	IPP	298.15	7.0	0.138	5.788
2	miglyol	293.15	30.0	0.571	5.559
3	PeG	298.15	45.6	1.482	9.684
		303.15	33.5	1.034	9.337
		308.15	25.0	0.754	9.286
		313.15	18.8	0.554	9.188
4	H2O-PeG (1:9)	303.15	30.0	0.685	6.901
		293.15	55.0	1.332	7.088
		298.15	41.0	0.948	6.879
		308.15	24.0	0.507	6.483
		313.15	18.0	0.384	6.644
5	H2O-PeG (1:3)	303.15	25.6	0.459	5.411
6	H2O-PeG (1:1)	303.15	14.6	0.328	6.767

As can be seen in the table, given V and K_B are constants, the K values are different in different vehicles. The highest K was exhibited by PeG and the lowest by the IPP and miglyol. Thus, despite viscosity is not an additive behavior [175], for the estimation of microviscosity of MEs, the average of the K values of the corresponding oil and PeG was taken. This was done considering the fact that the lipophilic phase is formed from oil-PeG mixture. Therefore, the KV/K_B value of TCPL4-based MEs was determined to be 7.53 for $\tau_c \leq 1.2$ ns and Eqn. 2.9 was used to describe the relationship between τ_c and η for TCPL4-based MEs.

$$\tau_c = 7.53 \left(\frac{\eta}{T} \right) + 0.0021 \dots \dots \dots \text{Eqn. 2.9}$$

The estimated microviscosity of selected TCPL4-based MEs is given in Table 2.5. a_N values were used to implicate the relative micropolarities of the MEs. The results showed that microviscosities were lesser than the corresponding viscosities of the MEs.

Table 2.5: Viscosities, microviscosities and relative micropolarities, of selected TCPL4-based MEs at 25°C and their proposed nanostructures.

No.	ME ^a	a_N	Microviscosity (mPa.s)	Viscosity (\pm RSD) (mPa.s)	Nanostructure
1	TAPOME2	0.968	47.98	85.9 (1.02)	W/O
2	TAPOME8	0.948	62.35	87.3 (0.77)	O/W

^a MEs prepared without addition of CER [AP]

Since the spin probe partitions almost in the oily phase (see detail in Appendix E) a_N values indicate the degree of partitioning of PeG into the oily phase. Thus, the higher a_N value in TAPOME2 shows that there is a high degree of partitioning of PeG in the oily phase, and it had to be followed by an increase in viscosity. In contrast, TAPOME8 showed the higher τ_c , and so microviscosity, which most likely attributes to the entrapment of the spin probe in the oil droplet. The significant increase in polarity of TAPOME2 might also be associated with the higher percentage of Lin A, which is more polar and viscous than IPP. Therefore, despite the MEs have more or less the similar viscosities, due to entrapment of the spin probe within the oil droplets in the O/W kind of MEs exhibited higher microviscosity than W/O MEs.

To investigate the effect of temperature on microviscosity, the EPR spectra of the above two MEs were obtained at - 35, -25, -15, -5, 5, 15, 25, 35, 45 and 60°C. However, the

MEs exhibited anisotropic motion below 5°C ($\tau_c > 3$ ns) [161-162] and yet the linearity was obtained for $\tau_c < 1.2$ ns. Hence, the microviscosities were calculated above 15°C and a sharp logarithmic decrease in microviscosity was observed as the temperature increases, Fig 2.8.

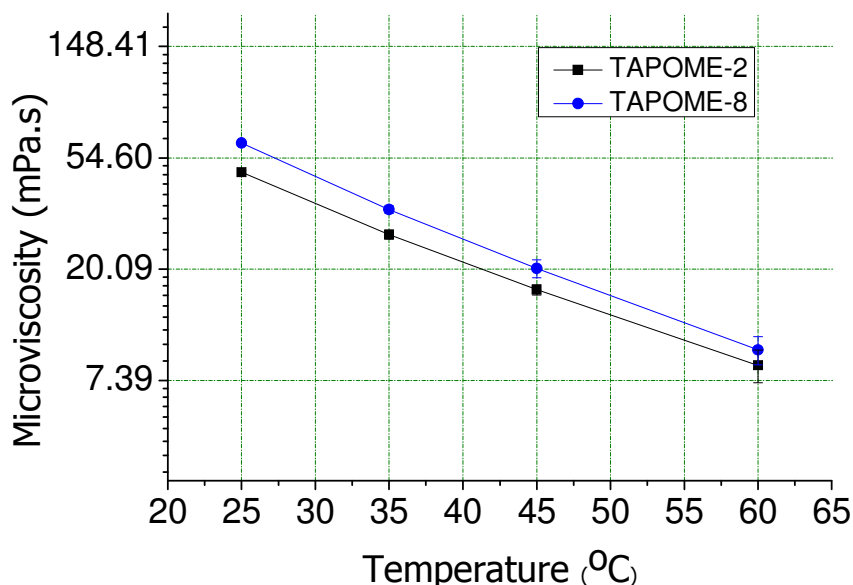


Figure 2.8: Effect of temperature on microviscosities of selected optimized TCPL4-based MEs.

2.3.1.1.4. Formulation and Characterisation of Lecithin-based CER [AP] MEs

Formulation

Miglyol, phosal and water-PeG mixture were selected as oil, amphiphilic and hydrophilic components, respectively, for the preparation of lecithin-based CER [AP] MEs (see detail in Appendix A). The effects of the percentage of each ME component as well as the ratio PeG in the hydrophilic component on stability of the MEs were thoroughly investigated in a region that potentially gives O/W MEs (low percentage of oil, (5-15) %). Due to safety reasons the level of SAA was maintained at ≤ 45 %. In general, formulations with higher ratio of PeG in the hydrophilic phase were found to have better stability. In contrary, as the ratio of PeG in the hydrophilic phase decreases it was necessary to increase the percentage of the oil and amphiphilic components in order to obtain stable MEs. The stable ME regions are shown in Fig 2.9 and ten MEs in the region were selected for further characterisation, Table 2.6.

Table 2.6: Compositions and stabilities of optimised lecithin-based CER [AP] MEs.

No.	ME	Migl yol %	Pho sal %	Water- PeG (1:9) %	Water- PeG (1.5:8.5) %	Water- PeG (1:3) %	CER [AP] ^a %	Stabilit y (± SD) (Mon)
1	PAPOME1	10	40	-	-	50	0.3	> 24
2	PAPOME2	10	45	-	-	45	0.3	> 24
3	PAPOME3	5	35	-	60	-	0.5	> 24
4	PAPOME4	10	45	-	45	-	0.5	> 24
5	PAPOME5	15	45	-	40	-	0.5	16 (1)
6	PAPOME6	10	30	60	-	-	0.5	15 (1)
7	PAPOME7	15	35	50	-	-	0.5	> 24
8	PAPOME8	10	40	50	-	-	0.5	> 24
9	PAPOME9	5	35	60	-	-	0.5	> 24
10	PAPOME10	15	45	40	-	-	0.5	> 24

^a percent per total mass of the MEs

Characterisation

▪ Pseudo-ternary Phase Diagram

Titration technique was employed to construct the PT-PD of lecithin-based MEs, Fig 2.9. Clear formulations that exhibited birefringence under cross-polarised light microscope were classified as LCs [72, 93, 103, 116-117].

As can be seen in Fig 2.9, only LCs were obtained at water-PeG (1:1, v/v) that most likely is a lamellar liquid crystalline phase formed due to less amount of the co-solvent, which provide the desired flexibility for the interfacial film to form MEs [176]. Mostly, twin tailed SAAs can form MEs without a co-SAA or a co-solvent. But lecithin, a twin-tailed SAA, needs a co-SAA in order to disrupt the lamellar structures that characterize its biological behavior [77]. In addition, unlike alcohols, alkanediols have to be used at high concentrations to obtain a stable ME [97]. Thus, the two-phase and LC regions contracted tremendously as the ration of PeG in the hydrophilic phase increases. The LC vanished completely at water-PeG \leq 1:3. The results in Appendix B also showed that the stability and CER loading capacity of lecithin-based MEs increased significantly as the percentage of PeG in the hydrophilic phase increases. There was a higher possibility of obtaining stable O/W MEs at a very low level of water in the hydrophilic phase suggesting the possibility of obtaining water free MEs, for drugs that are insoluble or poorly soluble in water, like CERs, or drugs that are susceptible to hydrolysis.

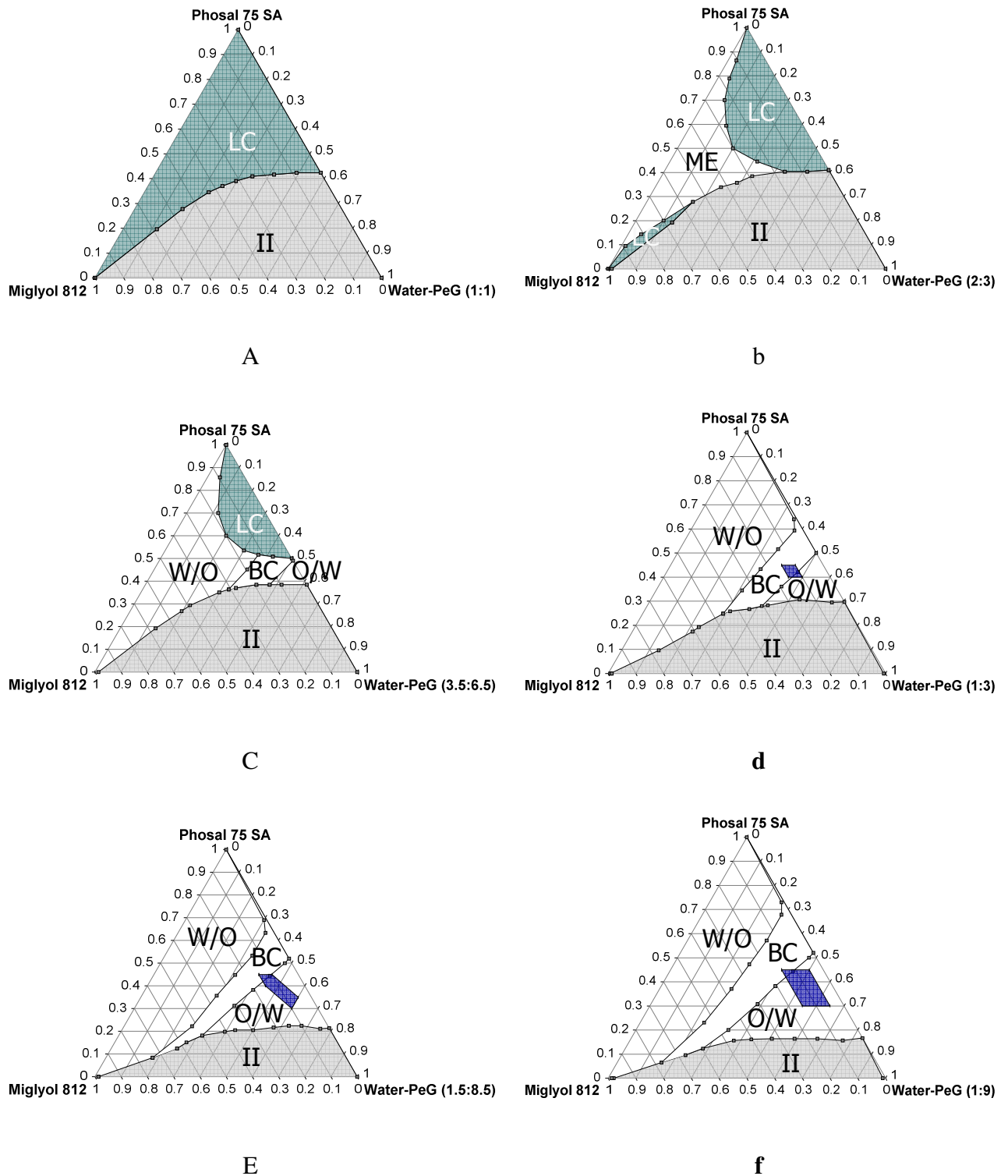


Figure 2.9: PT-PDs of lecithin-based MEs at different water-PeG ratios: a, 1:1; b, 2:3; c, 3.5:6.5; d, 1:3; e 1.5:8.5 and f, 1:9. II= 2 phase region; ME= ME region; O/W= O/W ME region; W/O= W/O ME region; BC= BC ME region, the blue band on the ME region=region of stable CER [AP] MEs.

ME Nanostructure

Like the case of TCPL4-based MEs, electrical conductivity results combined with DSC and EPR measurements were used to determine the nanostructures of lecithin-based MEs.

Electrical Conductivity

As has been mentioned under section 2.3.1.1.3, electrical conductivity is the simplest technique that can give valuable information about the nanostructure of MEs. Hence the electrical conductivity of the lecithin-based MEs was obtained at various dilution lines, Fig 2.10.

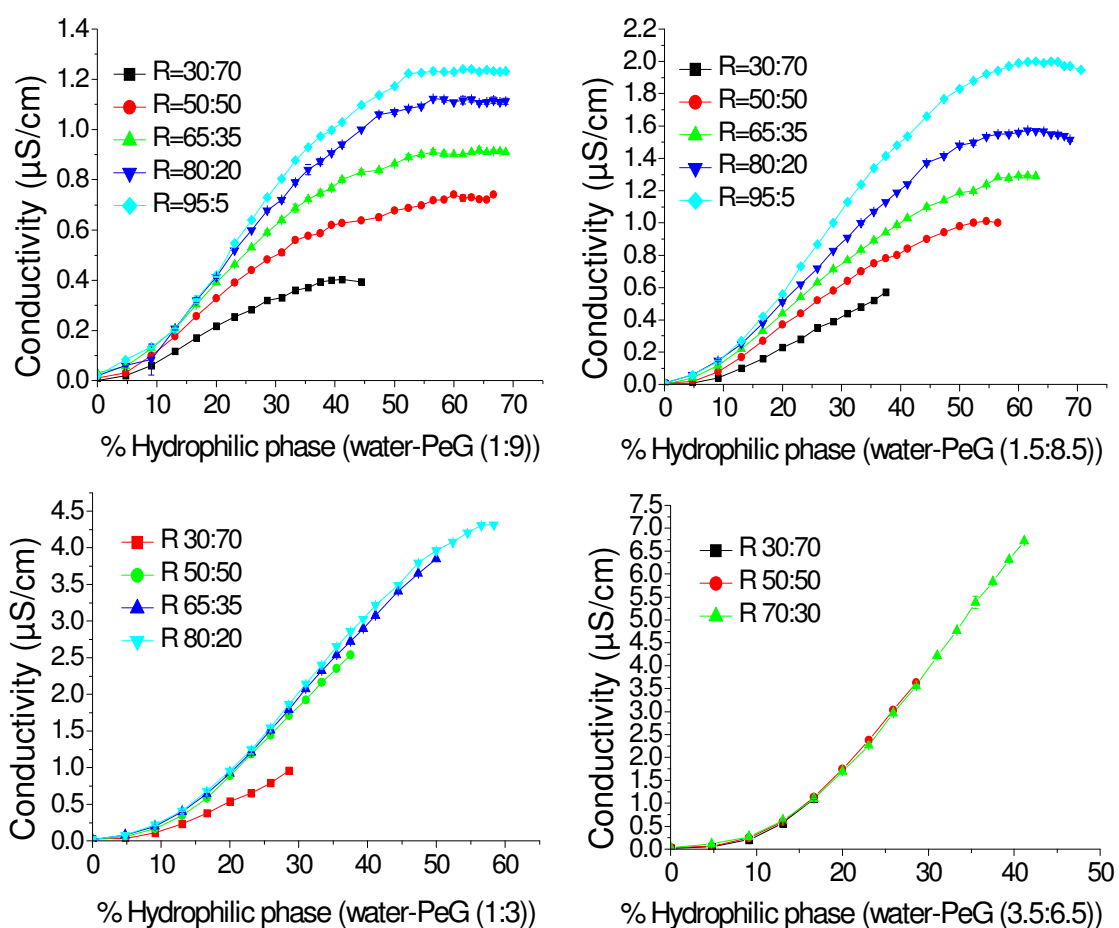


Figure 2.10: Electrical conductivity of lecithin-based MEs as a function of Wt. % of the hydrophilic phase (water-PeG 1:9-3.5:6.5). R= phosal-miglyol (% m/m) (N=3).

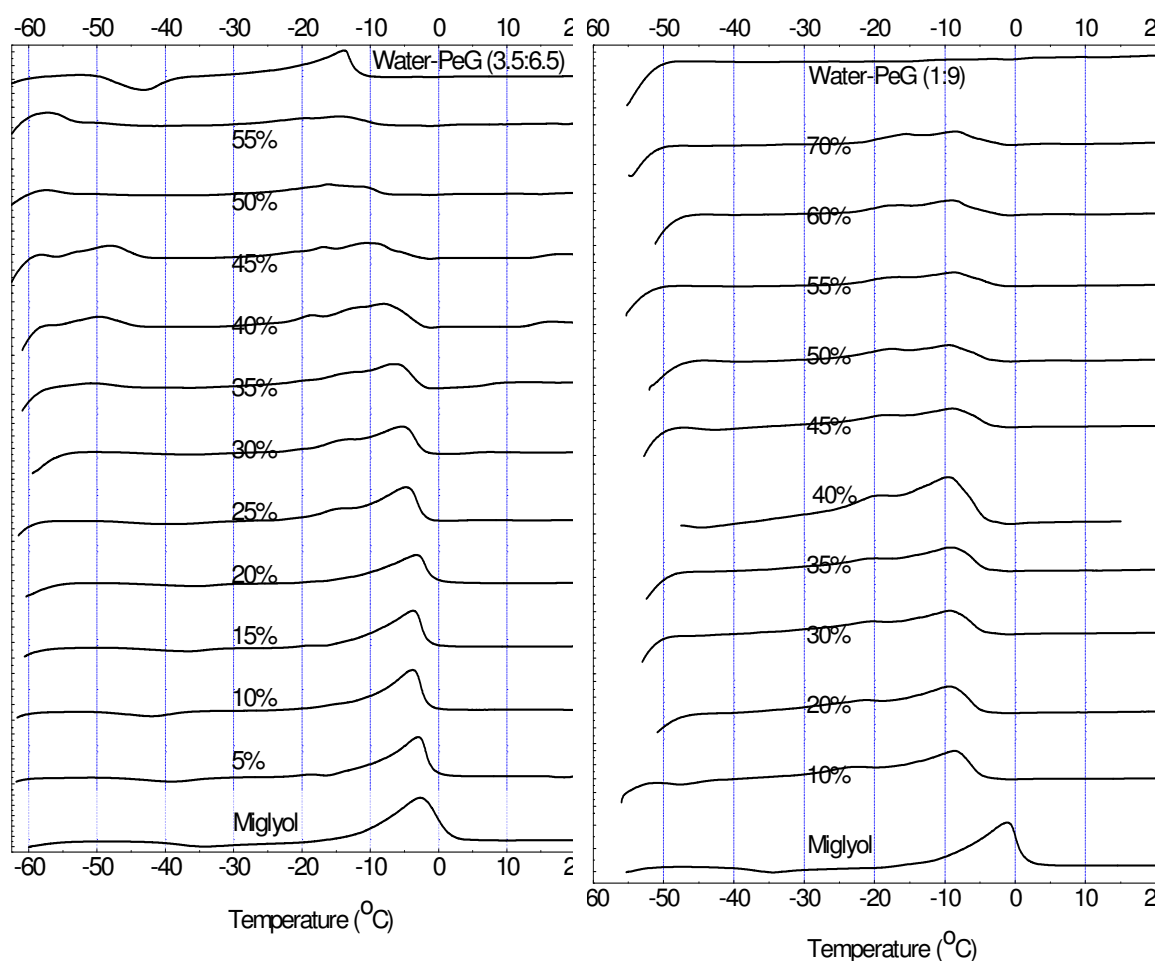
Like the case of TCPL4-based MEs, initially the electrical conductivity was zero and was followed by slow increase due to percolation of hydrophilic droplets into clusters

[104]. Then a rapid increase in electrical conductivity was observed due to formation of channels of hydrophilic phases, which are characteristics of the BC MEs. Finally, the electrical conductivity increased slowly suggesting formation of O/W MEs. Accordingly, the W/O, BC and O/W ME regions for some of the PT-PDs were obtained, Fig 2.9.

Differential Scanning Calorimetry

Like the case of TCPL4-based MEs, section 2.3.1.1.3, DSC results were used to corroborate the results of conductivity tests. The DSC thermograms of two lecithin-based ME systems were obtained at 40 % SAA dilution line using 3.5:6.5 and 1:9 water-PeG hydrophilic components, Fig 2.11. As can be seen in Fig 2.11 a, obtained using water-PeG (3.5:6.5), the oil peak, obtained at around -5°C , moved to the lower temperatures and vanished at 50 % of the hydrophilic phase. In addition, an exothermic peak was obtained at lower temperatures ($\approx -48^{\circ}\text{C}$) for MEs containing (35-45) % of the hydrophilic component, which might be attributed to the bound water to the head group of the SAA. Same DSC peak was observed by Hathout et al. (2010) in BC MEs [72] and the same peak was obtained in TCPL4-based MEs. However, due to the low percentage of water in the hydrophilic phase strong unbound water peak could not be obtained. Raising the ratio of water in the hydrophilic phase results in a very small ME region to be investigated. However, the oil and the bound water peaks suggested that the MEs, at the dilution line considered are (0-35) % W/O, (40-45) % BC and above 50 % O/W types. The results obtained are in agreement with the electrical conductivity results.

Unlike in Fig 2.11 a, in Fig 2.11 b (obtained using water-PeG 1:9 (v/v)) the characteristic BC peak was very weak due to the low ratio of water in the hydrophilic phase and was observed at 40 % of the hydrophilic phase. However, the oil peak almost vanished above 45 % of the hydrophilic phase suggesting the formation of O/W MEs above 45 % of the hydrophilic phase. Electrical conductivity results suggested BC region at about (27-39) % of the hydrophilic phase. The slight shift of the BC region to the right in DSC can be attributed to the very low temperature at phase transition in DSC. More or less, DSC results corroborate the results of electrical conductivity study.



a) ΔH along 40 % SAA dilution line as a function of water-PeG (3.5:6.5). b) ΔH at 65 % phosal and 35 % miglyol diluted with water-PeG (1:9).

Figure 2.11: DSC thermograms of lecithin-based MEs obtained along the 40 % SAA (a) and R=65:35 (b) dilution lines diluted with water-PeG 3.5:6.5 and 1:9, respectively.

Electron Paramagnetic Resonance

Like TCPL4-based MEs, section 2.3.1.1.3, the plot of the four EPR parameters, T_c , IF, LW and a_N , as a function of the percentage of hydrophilic phase was obtained at 25°C and 40°C, Fig 2.12, on the 40 % SAA dilution line and similar abrupt changes in the EPR parameters were observed and were associated with changes in ME nanostructure. Accordingly, at 25°C, (0-30) % was classified as W/O ME, (35-40) % was classified as BC ME and above 45 % water-PeG (1.5:8.5 w/w) the region was classified as O/W ME region. As the ratio of PeG in the hydrophilic phase decreases to water-PeG 3.5:6.5 the BC region moved to (40-45) % expanding the W/O ME region to (0-35) % of the

hydrophilic phase and contracting the O/W ME region to >50 % of the hydrophilic phase. As can be seen in the figure, temperature did not show a significant effect on ME nanostructure except that MEs obtained using water-PeG 3.5:6.5 w/w shifted slightly to the left at high temperature. This can explain that fact that the BC region obtained from DSC results moved slightly to the right at lower phase transition temperatures of the DSC. The results obtained are also in agreement with the results of electrical conductivity and DSC and the different nanostructures obtained for some of the PT-PDs are shown in Fig 2.9.

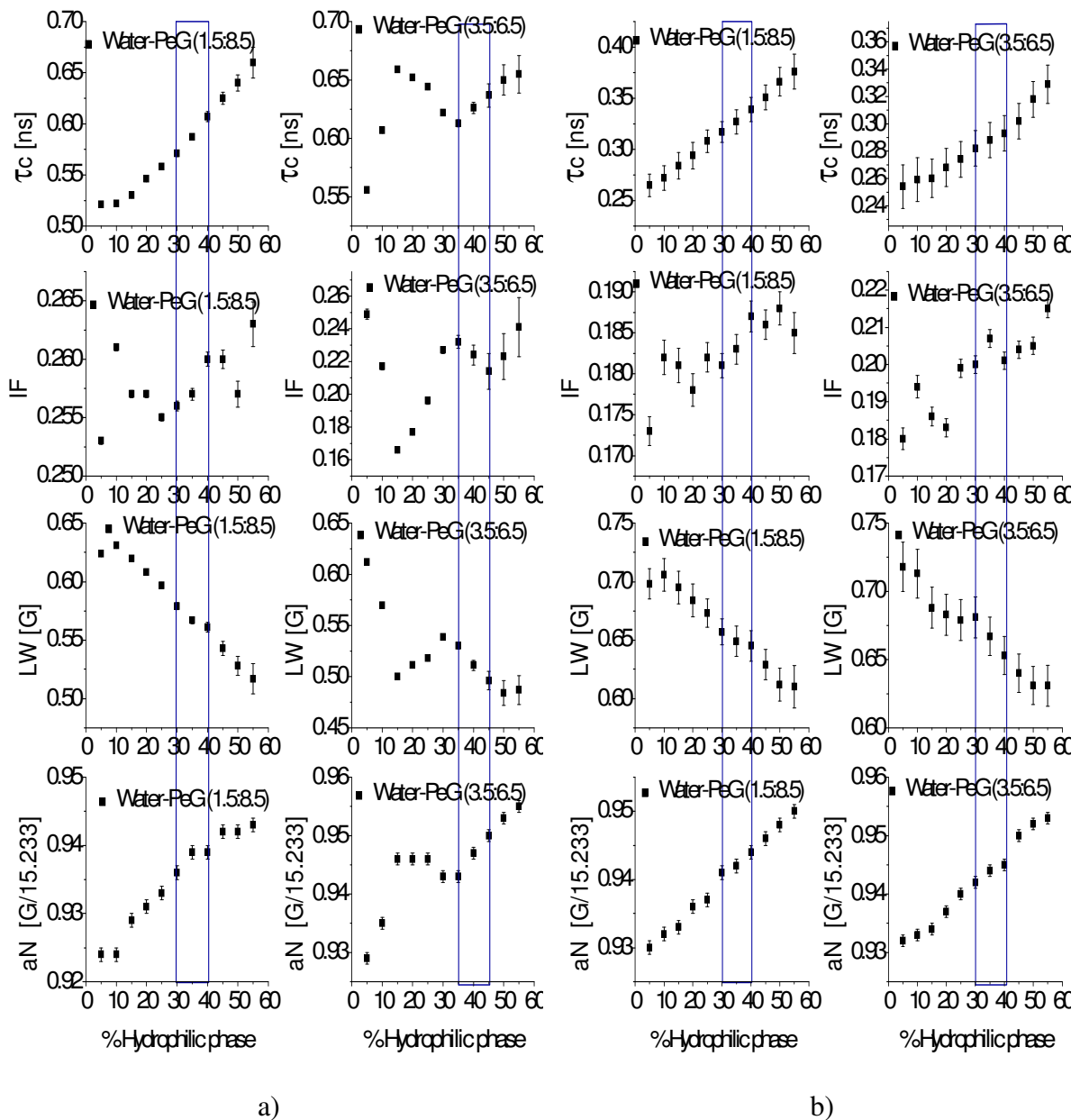


Figure 2.12: Change in EPR parameters of lecithin-based MEs at 40 % phosal dilution line at 25°C (a) and 40°C (b) as a function of percentage hydrophilic components containing 1.5:8.5 (left) and 3.5:6.5 (right) water-PeG.

As can be seen in Fig 2.9, as the level of PeG in the hydrophilic phase increases, the BC region expanded slightly and moved to the left contracting the W/O ME region and slightly expanding the O/W ME region. As has been shown under Appendix E, high level of PeG increased stability of lecithin-based CER MEs.

▪ Viscosity, Refractive Index and Droplet Size

The viscosity, refractive index, droplet diameter and the nanostructures of the 10 optimised lecithin-based CER [AP] MEs are shown in Table 2.7. Those MEs with higher percentage of SAA have higher viscosities. However, all the formulations had relatively lower viscosities and exhibited Newtonian kind of flow, which is typical characteristics of MEs [110, 117, 125].

Table 2.7: Viscosity, refractive index, droplet diameter and nanostructure of optimised lecithin-based CER [AP] MEs.

No.	ME	Viscosity (\pm RSD) ^a (mPa.s)	Refractive Index (\pm RSD)	Droplet diameter (\pm RSD) (nm)	Nanostructure
1	PAPOME1	52.3 (0.574)	1.442 (0.042)	204.2 (5.92)	O/W
2	PAPOME2	60.3 (1.227)	1.441 (0.042)	176.94 (7.49)	O/W
3	PAPOME3	49.6 (0.987)	1.440 (0.042)	194.74 (22.94)	O/W
4	PAPOME4	66.6 (0.975)	1.440 (0.000)	163.42 (12.18)	O/W
5	PAPOME5	66.4 (0.482)	1.442 (0.069)	214.6 (7.49)	O/W
6	PAPOME6	45.7 (0.241)	1.446 (0.042)	223.2 (6.99)	O/W
7	PAPOME7	58.6 (1.126)	1.441 (0.042)	167.9 (5.74)	O/W
8	PAPOME8	61.4 (1.726)	1.442 (0.042)	197.14 (5.47)	O/W
9	PAPOME9	52.6 (0.264)	1.440 (0.083)	196.94 (6.39)	O/W
10	PAPOME10	59.20 (0.785)	1.442 (0.042)	1848.8 (69.70)	BC

^a exhibited Newtonian kind of flow

Like TCPL4-based MEs, section 2.3.1.1.3, the droplet diameter of lecithin-based MEs was determined using PCS and during estimation of the droplet diameter the same equations and principles were applied. Interestingly, unlike TCPL4-based CER [AP] MEs, the D_{app} value of lecithin-based CER [AP] MEs were not angle dependent suggesting that the droplet are symmetrical, where a very low RSDs were observed, Table 2.7. In PAPOME10 the result was angle dependent and Γ/q^2 vs. q^2 graph showed no relationship, suggesting that it is a BC MEs and the results obtained were in agreement with PT-PD results, Fig 2.9, except PAPOME 2 and 5, which were identified as BC type MEs based on the PT-PD. This shift might be due to the incorporation of

CER [AP], which possibly altered the nanostructure of the MEs at the BC-O/W boarder owing to its amphiphilic nature.

As can be shown in Table 2.7, like TCPL4-based MEs, droplets of lecithin-based MEs containing higher concentration of the SAA and low oil concentration were relatively smaller. The same effect was observed by previous studies done on lecithin-based MEs [177-178]. In addition, lecithin-based MEs are smaller and exhibited better skin permeability, section 5.3.2, than TCPL4-based MEs.

▪ Micropolarity and Microviscosity

The same principle used during determination of micropolarities and microviscosities of TCPL4-based MEs, section 2.3.1.1.3, was applied in order to determine the micropolarity and microviscosity of lecithin-based CER [AP] MEs. Accordingly, based on the K values given in Table 2.4, the equation that describes the relationship between τ_c and η was obtained, Eqn. 2.10. The micropolarity and microviscosity of two selected lecithin-based CER [AP] MEs are shown in Table 2.8.

$$\tau_c = 7.41 \left(\frac{\eta}{T} \right) + 0.0021 \dots \dots \dots \text{Eqn. 2.10}$$

Table 2.8: Viscosities, microviscosities and relative a_N values of selected TCPL4 and lecithin-based MEs at 25°C along with their proposed nanostructures.

No.	ME ^a	a_N	Microviscosity (mPa.s)	Viscosity (± RSD) (mPa.s)	Nanostructure
1	PAPOME2	0.945	24.22	60.3 (1.227)	BC
2	PAPOME8	0.940	34.55	61.4 (1.726)	O/W

^a MEs prepared without addition of CER [AP]

a_N reflects the polarity of the immediate environment of the spin probe, irrespective of the spin probe entrapment [171, 179]. PAPOME2 exhibited higher micropolarity than PAPOME8 due to the higher percentage of water in the hydrophilic phase, which reduces the degree of partitioning of PeG into the oily phase. Although the higher SAA concentration in PAPOME2, which has more or less similar viscosity as that of PAPOME8, it has lower microviscosity than PAPOME8. The decrease in microviscosity can partially be attributed to the reduced partitioning of PeG into the oily

phase. However, compared to alteration in polarity values, the decrease in microviscosity in PAPOME2 was quite significant and this can be accounted to the higher level of entrapment of the spin probe in the O/W droplets of PAPOME8 [171]. The converse provides further information on the nanostructures of the MEs.

To investigate the effect of temperature on microviscosity, the EPR spectra of the above two MEs were obtained at - 35, -25, -15, -5, 5, 15, 25, 35, 45 and 60°C. However, the MEs exhibited anisotropic motion bellow 5°C ($\tau_c > 3$ ns) [161-162] and the linearity was obtained for $\tau_c < 1.2$ ns. Thus, the microviscosities were calculated above 15°C, Fig 2.13 showing that viscosity decreases logarithmically with temperature.

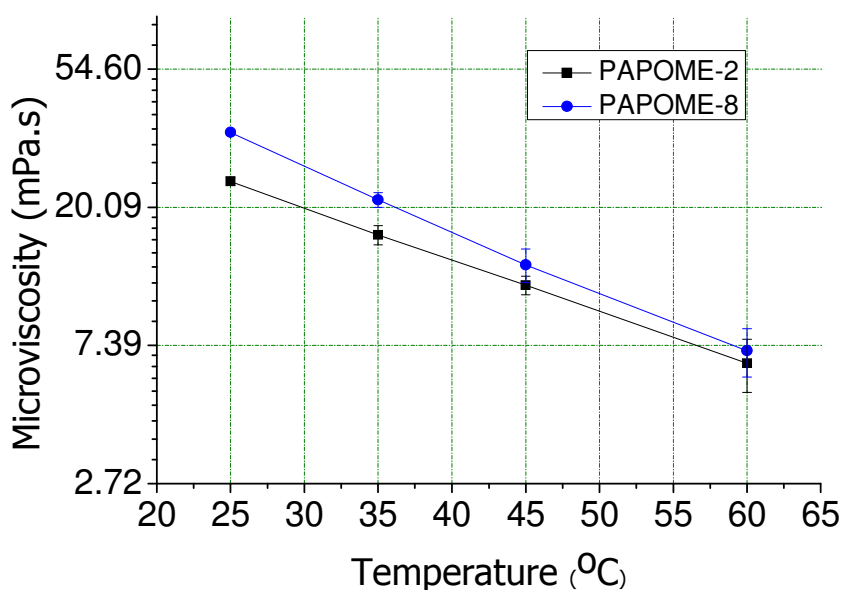


Figure 2.13: Effect of temperature on microviscosities of selected lecithin-based MEs.

2.3.1.2. Formulation and Characterisation of CER [EOS] MEs Containing other SC Lipids

CER [EOS], like CER [AP], plays a vital role in maintaining the barrier function of the SC and it might be used to treat affected or aged skin [13, 22]. Formulation of MEs may, therefore, help to facilitate its permeation into the SC. Since CERs have some structural similarities, Fig 1.2, and share some physicochemical properties in common the same ME components used during formulation of CER [AP] MEs were also used to develop CER [EOS] MEs. Like the CER [AP] MEs, attempt was made to formulate two types of CER [EOS] MEs, namely TCPL4-based and lecithin-based CER [EOS] MEs.

2.3.1.2.1. Formulation and Characterisation of TCPL4-based CER [EOS] and other SC Lipids MEs

Despite structural similarities between CERs results of preliminary experiments revealed that CER [EOS] needs a different microenvironment than CER [AP], which might be attributed to its bigger size and reduced polarity as compared to CER [AP], Fig 1.2. Hence, the effect of percent ME component on the stability of CER [EOS] MEs was thoroughly assessed (see detail in Appendix C) and the results showed that, compared to CER AP, the MEs have very low CER [EOS] loading capacity. However, since CER [EOS] is effective at a very low concentration (0.01-1 %) [180], stable TCPL4-based MEs that contain lower percentage of CER [EOS] (0.05 %) were obtained. The findings showed that, unlike CER [AP] MEs, stable CER [EOS] MEs could only be formulated at higher percentage of the oily phase, which can give BC MEs. With a view to incorporate CER [AP] into CER [EOS] MEs, the effect of CER [AP] on the stability of CER [EOS] MEs was assessed. Interestingly, CER [AP] improved the stability of CER [EOS] MEs considerably. Lin A increased stability of CER [EOS] MEs only when used along with CER [AP]: in the absence of CER [AP] Lin A had a slight negative effect on the stability of CER [EOS] MEs, which is statistically insignificant. Besides, like CER [AP] MEs, HPGMO4 and higher percentage of PeG in the hydrophilic component improved stability of CER [EOS] MEs and the most stable CER [EOS] MEs were obtained at moderate level of the SAA, which is again capable of forming BC MEs but near to the O/W-BC MEs border.

In addition, since several skin diseases are also associated with depleted levels of FFAs and/or CHOL in the SC, Table 1.1, an attempt was made to develop TCPL4-based MEs that contain CHOL and FFAs, besides CER [AP] and CER [EOS] (see details in Appendix C). However, incorporation of either FFAs (namely PA, SA, BA and LA) or CHOL considerably reduced stability of TCPL4-based CER [EOS] MEs. In contrary, the effect of CHOL was not significant. Besides, the effect of the FFAs was dependent on the chain length of the FFA, that is, as the chain length of the FFA increases stability of the resulting ME decreased significantly. Accordingly, LA reduced stability of the MEs very significantly and, hence, its inclusion alone or in combination with the other FFAs and/or CHOL to TCPL4-based CER [EOS] MEs was challenging. Combination of FFAs improved stability of the MEs. MEs that are prepared with BA/PA displayed better stability than single or pairs of FFAs used. Combining FFAs with CHOL, in

contrast, affected stability negatively and only stable TCPL4-based CER [EOS] MEs that contain either FFAs (Except LA) or CHOL could be obtained with stability slightly compromised. Accordingly, nine relatively stable TCPL4-based CER [EOS] MEs were obtained for further characterisation, Table 2.9.

Table 2.9: Compositions and stabilities of optimised TCPL4-based CER [EOS] MEs.

No.	ME	IP P %	IPP- Lin A (9:1) %	TCP L4 %	HPG MO4 %	Water r- PeG (1:9) %	Water r- PeG (1.5: 8.5) %	CER [AP] ^a %	CER [EO S] ^a %	PA- BA (1:1) ^a %	CH OL ^a %	Stability (± SD) (Mon)
1	TAPEOSME1	-	15	20	20	45	-	0.4	0.05	-	-	>24
2	TAPEOSME2	-	15	22.5	22.5	40	-	0.4	0.05	-	-	10 (3)
3	TAPEOSME3	-	15	35	-	-	50	0.4	0.05	-	-	15.5 (4.5)
4	TAPEOSME4	-	15	17.5	17.5	-	50	0.4	0.05	-	-	>24
5	TAPEOSME5	15	-	35	-	-	50	-	0.05	-	-	>24
6	TAPEOSME6	15	-	17.5	17.5	-	50	-	0.05	-	-	>24
7	TAPEOSME7	-	15	20	20	45	-	0.4	0.05	-	0.3	13 (3.5)
8	TAPEOSME8	-	15	22.5	22.5	40	-	0.4	0.05	0.3	-	11 (2.5)
9	TAPEOSME9	-	15	17.5	17.5	-	50	0.4	0.05	0.3	-	11 (0.5)

^a percent per total mass of the MEs

Characterisation

▪ Pseudo-ternary Phase Diagram

The PT-PDs of TCPL4-based MEs are shown in Fig 2.1 and all the stable MEs were found to be BC type, Table 2.10. It was not possible to obtain stable TCPL4-based O/W CER [EOS] MEs.

▪ Viscosity, Refractive Index and Dynamic Light Scattering

The viscosity and refractive index of the optimised TCPL4-based CER [EOS] MEs are shown in Table 2.10. All the MEs exhibited Newtonian kind of flow and the viscosity of the MEs was mainly dependent on the percentage of the SAA used.

In case of TCPL4-based CER [EOS] MEs, the D_{app} value was dependent on the angle of measurement and no relation was observed when Γ/q^2 was plotted against q^2 . In addition, there was a big variation in the diameter of the pseudo-droplet calculated based on the D_{app} obtained and thus the results suggested that all the MEs are BC types and the light scattering should be associated with the dynamics of the constantly changing BC channels. The results obtained are in agreement with the PT-PD results.

Table 2.10: Viscosity, refractive index, pseudo-droplet diameter, and nanostructures of optimised TCPL4-based CER [EOS] MEs.

No	ME	Viscosity (\pm RSD) ^a (mPa.s)	Refractive Index (\pm RSD)	Pseudo-droplet diameter (\pm RSD) (nm)	Nanostructure
1	TAPEOSME1	117.13 (0.709)	1.446 (0.000)	97.24 (19.89)	BC
2	TAPEOSME2	180.21 (0.324)	1.448 (0.001)	288.87 (53.93)	BC
3	TAPEOSME3	95.09 (0.562)	1.441 (0.000)	358.77 (40.72)	BC ^b
4	TAPEOSME4	87.56 (1.004)	1.442 (0.001)	259.85 (42.26)	BC ^b
5	TAPEOSME5	87.67 (0.935)	1.441 (0.001)	525.15 (37.53)	BC ^b
6	TAPEOSME6	91.43 (1.049)	1.441 (0.000)	427.24 (46.86)	BC ^b
7	TAPEOSME7	116.13 (0.656)	1.446 (0.000)	503.79 (37.57)	BC
8	TAPEOSME8	179.16 (0.511)	1.448 (0.001)	168.47 (63.10)	BC
9	TAPEOSME9	86.51 (1.158)	1.442 (0.000)	548.33 (49.21)	BC ^b

^a exhibited Newtonian kind of flow; ^b determined based on trend observed

2.3.1.2.2. Formulation and Characterisation of Lecithin-based CER [EOS] MEs with other SC Lipids

Despite structural similarities, the results of preliminary findings showed that CER [EOS] needed a different microenvironment than CER [AP]. Therefore, the effect of percent ME components on stability of lecithin-based CER [EOS] MEs was thoroughly investigated (see detail in Appendix C). The results showed that lecithin-based CER [EOS] MEs have relatively low CER [EOS] loading capacity as compared to CER [AP], which, however, was not a problem since CER [EOS] is active at lower concentrations (0.01-1 %) [180]. In addition, unlike lecithin-based CER [AP] MEs, stable lecithin-based CER [EOS] MEs could only be obtained at higher percentages of the SAA and the oil, which all were identified as BC MEs. CER [AP] had a positive influence on stability of lecithin-based CER [EOS] MEs and most stable CER [EOS] MEs were obtained at higher concentration of PeG in the hydrophilic phase. In addition, the effects of FFAs (PA, SA, BA and LA) and CHOL, alone or in combination, on the stability of relatively stable lecithin-based CER [EOS] MEs were thoroughly investigated. In general, except LA, all the FFAs and CHOL (especially at lower concentration of the SAA) enhanced stability of the resulting MEs. The effect of FFAs was also dependent on the chain length of the FFAs; where the shorter the chain length the better was the stability improving effect. In addition, despite LA showed a slight negative effect on stability, it was possible to incorporate it with stability slightly compromised. Combination of different FFAs with themselves or CHOL showed a better stabilising

effect than the FFAs or CHOL alone. Accordingly, twelve stable lecithin-based CER [EOS] MEs were formulated, Table 2.11.

Table 2.11: Compositions and stabilities of optimised lecithin-based CER [EOS] MEs.

N o.	ME	Mig lyol %	Pho sal %	Wat er- PeG (1:9) %	Water -PeG (1.5:8. 5) %	CER [AP] ^a %	CER [EO S] ^a %	SA- BA- LA (1:1.5: 1) ^a %	CH OL ^a %	Stability (± SD) (Mon)
1	PAPEOSME1	15	45	40	-	0.5	0.05	-	-	>21
2	PAPEOSME2	15	45	40	-	0.5	0.1	-	-	16 (4)
3	PAPEOSME3	20	45	35	-	0.5	0.1	-	-	>21
4	PAPEOSME4	15	45	-	40	0.5	0.1	-	-	>21
5	PAPEOSME5	20	45	-	35	0.5	0.1	-	-	>21
6	PAPEOSME6	10	45	40	-	0.5	0.1	-	-	>21
7	PAPEOSME7	15	45	40	-	0.5	0.05	0.35	0.3	>21
8	PAPEOSME8	15	45	40	-	0.5	0.1	0.35	0.3	15 (0.5)
9	PAPEOSME9	20	45	35	-	0.5	0.1	0.35	0.3	>21
10	PAPEOSME10	15	45	-	40	0.5	0.1	0.35	0.3	>21
11	PAPEOSME11	20	45	-	35	0.5	0.1	0.35	0.3	>21
12	PAPEOSME12	10	45	40	-	0.5	0.1	0.35	0.3	>21

^a percent per total mass of the MEs

Characterisation

ME Nanostructure

As can be referred from Fig 2.1, all the stable CER EOS MEs were found to be BC MEs. It was not possible to obtain stable lecithin-based O/W CER [EOS] MEs.

Viscosity, Refractive Index and Dynamic Light Scattering

The viscosity and refractive index of the optimised lecithin-based CER [EOS] MEs are shown in Table 2.12. The viscosity of the MEs was mainly dependent on the concentration of the SAA in the ME. Moreover, all the MEs had relatively lower viscosities as compared to the SAA and all exhibited Newtonian kind of flow.

Like TCPL4-based CER [EOS] MEs, the D_{app} values lecithin-based CER [EOS] MEs, obtained using PCS, were dependent on the angle of measurement and no relationship was obtained when Γ/q^2 was plotted against q^2 suggesting that the MEs are BC types. Calculation of the pseudo-particle diameter showed high RSD values (see Table 2.12). The results obtained were in agreement with the results of PT-PD.

Table 2.12: Viscosity, refractive index, pseudo-droplet diameter and nanostructure of optimised lecithin-based CER [EOS] MEs.

No.	ME	Viscosity (\pm RSD) ^a (mPa.s)	Refractive Index (\pm RSD)	Pseudo-droplet diameter (\pm RSD) (nm)	Nanostructure
1	PAPEOSME1	59.20 (1.326)	1.448 (0.001)	276.90 (25.50)	BC
2	PAPEOSME2	59.59 (0.161)	1.447 (0.001)	307.71 (25.23)	BC
3	PAPEOSME3	66.24 (1.287)	1.448 (0.000)	333.90 (32.48)	BC
4	PAPEOSME4	67.51 (0.995)	1.445 (0.000)	287.15 (54.61)	BC
5	PAPEOSME5	62.53 (1.198)	1.446 (0.001)	333.96 (22.59)	BC
6	PAPEOSME6	63.13 (1.316)	1.448 (0.000)	255.61 (34.26)	BC
7	PAPEOSME7	59.70 (0.161)	1.448 (0.001)	299.86 (49.52)	BC
8	PAPEOSME8	59.54 (0.581)	1.447 (0.001)	336.98 (23.57)	BC
9	PAPEOSME9	66.79 (0.498)	1.448 (0.000)	189.21 (34.27)	BC
10	PAPEOSME10	67.90 (0.616)	1.446 (0.001)	273.18 (48.40)	BC
11	PAPEOSME11	63.19 (0.547)	1.447 (0.000)	352.82 (17.35)	BC
12	PAPEOSME12	63.85 (0.397)	1.448 (0.000)	295.97 (24.68)	BC

^a exhibited Newtonian kind of flow

2.3.1.3. Formulation and Characterisation of CER [NP] MEs Containing other SC Lipids

Like CER [EOS] due to structural similarities between CER [AP] and CER [NP], the same ME components used for the preparation of CER [AP] MEs were also employed for the preparation of CER [NP] MEs. Accordingly, attempts were made to develop two sets of MEs, namely TCPL4 and lecithin-based CER [NP] MEs.

2.3.1.3.1. Formulation and Characterisation of TCPL4-based CER [NP] and other SC Lipids MEs

Despite structural similarities, preliminary studies showed that, like CER [EOS], CER [NP] needs a different microenvironment than CER [AP]. Hence, optimisation of the MEs was made by varying the proportions of the ME components (see detail in Appendix D) and the results showed that, unlike CER [AP] MEs, formulation of stable CER [NP] MEs needed relatively higher percentage of the oily phase. However, unlike CER [EOS] MEs, it was possible to obtain O/W type CER [NP] MEs and the MEs had higher loading capacity to CER [NP] than CER [EOS]. Lin A had slight negative effect on stability of CER [NP] MEs. Moreover, like CER [EOS] MEs, CER [AP] improved stability of CER [NP] MEs by several factors. CER [EOS] also enhanced stability of

CER [NP] MEs provided that the MEs are BC types. Like CER [AP] and CER [EOS] MEs, combination of HPGMO4 with TCPL4 (1:1) improved the stability of TCPL4-based CER [NP] MEs. CHOL affected stability positively, which might be attributed to its amphiphilic nature [159], whereas FFAs, especially BA, showed negative effect on the stability of CER [NP] MEs. Unlike CER [EOS] MEs, the negative effect of LA on stability of the MEs was not as pronounced as that of BA. Accordingly, ten TCPL4-based CER [NP] MEs were obtained for further characterisation (see Table 2.13).

Table 2.13: Compositions and stabilities of optimized TCPL4-based CER [NP] MEs.

No.	ME	IPP-Lin A (9:1) %	TCPL4-HPGMO4 (1:1) %	Water r-PeG (1:9) %	Water r-PeG (1.5:8.5) %	Water r-PeG (1:4) %	CER [AP] ^a %	CER [EOS] ^a %	CER [NP] ^a %	PA-SA-BA-LA (1:1:2:2) ^a %	CHOL ^a %	Stability (Month)
1	TNPOME1	15	30	-	55	-	0.2	-	0.1	-	-	>12
2	TNPOME2	15	35	-	50	-	0.2	-	0.1	-	-	>12
3	TNPOME3	20	30	-	50	-	0.2	-	0.1	-	-	>12
4	TNPOME4	15	30	55	-	-	0.2	0.05	0.1	-	-	>11
5	TNPOME5	15	35	-	50	-	0.2	0.05	0.1	-	-	>10
6	TNPOME6	20	30	-	50	-	0.2	0.05	0.1	-	-	>10
7	TNPOME7	15	35	-	50	-	0.2	0.05	0.1	0.1	0.15	>10
8	TNPOME8	20	30	-	50	-	0.2	0.05	0.1	0.1	0.15	>10
9	TNPOME9	20	35	45	-	-	0.2	0.05	0.1	0.1	0.15	>10
10	TNPOME10	15	35	-	-	50	0.2	0.05	0.1	-	0.15	>10

^a percent per total mass of the MEs

Characterisation

ME Nanostructure

Based on Fig 2.1, the nanostructures of TCPL4-based MEs of CER [NP] and other SC lipids were determined, Table 2.14.

Viscosity, Refractive Index and Droplet Size

The viscosity and refractive index of the 10 optimised TCPL4-based CER [NP] MEs are shown in Table 2.14. Despite the viscosity of the MEs was depended on the concentration of the SAA used, generally, the MEs had lower viscosities and all exhibited Newtonian kind of flow.

Table 2.14: Viscosity, refractive index, droplet diameter, and nanostructures of optimised TCPL4-based CER [NP] MEs.

No.	ME	Viscosity (\pm RSD) ^a (mPa.s)	Refractive Index (\pm RSD)	Droplet diameter (\pm RSD) (nm)	Nanostructure
1	TNPOME1	75.48 (0.890)	1.440 (0.040)	210.8 (30.36) ^b	O/W
2	TNPOME2	85.07 (0.851)	1.442 (0.000)	207.8 (78.63) ^b	O/W
3	TNPOME3	77.53 (4.404)	1.441 (0.069)	343.81 (21.20) ^b	O/W
4	TNPOME4	80.64 (0.315)	1.443 (0.040)	103.38 (39.18) ^b	O/W
5	TNPOME5	85.12 (0.406)	1.444 (0.040)	1193.05 (98.19)	BC
6	TNPOME6	82.41 (1.067)	1.442 (0.040)	723.43 (43.91)	BC
7	TNPOME7	85.23 (0.850)	1.443 (0.040)	259.13 (26.3) ^b	O/W
8	TNPOME8	83.07 (0.200)	1.442 (0.000)	266.34 (25.87) ^b	O/W
9	TNPOME9	112.81 (0.390)	1.446 (0.040)	207.2 (55.05) ^b	O/W
10	TNPOME10	88.50 (0.217)	1.441 (0.000)	611.6 (18.46) ^b	O/W

^a exhibited Newtonian kind of flow; ^b apparent RSD

Like TCPL4-based CER [AP] MEs, the D_{app} value of TCPL4-based CER [NP] MEs was dependent on the angle of measurement. However, in all the MEs, except TNPOME5 and TNPOME6, a linear relationship was obtained when Γ/q^2 was drawn against q^2 at different angles, suggesting that the MEs are droplet types. The droplet diameter was obtained by extrapolating the D values to 0° and the apparent RSD values that are calculated from the pseudo-droplet diameters were taken as indicator of the degree of droplet asymmetry, Table 2.14. In case of TNPOME5 and TNPOME6, no trend was observed when Γ/q^2 was drawn against q^2 and hence the MEs were classified as BC MEs. Most of the MEs obtained were near the O/W-BC MEs boundary, and unlike the nanostructures suggested by the PT-PDs, TNPOME2, TNPOME3, TNPOME7, TNPOME8, TNPOME9 and TNPOME10 were found to be O/W, which is most likely attributed to the incorporation of CERs, amphiphilic compounds, which can modify nanostructures of the MEs. Analysis of the results showed that, in general, MEs with higher percentage of SAA and lower oil percentage were smaller. The results also showed that the droplet diameter increased significantly as the ratio of water in the hydrophilic phase increases.

2.3.1.3.2. Formulation and Characterisation of Lecithin-based CER [NP] and other SC Lipids MEs

Preliminary studies revealed that CER [NP] needs a different microenvironment than CER [AP] and hence optimisation was made to select the right percentage of ME

components that can give stable lecithin-based CER [NP] MEs (see detail in Appendix D) and the results showed that, Unlike CER [AP] MEs, stable lecithin-based CER [NP] MEs needed a relatively higher percentage of the SAA. However, unlike CER [EOS] MEs stable CER [NP] MEs could be obtained at relatively lower percentage of oil and SAA. Like lecithin-based CER [EOS] MEs, incorporation of CER [AP] has increased stability of CER [NP] MEs tremendously. CER [EOS] has also increased stability of CER [NP] MEs but incorporation of CER [EOS] had to be followed by higher percentage of oil and SAA, which can form BC MEs. In the absence of the other stabilising CERs, generally, FFAs slightly decreased the stability of CER [NP] MEs, especially at lower percentages of oil and SAA. BA gave the least stable TCPL4-based CER [NP] MEs followed by PA, SA and LA. However, in the presence of CER [AP] and CER [EOS], the FFAs had, in general, positive influence on the stability of lecithin-based CER [NP] MEs. In all cases CHOL enhanced the stability of lecithin-based CER [NP] MEs. Consequently, optimum lecithin-based CER [NP] MEs were obtained for further characterization, Table 2.15.

Table 2.15: Compositions and stabilities of optimized TCPL4-based CER [NP] MEs.

No.	ME	M igl yo l %	Ph os al %	Wa ter- Pe G (1: 9) %	Wat er- PeG (1.5 :8.5) %	Wa ter- Pe G (1: 4) %	CE R [A P] ^a %	CE R [E OS] %	CE R [N P] ^a %	PA- SA- BA- LA (1:1: 2:2) ^a %	CH OL ^a %	Stabilit y (± SD) (Mon)
1	PNPOME1	5	35	60	-	-	0.3	-	0.2	-	-	10 (1)
2	PNPOME2	10	40	50	-	-	0.3	-	0.2	-	-	> 12
3	PNPOME3	15	45	40	-	-	0.3	-	0.2	-	-	> 12
4	PNPOME4	20	45	-	35	-	0.3	0.1	0.2	-	-	> 12
5	PNPOME5	20	45	-	35	-	0.2	0.1	0.2	0.15	0.2	>10
6	PNPOME6	20	40	-	-	40	0.2	0.1	0.2	0.15	0.2	>10

^a percent per total mass of the MEs

Characterisation

ME Nanostructure

Based on Fig 2.9, the nanostructures of lecithin-based MEs of CER [AP] and other SC lipids were determined, Table 2.16.

Viscosity, and Refractive Index and Droplet Size

The viscosity and refractive index of the optimized lecithin-based CER [NP] MEs are shown in Table 2.16. The viscosity of the MEs was mainly dependent on the concentration of the SAA. In addition, all the MEs had relatively low viscosities and exhibited Newtonian kind of flow.

Table 2.16: Viscosity, refractive index, droplet diameter and nanostructure of lecithin-based CER [AP] MEs.

No.	ME	Viscosity (\pm RSD) ^a (mPa.s)	Refractive Index (\pm RSD)	Droplet diameter (\pm RSD) (nm)	Nanostructure
1	PNPOME1	53.00 (1.437)	1.443 (0.000)	201.4 (14.22)	o/w
2	PNPOME2	58.21 (1.437)	1.446 (0.040)	259.2 (18.86)	o/w
3	PNPOME3	59.59 (0.161)	1.448 (0.040)	369.4 (65.89)	BC
4	PNPOME4	64.30 (0.517)	1.447 (0.040)	270 (9.39)	w/o
5	PNPOME5	64.08 (1.331)	1.447 (0.040)	257.6 (4.6)	w/o
6	PNPOME6	54.05 (0.470)	1.448 (0.000)	414.8 (7.31)	o/w

^a exhibited Newtonian kind of flow

The droplet diameter of lecithin-based MEs is given in Table 2.16. The D_{app} values of the MEs obtained were not angle dependent, with low RSD values, suggesting that the MEs are spherical droplet MEs. However, D_{app} values of PNPOME3 were dependent on the angle and there was observed no relationship when Γ/q^2 was plotted against q^2 , implicating the ME is BC type. The nanostructure suggested by PCS is in agreement with PT-PD. But according to the PT-PDs PNPOME4, PNPOME5 and PNPOME6 were BC MEs located at the borders, which however shifted into droplet type MEs due to the inclusion of CERs, which are amphiphilic in nature. In addition, like TCPL4-based CER [NP] MEs, those MEs with higher SAA, lower oil and lower ratio of water in the hydrophilic phase had smaller droplets.

2.4. Conclusion

Stable TCPL4 and lecithin-based CER [AP], CER [EOS] and CER [NP] MEs were formulated and characterised. It was also possible to incorporate other SC lipids along with the CERs. Generally, one CER improved the stability of MEs of other CERs. It was possible to obtain O/W and BC types of CER [AP] and CER [NP] and other SC lipid MEs. However, it was difficult to formulate O/W CER [EOS] MEs. The MEs

loading capacity was in the order of CER [AP] > CER [NP] > CER [EOS]. Formulation wise, generally, high percentage of PeG in the hydrophilic phase enhanced stability and formation of MEs. In addition, combination of HPGMO4 with TCPL4 enhanced the stability of TCPL4-based SC lipid MES. The formulations also contained small amount of the essential FFA Lin A, which was incorporated alone in case of TCPL4-based MEs or as part of safflower oil found in phosal, in case of lecithin-based MEs. In general, the MEs formed were bigger in diameter, which might help to control the depth of skin penetration of the lipids.

3. Skin Irritation/Corrosion Study

3.1. Introduction

MEs are promising colloidal drug delivery systems that have a very high active loading capacity, due to the existence of different microenvironments within a macroscopically homogenous system and their enormous interface area, and an excellent permeation enhancing effect [64, 67, 91-92]. However, the higher percentage of SAA(s) needed for their formulation could irritate or corrode tissues [130]: although most of the SAAs used during ME preparation are pharmaceutically approved they might be toxic at higher concentrations. Besides, the oils and co-SAAs used might irritate the skin when used at higher concentrations. Therefore, the irritation and corrosive potential of the MEs was investigated.

There are some established animal *in vivo* methods designed to conduct skin irritation and toxicity studies [98-99, 107]. Nonetheless, these methods need exploitation of experimental animals. However, over the years HET-CAM test was developed as a sound alternative to the animal *in vivo* tests used to investigate the corrosive potential of pharmaceutical preparations on the skin and mucus membrane [181-182]. Hence, it was used to evaluate the compatibility of both TCPL4-and lecithin-based MEs with the skin.

3.2. Materials and Method

3.2.1. Materials

TCPL4, Evonik-Goldschmidt GmbH, Essen, Germany; HPGMO4, Hydrior AG massgeschneiderte Tenside, Wettingen, Germany; PeG, Symrise GmbH & Co KG, Holzminden, Germany; Lin A, Sigma-Aldrich Chemie GmbH, Taufkirchen, Germany; IPP and miglyol, Caesar & Loretz GmbH, Hilden, Germany; phosal, Phospholipid GmbH, Köln, Germany were the major materials used for the study. Double distilled water was used throughout.

3.2.2. Method

Hen's Egg Test Chorioallantoic Membrane (HET-CAM)

An *ex vivo* toxicity study of the MEs was carried out using HET-CAM. For the study fertilised eggs of the New Hampshire hens were incubated at 37°C and relative humidity

of 55 % for 8 days, turning them every 12 h, except during the last 24 h. Then a circular hole with a diameter of about 1.5 cm was cut on the less convex pole of the eggs under a laminar air flow box. The amnion was then carefully removed to expose the CAM and 100 μ l of the test MEs, 1 % sodium lauryl sulphate (SLS) (positive control) and normal saline (negative control) were applied on the CAM. Finally, the CAMs were observed for 300 seconds for occurrence of any haemorrhage (H: bleeding from the vessels), vascular lyses (L: blood vessel disintegration) and coagulation (C: intra-and extra-vascular protein denaturation). The experiments were conducted in six replicates and the data were analysed for outliers using anomalous observations of the data.

3.3. Results and Discussion

The irritation scores (ISs) of different MEs were determined in order to evaluate the skin irritation or corrosion potential of selected TCPL4-based and lecithin-based MEs (Table 3.1) using HET-CAM.

Table 3.1: Compositions and ISs of selected TCPL4 and lecithin-based MEs (n=6).

N o.	Formulation	IPP %	Lin A %	Migl yol (%)	TCP L4 %	Phos al (%)	Water -PeG (1:9) %	Water -PeG (1.5:8.5) %	Water -PeG (1:3) %	IS (± RSD)
1	TCPME1	4	1	-	30	-	-	65	-	0.07 (0.00)
2	TCPME2	4	1	-	30	-	65 ^a	-	-	0.07 (0.00)
3	TCPME3	5	2 ^a	-	30	-	-	63	-	0.26 (0.46)
4	TCPME4	5	2 ^a	-	40 ^a	-	53 ^a	-	-	0.71 (1.57)
5	PHOSME1	-	-	5	-	30	-	65	-	0.07 (0.00)
6	PHOSME2	-	-	5	-	35	60 ^a	-	-	0.07 (0.00)
7	PHOSME3	-	-	15 ^a	-	35	-	-	50	0.07 (0.00)
8	PHOSME4	-	-	10	-	45 ^a	50 ^a	-	-	0.52 (1.09)
9	1% SLS	-	-	-	-	-	-	-	-	8.57 (1.61)
10	Normal saline	-	-	-	-	-	-	-	-	0.07 (0.00)

^a too high concentration of the component

Since SC lipids are endogenous substances, only the irritation potential of MEs without SC lipids was investigated. As can be seen in Table 3.1, the irritation potential of the MEs was assessed at low and relatively higher percentages of the oil, SAA and PeG in the hydrophilic phase. 1 % SLS and normal saline were used as positive and negative controls, respectively.

According to ICCVAM [183], the IS, calculated using Eqn. 3.1, can be used to assess the degree of irritation caused by pharmaceutical preparations: 0-0.9 non-irritant; 1-4.9 slight irritation potential; 5-8.9 moderate irritation potential and 9-21 severe irritation potential.

$$IS = \left(\frac{301 - sekH}{300} * 5 \right) + \left(\frac{301 - sekL}{300} * 7 \right) + \left(\frac{301 - sekC}{300} * 9 \right) \dots \text{Eqn. 3.1}$$

Where; sek is seconds before the start of the event, H=haemorrhage; L= lyses; C= coagulation

As can be seen in Table 1, in TCPL4-based MEs, as the levels of Lin A and SAA increase the IS value also increased slightly. While, in lecithin-based MEs, as the percentage of phosal increases IS increased slightly. However, the results clearly showed that all the MEs were non-irritant with most of them have IS values close to normal saline. 1 % SLS had higher IS values and was classified as moderately irritant.

3.4. Conclusion

The HET-CAM result of both TCPL4-based MEs and lecithin-based MEs showed no sign of irritation or inflammation suggesting that they are safe to be applied on the skin and mucus membrane. MEs with low percent of Lin A and SAA were, however, preferable.

4. *In Vitro* Release and Penetration Study

4.1. Introduction

The process of drug absorption through the skin involves liberation of the active from the dosage form, penetration through the SC, permeation through the epidermis and absorption into the blood vessels and lymphatic system in the dermal layer. However, the objective of this work is to strengthen the barrier function of affected and/or aged skin through administration of SC lipids, which will be mingled into the lipid lamellae at the SG-SC interface [11, 14-16]. Thus, the release and penetration of the lipids into the SC are vital steps that need to be investigated.

4.2. Materials and Methods

4.2.1. Materials

CER [AP] and TCPL4, Evonik-Goldschmidt GmbH, Essen, Germany; HPGMO4, Hydrior AG massgeschneiderte Tenside, Wettingen, Germany; PeG, Symrise GmbH & Co KG, Holzminden, Germany; Lin A, Sigma-Aldrich Chemie GmbH, Taufkirchen, Germany; 4 % collodion, IPP and miglyol, Caesar & Loretz GmbH, Hilden, Germany; phosal, Phospholipid GmbH, Köln, Germany; acetic acid (HAC), Grüssing GmbH, Filsum, Germany; n-hexane, NeoLab Migge GmbH, Heidelberg, Germany; chloroform, Merck, Darmstadt, Germany; diethyl ether, Overlack GmbH, Leipzig, Germany; HPLC grade methanol, VWR international, Darmstadt, Germany; absolute ethanol, Bundesmonopolverwaltung für Branntwein, Offenbach, Germany; non-ionic emulsifying alcohol and glycerol (85 %), Bombastus-Werke AG, Freital, Germany; liquid paraffin, Hansen & Rosenthal KG, Hamburg, Germany; DMSO and anhydrous citric acid, Carl Roth GmbH, Karlsruhe, Germany; potassium sorbate, Fluka, Buchs, Switzerland; octanol and dodecanol, Sasol Germany GmbH, Brunsbüttel, Germany, were the major materials used for the study. Double distilled water was used throughout.

4.2.2. Methods

4.2.2.1. Solubility Study

Excess amount of CER [AP] was added into an ampoule containing a solvent of interest and the ampoule was sealed and kept for 48 hrs at 32°C in a water bath, which was

subjected to vibration. Then, the solvent was rapidly filtered using a 0.45 μm hydrophobic PERFECT-flow[®] PTFE membrane filter (WICOM Germany, Heppenheim, Germany) and was sufficiently diluted in excess methanol preceding quantification of the amount of CER [AP] dissolved using AMD-HPTLC (see Section 4.2.2.4). The experiment was conducted in triplicates.

4.2.2.2. Model Membrane Preparation

100 g of the membrane solution was prepared by mixing 50 g 4 % (m/m) collodion solution and 50 g 8 % (m/m) dodecanol mixture (dodecanol/octanol/DMSO, 80:10:10, v/v/v) in 15 % (v/v) ethanol in diethyl ether. The membrane solution was then spread evenly over a glass surface of about (500 mm x 300 mm) on a film applicator with adjustable clearance (Institute of Pharmacy, Martin Luther University Halle-Wittenberg Workshop) and was allowed to dry in a fume hood for about 12 hrs. The film was, finally, removed and cut into 40 mm diameter discs.

4.2.2.3. *In Vitro* release and Penetration Study

The rate and extent of release and penetration of CER [AP] from various dosage forms was investigated by an *in-vitro* multi-layer membrane model described by Neubert et al. (1991) [184]. The model contains penetration cells arranged one over the other in a penetration cell stand. Each penetration cell comprised four layers of circular 40 mm membrane films arranged one over the other. The membrane stack was placed on a circular base plate, Fig 4.1. To prevent adhesion of the bottom membrane to the base plate a nitrocellulose film was put between the bottom membrane and the base plate. A stencil, with a square opening of 4 cm² at the centre, was put above the membranes to enable application of the formulations and the whole cell was covered by a covering plate. During release and penetration investigation an equivalent mass of the formulation that contain 50 μg CER [AP] was evenly spread through the stencil over the upper membrane and the cells were kept at 32°C in a thermostatic chamber for predetermined time intervals (15, 30, 60,120 and 180 min) allowing release and penetration of CER [AP]. Then the cells were taken, the formulation remained unabsorbed over the surface of the first layer was removed with a tissue paper (except those cells used to calculate the percentage recovery), the membranes were separated, put in test tubes and were extracted by sonication at 50°C for 30 min in 1 ml n-Hexane-ethanol (2:1, v/v). The amount of CER [AP] extracted was quantified using AMD-

HPTLC (see Section 4.2.2.4). Five and three replicate studies were conducted for test and recovery samples, respectively. To assess the interaction of formulation and membrane components peaks with CER [AP] peak, the experiment was also conducted for blank formulation at 180 min. One-way ANOVA at $p < 0.05$ was conducted followed by Tukey's test as post hoc analysis to indicate the existence of significant differences between sets of data.

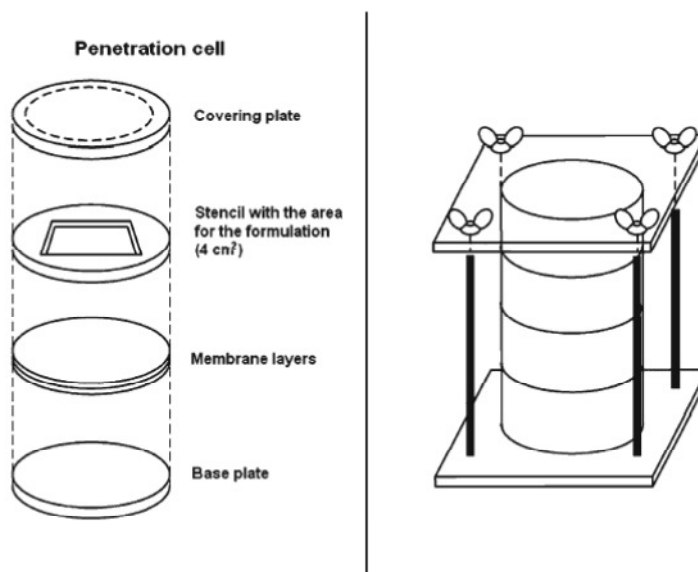


Figure 4.1: Schematic representation of a multi-layer membrane model described by Neubert et al (1991) adopted from [184].

4.2.2.4. Automated Multiple Development (AMD)-HPTLC

A Camag HPTLC system with CAMAG win CATS planer chromatographic manager (Camag, Muttenz, Switzerland) was used for the quantification of CER [AP] during the *in-vitro* release and penetration study. 5 μ l of test and standard samples were applied as 3 mm bands at 6 mm intervals under N_2 stream on a TLC plate (TLC silica gel 60 F254, 20cm x 10cm, Merck KGaA, Darmstadt, Germany) using CAMAG Automatic TLC sampler 4. Chromatographic development was conducted twice using chloroform-methanol-HAC (94.5:5:0.5, v/v/v) as a mobile phase over a distance of 70 mm using CAMAG AMD 2. Then the HPTLC plate was dipped in an aqueous $CuSO_4$ solution (10 % $CuSO_4$ (W/v), 8 % phosphoric acid (w/v) and 5 % methanol (V/V)) for 20 seconds and was charred at 160°C for 20 min in an oven. Finally, the plate was scanned by CAMAG TLC Scanner 3 in absorbance mode (358 nm) and the results were analyzed.

4.3. Results and Discussion

4.3.1.1. Solubility of CER [AP] in Dodecanol and Dodecanol Containing Solvent Mixtures

Before assessing the release and penetration of CER [AP], its solubility in dodecanol and dodecanol containing mixtures was determined at 32°C, Table 4. 1. The results showed that CER [AP] is very slightly soluble in dodecanol and the other solvent mixtures. However, incorporation of small percentages of octanol and especially DMSO enhanced solubility of CER [AP] approximately two to four folds.

Table 4.1: Solubility of CER [AP] in dodecanol and other dodecanol containing mixtures at 32°C (N=3).

No.	Solvent/solvent mixture	Solubility (± SD) at 32°C (mg/ml)
1	Dodecanol	1.53 (0.32)
2	Dodecanol-octanol (9:1, v/v)	2.37 (0.13)
3	Dodecanol-octanol-DMSO (8.5:1:0.5, v/v/v)	4.06 (0.51)
4	Dodecanol-octanol-DMSO (8:1:1, v/v/v)	6.52 (0.43)

4.3.1.2. *In Vitro* Release and Penetration Studies

Assessment of release and penetration of CER [AP] from various dosage forms was carried out using a multi-layer membrane model described by Neubert et al. (1991) [184]. For the assessment, 2 TCPL4-based and 2 lecithin-based CER [AP] MEs, which exhibited excellent stability, were chosen (see Table 4.2). Besides, a hydrophilic cream containing CER [AP] was used as a reference formulation, Table 4.3.

Table 4.2: Characteristics of TCPL4 and lecithin-based CER [AP] MEs chosen for release and penetration study.

No.	ME	Droplet diameter (± RSD) (nm)	Viscosity (± RSD) (mPa.s)	Microviscosity (mPa.s)	Nanostructure
1	TAPOME2	234.4 (84.83) ^a	85.9 (1.02)	47.98	W/O
2	TAPOME8	244.0 (110.12) ^a	87.3 (0.77)	62.35	O/W
3	PAPOME2	176.94 (7.49)	60.3 (1.227)	24.22	O/W
4	PAPOME8	197.14 (5.47)	61.4 (1.726)	34.55	O/W

^a apparent RSD

As can be seen in Table 4.2, apart from excellent stability, the MEs chosen have different diameters and nanostructures, where their effect on the release and penetration of the CERs was assessed.

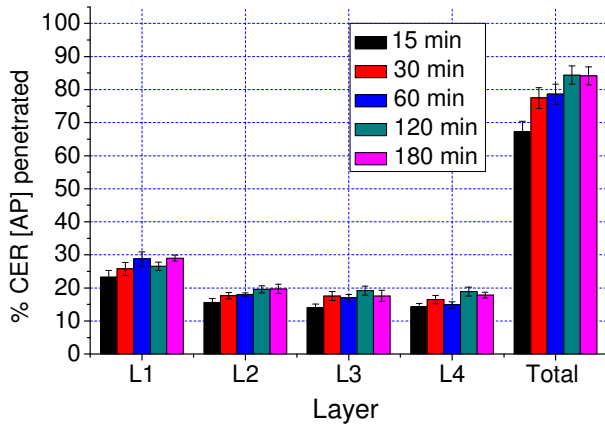
Table 4.3: Compositions of a conventional hydrophilic cream (DAC) used as reference formulation during release and penetration studies of CER [AP] from MEs.

No.	Ingredient	Hydrophilic cream (%)
1	CER [AP]	0.5
2	Non-ionic emulsifying alcohol	21
3	Liquid paraffin	10
4	Glycerol (85 %)	4.5
5	Potassium sorbate	0.14
6	Anhydrous citric acid	0.07
7	Double distilled water	63.79

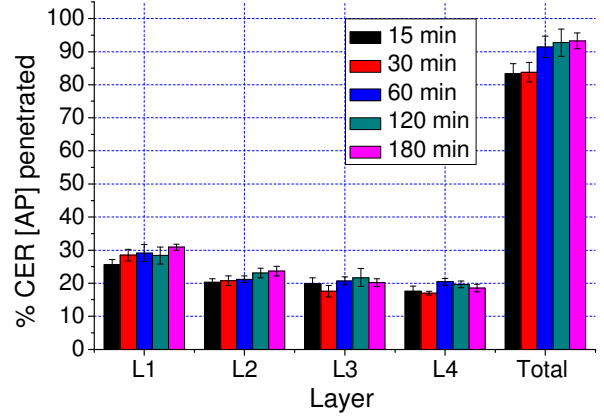
Generally, *in vitro* models should simulate *in vivo* conditions and, hence, during assessment of release and penetration of actives using such models it is vital to maintain the sink condition. In multi-layer membrane model, the total number of membranes that contains equivalent amount of dodecanol mixture, in which the maximum concentration of the active remain bellow (10-15) % of it saturation solubility, supposing 100 % of active is penetrated, was assumed to maintain the sink condition. Therefore, for this particular experiment 4 membranes were sufficient to maintain the sink condition.

In the collodion-dodecanol membrane, the collodion forms a mesh and provides mechanical support for dodecanol, which will be embedded in and simulate the SC lipids by virtue of its lipophilicity [184]. The dodecanol mixture also contains 10 % octanol to provide membrane stability and, in our case, it also enhanced the solubility of CER [AP] in the membrane along with the 10 % DMSO added in the dodecanol mixture, Table 4.1, enabling attainment of the sink condition with less number of the membranes. That is, for the quantity of CER [AP] applied on the surface, in the absence of octanol and DMSO, to maintain the level of CER [AP] bellow 15 % of its saturation solubility, more than 10 membranes should have been used and it is practically difficult to handle. However, incorporation of 5 and 10 % of DMSO, besides octanol, improved the solubility of CER [AP] by about 100 and 200 % and reduced the number of membranes needed to maintain the sink condition to 8 and 4 membranes, respectively.

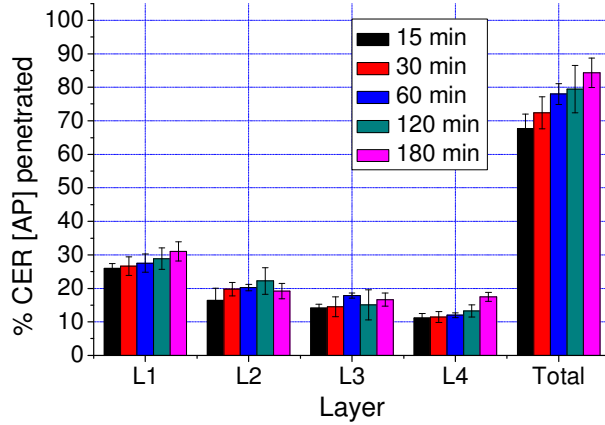
Therefore, dodecanol-octanol-DMSO (8:1:1, v/v/v) was chosen for the preparation of the artificial membrane.



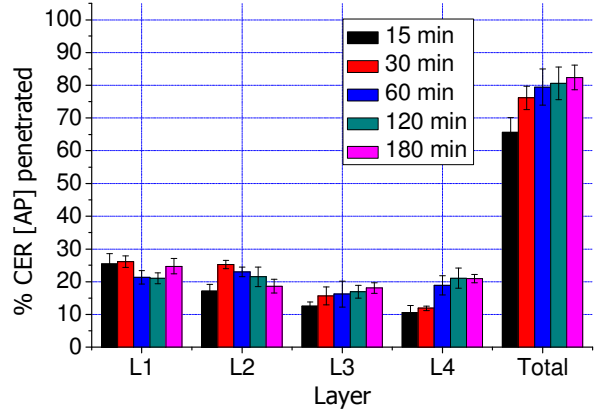
a) TAPOME2



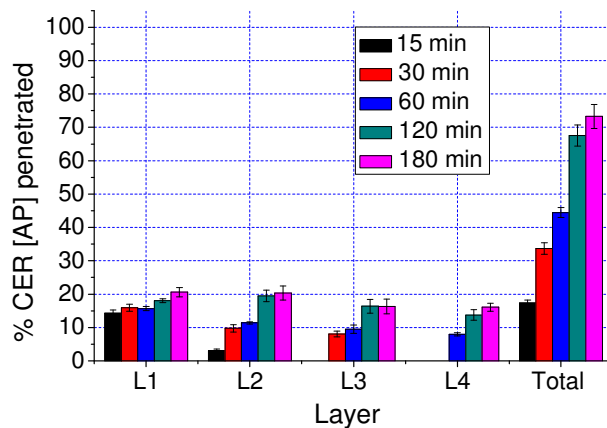
b) TAPOME8



c) PAPOME2



d) PAPOME8



e) Hydrophilic cream

Figure 4.2: Rate of CER [AP] released and penetrated into the deeper layers of the multi-layer membrane model comprised of 4 membranes (N=5).

The result of release and penetration study of the formulations into different layers of the model membrane is shown in Figs 4.2 (a-e). As can be seen in the figures, within 15 min a higher percentage of CER [AP] was released and penetrated from the MEs into the deeper membrane layers. However, from the hydrophilic cream, unlike the MEs, a very small percentage of the CER penetrated into the second layer and no CER [AP] was detected on the third and fourth layers after 15 min. This suggests that release and especially penetration of the CER from the MEs is by far better than the hydrophilic cream. Besides, the degree of penetration of the CER into the deeper layers from TAPOME8 was better than the other MEs. This can be attributed to its nanostructure, which is O/W, and composition.

The release and penetration profile of the total amount of CER [AP] into the four membrane layers is shown in Fig 4.3. As can clearly be seen in the figure, the rate and extent of release and penetration of CER [AP] from the MEs was by far better than the conventional hydrophilic cream, suggesting that MEs could significantly enhance the rate and extent of CER [AP] release and penetration. Table 4.4 also designates the key *in vitro* pharmacokinetic parameters describing the release and penetration process, which includes area under the curve (AUC), area between the curves (ABC); total percent CER [AP] released and penetrated (Mo) and mean dissolution time (MDT). Pharmaceutical formulations, which exhibit lower MDT and higher AUC have better rate and extent release and penetration, respectively. Accordingly, the results in Table 4.4 showed that the MEs have tremendously improved the rate and extent of CER [AP] penetration in comparison to the hydrophilic cream.

In addition, the results showed that the rate and extent of CER [AP] released and penetrated from TAPOME8 was better than TAPOME2, suggesting release and penetration from O/W MEs is better than that of W/O MEs. It was also supported in the literature that release and penetration of lipophilic substances is better from O/W MEs than W/O MEs [93]. The release and penetration of CER [AP] from TAPOME8 was also much better than PAPOME2 and PAPOME8 and, given all the three MEs are O/W types, the results suggested that the release and penetration from TCPL4-based MEs is better than that of lecithin-based MEs. Moreover, those MEs with higher microviscosity showed better release and penetration: higher microviscosity partly indicates high level of probe entrapment and formation of smaller O/W MEs. However, the difference in release and penetration observed between TAPOME2, PAPOME2 and PAPOME8 was

statistically insignificant ($P < 0.05$). Concluding MEs tremendously improved the release and penetration of CER [AP] into the model membranes and the release and penetration from TCPL4-based and O/W type MEs was faster and deeper than lecithin-based and W/O type MEs.

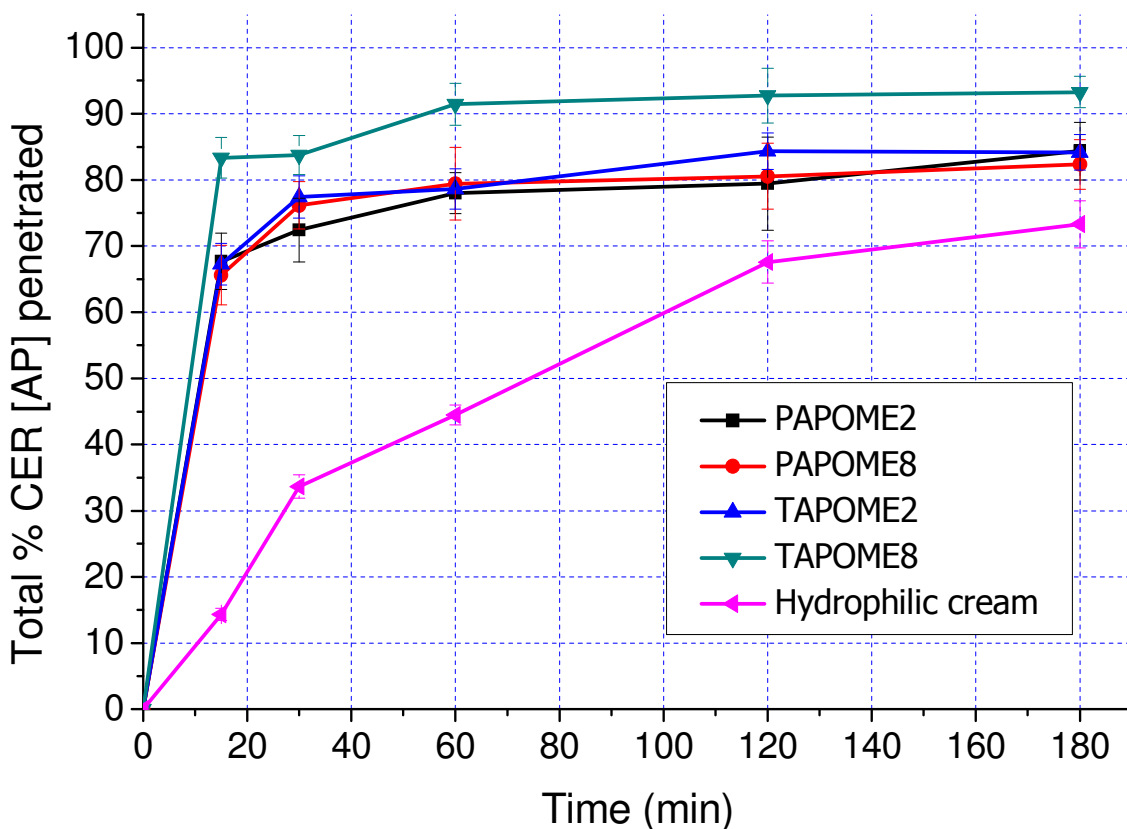


Figure 4.3: Overall release and penetration profile of CER [AP] from various formulations into membranes of multi-layer membrane model (N=5).

Table 4.4: *In vitro* pharmacokinetic parameters obtained from release and penetration study of CER [AP] from selected dosage forms (n=5)

No.	Formulation	AUC \pm SD (% . min)	M ₀ \pm SD (%)	ABC \pm SD (% . min)	MDT \pm SD (min)
1	TAPOME2	13502.80 (263.16)	84.19 (2.90)	1651.18 (298.27)	19.53 (2.86)
2	TAPOME8	15581.40 (304.00)	93.40 (2.31)	1282.59 (207.06)	13.66 (1.96)
3	PAPOME2	13521.23 (183.12)	84.80 (2.79)	1745.84 (406.81)	20.44 (4.21)
4	PAPOME8	13592.48 (233.54)	82.84 (1.56)	1331.05 (361.18)	16.04 (4.11)
5	Hydrophilic cream	9185.625 (283.06)	73.29 (3.32)	4127.11 (561.19)	55.60 (5.45)

4.4. Conclusion

The results of the *in vitro* release and penetration study showed that release and penetration from MEs was much better than a conventional cream. Besides, the rate and extent of release and penetration from O/W ME was much better than W/O type ME: O/W ME could penetrate to a greater extent into the deeper layers than W/O ME. Hence, the results obtained inspired *ex vivo* and *in vivo* permeability studies from MEs containing CER [AP]. In addition, since CERs share some physicochemical characteristic and CER [EOS], CER [NP] and FFAs have reduced polarities than CER [AP] similar or slightly improved release and penetration profiles are expected from both TCPL4-based and lecithin-based MEs of other SC lipids.

5. *Ex Vivo* Skin Permeability Study

5.1. Introduction

Skin is the largest organ of the body [185] that plays a significant role in maintaining the body homeostasis through provision of an excellent barrier against environmental insults and preventing the loss of water and other essential compounds from the body [17]. Its barrier function lies mainly on the highly impermeable outer most layer of the epidermis, the SC. It contains corneocytes, the dead *keratin*-filled squamous cells, embedded in a lipid matrix, which forms the only continuous pathway along the SC and, subsequently, provides the barrier [11, 17-18, 20-21, 23-24]. The lipid matrix exists in the form of lipid lamellae that have a unique composition and form a unique and impervious lipid organisation. Although the spatial organisation of the lipids within the matrix is not yet fully understood, any disruption of the composition may lead to disruption of the lipid organisation, that in return perturb the barrier function of the skin, which may further lead to inflammatory conditions. The inflammation may also cause further perturbation of the barrier function and could result in diseased skin [16, 59]. Conversely, several skin disease conditions, such as psoriasis [147], AD [13, 16, 148] and irritant/allergic contact dermatitis [148] are associated with depletion or disturbance of SC lipids in the SC [11]. Therefore, to treat the cause and/or the effect and break the vicious cycle it might be necessary to supply adequate amount of the depleted SC lipids, which can be CERs, FFAs and/or CHOL. However, organisation of the SC lipid into lipid bilayers takes place at the SG-SC interface [11, 14-16] and hence it is necessary to deliver the lipids deep into the interface.

Usually it is difficult to deliver the lipids deep into the interface using conventional dosage forms like ointments and creams [91-93]. Nonetheless, unlike conventional topical preparations permeation of substances from colloidal drug delivery systems, like MEs and ME gels, was found to be promising [93, 99, 114]. ME gels have an added advantage of easy pharmaceutical application owing to their higher viscosity and better adhesion to the skin [98-99]. Thus, with this premise in mind, MEs and ME gels, which are safe to be applied on the skin, were developed and characterised to enhance permeation of the SC lipids into the lower layers of the epidermis and showed an excellent release and penetration *in vitro* and it should be followed by *in vivo* permeability experiments. However, preceding *in vivo* investigations, few *ex vivo* models, such as Franz diffusion cell [72, 93, 107, 181], has been proposed to investigate

the permeability of drugs through the skin. Therefore, the permeability of the SC lipids from the MEs and ME gels was assessed *ex vivo* using Franz diffusion cell and CER [NP] as a model lipid.

5.2. Material and Methods

5.2.1. Materials

CER [AP], CER [EOS], phytosphingosine (1,3,4-octadecanetriol, 2-amino-, (2S, 3S, 4R)-) and TCPL4, Evonik-Goldschmidt GmbH, Essen, Germany; HPGMO4, Hydrior AG massgeschneiderte Tenside, Wettingen, Germany; PeG, Symrise GmbH & Co KG, Holzminden, Germany; Lin A, Sigma-Aldrich Chemie GmbH, Taufkirchen, Germany; IPP and miglyol, Caesar & Loretz GmbH, Hilden, Germany; phosal, Phospholipid GmbH, Köln, Germany; octadecanoic-18,18,18-d₃ acid (deuterated SA), Dr. Ehrenstorfer GmbH, Augsburg, Germany; tris(hydroxymethyl)aminomethane (tris), potassium sorbate and 2-Ethoxy-1-ethoxycarbonyl-1, 2-dihydrochinolin (EEDQ), Fluka, Buchs, Switzerland; HAC, Grüssing GmbH, Filsum, Germany; n-hexane, NeoLab Migge GmbH, Heidelberg, Germany; non-ionic emulsifying alcohol and glycerol (85 %) Bombastus-Werke AG, Freital, Germany; liquid paraffin, Hansen & Rosenthal KG, Hamburg, Germany; anhydrous citric acid, Carl Roth GmbH, Karlsruhe, Germany; Carbopol[®] 940 (carbopol), Noveon, Inc., Cleveland, Ohio, USA; chloroform and silica gel 60, 0.06-0.200 mm, Merck, Darmstadt, Germany; HPLC grade tetrahydrofuran (THF), Sigma-Aldrich, Steinheim, Germany; HPLC grade methanol, VWR international, Darmstadt, Germany; absolute ethanol, Bundesmonopolverwaltung für Branntwein, Offenbach, Germany were the major materials used for the study. Double distilled water was used throughout. A human thigh skin was kindly donated by the Department of Dermatology and Venereology of the Faculty of Medicine, Martin Luther University Halle-Wittenberg, after approval by the independent ethics committee of the Faculty.

5.2.2. Methods

5.2.2.1. Synthesis of CER [NP]-D₃-18 (Deuterated CER [NP])

Deuterated CER [NP] was synthesized by dissolving 0.98 mmol 18, 18, 18-D₃-octadecanoic acid, 1.46 mmol EEDQ and 0.98 mmol phytosphingosine in 30 ml ethanol. The reaction mixture was stirred continuously for 24 hrs at 55°C. Then 1 mmol

EEDQ was further added and the reaction was allowed another 12 hrs. During the reaction, the reaction process was controlled by TLC. Upon completion of the reaction process, the reacting mixture was concentrated to 1/5 of its original volume and 52.5 ml chloroform-methanol (20:1, v/v) was added. Then, the mixture was transferred into a separatory funnel, 100 ml 3 % HCl (36 % v/v) solution was added and the mixture was thoroughly mixed. Emulsion developed through the reaction process was broken by filtration and the filter was rinsed twice using 25 ml warm chloroform. Finally, the two layers were allowed to equilibrate and the organic layer was separated, dried for 24 hrs over sodium sulfate, filtered and the solvent was evaporated leaving deuterated CER [NP]. Chloroform was dried through refluxing over P₂O₅ for 2 hrs before use.

5.2.2.2. Column Chromatography

Purification of the synthesized deuterated CER [NP] was conducted by a column chromatographic technique. A conditioned chromatographic column was used, which was filled with a slurry of silica gel 60 (100 g silica gel per 1 g substance) in chloroform and was allowed to settle. The substance was also dissolved in chloroform and was poured slowly into the column. A gradient system, comprising 200 ml of increasing percentages of methanol in chloroform (0, 1, 2, 3, 4 and 5 %), was used as a mobile phase and, subsequently, about 30 ml chromatographic fractions were collected. Deuterated CER [NP] containing fractions were identified by TLC. Chloroform was dried before use through refluxing over P₂O₅ for 2 hrs.

5.2.2.3. Thin Layer Chromatography

Identification of deuterated CER [NP] during the synthesis and purification steps was made by TLC. Silica gel 60 F254 plate (5x10 cm, Merck KGaA, Darmstadt, Germany) was used as a stationary phase and before chromatographic development the chromatographic chamber was saturated with a mobile phase, Chloroform-ethanol (9:1, v/v). Chromatographic development was carried out until the solvent front reached the end of the TLC plate and it was then removed, dried and sprayed with bromothymol blue indicator solution, which formed a yellowish molecular complex that turned to blue when fumigated with ammonia vapor. Since EEDQ is fluorescent active it was identified under UV-lump before spraying the plate with indicator solution. Other components were identified by comparing their R_f values with reference compounds.

5.2.2.3.1. LC/ESI-MS Method Development

An Agilent 6100 series HPLC (Agilent Technologies, Waldbronn, Germany) coupled with Agilent Technologies 6120 Quadrupole MS (Agilent Technologies, Waldbronn, Germany) with ESI ionization interface was used for the analysis of deuterated CER [NP] during permeability studies. A reversed phase Nucleosil® C-18 HPLC column (125 mm x 2 mm, 120-3, Macherey-Nagel, Düren, Germany), fitted with a C-18 precolumn, was used as a stationary phase while an isocratic system containing methanol-THF-water-HAC (80:10:10:0.2, v/v/v/v) was used as a mobile phase. The mobile phase flow rate, injection volume and column temperature were set at 0.2 ml/min, 10 µl and 25°C, respectively. Samples were prepared in methanol. ESI-MS was used as a detector with negative ionisation mode and at a fragmentor voltage of 180; capillary voltage of 4000 V; nebulizer pressure of 20 psig; drying gas flow rate of 11 L/min and drying gas temperature of 350°C. N₂ was used as both nebulizer and drying gas.

5.2.2.4. LC/ESI-MS Method Validation

Calibration curve and method linearity was determined following linear regression analysis of the peak areas of 7 standard deuterated CER [NP] solutions in methanol (10, 50, 100, 200, 400, 600 and 800 ng/ml). The peak areas obtained from the standard concentrations were plugged into the calibration equation and the standard concentrations were back calculated to determine accuracy of the calibration equation. The LOD and LOQ of the method were determined according to the 1996 analytical detection limit guidance [186]. Consequently, the peak areas of eleven 10 ng/ml deuterated CER [NP] solutions were determined and their concentrations were calculated to calculate LOD and LOQ. The within-run and between-run precision and accuracy of the method were determined by analyzing five replicates of the control sample containing 10, 30, 300 and 700 ng/ml solutions of deuterated CER [NP] in methanol over a single run and five runs over three days, respectively. Method selectivity was analysed by observing the interactions of the chromatographic peaks of six pure SC extracts obtained from different sources with the pure deuterated CER [NP] peak. Whereas, matrix effect was determined through determination the matrix factor (MF= peak area in the presence of matrix/ peak area in the absence of matrix) of six SC extracts, which were spiked with 30 ng/ml of the deuterated CER [NP]. The occurrence of any MS peak within the retention window of deuterated CER [NP] after injecting

blank samples preceded by three CER [NP] samples dissolved in the SC extract (800 ng/ml) was observed to investigate method carry-over effect. Unless specified all the experiments were done in triplicates.

5.2.2.5. Preparation of MEs and ME Gels

During ME preparation, all the ME components were mixed in a test tube and were sonication for 45 min at 50°C. ME gels were prepared by slowly dispersing carbopol 940 in MEs, avoiding lump and air bubble formation, followed by pH adjustment using 10 µl 7.5 % tris per 1g ME.

5.2.2.6. *Ex Vivo* Permeability Experiment

A piece of excised human thigh skin (postoperatively cleaned and the subcutaneous tissue mechanically dissected) was mounted on a Franz diffusion cell (Crown Glass Company, Somerville, NJ, USA) the outer side of the skin facing the donor compartment. The acceptor compartment was filled with distilled water and 20 mg of the formulation was applied uniformly on the skin surface (3.1416 cm²) and was allowed to permeate for 300 min. The temperature of the cell was maintained at 32°C using circulating water. After 300 min the apparatus was disassembled, the remaining formulation on the skin surface was thoroughly wiped with a cotton swab and the SC layer was removed by tape striping: 10 tape strips each representing two layers of the SC, over an area of 2.016 cm². Subsequently, three 0.6 cm dm discs were punched out using a Kromayer punch (Stiefel-Laboratorium, Offenbach, Germany) and the epidermal layer (EP), four 20 µm slices, was removed using a cryo-microtome (Jung, Heidelberg, Germany). Other five 40 µm thick slices were cut out to represent the dermal layer (DR) together with the remaining piece of tissue. Then each skin layer, including the swab, was sonicated at 50°C for 2 hrs in n-Hexane-ethanol (2:1, v/v) and was left overnight for maximum lipid extraction. Following extraction, the supernatant was taken, the solvent was evaporated at 60°C under a stream of N₂ gas, the residue was reconstituted in methanol, sonicated at 50°C for 15 min, filtered (0.45µm, Mini-UniPrepTM, GE healthcare UK Limited, Buckinghamshire, UK) and the deuterated CER [NP] was quantified using LC/ESI-MS. During extraction, the 5 tape strips obtained from the SC were considered as upper SC (USC) layers, whereas, the lower 5 tape strips of the SC were considered as lower SC (LSC) layers. The volume of liquid in the acceptor compartment was lyophilized (Alpha 2-4 Christ, Martin Christ

Gefriertrocknungsanlagen GmbH, Osterode, Germany) and was treated like the other skin layers. Prior to the experiment an ethical clearance was obtained from the independent ethics committee of the Faculty of Medicine, Martin Luther University Halle-Wittenberg. One-way ANOVA at $p < 0.05$ was conducted followed by Tukey's test as post hoc analysis to indicate the existence of significant differences between sets of data.

5.3. Results and Discussion

5.3.1. Method Development and Validation

- **Synthesis of Deuterated CER [NP]**

Several skin diseases are associated with the depletion or perturbation of SC lipids, Table 1.1, and hence administration of SC lipids to the SC is believed to help restore the barrier function of affected and aged skin. To that end there are few preparations in the market that contain CERs (e.g. CeraVe, TriCeram, Atopiclair, and Mimyx Cream). However, to our knowledge their permeation deep into the target site at which they assemble into a meaningful barrier was not assessed. Despite the availability of several methods developed for the quantification of SC lipids [35, 58, 187], this may mainly attribute to unavailability of a selective analytical method that can discriminately identify and quantify the CERs penetrated into the SC and other layers of the skin. Our main objective was also to administer and quantify SC lipids deep into the SC. Therefore, it was mandatory to develop a selective analytical method that can quantify the amount of exogenous SC lipids permeated. Hence, a selective and sensitive LC/ESI-MS method was developed for the quantification of CER [NP], as a model SC lipid, permeated deep in the SC. The method involved synthesis of deuterated CER [NP] from phytosphingosine and 18,18,18-D₃-octadecanoic acid using EEDQ as a condensing agent [188], Fig 5.1. The reaction started as the nucleophilic carboxylate anion of the FFA attacks the electrophilic carbon atom of EEDQ ring at position 2. Since the formed intermediate product is extremely unstable, it was broken down very rapidly into a mixed anhydride and quinoline. The formed mixed anhydride reacted with the amino group of phytosphingosine forming deuterated CER [NP]. The ethyl ester of carbonic acid formed during the reaction process was unstable and rapidly broken down into carbon dioxide and ethanol. Following its synthesis, the CER was purified using column chromatography. A gradient system containing chloroform-methanol was used to

efficiently separate the compounds and the CER was eluted at chloroform-methanol (95:5 v/v). Identification of the compounds of interest during synthesis and purification steps was done by TLC through comparison of R_f values of the samples with the references. MS of the pure compound showed only single mass of deuterated CER [NP], ($m/z=585.5$).

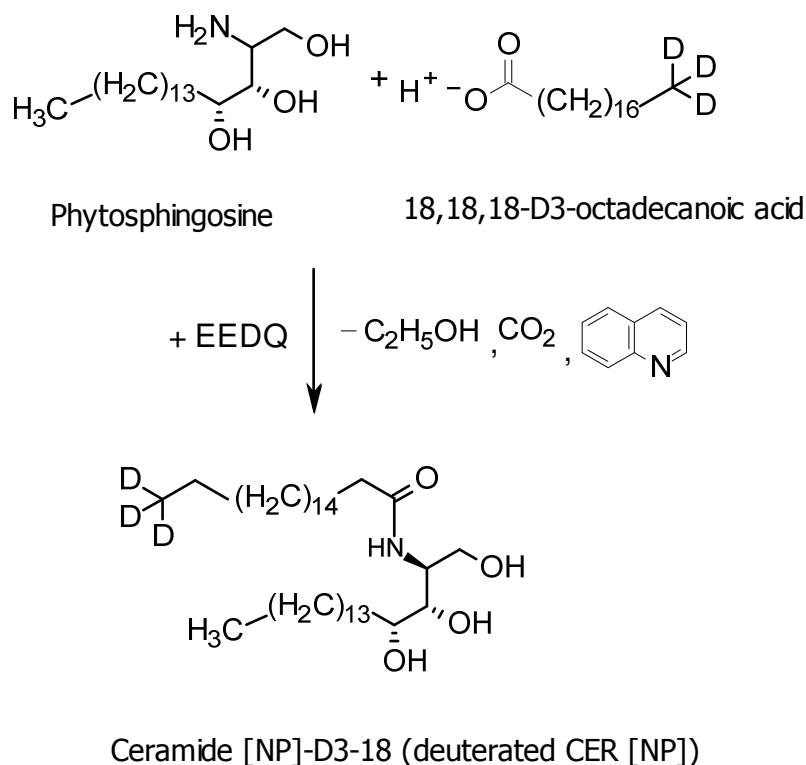


Figure 5.1: Schematic representation of the mechanism by which phytosphingosine couples with octadecanoic-18, 18, 18-D3 acid to form deuterated CER [NP].

▪ **Method Development**

Development of sensitive LC/MS method for quantification of traces amounts of compounds in biological samples needs maximum separation of the compound of interest from other interfering components of the matrix in order to avoid ion suppression [189-190]. Since extracts of the SC and other skin layers contain spectral of compounds, an optimum HPLC method that separates the CER from other components was developed and validated.

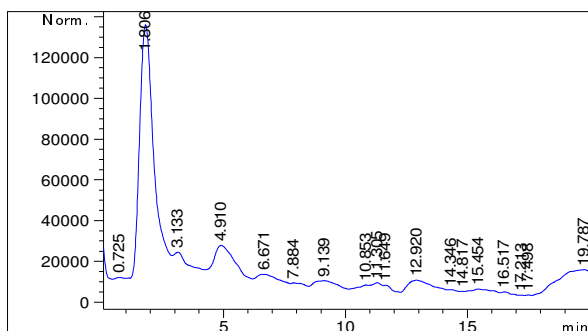
During method development, three standard reversed-phase HPLC columns (C4, C8 and C18) were assessed as stationary phases and higher degree of peak separation was attained with the C18 column. Methanol was used as the principal mobile phase and

raising the level of water and THF in methanol form (0-10) %, each, resulted in a higher degree of peak separation. Any further change in THF and/or water percent resulted either in poor peak separation and/or increased peak retention time. In addition, incorporation of small percentage of HAC into the mobile phase reduced the retention time of the deuterated CER [NP] peak with better peak separation and significant increase in LC/MS peak intensity. The effect of HAC percent on the chromatogram was investigated and maximum peak separation and peak intensity was obtained at 0.2 % HAC. Moreover, the effects of temperature (25, 30, 35 and 40°C), flow rate (1, 1.5, 2, 2.5 and 3 ml/min) and injection volume (5, 10 and 20 μ l) on peak separation were studied and sharp and better separated peak was obtained at lower temperature (25°C), medium flow rate (2 ml/min) and medium injection volume (10 μ l). Moreover, using the same chromatographic conditions, sufficient degree of CER [NP] peak separation was obtained in other skin layer extracts. Optimization of the MS parameters showed that at low fragmentor voltage (60), HAC (M. Wt=60) formed adduct with the CER ($m/z= 645.5$ Da) and almost no deuterated CER [NP] peak was obtained ($m/z= 585.5$). However, as the fragmentor voltage increased the CER [NP] peak dominated and at a fragmentor voltage of 180 only trace amount of adduct was detected. Higher degree of ionization was attained at high drying gas temperature (350°C), higher capillary voltage (4 kV), lower nebulizer pressure (20 psig) and higher drying gas flow rate (11 L/min).

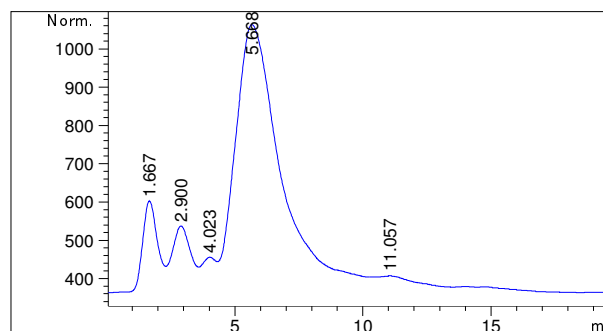
▪ **Method Validation**

The method was validated according to the EMA guideline on validation of bioanalytical methods [191]. Using the above LC/ESI-MS method, the retention window of CER [NP] was found to be roughly 10-12 min. The MS of pure SC extract, Fig 5.2 a, in full ion monitoring mode [$m/z=300-1000$ Da] showed spectral of compounds are present within the extract. However, at selective ion monitoring (SIM) mode ($m/z=585.5$ Da), no MS peak was obtained within the retention window of CER [NP] Fig 5.2 b. Interestingly, MS spectra of the SC extract at $m/z=582.5$ Da gave a sharp MS peak of CER [NP], Fig 5.2 c. Unlike the MS of the SC extract at SIM at $m/z=585.5$ Da the MS of the SC extract spiked with 10 ng/ml deuterated CER [NP], Fig 5.2 d gave a sharp deuterated CER [NP] peak within the retention window of the CER. Hence no other peak was obtained within the retention window of CER [NP], suggesting the method is selective. In addition, the appearance of no MS peak within the retention window of CER [NP] after injection of blank samples, preceded by three

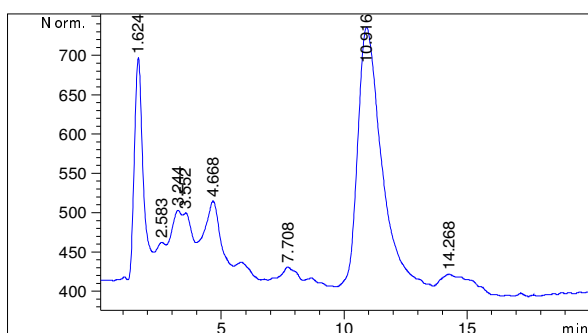
high concentrations (800 ng/ml) deuterated CER [NP] in the SC extract indicated that the method is not affected by carry-over effect.



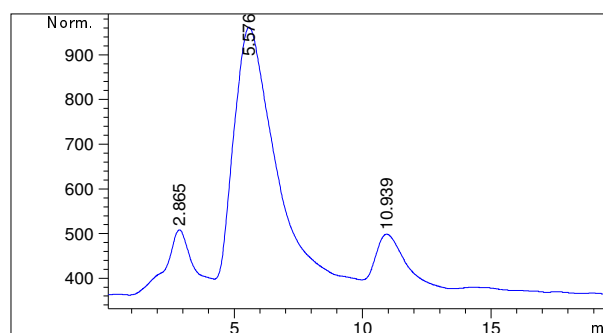
a) LC/ESI-MS chromatogram of SC extract obtained in full ion monitoring mode [m/z=300-1000 Da].



b) LC/ESI-MS chromatogram of SC extract obtained in SIM mode [m/z=585.5 Da].



c) LC/ESI-MS chromatogram of SC extract obtained in SIM mode [m/z=582.5 Da].



d) LC/ESI-MS chromatogram of deuterated CER [NP] (10 ng/ml) in SC extract obtained in SIM mode [m/z=585.5 Da].

Figure 5.2: LC/ESI-MS chromatograms and spectrum of deuterated CER [NP] and SC extracts obtained in negative ionization mode.

The results of a linear regression analysis showed that the method is linear over 10-800 ng/ml ($R^2 = 0.9993 \pm 0.0004$) with slope and intercept values of 268.9 ± 7.44 and 2884 ± 524.2 , respectively. For concentrations higher than 800 ng/ml, the relationship between peak area and concentration was polynomial. Back calculation of the calibration standards has a mean accuracy values of (89.2-104.8) %. LOD and LOQ of the method were determined based on “the Analytical Detection Limit Guidance - April 1996” [186] and were found to be 3 and 10 ng/ml, respectively. The method was also found to be precise and accurate, Table 5.1. The SC extracts, spiked with 3x LOD of the deuterated CER [NP], has an MF value of 1.002 (± 0.046). MF close to 1 and a very

small RSD value showed that the matrix has no or little effect on the ionization of the CER suggesting that the matrix effect can be neglected in the method developed.

Table 5.1: Values depicting the precision and accuracy of the LC/ESI-MS method for quantification of exogenous deuterated CER [NP] in SC and other layers of the skin.

No.	Nominal Concentration (ng/ml)	Calculated concentration (ng/ml) (n=5)		Deuterated CER [NP] recovered (%)		RSD (%) (n=5)	
		Within-run	Between-run	Within-run	Between-run	Within-run	Between-run
1	10	10.3	10.2	103.2	102.1	2.3	2.5
2	30	29.7	31.5	98.8	104.9	5.4	7.4
3	300	306.3	307.6	102.1	102.5	2.1	2.5
4	700	679.5	693.2	97.1	99.0	0.9	2.1

5.3.2. *Ex Vivo* Permeability Study

Permeation of drug molecules from MEs is dependent on the composition and nanostructure of the MEs. Araujo et al. (2010) showed that permeation of 5-ALA from O/W ME was far greater than W/O type MEs: W/O ME did not improve permeation of the drug through the skin when compared with the drug dissolved in phosphate buffer [93]. Thus, given the different types (lecithin-based and TCPL4-based) and nanostructures (O/W and BC) of MEs developed, it was necessary to conduct some screening studies. In addition, since MEs with higher viscosity are easier to be applied on the skin [99] and may have less penetration into the deeper layers of the epidermis and dermis, the effect of MEs viscosity, as ME gel, was investigated. Putting together, the extent of permeability of deuterated CER [NP] from different MEs (Table 5.2) with different nanostructures and viscosities, was investigated over a period of 300 min. Carbomer 940 was used to prepare ME gels [98-100]. In addition, the effect of CER [EOS] on the permeability behaviour of deuterated CER [NP] MEs was investigated with the aim to investigate the effect of one lipid on the permeability of other lipid. A standard hydrophilic cream containing deuterated CER [NP] (Table 4.3; where CER [AP] was replaced by 0.2 % deuterated CER [NP]) was used as a reference formulation.

The physicochemical characteristics of the MEs investigated are shown in Table 5.3. The apparent RSD is an indicator of shape irregularity, section 2.3.1.1.3, and hence the higher the value the higher is the asymmetry of the droplets.

Table 5.2: Compositions of MEs and ME gels selected for *ex vivo* permeability study.

No.	ME/ME gel	IPP - Lin A (9:1) %	Mi gly col % MO4 (1:1) %	TCP L4- HPG (1:1) %	Ph os al % %	Wate r- PeG (1:9) %	Wate r- PeG (1.5: 8.5) %	CE R [A P] ^a %	CE R ^a [E OS] %	Deut rated CER ^a [NP] %	Car bo me r ^a %
1	Lecithin B O/W ME-1	-	5	-	35	60	-	0.2	-	0.2	-
2	Lecithin B O/W ME-2	-	15	-	45	-	40	0.2	-	0.2	-
3	TCPL4 B O/W ME	10	-	30	-	-	60	0.2	-	0.1	-
4	TCPL4 B BC ME	15	-	35	-	-	50	0.2	-	0.1	-
5	CER EOS containing TCPL4 B BC ME	15	-	35	-	-	50	0.2	0.0 5	0.1	-
6	TCPL4 B O/W ME gel ^b	10	-	30	-	-	60	0.2	-	0.1	2.5
7	TCPL4 B BC ME gel ^b	15	-	35	-	-	50	0.2	-	0.1	2.5
8	CER EOS containing TCPL4 B BC ME gel ^b	15	-	35	-	-	50	0.2	0.0 5	0.1	2.5

^a percent per total mass of the MEs; ^b 0.075 % tris was added to adjust the pH

The extent of permeability of the deuterated CER [NP] into the different layers of the skin after 300 min from the formulations is shown in Fig 5.3.

Table 5.3: Viscosity, refractive index, droplet diameter, and nanostructure of lecithin and TCPL4-based CER [NP] MEs selected for permeability study.

No.	ME	Viscosity (± RSD) ^a (mPa.s)	Refractive Index (± RSD)	Droplet diameter (± RSD) (nm)	Nanost ructure
1	Lecithin B O/W ME-1	54.27(1.686)	1.448 (0.000)	203.4 (7.27)	O/W
2	Lecithin B O/W ME-2	67.34(1.112)	1.447 (0.000)	248.2 (7.33)	O/W
3	TCPL4 B O/W ME	73.27(0.600)	1.441 (0.040)	207.6 (81.21) ^b	O/W
4	TCPL4 B BC ME	83.79(0.637)	1.444 (0.000)	718.8 (82.08)	BC
5	CER EOS containing TCPL4 B BC ME	85.01(0.299)	1.444 (0.040)	1279.6 (70.68)	BC

^a exhibited Newtonian flow; ^b apparent RSD

As can be seen in Fig 5.3, permeation from MEs was much better and deeper than the hydrophilic cream and ME gels. From the hydrophilic cream, deuterated CER [NP] could not permeate into the deeper layers of the SC and other skin layers after 300 min. However, permeation from ME gels was better than the hydrophilic cream and it reduced degree of permeation into deeper layers of the skin, which can be attributed to its high viscosity. Yuan et al. (2010) showed that the degree of actives permeation from MEs is dependent on the percentage of the SAA in the MEs [92]. However, in this

case, permeation was governed more by the size, nanostructure and viscosity of the MEs. Smaller droplet and less viscous MEs permeated more into deeper layers and to a higher extent, as a result significant amount of the CER was found in the acceptor compartment. Even in case of ME gels, CER [NP] penetrated deeper from the O/W type ME gel than that of the BC ME gel. The same effect was observed by Araujo et al. (2010) [93]. Interestingly, unlike the *in vitro* release and penetration studies, lecithin-based MEs penetrated more into deeper layers of the skin than TCPL4-based MEs. However, the impact of CER [EOS] on the permeability of the deuterated CER [NP] into the SC and other layers of the skin was insignificant in both TCPL4-based MEs and ME gels giving a hint that the permeation of SC lipids from MEs into different skin layers is independent. Thus, the deepest permeation was obtained from the smaller, O/W based lecithin-based MEs, whereas, the permeation from TCPL4-based BC ME gels was shallow. Permeation from conventional hydrophilic cream was poor and no deuterated CER [NP] was identified in the lower layers of the SC and other skin layers.

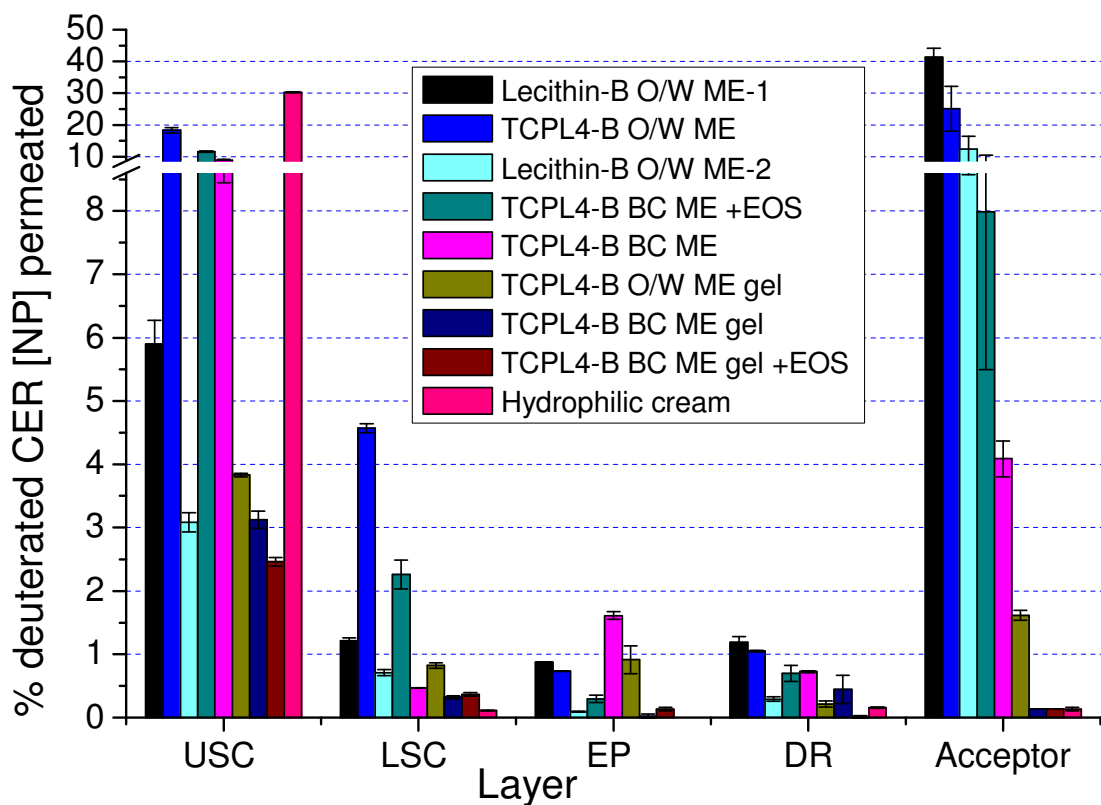


Figure 5.3: Percentage deuterated CER [NP] permeated into the different layers of the skin from various formulations.

5.4. Conclusion

A very simple, highly selective, accurate, precise and sensitive LC/ESI-MS method was developed and validated for the detection and quantification of exogenous CER [NP] in the SC and other layers of the skin. The concept of the method can be extrapolated to the quantification of other exogenous CERs and SC lipids permeated into the SC and other layers of the skin.

MEs enhanced the permeability of the deuterated CER [NP] through the skin significantly. Lecithin-based MEs permeated into deeper skin layers than those TCPL4-based MEs. Also smaller and/or O/W MEs permeated more into the deeper skin layers than bigger and/or BC MEs. Penetration from ME gels was minimal and shallow as compared to MEs. Therefore, the BC MEs have an added advantage of being localized into the upper layers the epidermis or, alternatively, preparation of gels of O/W MEs can be used as a means of localising the MEs into the desired site. Incorporation of CER [EOS] did not significantly affect permeation of CER [NP] and, hence, the result suggested that the MEs can be used to administer combinations of CERs without impeding each other's permeation.

6. Summary and Perspectives

6.1. English version

Skin represents the largest organ of the body [185] that provide barrier against environmental insults and loss of water and other essential components of the body [17]. As has been understood so far, its barrier function lies on the lipid lamellae of the SC, whose main components are CERs, FFAs and CHOL [4, 17, 27]. Analysis of various skin disease conditions such as AD [57], psoriasis [3-4], Lamellar ichthyosis [11] are associated with depletion or disturbance of these SC lipids, which are responsible for the formation of the uniquely organised lipid lamellae that is believed to be assembled at the SG-SC interface of the epidermis [11, 14-16]. Thus, this work was founded on the hypothesis that incorporation of essential SC lipids into the lipid lamellae can help to restore the barrier function of affected and/or aged skin.

There are some preparations in the market such as creams and gels that contain CERs (e.g. TriCeram, Atopiclair and Mimyx Cream). However, larger extremely lipophilic molecules, like SC lipids, can hardly permeate the skin from these conventional dosage forms. Thus, with these premises in mind, it was necessary to look for a very simple but effective method by which these lipids can permeate into their target site. On the other hand, researches over the last few decades showed that MEs are promising dosage forms to enhance permeation of actives through the SC [75, 77, 91-94], provided that they are safe to be applied topically. Therefore, it was decided to formulate MEs of the SC lipids and investigate their release, penetration into and permeation through the SC.

To date about 12 types of CERs have been identified in human SC [1]. However, as has been discussed under section 1.1.3.2 some of the CERs, like CER [AP], CER [EOS], and CER [NP] are playing a major role in maintaining the unique organisation of the lipid lamellae in the SC. In addition, the rate and extent of permeation of actives from MEs is dependent on the composition, nanostructure as well as other physicochemical characteristics of the MEs. Hence, as has been summarised in Table 6.1 stable lecithin and TCPL4-based CER [AP], CER [EOS], CER [NP], and other SC lipids MEs were developed.

Table 6.1: Compositions and stabilities of TCPL4 and lecithin-based MEs of SC lipids developed.

No	ME-Type	Composition: TCPL4-based MEs	Stability (Mon)	Composition: lecithin-based MEs	Stability (Mon)
1	CER [AP]	0.4 % CER [AP]	10 to >24	0.5 % CER [AP]	13 to >24
2	CER [EOS]	0.05 % CER EOS]; 0.4 % CER [AP]; 0.3 % CHOL; 0.25 % FFAs (BA and LA)	7 to > 24	0.1 % CER [EOS]; 0.5 % CER [AP]; 0.3 % CHOL; 0.35 % FFAs (SA,BA and LA)	15 to >21
3	CER [NP]	0.1 % CER [NP]; 0.05 % CER [EOS]; 0.2 % CER [AP]; 0.15 % CHOL; 0.1 % FFAs (PA,SA,BA and LA)	>10	0.2 % CER [NP]; 0.1 % CER [EOS]; 0.3 % CER [AP]; 0.2 % CHOL; 0.15 % FFAs (PA,SA,BA and LA)	>10

During development of the MEs, safety was given priority and hence both sets of MEs were prepared from mild SAAs, co-solvent and oils. Therefore, for the preparation of TCPL4-based MEs, TCPL4, IPP and water-PeG were used as principal MEs components: as amphiphilic, oily and hydrophilic components, respectively. The effects of HPGMO4 as a co-SAA, Lin A as part of the oil phase and the percentage of PeG in the hydrophilic phase on the stability and physicochemical characteristics of the MEs were thoroughly investigated and it was found out that high level of PeG in the hydrophilic phase was important to obtain stable MEs. HPGMO4 also increased stability of the MEs. Small percent of Lin A was added as it is an essential FFA, which is important for normal functioning of the skin [182]. It also increased the stability of CER [AP] MEs but had no significant effect on other SC lipids. In addition, all PeG, Lin A and HPGMO4 expanded the MEs region through contraction of both LC and two-phase regions.

Phosal, miglyol and water-PeG were used as amphiphilic, oily and hydrophilic components, respectively, to prepare stable lecithin-based MEs. It was not necessary to incorporate Lin A in lecithin-based MEs as it is present in small amounts in phosal, which contains safflower oil, which is rich in Lin A. Generally, it was found out that lecithin-based MEs showed better stability and loading capacity for the lipids than TCPL4-based MEs. Like TCPL4-based MEs, a high level of PeG was necessary in order to formulate a stable lecithin-based SC lipid MEs. In addition, it expanded the ME regions significantly, through contraction of the two-phase as well as the LC regions.

Interestingly, CER [AP] increased the stability of both CER [EOS] and CER [NP] MEs and CER [EOS] increased the stability of CER [AP] MEs, suggesting that one CER increases the stability of other CERs in both TCPL4- and lecithin-based MEs. In general, CHOL improved the stability of CER MEs, especially at lower levels of the SAAs. FFAs decreased the stability of TCPL4-based MEs, especially in O/W type of MEs, and improved the stability of lecithin-based MEs. The shorter the FFA (C-16 is the shortest chain) the better was the stability.

Several techniques were employed to characterise the MEs. Titration technique combined with cross-polarised light microscopy helped to differentiate two-phase and LC regions from MEs within the PT-PD [72, 117]. Electrical conductivity technique combined with DSC and EPR results was used to identify MEs nanostructures. A simple EPR method was used for the first time to identify MEs nanostructures and the results obtained were very informative. Unlike DSC, it was also possible to control the effect of temperature on MEs nanostructures.

Identification of MEs nanostructure showed that unlike CER [AP] and CER [NP] MEs, it was only possible to obtain BC type CER [EOS] MEs of both TCPL4 and lecithin-based MEs. CER [NP] was stable more in BC type MEs. Interesting to mention, generally, the most stable MEs were obtained at the BC-O/W ME border. In addition, the effect of Lin A, HPGMO4 and level of PeG on the nanostructure was investigated. Lin A and PeG expanded the W/O region of TCPL4-based MEs contracting the BC and O/W type ME regions. In contrary, HPGMO4 contracted the W/O region expanding the O/W and BC regions. In lecithin-based MEs, high PeG in hydrophilic phase slightly expanded the BC region, contracting the W/O ME region.

The micropolarities and the microviscosities of the colloidal phase of the stable MEs were also determined using EPR and their microviscosity was different from their viscosity. Droplet diameter and diameter distribution of droplet MEs was also measured using PCS. The Γ values were obtained at different angles and the D values were taken as the intercept of Γ/q^2 vs. q^2 curve, which had a negative slope and was taken as indicator of the degree of asymmetry of the droplets. The results showed that the MEs are not spherical and the droplets were bigger, especially in those MEs containing low level of SAA and high levels of oil. One of the reasons could be associated with aggregation of droplets, which can be accounted for a high concentration of droplets that may lead to strong droplet-droplet interaction [72]. Viscosities and refractive

indexes of the MEs were also measured and were used during calculation of the droplet diameter.

The toxicities and irritation potential of selected MEs was assessed using HET-CAM. During the test, normal saline was used as a positive control and 1 % SLS solution was used as a negative control. The IS was calculated as irritation indicator and all the MEs showed no irritation potential.

The release and penetration behaviours of the MEs was assessed *in vitro*, using CER [AP] as a model lipid, using a multi-layer membrane model [184] over 180 min and the results were compared with a hydrophilic cream (DAC). The results showed that the release and penetration of the lipid from the MEs was superior as compared to the cream. Release and penetration from TCPL4-based MEs was better than lecithin-based MEs. Also the rate and extent of release from droplet type MEs was far better than the BC type MEs.

The rate and extent of permeability of the lipids from the MEs was also investigated *ex vivo* using Franz diffusion cell, on which an excised human skin was mounted, and CER [NP] as a model lipid. However, before permeability investigation it was necessary to develop a sensitive analytical method that can selectively quantify the exogenous CER [NP] in the SC and other layers of the skin. Thus, a terminally deuterated analogue of CER [NP] was synthesised using phytosphingosine and terminally deuterated SA as reactants and EEDQ as a condensing agent. The synthesised CER was purified using a fine column chromatographic technique. Then, a sensitive, selective precise and accurate LC/ESI-MS method was developed. To avoid the matrix effect and enhance selectivity the method was extensively optimised and had MF=0.1002 (\pm 0.46). A mobile phase of methanol-water-THF-HAC (80:10:10:0.2) was used as a mobile phase and C-18 column was selected as a stationary phase, at 25°C and flow rate of 0.2 ml/min. The method was sensitive with LOD and LOQ 3 and 10ng/ml, respectively.

Permeability results showed that MEs extensively enhanced the permeation of the CER into the SC and other layers of the skin. No detectable amount of the CER was permeated from a hydrophilic cream into lower SC layers as well as other layers of the skin. Unlike release and penetration results, permeability of the model CER from lecithin-based MEs was deeper than TCPL4-based MEs. But like release and permeability results, permeation from droplet type MEs was more into deeper layers

and a considerable amount of deuterated CER [NP] traversed into the acceptor compartment. However, formation of ME gel minimises the depth of permeation of O/W MEs and it was suggested as means of localising the lipids into the upper epidermal layers. Thus, using BC type MEs and/or changing the viscosities droplet type MEs using gelling agent could be used as a tool to control the depth of SC lipid permeation. ME gels have also an added advantage of easy pharmaceutical application owing to their higher viscosity and better adhesion to the skin [99]. Generalising, the results obtained showed that reasonable stability and permeability were obtained from BC type MEs.

Concluding, stable and safe TCPL4-and lecithin-based O/W and BC type MEs of various SC lipids were developed. Nonetheless, the *ex vivo* permeability all the SC lipids used should be studied in detail over a range of time followed by *in vivo* toxicity and permeability experiments on animals and humans. It will be also helpful to thoroughly investigate alterations in SC lipid composition and organisation in diseased and affected skin and recommend the best combination of SC lipids for respective skin conditions. Following *in vivo* investigations clinical studies can be undertaken to fully understand the potential of the MEs to treat diseased and affected skin.

6.2. German version

Die Haut ist das größte Organ des Körpers [185] und bietet sowohl einen Schutz gegen Umwelteinflüsse als auch gegen Wasserverlust [17]. Nach bisherigen Erkenntnissen beruht die Barrierefunktion auf den Lipidlamellen des SC, deren Hauptbestandteile CERs, FFAs und CHOL sind [4, 17, 27]. Die Analyse der verschiedenen Hautkrankheiten wie AD [57], Psoriasis [3-4] oder lamellärer Ichthyose [11] ergab, dass diese Krankheitsbilder auf einer Erschöpfung oder Störung der SC-Lipide beruhen, die für die Bildung der einzigartig organisierten Lipidlamellen verantwortlich sind und in der SG-SC-Schnittstelle der Epidermis [11, 14-16] montiert werden. Diese Arbeit geht von der Hypothese aus, dass der Einbau wesentlicher SC Lipide in die Lipidlamellen helfen könnte, die Barrierefunktion der betroffenen/erkrankten und gealterte Haut wieder herzustellen.

Es gibt einige Cremes und Gele auf dem Markt, die CERs enthalten (z.B. Triceram[®], Atopiclair[®] und Mimyx[®] Cream). Allerdings können größere, extrem lipophile Moleküle wie SC-Lipide die Haut aus diesen herkömmlichen Formulierungen kaum

durchdringen. Mit dieser Prämisse im Kopf wurde eine sehr einfache, aber effektive Methode, mit der diese Lipide an ihren Zielort (target-site) durchdringen können, gesucht. In den letzten Jahrzehnten zeigten Untersuchungen an MEs, dass sie vielversprechende Arzneiformen zur Permeation von Wirkstoffen durch die SC sind [75, 77, 91-94], vorausgesetzt, dass sie sicher topisch appliziert werden können. Daher wurde beschlossen, MEs der SC-Lipide zu formulieren und ihre Freilassung, das Eindringen in und Permeation durch die SC zu untersuchen.

Bisher wurden 12 Arten von CERen im menschlichen SC identifiziert [1]. Wie jedoch in Abschnitt 1.1.3.2 diskutiert, spielen einige der CERs, wie CER [AP], CER [EOS] und CER [NP] eine wichtige Rolle/Hauptrolle bei der Aufrechterhaltung der einzigartigen Organisation der Lipidlamellen im SC. Darüber hinaus ist die Geschwindigkeit und das Ausmaß der Permeation der Wirkstoffe aus MEs abhängig von der Zusammensetzung, der Nanostruktur sowie anderen physikalisch-chemischen Eigenschaften des ME. Tabelle 6.2 zeigt die Lecithin- und TCPL4-basierenden stabilen MEen, die mit CER [AP], CER [EOS], CER [NP] und andere SC Lipide entwickelt wurden.

Table 6.2: Zusammensetzungen und Stabilitäten von Lecithin- und TCPL4-basierten SC-Lipid-MEs.

Nr.	ME-Typ	Zusammensetzung: TCPL4-basierte MEen	Stabilität (Monate)	Zusammensetzung: lecithin-basierte MEen	Stabilität (Monate)
1	CER [AP]	0.4 % CER [AP]	10 to >24	0.5 % CER [AP]	13 to >24
2	CER [EOS]	0.05 % CER EOS]; 0.4 % CER [AP]; 0.3 % CHOL; 0.25 % FFAs (BA und LA)	7 to > 24	0.1 % CER [EOS]; 0.5 % CER [AP]; 0.3 % CHOL; 0.35 % FFAs (SA,BA und LA)	15 to >21
3	CER [NP]	0.1 % CER [NP]; 0.05 % CER [EOS]; 0.2 % CER [AP]; 0.15 % CHOL; 0.1 % FFAs (PA,SA,BA und LA)	>10	0.2 % CER [NP]; 0.1 % CER [EOS]; 0.3 % CER [AP]; 0.2 % CHOL; 0.15 % FFAs (PA,SA,BA und LA)	>10

Unter Berücksichtigung des Sicherheitsaspekts wurde beide Arten von MEs mit mildem SAA, Co-SAA und Ölen hergestellt. Für die Bildung der ME wurden TCPL4-basierte SAAs, TCPL4, IPP und Wasser-PeG-Mischungen als amphiphile, fettige beziehungsweise hydrophilen Hauptkomponenten verwendet. Die Auswirkungen von HPGMO4 als Co-SAA, Lin A als Teil der Öl-Phase und des Anteils von PeG in der

hydrophilen Phase auf die Stabilität und physikalisch-chemischen Eigenschaften des MEen wurden gründlich untersucht und es wurde festgestellt, dass hohe PeG-Anteile in der hydrophilen Phase wichtig sind, um stabile MEs zu erhalten. HPGMO4 erhöht auch die Stabilität des MEen. Kleine Anteile von Lin A, die eine wesentliche FFA für die normale Funktion der Haut ist [182], erhöhten die Stabilität des CER [AP] MEs, hatten aber keinen signifikanten Einfluss auf MEen von andere SC Lipide. Darüber hinaus erweiterte die Zugabe von PeG, Lin A und HPGMO4 den Bereich der ME-Bildung durch Kontraktion sowohl der LC- als auch der Zwei-Phasenregionen.

Phosal, Miglyol und Wasser-PEG wurden als amphiphile, fettige und hydrophilen Komponenten verwendet bzw. um stabile Lecithin-basierte MEs herzustellen. Es war nicht nötig, Lin A in Lecithin-basierte MEs zu integrieren, da es in kleinen Mengen bereits in Phosal enthalten. Im Allgemeinen zeigten Lecithin-basierte MEs eine bessere Stabilität und bessere Beladungsfähigkeit für die Lipide. Wie in TCPL4-basierten ME war auch in Lecithin-basierte SC-Lipid ME ein hoher Anteil von PeG nötig, um eine stabile Formulierung zu finden. Darüber hinaus erweitert es den ME-Bereich deutlich indem es beiden Phasen sowie der LC Region kontrahierte.

Interessanterweise erhöhte CER [AP] die Stabilität der beiden ME mit CER [EOS] und CER [NP] und CER [EOS] erhöhte die Stabilität der ME mit CER [NP]. Dies legt nahe, dass ein CER die Stabilität des anderen CERen in beiden TCPL4- und Lecithin-basierenden MEen erhöht. Generell verbessert CHOL die Stabilität des CER MEen, vor allem bei niedrigeren Konzentrationen von SAA. FFAen verringerten die Stabilität der TCPL4-basierten ME vom O/W-Typ, aber verbesserten die Stabilität der Lecithin-basierte MEen. Je kürzer die FFA (C-16 ist die kürzeste Kette), desto besser wurde die Stabilität.

Verschiedene Techniken wurden verwendet, um die MEen zu charakterisieren. Mit Hilfe von Titration in Kombination mit Cross-Polarisationsmikroskopie konnten zwei Phasen und LC-Regionen der MEen im PT-PD [72, 117] identifiziert werden. Unter Nutzung der elektrischen Leitfähigkeitsmessung mit DSC und EPR wurde MEen Nanostrukturen zu identifiziert. Eine einfache EPR-Methode wurde zum ersten Mal verwendet, um MEen Nanostrukturen zu identifizieren deren Ergebnisse sehr informativ/aussagekräftig waren. Im Gegensatz zu DSC, war es außerdem möglich, den Einfluss der Temperatur auf Nanostrukturen zu kontrollieren.

Die Identifizierung von ME-Nanostrukturen hat gezeigt, dass im Gegensatz zu MEen mit CER [AP] und CER [NP], es nur möglich war CER [EOS] TCPL4- und Lecithin-Basierten BC-Typ MEen zu erhalten. CER [NP] war mehr stabil in BC-Typ MEen. In der Regel wurden die stabilsten MEs an der BC-O/W ME-Grenze erhalten. Neben der Wirkung von Lin A, wurden HPGMO4 und der PeG-Anteil auf ihre Wirkung auf die Nanostruktur untersucht. Lin A und PeG erweiterten den W/O-Bereich von TCPL4-basierten MEs. Im Gegensatz dazu verminderte HPGMO4 den W/O-Bereich. In Lecithin-basierten MEen erweiterten hohe PeG-Anteile den BC-Bereich und verminderten den W/O-ME-Bereich leicht.

Die Mikropolarität und die Mikroviskosität der kolloidalen Phase des stabilen MEen wurden auch mittels EPR gemessen. Die Mikroviskosität verhielt sich anders als die Viskosität des MEen. Die Tropfendurchmesser der MEen und ihre Verteilung wurde mit PCS gemessen. Die Γ -Werte wurden bei verschiedenen Winkeln ermittelt und die D-Werte wurden als der Schnittpunkt der Γ/q^2 vs. q^2 -Kurve verwendet, die eine negative Steigung hatte und als Indikator für den Grad der Asymmetrie der Tropfen entnommen wurden. Die Ergebnisse zeigten, dass die Tropfen der MEen nicht kugelförmig sind und dass die Tropfen größer wurden mit niedrigen SAA- und hohen Ölgehalt. Einer der Gründe könnte in der Aggregation von Tröpfchen liegen, was bei einer hohen Tröpfchenkonzentration mit einer starken Tropfen-Tropfen-Interaktionen [72] verbunden sein kann. Die Viskositäten und Brechungsindizes der MEs wurden ebenfalls bestimmt und wurden bei der Berechnung der Tropfendurchmesser verwendet.

Die Toxizitäten und irritierende Potenzial von MEen wurde mittels HET-CAM-Test ermittelt. Während des Test wurde Physiologischer Kochsalzlösung als positive Kontrolle verwendet und 1 % SLS-Lösung wurde als negative Kontrolle verwendet. Beide TCPL4- und Lecithin-basierten MEen wurden ausgewählt, die eine höheren Anteil von SAA, Öl und/oder PeG enthielten. Der IS wurde als Irritation Indikator berechnet. Keine ME hat ein Irritationspotenzial.

Die Freisetzung des MEen wurde in-vitro mit CER [AP] als Modell Lipid mit einem Multi-Layer-Membran-Modell [184] über 180 Minuten untersucht und die Ergebnisse wurden mit denen von hydrophiler Creme (DAC) verglichen. Die Ergebnisse zeigten, dass mehr Lipide aus der MEen als aus der Creme freigesetzt wurden. Es wurde auch gezeigt, dass PeG die Freisetzung und Penetration des Lipiden umfassend verbessert. Die Freisetzung von Lipiden aus TCPL4-basierten MEen war besser als aus Lecithin-

basierten MEen. Auch die Geschwindigkeit und das Ausmaß der Freisetzung von Lipiden aus MEen des Tröpfchen-typ war viel besser als aus denen des BC-Typs.

Die Geschwindigkeit und das Ausmaß der Permeation der Lipide wurde *ex vivo* mit der Franz Diffusionszelle untersucht. Vor den Permeationuntersuchungen war es notwendig, eine empfindliche analytische Methode für die selektive Quantifizierung von exogenem CER im SC und anderen Hautschichten zu entwickeln. Dafür wurde ein terminal deuteriertes CER [NP]-Analogon aus Phytosphingosin, terminal deuteriertem SA als Reaktionspartner und EEDQ als Kondensationsmittel hergestellt. Die synthetisierten CER wurde unter Verwendung einer Säulenchromatographie gereinigt. Damit konnte eine empfindliche und selektive, präzise und genaue LC / ESI-MS-Methode entwickelt werden. Um die Matrix-Effekt zu vermeiden und die Selektivität zu steigern wurde die Methode umfassend optimiert und zeigte zum Schluss MF = 0,1002 ($\pm 0,46$). Methanol-Wasser-THF-HAC (80:10:10:0.2) wurde als mobile Phase und eine C-18 Säule als stationäre Phase ausgewählt. Es wurde bei 25°C und einer Flussrate von 0,2 ml / min gearbeitet. Die Methode war empfindlich und zeigte ein LOD von 3 und ein LOQ von 10 ng/ml.

Die Permeationsergebnisse zeigten, dass die Bildung von MEs die Permeation der CER in die SC und andere Schichten der Haut sehr stark erhöhten. Aus der hydrophile Creme permeierte kein CER in die tieferen Schichten des SC oder in andere Schichten der Haut. Im Gegensatz zu den Freisetzungs- und Penetrationsuntersuchungen war die Permeabilität des CER aus Lecithin-basierten MEs tiefer als aus TCPL4-basierten MEs. Aber genau wie in den Freisetzungs- und Penetrationsstudien permeierte CER aus MEs des Tröpfchentyps stärker in tiefere Schichten und eine erhebliche Menge an deuterierten CER [NP] wurde im Akzeptor-Kompartiment gefunden. Jedoch minimiert die Bildung von ME-Gel die Tiefe der Durchdringung der O/W MEs und wird als Mittel zur Lokalisierung der Lipide in den oberen Hautschichten vorgeschlagen. D.h. durch Verwendung von ME vom BC-Typ und/oder Veränderung der Viskosität der ME vom Tropfentyp mit verschiedenen Geliermittel kann die Tiefe der Durchdringung der SC-Lipid kontrolliert werden. ME-Gele haben den zusätzlichen Vorteil der einfacheren Applikation aufgrund ihrer höheren Viskosität und einer besseren Haftung auf der Haut [99]. Darüber hinaus zeigten die bisher erzielten Ergebnisse, dass ME des BC-Typs stabiler sind und besser permeieren.

Es wurden also stabile und sichere O/W- und BC-Typ-MEs mit verschiedenen SC-Lipide entwickelt. Allerdings sollte die *ex-vivo* Permeationstudien für alle SC-Lipide im Detail über einen längeren Beobachtungszeitraum durchgeführt und von *in-vivo* Toxizitäts- und Permeationsversuchen an Tieren und Menschen begleitet werden. Dies würde auch hilfreich, um Veränderungen in der SC-Lipidzusammensetzung und -organisation in kranken und betroffenen Haut nachvollziehen zu können und Empfehlungen für die beste Kombination von SC-Lipide bei den jeweiligen Hautprobleme geben zu können. Nach *in-vivo* Untersuchungen sollten klinische Studien durchgeführt werden, um Potential der MEen an kranker und betroffener Haut zu behandeln verstehen und nutzen zu können.

7. References

1. van Smeden, J., et al., *LC/MS analysis of stratum corneum lipids: ceramide profiling and discovery*. J Lipid Res, 2011. **52**(6): p. 1211-21.
2. Zhang, L., L.I. Hellgren, and X. Xu, *Enzymatic production of ceramide from sphingomyelin*. J Biotechnol, 2006. **123**(1): p. 93-105.
3. Farwanah, H., et al., *Ceramide profiles of the uninvolved skin in atopic dermatitis and psoriasis are comparable to those of healthy skin*. Arch Dermatol Res, 2005. **296**(11): p. 514-21.
4. Holleran, W.M., Y. Takagi, and Y. Uchida, *Epidermal sphingolipids: metabolism, function, and roles in skin disorders*. FEBS Lett, 2006. **580**(23): p. 5456-66.
5. Kang, J.S., et al., *Inhibition of atopic dermatitis-like skin lesions by topical application of a novel ceramide derivative, K6PC-9p, in NC/Nga mice*. Exp Dermatol, 2008. **17**(11): p. 958-64.
6. Lambers, J.W.J.P., (NL) and J.L. Verweij, (NL), *Ceramide 3 derivatives based on monounsaturated fatty acids*, 1997, Gist-brocades N.V. (NL): United States.
7. Stover, T.C., et al., *Systemic delivery of liposomal short-chain ceramide limits solid tumor growth in murine models of breast adenocarcinoma*. Clin Cancer Res, 2005. **11**(9): p. 3465-74.
8. El Maghraby, G.M., B.W. Barry, and A.C. Williams, *Liposomes and skin: from drug delivery to model membranes*. Eur J Pharm Sci, 2008. **34**(4-5): p. 203-22.
9. Shah, B., N. Surti, and A. Misra, *12 - Other Routes of Protein and Peptide Delivery: Transdermal, Topical, Uterine, and Rectal*, in *Challenges in Delivery of Therapeutic Genomics and Proteomics*, A. Misra, Editor 2011, Elsevier: London. p. 623-671.
10. Shah, U.U., et al., *Needle-free and microneedle drug delivery in children: A case for disease-modifying antirheumatic drugs (DMARDs)*. Int J Pharm, 2011. **416**(1): p. 1-11.
11. Bouwstra, J.A. and M. Ponec, *The skin barrier in healthy and diseased state*. Biochim Biophys Acta, 2006. **1758**(12): p. 2080-95.
12. Lampe, M.A., M.L. Williams, and P.M. Elias, *Human epidermal lipids: characterization and modulations during differentiation*. J Lipid Res, 1983. **24**(2): p. 131-40.
13. Proksch, E., J.M. Jensen, and P.M. Elias, *Skin lipids and epidermal differentiation in atopic dermatitis*. Clin Dermatol, 2003. **21**(2): p. 134-44.
14. Bonte, F., et al., *Thermotropic phase behavior of in vivo extracted human stratum corneum lipids*. Lipids, 1997. **32**(6): p. 653-60.
15. Weerheim, A. and M. Ponec, *Determination of stratum corneum lipid profile by tape stripping in combination with high-performance thin-layer chromatography*. Arch Dermatol Res, 2001. **293**(4): p. 191-9.
16. Loden, M., *The skin barrier and use of moisturizers in atopic dermatitis*. Clin Dermatol, 2003. **21**(2): p. 145-57.
17. Ponec, M., et al., *New acylceramide in native and reconstructed epidermis*. J Invest Dermatol, 2003. **120**(4): p. 581-8.
18. Bonte, F., et al., *Analysis of all stratum corneum lipids by automated multiple development high-performance thin-layer chromatography*. J Chromatogr B Biomed Appl, 1995. **664**(2): p. 311-6.
19. de Jager, M.W., et al., *The phase behaviour of skin lipid mixtures based on synthetic ceramides*. Chem Phys Lipids, 2003. **124**(2): p. 123-34.
20. Hatfield, R.M. and L.W. Fung, *Molecular properties of a stratum corneum model lipid system: large unilamellar vesicles*. Biophys J, 1995. **68**(1): p. 196-207.
21. Groen, D., et al., *Two new methods for preparing a unique stratum corneum substitute*. Biochim Biophys Acta, 2008. **1778**(10): p. 2421-9.
22. Mizutani, Y., et al., *Ceramide biosynthesis in keratinocyte and its role in skin function*. Biochimie, 2009. **91**(6): p. 784-90.
23. de Jager, M.W., et al., *Modelling the stratum corneum lipid organisation with synthetic lipid mixtures: the importance of synthetic ceramide composition*. Biochim Biophys Acta, 2004. **1664**(2): p. 132-40.
24. Kang, L., P.C. Ho, and S.Y. Chan, *Interactions between a skin penetration enhancer and the main components of human stratum corneum lipids Isothermal titration calorimetry study*. J Therm Anal Calorim, 2006. **83**(1): p. 27-30.
25. Hatta, I., et al., *Coexistence of two domains in intercellular lipid matrix of stratum corneum*. Biochim Biophys Acta, 2006. **1758**(11): p. 1830-6.
26. de Jager, M.W., et al., *Novel lipid mixtures based on synthetic ceramides reproduce the unique stratum corneum lipid organization*. J Lipid Res, 2004. **45**(5): p. 923-32.
27. Norlen, L., et al., *Human stratum corneum lipid organization as observed by atomic force microscopy on Langmuir-Blodgett films*. J Struct Biol, 2007. **158**(3): p. 386-400.

28. Bonte, F., et al., *Existence of a lipid gradient in the upper stratum corneum and its possible biological significance*. Arch Dermatol Res, 1997. **289**(2): p. 78-82.
29. Jungersted, J.M., et al., *Ethnicity and stratum corneum ceramides*. Brit J Dermatol, 2010. **163**(6): p. 1169-1173.
30. Norlen, L., et al., *Inter- and intra-individual differences in human stratum corneum lipid content related to physical parameters of skin barrier function in vivo*. J Invest Dermatol, 1999. **112**(1): p. 72-7.
31. Masukawa, Y., et al., *Characterization of overall ceramide species in human stratum corneum*. J Lipid Res, 2008. **49**(7): p. 1466-76.
32. Kessner, D., et al., *Properties of ceramides and their impact on the stratum corneum structure. Part 2: stratum corneum lipid model systems*. Skin Pharmacol Physiol, 2008. **21**(2): p. 58-74.
33. Hinder, A., et al., *Investigation of the Molecular Structure of the Human Stratum Corneum Ceramides [NP] and [EOS] by Mass Spectrometry*. Skin Pharmacol Physiol, 2011. **24**(3): p. 127-135.
34. T'Kindt, R., et al., *Profiling and Characterizing Skin Ceramides Using Reversed-Phase Liquid Chromatography-Quadrupole Time-of-Flight Mass Spectrometry*. Anal Chem, 2012. **84**(1): p. 403-11.
35. Farwanah, H., et al., *Profiling of human stratum corneum ceramides by means of normal phase LC/APCI-MS*. Anal Bioanal Chem, 2005. **383**(4): p. 632-7.
36. Ramesh, G. and U.N. Das, *Effect of free fatty acids on two-stage skin carcinogenesis in mice*. Cancer Lett, 1996. **100**(1-2): p. 199-209.
37. Ziboh, V.A., C.C. Miller, and Y. Cho, *Metabolism of polyunsaturated fatty acids by skin epidermal enzymes: generation of antiinflammatory and antiproliferative metabolites*. Am J Clin Nutr, 2000. **71**(1 Suppl): p. 361S-6S.
38. Ansari, M.N.A., Nicolaid.N, and H.C. Fu, *Fatty Acid Composition of Living Layer and Stratum Corneum Lipids of Human Sole Skin Epidermis*. Lipids, 1970. **5**(10): p. 838-&.
39. Terashi, H., et al., *Human stratified squamous epithelia differ in cellular fatty acid composition*. J Dermatol Sci, 2000. **24**(1): p. 14-24.
40. Jiang, W.G., R.P. Bryce, and D.F. Horrobin, *Essential fatty acids: molecular and cellular basis of their anti-cancer action and clinical implications*. Crit Rev Oncol Hematol, 1998. **27**(3): p. 179-209.
41. Takigawa, H., et al., *Deficient production of hexadecenoic acid in the skin is associated in part with the vulnerability of atopic dermatitis patients to colonization by Staphylococcus aureus*. Dermatology, 2005. **211**(3): p. 240-8.
42. Chen, X., et al., *Fatty acids influence "solid" phase formation in models of stratum corneum intercellular membranes*. Langmuir, 2007. **23**(10): p. 5548-56.
43. Brody, I., *A Light and Electron-Microscopy Study of Normal Human Stratum-Corneum with Particular Reference to the Intercellular Space*. Upsala J Med Sci, 1989. **94**(1): p. 29-45.
44. Bouwstra, J.A., et al., *The lipid organisation in the skin barrier*. Acta Derm Venereol Suppl (Stockh), 2000. **208**: p. 23-30.
45. Forslind, B., *A Domain Mosaic Model of the Skin Barrier*. Acta Dermato-Venereologica, 1994. **74**(1): p. 1-6.
46. Kiselev, M.A., et al., *New insights into the structure and hydration of a stratum corneum lipid model membrane by neutron diffraction*. Eur Biophys J, 2005. **34**(8): p. 1030-40.
47. ten Grotenhuis, E., et al., *Phase behavior of stratum corneum lipids in mixed Langmuir-Blodgett monolayers*. Biophys J, 1996. **71**(3): p. 1389-99.
48. Schroter, A., et al., *Basic nanostructure of stratum corneum lipid matrices based on ceramides [EOS] and [AP]: a neutron diffraction study*. Biophys J, 2009. **97**(4): p. 1104-14.
49. Norlen, L., *Skin barrier structure and function: the single gel phase model*. J Invest Dermatol, 2001. **117**(4): p. 830-6.
50. Kiselev, M.A., *Conformation of ceramide 6 molecules and chain-flip transitions in the lipid matrix of the outermost layer of mammalian skin, the stratum corneum*. Crystallogr Rep+, 2007. **52**(3): p. 525-528.
51. Norlén, L., *Molecular Structure of the SC Lipids in vivo*, in *Skin Forum 12th Annual Meeting 2011*, International Association for Pharmaceutical Technology in partnership with Skin Forum: Campus Westend, Goethe Universität Frankfurt, Germany.
52. Boncheva, M., F. Damien, and V. Normand, *Molecular organization of the lipid matrix in intact Stratum corneum using ATR-FTIR spectroscopy*. Biochim Biophys Acta, 2008. **1778**(5): p. 1344-55.
53. Caussin, J., G.S. Gooris, and J.A. Bouwstra, *FTIR studies show lipophilic moisturizers to interact with stratum corneum lipids, rendering the more densely packed*. Biochim Biophys Acta, 2008. **1778**(6): p. 1517-24.

54. Caussin, J., et al., *Lipid organization in human and porcine stratum corneum differs widely, while lipid mixtures with porcine ceramides model human stratum corneum lipid organization very closely*. *Biochim Biophys Acta*, 2008. **1778**(6): p. 1472-82.
55. Bouwstra, J.A. and P.L. Honeywell-Nguyen, *Skin structure and mode of action of vesicles*. *Adv Drug Deliv Rev*, 2002. **54 Suppl 1**: p. S41-55.
56. Corbe, E., et al., *Role of ceramide structure and its microenvironment on the conformational order of model stratum corneum lipids mixtures: an approach by FTIR spectroscopy*. *Chem Phys Lipids*, 2007. **146**(2): p. 67-75.
57. Jacobs, R.J., *Depleted skin barrier replenishing skin creams composition and method of application*, 2004: United States.
58. Farwanah, H., et al., *Improved procedure for the separation of major stratum corneum lipids by means of automated multiple development thin-layer chromatography*. *J Chromatogr B Analyt Technol Biomed Life Sci*, 2002. **780**(2): p. 443-50.
59. Vavrova, K., et al., *Ceramide analogue 14S24 ((S)-2-tetracosanoylamino-3-hydroxypropionic acid tetradecyl ester) is effective in skin barrier repair in vitro*. *Eur J Pharm Sci*, 2004. **21**(5): p. 581-7.
60. Nakajima, K., et al., *Altered lipid profiles in the stratum corneum of Sjogren-Larsson syndrome*. *J Dermatol Sci*, 2011. **63**(1): p. 64-6.
61. Janssens, M., et al., *Lamellar Lipid Organization and Ceramide Composition in the Stratum Corneum of Patients with Atopic Eczema*. *J Invest Dermatol*, 2011. **131**(10): p. 2136-2138.
62. Zhao, X., et al., *Enhancement of transdermal delivery of theophylline using microemulsion vehicle*. *Int J Pharm*, 2006. **327**(1-2): p. 58-64.
63. Boonme, P., et al., *Characterization of microemulsion structures in the pseudoternary phase diagram of isopropyl palmitate/water/Brij 97:1-butanol*. *AAPS PharmSciTech*, 2006. **7**(2): p. E45.
64. Kogan, A., et al., *Characterization of the nonionic microemulsions by EPR. I. Effect of solubilized drug on nanostructure*. *J Phys Chem B*, 2009. **113**(3): p. 691-9.
65. Djekic, L. and M. Primorac, *The influence of cosurfactants and oils on the formation of pharmaceutical microemulsions based on PEG-8 caprylic/capric glycerides*. *Int J Pharm*, 2008. **352**(1-2): p. 231-9.
66. Xu, J., et al., *The preparation of neem oil microemulsion (Azadirachta indica) and the comparison of acaricidal time between neem oil microemulsion and other formulations in vitro*. *Vet Parasitol*, 2010. **169**(3-4): p. 399-403.
67. Pakpayat, N., et al., *Formulation of ascorbic acid microemulsions with alkyl polyglycosides*. *Eur J Pharm Biopharm*, 2009. **72**: p. 444-452.
68. Cheng, M.B., et al., *Characterization of water-in-oil microemulsion for oral delivery of earthworm fibrinolytic enzyme*. *J Control Release*, 2008. **129**(1): p. 41-8.
69. Graf, A., et al., *Protein delivery using nanoparticles based on microemulsions with different structure-types*. *Eur J Pharm Sci*, 2008. **33**(4-5): p. 434-44.
70. Graf, A., et al., *Microemulsions containing lecithin and sugar-based surfactants: nanoparticle templates for delivery of proteins and peptides*. *Int J Pharm*, 2008. **350**(1-2): p. 351-60.
71. Wellert, S., et al., *Structure of biodiesel based bicontinuous microemulsions for environmentally compatible decontamination: A small angle neutron scattering and freeze fracture electron microscopy study*. *J Colloid Interface Sci*, 2008. **325**(1): p. 250-8.
72. Hathout, R.M., et al., *Microemulsion formulations for the transdermal delivery of testosterone*. *Eur J Pharm Sci*, 2010. **40**(3): p. 188-96.
73. Sathishkumar, M., et al., *Role of bicontinuous microemulsion in the rapid enzymatic hydrolysis of (R,S)-ketoprofen ethyl ester in a micro-reactor*. *Bioresour Technol*, 2010.
74. Yuan, J.S. and E.J. Acosta, *Extended release of lidocaine from linker-based lecithin microemulsions*. *Int J Pharm*, 2009. **368**(1-2): p. 63-71.
75. Yuan, J.S., et al., *Linker-based lecithin microemulsions for transdermal delivery of lidocaine*. *Int J Pharm*, 2008. **349**(1-2): p. 130-43.
76. Kreilgaard, M., E.J. Pedersen, and J.W. Jaroszewski, *NMR characterisation and transdermal drug delivery potential of microemulsion systems*. *J Control Release*, 2000. **69**(3): p. 421-33.
77. Lawrence, M.J. and G.D. Rees, *Microemulsion-based media as novel drug delivery systems*. *Adv Drug Deliver Rev*, 2000. **45**(1): p. 89-121.
78. Safavi, A., N. Maleki, and F. Farjami, *Phase behavior and characterization of ionic liquids based microemulsions*. *Colloids and Surfaces A: Physicochem. Eng. Aspects*, 2010. **355**(1-3): p. 61-66.
79. Zhu, W., et al., *Formulation design of microemulsion for dermal delivery of penciclovir*. *Int J Pharm*, 2008. **360**(1-2): p. 184-90.

80. Rozman, B., et al., *Temperature-sensitive microemulsion gel: an effective topical delivery system for simultaneous delivery of vitamins C and E*. AAPS PharmSciTech, 2009. **10**(1): p. 54-61.
81. Mendonca, C.R., et al., *Role of the co-surfactant nature in soybean w/o microemulsions*. J Colloid Interface Sci, 2009. **337**(2): p. 579-85.
82. Sharma, G., et al., *Microemulsions for oral delivery of insulin: design, development and evaluation in streptozotocin induced diabetic rats*. Eur J Pharm Biopharm, 2010. **76**(2): p. 159-69.
83. Kale, A.A. and V.B. Patravale, *Development and evaluation of lorazepam microemulsions for parenteral delivery*. AAPS PharmSciTech, 2008. **9**(3): p. 966-71.
84. Chaiyana, W., et al., *Characterization of potent anticholinesterase plant oil based microemulsion*. Int J Pharm, 2010. **401**(1-2): p. 32-40.
85. Narang, A.S., D. Delmarre, and D. Gao, *Stable drug encapsulation in micelles and microemulsions*. Int J Pharm, 2007. **345**(1-2): p. 9-25.
86. Pestana, K.C., et al., *Oil-in-water lecithin-based microemulsions as a potential delivery system for amphotericin B*. Colloids Surf B Biointerfaces, 2008. **66**(2): p. 253-9.
87. Nguyen, T.T., et al., *Biocompatible lecithin-based microemulsions with rhamnolipid and sophorolipid biosurfactants: formulation and potential applications*. J Colloid Interface Sci, 2010. **348**(2): p. 498-504.
88. Castellino, V., Y.L. Cheng, and E. Acosta, *The hydrophobicity of silicone-based oils and surfactants and their use in reactive microemulsions*. J Colloid Interface Sci, 2011. **353**(1): p. 196-205.
89. Heuschkel, S., A. Goebel, and R.H. Neubert, *Microemulsions--modern colloidal carrier for dermal and transdermal drug delivery*. J Pharm Sci, 2008. **97**(2): p. 603-31.
90. Tan, G., et al., *Cryo-field emission scanning electron microscopy imaging of a rigid surfactant mesophase*. Langmuir, 2008. **24**(19): p. 10621-4.
91. Liu, C.H., F.Y. Chang, and D.K. Hung, *Terpene microemulsions for transdermal curcumin delivery: effects of terpenes and cosurfactants*. Colloids Surf B Biointerfaces, 2011. **82**(1): p. 63-70.
92. Yuan, J.S., et al., *Effect of surfactant concentration on transdermal lidocaine delivery with linker microemulsions*. Int J Pharm, 2010. **392**(1-2): p. 274-84.
93. Araujo, L.M., J.A. Thomazine, and R.F. Lopez, *Development of microemulsions to topically deliver 5-aminolevulinic acid in photodynamic therapy*. Eur J Pharm Biopharm, 2010. **75**(1): p. 48-55.
94. Rogerio, A.P., et al., *Anti-inflammatory effect of quercetin-loaded microemulsion in the airways allergic inflammatory model in mice*. Pharmacol Res, 2010. **61**(4): p. 288-97.
95. Fanun, M., *Oil type effect on diclofenac solubilization in mixed nonionic surfactants microemulsions*. Colloids and Surfaces A: Physicochem. Eng. Aspects, 2009. **343**(1-3): p. 75-82.
96. Zhao, X.Y., et al., *Rheological properties and microstructures of gelatin-containing microemulsion-based organogels*. Colloids and Surfaces A: Physicochem. Eng. Aspects, 2006. **281**(1-3): p. 67-73.
97. Date, A.A. and M.S. Nagarsenker, *Parenteral microemulsions: an overview*. Int J Pharm, 2008. **355**(1-2): p. 19-30.
98. Chen, H., et al., *Hydrogel-thickened microemulsion for topical administration of drug molecule at an extremely low concentration*. Int J Pharm, 2007. **341**(1-2): p. 78-84.
99. Zhu, W., et al., *Microemulsion-based hydrogel formulation of penciclovir for topical delivery*. Int J Pharm, 2009. **378**(1-2): p. 152-8.
100. Luo, M., Q. Shen, and J. Chen, *Transdermal delivery of paeonol using cubic gel and microemulsion gel*. Int J Nanomedicine, 2011. **6**: p. 1603-10.
101. Guillard, E.C., C. Laugel, and A. Baillet-Guffroy, *Molecular interactions of penetration enhancers within ceramides organization: a FTIR approach*. Eur J Pharm Sci, 2009. **36**(2-3): p. 192-9.
102. El-Galeel, M.A.S.A., *Solubility and Stability of Natural Food Colorants in Microemulsions*, in *Institut für Lebensmitteltechnologie2002*, Rheinschen Friedrich-Wilhelms-Universität: Bonn. p. 105.
103. El Maghraby, G.M., *Self-microemulsifying and microemulsion systems for transdermal delivery of indomethacin: effect of phase transition*. Colloids Surf B Biointerfaces, 2010. **75**(2): p. 595-600.
104. Fanun, M., *Formulation and characterization of microemulsions based on mixed nonionic surfactants and peppermint oil*. J Colloid Interface Sci, 2010. **343**(2): p. 496-503.
105. Coppola, L., et al., *Phase equilibria and physical-chemical properties of sugar-based surfactants in aqueous solutions*. Colloids and Surfaces A: Physicochem. Eng. Aspects, 2002. **196**(2-3): p. 175-187.

106. Teichmann, A., et al., *Comparison of stratum corneum penetration and localization of a lipophilic model drug applied in an o/w microemulsion and an amphiphilic cream*. Eur J Pharm Biopharm, 2007. **67**(3): p. 699-706.
107. Gannu, R., et al., *Enhanced bioavailability of lacidipine via microemulsion based transdermal gels: formulation optimization, ex vivo and in vivo characterization*. Int J Pharm, 2010. **388**(1-2): p. 231-41.
108. Shukla, A., et al., *Investigation of pharmaceutical oil/water microemulsions by small-angle scattering*. Pharm Res, 2002. **19**(6): p. 881-886.
109. Peira, E., et al., *Positively charged microemulsions for topical application*. Int J Pharm, 2008. **346**(1-2): p. 119-23.
110. Sintov, A.C., H.V. Levy, and S. Botner, *Systemic delivery of insulin via the nasal route using a new microemulsion system: In vitro and in vivo studies*. J Control Release, 2010. **148**(2): p. 168-76.
111. Piao, H.M., et al., *Preparation and evaluation of fexofenadine microemulsions for intranasal delivery*. Int J Pharm, 2010. **395**(1-2): p. 309-16.
112. Fanun, M., *Properties of microemulsions with mixed nonionic surfactants and citrus oil*. Colloids and Surfaces A: Physicochem. Eng. Aspects, 2010. **369**(1-3): p. 246-252.
113. Lin, C.C., et al., *Stability and characterisation of phospholipid-based curcumin-encapsulated microemulsions*. Food Chem, 2009. **116**(4): p. 923-928.
114. Heuschkel, S., J. Wohlrab, and R.H. Neubert, *Dermal and transdermal targeting of dihydroavenanthramide D using enhancer molecules and novel microemulsions*. Eur J Pharm Biopharm, 2009. **72**(3): p. 552-60.
115. Neubert, R.H.H., et al., *Microemulsions as colloidal vehicle systems for dermal drug delivery. Part V: Microemulsions without and with glycolipid as penetration enhancer*. J Pharm Sci, 2005. **94**(4): p. 821-827.
116. Constantinides, P.P. and J.P. Scalart, *Formulation and physical characterization of water-in-oil microemulsions containing long- versus medium-chain glycerides*. Int J Pharm, 1997. **158**(1): p. 57-68.
117. Margulis-Goshen, K., et al., *Formation of organic nanoparticles from volatile microemulsions*. J Colloid Interface Sci, 2010. **342**(2): p. 283-92.
118. Zech, O., et al., *Ethylammonium nitrate in high temperature stable microemulsions*. J Colloid Interface Sci, 2010. **347**(2): p. 227-32.
119. Shrikhande, J.J., P.A. Hassan, and R.V. Jayaram, *Condensation reaction of benzaldehyde and acetone in o/w microemulsions: Effect of microemulsion compositions*. Colloids and Surfaces A: Physicochem. Eng. Aspects, 2010. **370**(1-3): p. 64-71.
120. Shukla, A., A. Krause, and R.H.H. Neubert, *Microemulsions as colloidal vehicle systems for dermal drug delivery. Part IV: investigation of microemulsion systems based on a eutectic mixture of lidocaine and prilocaine as the colloidal phase by dynamic light scattering*. J Pharm Pharmacol, 2003. **55**(6): p. 741-748.
121. Shukla, A., et al., *Microemulsions for dermal drug delivery studied by dynamic light scattering: Effect of interparticle interactions in oil-in-water microemulsions*. J Pharm Sci, 2003. **92**(4): p. 730-738.
122. Papadimitriou, V., et al., *Microemulsions based on virgin olive oil: A model biomimetic system for studying native oxidative enzymatic activities*. Colloids and Surfaces A: Physicochem. Eng. Aspects, 2011. **382**(1-3): p. 232-237.
123. Xie, Y.W., R.Q. Ye, and H.L. Liu, *Microstructure studies on biosurfactant-rhamnolipid/n-butanol/water/n-heptane microemulsion system*. Colloids and Surfaces A: Physicochem. Eng. Aspects, 2007. **292**(2-3): p. 189-195.
124. Rozner, S., et al., *Do food microemulsions and dietary mixed micelles interact?* Colloid Surface B, 2010. **77**(1): p. 22-30.
125. Rojas, O., et al., *A new type of microemulsion consisting of two halogen-free ionic liquids and one oil component*. Colloids and Surfaces A: Physicochem. Eng. Aspects, 2010. **369**(1-3): p. 82-87.
126. Boonme, P., et al., *Characterization of microemulsion structures in the pseudoternary phase diagram of isopropyl palmitate/water/Brij 97 : 1-butanol*. AAPS PharmSciTech, 2006. **7**(2).
127. Yu, A.H., et al., *Skin irritation and the inhibition effect on HSV-1 in vivo of penciclovir-loaded microemulsion*. Int Immunopharmacol, 2010. **10**(10): p. 1305-1309.
128. Chen, X., et al., *Interfacial tension and the behavior of microemulsions and macroemulsions of water and carbon dioxide with a branched hydrocarbon nonionic surfactant*. J Supercrit Fluid, 2010. **55**(2): p. 712-723.
129. Feng, J.-L., et al., *Study on food-grade vitamin E microemulsions based on nonionic emulsifiers*. Colloids and Surfaces A: Physicochem. Eng. Aspects, 2009. **339**: p. 1-6.

130. Zhong, F., et al., *Formation and characterisation of mint oil/S and CS/water microemulsions*. Food Chem, 2009. **115**(2): p. 539-544.
131. Avramiotis, S., et al., *EPR studies of proteolytic enzymes in microemulsions*. Colloids and Surfaces A: Physicochem. Eng. Aspects, 1998. **144**: p. 295-304.
132. Wilk, K.A., et al., *Biocompatible microemulsions of dicephalic aldonamide-type surfactants: formulation, structure and temperature influence*. J Colloid Interface Sci, 2009. **334**(1): p. 87-95.
133. Vodolazkaya, N.A., et al., *Molecular spectroscopy studies of solvent properties of dispersed 'water pools' Fluorescein and 2,7-dichlorofluorescein in reversed AOT-based microemulsions*. J Mol Liq, 2010. **157**(2-3): p. 105-112.
134. Zhang, W.N. and Q.X. Zhong, *Microemulsions as nanoreactors to produce whey protein nanoparticles with enhanced heat stability by thermal pretreatment*. Food Chem, 2010. **119**(4): p. 1318-1325.
135. Lu, C.H., C.H. Lee, and C.H. Wu, *Microemulsion-mediated solvothermal synthesis of copper indium diselenide powders*. Sol Energ Mat Sol C, 2010. **94**(10): p. 1622-1626.
136. Zhuang, Y.Q., et al., *Particle kinetics and physical mechanism of microemulsion polymerization of octamethylcyclotetrasiloxane*. Powder Technol, 2010. **201**(2): p. 146-152.
137. Patole, A.S., et al., *A facile approach to the fabrication of graphene/polystyrene nanocomposite by in situ microemulsion polymerization*. J Colloid Interface Sci, 2010. **350**(2): p. 530-7.
138. Lyons, K.C., et al., *Factors limiting the oral bioavailability of N-acetylglucosaminyl-N-acetylmuramyl dipeptide (GMDP) and enhancement of absorption in rats by delivery in a water-in-oil microemulsion*. Int J Pharm, 2000. **199**(1): p. 17-28.
139. Graf, A., T. Rades, and S.M. Hook, *Oral insulin delivery using nanoparticles based on microemulsions with different structure-types: optimisation and in vivo evaluation*. Eur J Pharm Sci, 2009. **37**(1): p. 53-61.
140. Liang, M., N.M. Davies, and I. Toth, *Increasing entrapment of peptides within poly(alkyl cyanoacrylate) nanoparticles prepared from water-in-oil microemulsions by copolymerization*. Int J Pharm, 2008. **362**(1-2): p. 141-6.
141. Solanki, J.N., R. Sengupta, and Z.V.P. Murthy, *Synthesis of copper sulphide and copper nanoparticles with microemulsion method*. Solid State Sci, 2010. **12**(9): p. 1560-1566.
142. Chen, W., et al., *Synthesis of PMMA and PMMA/PS nanoparticles by microemulsion polymerization with a new vapor monomer feeding system*. Colloids and Surfaces A: Physicochem. Eng. Aspects, 2010. **364**(1-3): p. 145-150.
143. Keswani, R.K., et al., *Room temperature synthesis of titanium dioxide nanoparticles of different phases in water in oil microemulsion*. Colloids and Surfaces A: Physicochem. Eng. Aspects, 2010. **369**(1-3): p. 75-81.
144. Zhao, M.W., et al., *Fabrication of hollow silica spheres in an ionic liquid microemulsion*. Mater Lett, 2008. **62**(30): p. 4591-4593.
145. Hathout, R.M., et al., *Visualization, dermatopharmacokinetic analysis and monitoring the conformational effects of a microemulsion formulation in the skin stratum corneum*. J Colloid Interface Sci, 2011. **354**(1): p. 124-30.
146. Moniruzzaman, M., N. Kamiya, and M. Goto, *Ionic liquid based microemulsion with pharmaceutically accepted components: Formulation and potential applications*. J Colloid Interface Sci, 2010. **352**(1): p. 136-42.
147. Cho, Y., et al., *An inverse relationship between ceramide synthesis and clinical severity in patients with psoriasis*. J Korean Med Sci, 2004. **19**(6): p. 859-63.
148. Berardesca, E., et al., *Evaluation of efficacy of a skin lipid mixture in patients with irritant contact dermatitis, allergic contact dermatitis or atopic dermatitis: a multicenter study*. Contact Dermatitis, 2001. **45**(5): p. 280-5.
149. Macheleidt, O., H.W. Kaiser, and K. Sandhoff, *Deficiency of epidermal protein-bound omega-hydroxyceramides in atopic dermatitis*. J Invest Dermatol, 2002. **119**(1): p. 166-73.
150. Teichmann, A., et al., *Comparison of stratum corneum penetration and localization of a lipophilic model drug applied in an o/w microemulsion and an amphiphilic cream*. Eur J Pharm Biopharm, 2007. **67**(3): p. 699-706.
151. Santos, P., et al., *Application of microemulsions in dermal and transdermal drug delivery*. Skin Pharmacol Physiol, 2008. **21**(5): p. 246-59.
152. Raith, K., et al., *Profiling of human stratum corneum ceramides by liquid chromatography-electrospray mass spectrometry*. Analytica Chimica Acta, 2000. **418**(2): p. 167-173.
153. Phospholipid-GmbH, *Phosal[®] 75 SA*, 2007, Phospholipid-GmbH, Nattermannallee 1, D - 50829 Cologne, Germany.
154. Evonik-Goldschmidt-GmbH, *TEGO[®] Care PL 4*, 2008, Goldschmidtstr. 100, 45127 Essen, Germany.

155. Göbel, A.S.B., *Mikroemulsionen als moderne Formulierungen zum Einsatz bei chronisch entzündlichen Hauterkrankungen am Beispiel Tacrolimus und Linolsäure*, in *Institute of Pharmacy, Department of Pharmaceutical Technology and Biopharmaceutics* 2009, Martin Luther University, Halle-Wittenberg: Halle (Saale). p. 115.
156. Heuschkel, S., et al., *Modulation of dihydroavenanthramide D release and skin penetration by 1,2-alkanediols*. *Eur J Pharm Biopharm*, 2008. **70**(1): p. 239-47.
157. Fu, X., et al., *Conductivity study on the w/o microemulsion of a saponified mono(2-ethylhexyl) phosphoric acid extractant system*. *Colloids and Surfaces A: Physicochem. Eng. Aspects*, 1996. **110**: p. 55-61.
158. Szajdzinska-Pietek, E., et al., *ESR study of aqueous micellar solutions of perfluoropolyether surfactants with the use of fluorinated spin probes*. *J Colloid Interf Sci*, 2007. **312**(2): p. 405-412.
159. Rozner, S., et al., *Characterization of nonionic microemulsions by EPR. Part II. The effect of competitive solubilization of cholesterol and phytosterols on the nanostructure*. *J Phys Chem B*, 2009. **113**(3): p. 700-7.
160. Zielinska, K., et al., *Microstructure and structural transition in microemulsions stabilized by aldonamide-type surfactants*. *J Colloid Interface Sci*, 2008. **321**(2): p. 408-17.
161. Nakagawa, K., *EPR Investigations of Spin-Probe Dynamics in Aqueous Dispersions of a Nonionic Amphiphilic Compound*. *J Am Oil Chem Soc*, 2009. **86**(1): p. 1-17.
162. Lucaciu, C.M., et al., *EPR study of the dynamics of some spin labels inclusion in cyclodextrins*. *Romanian J. Biophys.*, 2005. **15**(1-4): p. 15-60.
163. Kristl, J., et al., *Effect of colloidal carriers on ascorbyl palmitate stability*. *Eur J Pharm Sci*, 2003. **19**(4): p. 181-9.
164. Abdalla, A. and K. Mader, *ESR studies on the influence of physiological dissolution and digestion media on the lipid phase characteristics of SEDDS and SEDDS pellets*. *Int J Pharm*, 2009. **367**(1-2): p. 29-36.
165. Kempe, S., H. Metz, and K. Mader, *Application of electron paramagnetic resonance (EPR) spectroscopy and imaging in drug delivery research - chances and challenges*. *Eur J Pharm Biopharm*, 2010. **74**(1): p. 55-66.
166. Shirahama, K., M. Tohdo, and M. Murahashi, *Esr-Linewidth Broadening of a Hydrophobic Probe in Some Surfactant Solutions*. *Colloid Polym Sci*, 1984. **262**(12): p. 978-981.
167. Persson, K. and B.L. Bales, *Epr Study of an Associative Polymer in Solution - Determination of Aggregation Number and Interactions with Surfactants*. *J Chem Soc Faraday T*, 1995. **91**(17): p. 2863-2870.
168. Shukla, A. and R.H.H. Neubert, *Diffusion behavior of pharmaceutical O/W microemulsions studied by dynamic light scattering*. *Colloid Polym Sci*, 2006. **284**(5): p. 568-573.
169. Shukla, A., H. Graener, and R.H.H. Neubert, *Observation of two diffusive relaxation modes in microemulsions by dynamic light scattering*. *Langmuir*, 2004. **20**(20): p. 8526-8530.
170. Gohy, J.F., S.K. Varshney, and R. Jerome, *Water-soluble complexes formed by poly(2-vinylpyridinium)-block-poly(ethylene oxide) and poly(sodium methacrylate)-block-poly(ethylene oxide) copolymers*. *Macromolecules*, 2001. **34**(10): p. 3361-3366.
171. Hou, Z.S., Z.P. Li, and H.Q. Wang, *Solubilization of poly(ethylene oxide) in sodium dodecyl sulfonate/octane/butanol/water reverse microemulsion*. *Colloids and Surfaces A: Physicochem. Eng. Aspects*, 2000. **168**(2): p. 109-113.
172. Hemminga, M.A. and I.J.v.d. Dries, *Spin label applications to food science*, in *Bio Magn Re*, L.J. Berliner, Editor 1998. p. 345-347.
173. Bahri, M.A., et al., *Investigation of SDS, DTAB and CTAB micelle microviscosities by electron spin resonance*. *Colloids and Surfaces A: Physicochem. Eng. Aspects*, 2006. **290**(1-3): p. 206-212.
174. Jadzyn, J., G. Czechowski, and T. Stefaniak, *Viscosity of a series of 1,2-alkanediols*. *J Chem Eng Data*, 2002. **47**(4): p. 978-979.
175. Czechowski, G. and J. Jadzyn, *The viscous properties of diols. II. 1,2- and 1,5-pentanediol in water and 1-pentanol solutions*. *Z Naturforsch A*, 2003. **58**(5-6): p. 321-324.
176. Kayali, I.H., S.H. Liu, and C.A. Miller, *Microemulsions containing mixtures of propoxylated sulfates with slightly branched hydrocarbon chains and cationic surfactants with short hydrophobes or PO chains*. *Colloids and Surfaces A: Physicochem. Eng. Aspects*, 2010. **354**(1-3): p. 246-251.
177. Saintruth, H., et al., *Phase Studies and Particle-Size Analysis of Oil-in-Water Phospholipid Microemulsions*. *Int J Pharm*, 1995. **116**(2): p. 253-261.
178. Trotta, M., et al., *Phase behaviour of microemulsion systems containing lecithin and lysolecithin as surfactants*. *Int J Pharm*, 1996. **143**(1): p. 67-73.

References

179. Zoumpanioti, M., et al., *Spectroscopic and catalytic studies of lipases in ternary hexane-1-propanol-water surfactantless microemulsion systems*. Colloid Surface B, 2006. **47**(1): p. 1-9.
180. Evonik-Goldschmidt-GmbH, *Ceramide I: Reinforcing the skins natural protective lipid barrier*, 2003, Goldschmidtstr. 100, 45127 Essen, Germany.
181. Moniruzzaman, M., et al., *Ionic liquid-in-oil microemulsion as a potential carrier of sparingly soluble drug: Characterization and cytotoxicity evaluation*. Int J Pharm, 2010. **400**(1-2): p. 243-250.
182. Goebel, A.S., et al., *Dermal targeting using colloidal carrier systems with linoleic acid*. Eur J Pharm Biopharm, 2010. **75**(2): p. 162-72.
183. ICCVAM-Test, *ICCVAM Recommended Protocol for Future Studies Using the Hen's Egg Test-Chorioallantoic Membrane (HET-CAM) Test Method*, 2006.
184. Neubert, R., et al., *A multilayer membrane system for modelling drug penetration into skin*. Int J Pharm, 1991. **75**(1): p. 89-94
185. Sand, M., et al., *MicroRNAs and the skin: Tiny players in the body's largest organ*. J Dermatol Sci, 2009. **53**(3): p. 169-175.
186. Resources, W.D.o.N., *Analytical detection limit guidance & laboratory guide for determining method detection limits*, 1996, Wisconsin Department of Natural Resources Laboratory Certification Program.
187. Opitz, A., et al., *Improved Method for Stratum Corneum Lipid Analysis by Automated Multiple Development HPTLC*. Chromatographia, 2011. **73**(5-6): p. 559-565.
188. Belleau, B. and G. Malek, *A new convenient reagent for peptide syntheses*. J Am Chem Soc, 1968. **90**(6): p. 1651-2.
189. Annesley, T.M., *Ion suppression in mass spectrometry*. Clin Chem, 2003. **49**(7): p. 1041-4.
190. Jessome, L.L. and D.A. Volmer, *Ion suppression: A major concern in mass spectrometry*. Lc Gc North America, 2006. **24**(5): p. 498-+.
191. EMEA, *Draft guideline on validation of bioanalytical methods*, 2009, European Medicines Agency: London,.
192. Norris, L.E., et al., *Comparison of dietary conjugated linoleic acid with safflower oil on body composition in obese postmenopausal women with type 2 diabetes mellitus*. Am J Clin Nutr, 2009. **90**(3): p. 468-476.
193. Rübe, A., *Development and physico-chemical characterization of nanocapsules*, in *Mathematisch-Naturwissenschaftlich-Technischen Fakultät* 2006, Martin-Luther-Universität Halle-Wittenberg: Halle (Saale). p. 136.
194. Caldararu, H., et al., *Structure of the Polar Core in Reverse Micelles of Nonionic Poly(Oxyethylene) Surfactants, as Studied by Spin-Probe and Fluorescence Probe Techniques*. J PHYS CHEM-US, 1994. **98**(20): p. 5320-5331.

8. Appendixes

Appendix A: Selection of appropriate ME Ingredients

The thermodynamics stability and the physicochemical properties of MEs of a certain active is dependent on the composition as well as proportion of the ME components. Hence, appropriate ME components have to be chosen for a particular active ingredient. Since CERs have similar structures and share some common properties, during selection of MEs component CER [AP] was chosen as a representative CER. Thus, the effects of the type of various ME components on the stability of CER [AP] MEs was thoroughly investigated and the appropriate ME components were chosen. In the process, thermodynamic stability of the MEs was expressed as lack of any turbidity, phase separation, sedimentation of droplets, aggregation or precipitation of the lipid that is molecularly dispersed in the ME. Any ME regarded as stable remained clear over the stated period of time.

I-Selection of Appropriate SAA (s)

Since MEs of non-ionic SAAs have high stability, low toxicity, low irritancy and biodegradability [72], for the preparation of CER MEs, various non ionic and zwitterions SAAs were assessed. The SAAs used were from various SAA classes and have different HLB values and were used at various percentages, Table A1. During the investigation, since the objective of the research was to obtain O/W MEs, the level of the oily component was maintained lower. At the initial stages PeG and Lin A were chosen a co-solvent and oil, respectively.

As can be seen in the table, the alkyl glycosides (Plantacare[®] 818 and Plantacare[®] 2000: sugar based SAAs that are safe and environmental friendly [105]), poloxamers (Synperonic[®] PE/L 101 and Synperonic[®] PE/L 44) and Tego[®] Betain 810 (Capryl/Capramidopropyl Betain: a very mild amphoteric SAA) gave the most unstable MEs. The polysorbate Tween 80 gave MEs with better stability than the above five SAAs but was not as good as Tagat and high concentration of Tego[®] Sis 40 (PEG-40 Sorbitanperisostearate).

Table A1: Effect of type and HLB value of hydrophilic SAAs on stability of CER [AP] MEs.

Formulation	Lin A %	Tego® Betain 810 %	Synperonic® PE/L 44 %	Synperonic® PE/L 101 %	Plantacare® 818 %	Plantacare® 2000 %	Tween 80 %	Tagat %	Tego® Sis 40 %	HPG CH4 %	Phosail 75 %	TCPL 4 %	Water-PeG (3:1) %	CER [AP] %	Stability (Days)
PAPME99	5	20	-	-	-	-	-	-	-	-	-	-	75	0.3	ON
PAPME100	5	25	-	-	-	-	-	-	-	-	-	-	70	0.3	ON
PAPME101	5	35	-	-	-	-	-	-	-	-	-	-	60	0.3	ON
PAPME102	5	-	20	-	-	-	-	-	-	-	-	-	75	0.3	ON
PAPME103	5	-	25	-	-	-	-	-	-	-	-	-	70	0.3	ON
PAPME104	5	-	35	-	-	-	-	-	-	-	-	-	60	0.3	ON
PAPME79	5	-	-	20	-	-	-	-	-	-	-	-	75	0.3	ON
PAPME80	5	-	-	25	-	-	-	-	-	-	-	-	70	0.3	ON
PAPME82	5	-	-	35	-	-	-	-	-	-	-	-	60	0.3	ON
PAPME108	5	-	-	-	20	-	-	-	-	-	-	-	75	0.3	ON
PAPME109	5	-	-	-	25	-	-	-	-	-	-	-	70	0.3	ON
PAPME110	5	-	-	-	35	-	-	-	-	-	-	-	60	0.3	ON
PAPME75	5	-	-	-	-	20	-	-	-	-	-	-	75	0.3	ON
PAPME76	5	-	-	-	-	25	-	-	-	-	-	-	70	0.3	ON
PAPME78	5	-	-	-	-	35	-	-	-	-	-	-	60	0.3	ON
PAPME204	5	-	-	-	-	-	20	-	-	-	-	-	75	0.3	2
PAPME205	5	-	-	-	-	-	25	-	-	-	-	-	70	0.3	2
PAPME206	5	-	-	-	-	-	35	-	-	-	-	-	60	0.3	2
PAPME83	5	-	-	-	-	-	-	20	-	-	-	-	75	0.3	7
PAPME85	5	-	-	-	-	-	-	25	-	-	-	-	70	0.3	7
PAPME86	5	-	-	-	-	-	-	35	-	-	-	-	60	0.3	7
PAPME114	5	-	-	-	-	-	-	-	20	-	-	-	75	0.3	2
PAPME115	5	-	-	-	-	-	-	-	25	-	-	-	70	0.3	10
PAPME116	5	-	-	-	-	-	-	-	35	-	-	-	60	0.3	10
PAPME89	5	-	-	-	-	-	-	-	-	20	-	-	75	0.3	10
PAPME90	5	-	-	-	-	-	-	-	-	25	-	-	70	0.3	10
PAPME92	5	-	-	-	-	-	-	-	-	35	-	-	60	0.3	10
PAPME111	5	-	-	-	-	-	-	-	-	-	20	-	75	0.3	ON
PAPME112	5	-	-	-	-	-	-	-	-	-	25	-	70	0.3	10
PAPME113	5	-	-	-	-	-	-	-	-	-	35	-	60	0.3	>120
PAPME105	5	-	-	-	-	-	-	-	-	-	-	20	75	0.3	>120
PAPME106	5	-	-	-	-	-	-	-	-	-	-	25	70	0.3	50
PAPME107	5	-	-	-	-	-	-	-	-	-	-	35	60	0.3	70

The polyglycerol fatty acid ester SAAs, TCPL4 and HYDRIOL[®] PGCH.4 (HPGCH4: polyglyceryl-4-caprate), gave clear CER [AP] MEs with better stability than the other SAAs tested except phosal. Yet among the two polyglycerol fatty acid ester SAAs, TCPL4 (HLB=11 [154]) gave MEs with better stability than HPGCH4 (HLB=16). Given both SAAs belong to the same SAA group, the difference in microemulsification power should be attributed to the optimal HLB value of TCPL4 where for preparation of stable MEs SAAs. In general, the results in Table A1 indicated that SAAs with HLB values close to 10-11 gave relatively stable MEs: TCPL4 (HLB=11) was much better than HPGCH4 (HLB=16) and Tego[®] Sis 40 (HLB=10) was better than Tween 80 (HLB=15). Phosal, a lecithin-based SAA containing 75 % phosphatidylcholine and (8-10) % ethanol [153], gave the most stable CER [AP] MEs when used at relatively higher concentration.

Since the type of the oil component used also affects the choice of a SAA, further assessments were made using IPP as an oily phase for SAAs that gave relatively stable MEs, Table A2. As can be seen in the table, phosal, when used at higher concentration, gave the most stable ME followed by TCPL4.

Table A2: Effect of SAA type on stability of CER [AP] MEs containing IPP as the oily component.

Formulation	IPP %	Tagat %	TCPL4 %	Phosal %	Water-PeG (3.5:6.5) %	CER [AP] %	Stability (Days)	Remark
PAPME129	5	20	-	-	75	0.3	-	Emulsion
PAPME130	10	20	-	-	70	0.3	-	Emulsion
PAPME131	5	35	-	-	60	0.3	ON	
PAPME132	10	35	-	-	55	0.3	ON	
PAPME133	5	-	20	-	75	0.3	2 ^a	
PAPME134	10	-	20	-	70	0.3	-	Emulsion
PAPME135	5	-	35	-	60	0.3	5	
PAPME136	10	-	35	-	55	0.3	5	
PAPME137	5	-	-	20	75	0.3	-	Emulsion
PAPME138	10	-	-	20	70	0.3	-	Emulsion
PAPME139	5	-	-	35	60	0.3	5	
PAPME140	10	-	-	35	55	0.3	>120	

^aEmulsion turned to clear ME upon incorporation of CER [AP]

Both TCPL4 and phosal were further challenged using a hydrophilic phase containing lower proportion of the co-solvent, Table A3. The results showed that at low percentage of the co-solvent TCPL4 gave relatively stable MEs than phosal. Therefore, TCPL4 gave stable MEs at lower percentages of the SAA and the co-solvent while phosal gave the most stable MEs when used at higher level accompanied by a higher proportion of the co-solvent. Consequently, both SAAs were chosen to prepare MEs for further stability, safety and bioavailability investigations.

Table A3: Comparison of stability of TCPL4-based and lecithin-based CER [AP] MEs at low PeG content.

Formulation	IPP %	TCPL4 %	Phosal %	Water-PeG (4.5:5.5) %	CER [AP] %	Stability (Days)	Remark
PAPME141	5	25	-	70	0.3	2	-
PAPME142	10	25	-	65	0.3	-	Emulsion
PAPME143	5	35	-	60	0.3	2	-
PAPME144	10	35	-	55	0.3	2	-
PAPME145	5	-	25	70	0.3	-	Emulsion
PAPME146	10	-	25	65	0.3	-	Emulsion
PAPME147	5	-	35	60	0.3	ON	-
PAPME148	10	-	35	55	0.3	2	-

II-Selection of Appropriate Co-SAA

In most cases combination of SAAs results in MEs that have better physicochemical characteristics, stability and tolerability [77, 85, 97]. However, preliminary studies showed that combination of other SAAs with phosal did not improve stability of lecithin-based CER [AP] MEs. Whereas the effects of various lipophilic SAAs (HPGMO4 (HLB=8); Span[®] 80 (HLB=4.3), Span[®] 20 (HLB=8.6) and Synperonic[®] PE/L 101 (HLB=4.3)) on the stability of TCPL4-based CER [AP] MEs was investigated at SAA/co-SAA of (2:1 and 4:1), Table A4.

Table A4: Effects of selected lipophilic SAAs as co-SAAs on stability of TCPL4-based CER [AP] MEs at a SAA/co-SAA of 2:1 and 4:1.

Formulation	IP P %	TCP L4 %	Span [®] 80 %	Span [®] 20 %	HPG MO4 %	Synperoni c [®] PE/L 101 %	Water-PeG (3:7) %	CER [AP] %	Stability (Days)
PAPME177	5	25	-	-	-	-	70	0.5	ON
PAPME178	5	30	-	-	-	-	65	0.5	ON
PAPME179	5	35	-	-	-	-	60	0.5	2
PAPME180	5	20	5	-	-	-	70	0.5	Cloudy
PAPME181	5	24	6	-	-	-	65	0.5	ON
PAPME182	5	28	7	-	-	-	60	0.5	ON
PAPME183	5	17	8	-	-	-	70	0.5	Cloudy
PAPME184	5	20	10	-	-	-	65	0.5	Cloudy
PAPME185	5	23	12	-	-	-	60	0.5	ON
PAPME186	5	20	-	5	-	-	70	0.5	ON
PAPME187	5	24	-	6	-	-	65	0.5	ON
PAPME188	5	28	-	7	-	-	60	0.5	ON
PAPME189	5	17	-	8	-	-	70	0.5	ON
PAPME190	5	20	-	10	-	-	65	0.5	ON
PAPME191	5	23	-	12	-	-	60	0.5	ON
PAPME192	5	20	-	-	5	-	70	0.5	ON
PAPME193	5	24	-	-	6	-	65	0.5	2
PAPME194	5	28	-	-	7	-	60	0.5	2
PAPME195	5	17	-	-	8	-	70	0.5	ON
PAPME196	5	20	-	-	10	-	65	0.5	ON
PAPME197	5	23	-	-	12	-	60	0.5	ON

PAPME198	5	20	-	-	-	5	70	0.5	2
PAPME199	5	24	-	-	-	6	65	0.5	2
PAPME200	5	28	-	-	-	7	60	0.5	2
PAPME201	5	17	-	-	-	8	70	0.5	2
PAPME202	5	20	-	-	-	10	65	0.5	ON
PAPME203	5	23	-	-	-	12	60	0.5	ON

Span[®] 80 and span 20[®] reduced the stability, whereas, low concentrations of HPGMO4 and Synperonic[®] PE/L 101 slightly improved stability. Hence, HPGMO4 was chosen for further investigations as a co-SAA as it is relatively safer. Unlike Span[®] 20, Span[®] 80 gave cloudy formulations, supporting the idea that the use of SAAs with too low HLB value is not good for preparation of MEs. Similarly, focusing on synergistic effect of SAAs, the stability enhancing effects of other hydrophilic SAAs (Tween 80 (HLB=15), Tagat (HLB=15), HYDRIOL[®] PGC.3 (polyglyceryl-3-caprate: polyglycerol FA ester SAA, HLB=14), HPGCH4 (HLB=16), Tego[®] Sis 40 (HLB≈9), Synperonic[®] PE/L 44 (HLB=16), and phosal) on TCPL4-based MEs was investigated but none of the SAA improved stability of TCPL4-based CER [AP] MEs.

III: Selection of Appropriate Oil (s)

The results in Table A1 as well as some preliminary study results indicated the possibility of obtaining stable CER [AP] MEs using Lin A. Lin A is an essential FFA, which is vital for the normal functioning of the skin [182]. However a study by Göbel, A (2009) showed that a high percentage of Lin A in the MEs could be irritant to the skin [155]. Hence, for the preparation of stable CER [AP] MEs, Lin A had to be partly replaced by other safe oils. Therefore the effects IPP and miglyol, alone or in combination with Lin A, on the stability of TCPL4 and lecithin-based CER [AP] MEs was studied, Table A5.

Table A5: Effect of type of oil on the stability of lecithin and TCPL4-based CER [AP] MEs.

Formulation	Miglyol %	IPP %	Miglyol-Lin A (2:1) %	IPP-Lin A (2:1) %	TCP L4 %	Phosal %	Water-PeG (1:3) %	CER [AP] %	Stability (Mon)
PAPME118	5	-	-	-	20	-	75	0.3	Emulsion
PAPME119	5	-	-	-	-	35	60	0.3	>4
PAPME121	-	5	-	-	20	-	75	0.3	>4
PAPME122	-	5	-	-	-	35	60	0.3	4
PAPME124	-	-	5	-	20	-	75	0.3	2
PAPME125	-	-	5	-	-	35	60	0.3	>4
PAPME127	-	-	-	5	20	-	75	0.3	>4
PAPME128	-	-	-	5	-	35	60	0.3	4

As can be seen in the table, IPP gave stable MEs with TCPL4 than miglyol. It also showed the possibility of combining small percentage of Lin A with IPP without affecting the stability significantly. Thus IPP alone or in combination with small percentage of Lin A was chosen as oil component for the preparation of TCPL4-based CER [AP] MEs.

In contrast to TCPL4-based MEs, relatively stable lecithin-based MEs were obtained with miglyol than IPP. However, the effect of combining Lin A with miglyol was not clearly seen and hence further investigations were made, Table A6. As can be seen in the table Lin A decreased stability of lecithin-based CER [AP] MEs considerably. Hence miglyol alone was chosen as oil component for lecithin-based MEs. Nonetheless, it was not necessary to incorporate Lin A in lecithin-based MEs as phosal contains some percent of safflower oil, which is known to contain a certain amount of Lin A [192].

Table A6: Effect of Lin A on stability of lecithin-based CER [AP] MEs.

Formulation	Miglyol %	Lin A %	Phosal %	Water-PeG (1.5:8.5) %	CER [AP] %	Stability (Days)
PAPME464	5	-	35	60	0.7	27
PAPME465	5	-	40	55	0.7	2
PAPME472	5	1	35	59	0.7	ON
PAPME473	5	1	40	54	0.7	ON

IV: Selection of Appropriate Co-solvent

Preparation of stable MEs in most cases demands the use of co-solvents like short chain alcohols, alkanediols and alkanetriols. Although, unlike alkanediols and alkanetriols, relatively lower concentration the short chain alcohols suffices to prepare a stable MEs [97], the alkanediols and alkanetriols are safer to be applied on the skin [89]. Therefore, giving safety priority, alkanediols and alkanetriols were selected for the preparation of CER [AP] MEs. In addition, different alkanediols and alkanetriols have different stabilisation and safety profiles and hence the effects of two alkanediols, PeG and PG, and one alkanetriols, glycerol, on stability of TCPL4-based CER [AP] MEs was investigated as has been shown in Table A7.

Table A7: The role of type of co-solvent on stability of CER [AP] MEs.

Formulation	IPP %	Lin A %	TCPL4 %	PeG %	PG %	Glyce rol %	Water %	CER [AP] %	Stability (Days)
PAPME312	5	2	30	44.1			18.9	0.6	2
PAPME313	5	2	30	53.55			9.45	0.6	2
PAPME314	5	2	35	40.6			17.4	0.6	2
PAPME315	5	2	35	49.3			8.7	0.6	2
PAPME316	5	2	30		44.1		18.9	0.6	Gel
PAPME317	5	2	30		53.55		9.45	0.6	VS
PAPME318	5	2	35		40.6		17.4	0.6	VS
PAPME319	5	2	35		49.3		8.7	0.6	VS
PAPME320	5	2	30			44.1	18.9	0.6	Gel
PAPME321	5	2	30			53.55	9.45	0.6	Gel
PAPME322	5	2	35			40.6	17.4	0.6	Gel
PAPME323	5	2	35			49.3	8.7	0.6	ON
PAPME324	5	2	30	22.05	22.05		18.9	0.6	ON
PAPME325	5	2	30	26.78	26.78		9.45	0.6	ON
PAPME326	5	2	35	20.3	20.3		17.4	0.6	ON
PAPME327	5	2	35	24.65	24.65		8.7	0.6	ON

PAPME328	5	2	30	22.05	22.05	18.9	0.6	ON
PAPME329	5	2	30	26.78	26.78	9.45	0.6	ON
PAPME330	5	2	35	20.3	20.3	17.4	0.6	ON
PAPME331	5	2	35	24.65	24.65	8.7	0.6	ON

VS=viscous suspension

The results in Table A7 showed that glycerol and PG resulted into gel or a viscous media at which the CER [AP] remained suspended. Moreover, combination of PG or glycerol with PeG was not as efficient as PeG alone.

As can be seen in Table A8, further investigation was made comparing PeG with HeG. According to the results obtained, although relatively stable MEs were obtained using HeG at higher concentration of water, the MEs obtained were not sufficiently stable. Relatively stable MEs could only be obtained at higher concentration of the co-solvent, in which case PeG was excessively superior. During preliminary studies the same effect was observed with lecithin-based CER [AP] MEs and hence PeG was selected as a co-solvent for the preparation of both lecithin and TCPL4-based CER [AP] MEs. Hence, a mixture of PeG and water will constitute the hydrophilic component of the MEs.

Table A8: Effect of HeG on stability of CER [AP] MEs in comparison with PeG.

Formulation	IPP-Lin A (4:1) %	TCPL4 %	PeG %	HeG %	Water %	CER [AP] %	Stability (Days)
PAPME276	5	25	45.5		24.5	0.5	ON
PAPME277	5	35	39		21	0.5	ON
PAPME278	5	25	52.5		17.5	0.5	Cloudy
PAPME264	5	35	45		15	0.5	ON
PAPME279	5	25	59.5		10.5	0.5	65
PAPME266	5	35	51		9	0.5	105
PAPME280	5	25		45.5	24.5	0.5	2
PAPME281	5	35		39	21	0.5	2
PAPME282	5	25		52.5	17.5	0.5	Cloudy
PAPME283	5	35		45	15	0.5	7
PAPME284	5	25		59.5	10.5	0.5	7
PAPME285	5	35		51	9	0.5	7

As has been depicted in Tables A9 and A10 the effect of percent PeG in the hydrophilic phase on stability of TCPL4 and lecithin-based CER [AP] MEs, respectively, was investigated. In both cases stable MEs could be obtained only at relatively higher proportion of PeG in the hydrophilic phase (lower proportion of water). Interestingly, the results in Table A9 and Table A10 showed that water was important in order to obtain stable MEs. In addition, although miglyol is not completely miscible with water and may give MEs without water, it was evidenced that water enhanced the stability of lecithin-based MEs. Preliminary studies also showed that the level of PeG should increase with the level of CER [AP] in the MEs.

Table A9: Effect of percentage of PeG in the hydrophilic phase on stability of TCPL4-based CER [AP] MEs.

ME	IPP-Lin A (4:1) %	TCPL4 %	PeG %	Water %	CER [AP] %	Stability (Days)
PAPME264	5	35	45	15	0.5	ON
PAPME265	5	35	48	12	0.5	7
PAPME266	5	35	51	9	0.5	105
PAPME267	5	35	54	6	0.5	115
PAPME268	5	35	57	3	0.5	115
PAPME269	5	35	60	0	0.5	7
PAPME270	5	30	48.75	16.25	0.5	7
PAPME271	5	30	52	13	0.5	7
PAPME272	5	30	55.25	9.75	0.5	105
PAPME273	5	30	58.5	6.5	0.5	120
PAPME274	5	30	61.75	3.25	0.5	>120
PAPME275	5	30	65	0	0.5	7

Table A10: Effect of percentage of PeG in the hydrophilic phase on stability of lecithin-based CER [AP] MEs.

Formulation	Miglyol %	Phosal %	PeG %	Water %	CER [AP] %	Stability (Days)
PAPME450	5	35	48	12	0.5	3
PAPME451	5	35	51	9	0.5	1.9 yrs
PAPME452	5	35	54	6	0.5	>2 yrs
PAPME453	5	35	57	3	0.5	1.9 yrs
PAPME454	5	35	60	0	0.5	1.5 Yrs
PAPME455	10	35	44	11	0.5	5
PAPME456	10	35	49.5	5.5	0.5	1.9 yrs
PAPME457	10	35	55	0	0.5	1.5 yrs
PAPME458	15	35	40	10	0.5	4
PAPME459	10	30	48	12	0.5	Cloudy
PAPME460	10	40	10	10	0.5	4
PAPME461	10	45	44	11	0.5	6

Therefore, IPP (alone or in combination with Lin A), TCPL4 (alone or in combination with HPGMO4 (1:1)) and water-PeG mixture were chosen as oily, amphiphilic and hydrophilic components, respectively, for the preparation of TCPL4-based MEs. Miglyol, phosal and water-PeG were chosen as oily, amphiphilic and hydrophilic components, respectively, for the preparation of lecithin-based MEs.

Appendix B: Development of CER [AP] MEs

Appropriate ME components were chosen for the preparation of TCPL4 and lecithin-based CER [AP] MEs, Appendix A. However, the thermodynamic stability and the physicochemical properties of MEs is highly dependent on the percentage compositions of each ME component. Thus, the effect of percentage ME component on the physical stability of the MEs was

investigated at large and optimum MEs with better thermodynamic stability were chosen for further characterisation.

During stability study, instability of TCPL4-based CER [AP] MEs was expressed as formation of fine suspended particles, which subsequently form bigger aggregates and precipitated. The degree of precipitation indicates the degree of instability. However, in lecithin-based CER [AP] MEs instability was mainly expressed as sedimentation of MEs droplets, although in some cases precipitation of the CER was observed. In those MEs prepared without CER [AP], neither precipitation nor sedimentations were observed.

I-Development of TCPL4-based CER [AP] MEs

A set of MEs that represent the effect of the percentage ME component on the thermodynamic stability of the MEs is shown in Table B1. Since the objective of the research was to obtain O/W MEs, the level of oil was maintained low, 5-15 %. The upper and lower limits of SAA (SAA mixture) were maintained at 30 % and 45 % due to safety concerns and stability reasons, respectively. However, in those MEs that contain Lin A as part of the oily component, the SAA level was maintained lower, (25-40 %) since the preliminary study showed that Lin A plays an amphiphilic role. The MEs were prepared and kept at ambient conditions and were observed over a period of time for instability. To further challenge the physical stability, the MEs were centrifuged at 3500rpm for 30 min after 1 week of preparation. Besides the effect of percent ME component, the effects of the level of Lin A in the oily phase, level of PeG in the hydrophilic phase and HPGMO4 as a co-SAA on the stability of the MEs were investigated at large.

Table B1: Effects of Lin A, level of PeG in the hydrophilic phase and HPGMO4 as a co-SAA on the stability of TCPL4-based MEs at various percents of ME components.

ME	IPP %	IPP-Lin A (9:1) %	IPP-Lin A (5:2) %	TCP L4 %	HPG MO4 %	Water-PeG (1.5:8.5) %	Water-PeG (1:9) %	CER [AP] %	Stability (Mon)
SST101	5	-	-	30	-	65	-	0.4	3
SST102	10	-	-	30	-	60	-	0.4	2
SST103	15	-	-	30	-	55	-	0.4	2.3
SST104	5	-	-	35	-	60	-	0.4	3
SST105	10	-	-	35	-	55	-	0.4	2.2
SST106	15	-	-	35	-	50	-	0.4	2
SST107	5	-	-	40	-	55	-	0.4	2
SST108	10	-	-	40	-	50	-	0.4	3
SST109	15	-	-	40	-	45	-	0.4	2.2
SST110	5	-	-	45	-	50	-	0.4	1.3
SST111	10	-	-	45	-	45	-	0.4	1.3
SST112	15	-	-	45	-	40	-	0.4	1.3
SST201	-	5	-	25	-	70	-	0.4	2.3
SST202	-	10	-	25	-	65	-	0.4	0.7
SST203	-	15	-	25	-	60	-	0.4	1.5
SST204	-	5	-	30	-	65	-	0.4	2.7
SST205	-	10	-	30	-	60	-	0.4	2
SST206	-	15	-	30	-	55	-	0.4	0.7

Appendixes

SST207	-	5	-	35	-	-	60	-	0.4	0.8
SST208	-	10	-	35	-	-	55	-	0.4	2
SST209	-	15	-	35	-	-	50	-	0.4	1.7
SST210	-	5	-	40	-	-	55	-	0.4	4
SST211	-	10	-	40	-	-	50	-	0.4	1
SST212	-	15	-	40	-	-	45	-	0.4	1.5
SST301	-	-	5	25	-	-	70	-	0.4	0.7
SST302	-	-	10	25	-	-	65	-	0.4	14
SST303	-	-	15	25	-	-	60	-	0.4	2.3
SST304	-	-	5	30	-	-	65	-	0.4	0.8
SST305	-	-	10	30	-	-	60	-	0.4	5
SST306	-	-	15	30	-	-	55	-	0.4	7
SST307	-	-	5	35	-	-	60	-	0.4	2.2
SST308	-	-	10	35	-	-	55	-	0.4	14
SST309	-	-	15	35	-	-	50	-	0.4	14
SST310	-	-	5	40	-	-	55	-	0.4	2.2
SST311	-	-	10	40	-	-	50	-	0.4	5
SST312	-	-	15	40	-	-	45	-	0.4	5
SST401	5	-	-	30	-	-	-	65	0.4	2.3
SST402	10	-	-	30	-	-	-	60	0.4	5
SST403	15	-	-	30	-	-	-	55	0.4	2.2
SST404	5	-	-	35	-	-	-	60	0.4	0.8
SST405	10	-	-	35	-	-	-	55	0.4	1
SST406	15	-	-	35	-	-	-	50	0.4	2
SST407	5	-	-	40	-	-	-	55	0.4	2.3
SST408	10	-	-	40	-	-	-	50	0.4	2.2
SST409	15	-	-	40	-	-	-	45	0.4	2.6
SST410	5	-	-	45	-	-	-	50	0.4	2.6
SST411	10	-	-	45	-	-	-	45	0.4	0.7
SST412	15	-	-	45	-	-	-	40	0.4	2
SST501	-	5	-	25	-	-	-	70	0.4	2.3
SST502	-	10	-	25	-	-	-	65	0.4	12
SST503	-	15	-	25	-	-	-	60	0.4	>24
SST504	-	5	-	30	-	-	-	65	0.4	5
SST505	-	10	-	30	-	-	-	60	0.4	3
SST506	-	15	-	30	-	-	-	55	0.4	3
SST507	-	5	-	35	-	-	-	60	0.4	2.3
SST508	-	10	-	35	-	-	-	55	0.4	5
SST509	-	15	-	35	-	-	-	50	0.4	>24
SST510	-	5	-	40	-	-	-	55	0.4	10
SST511	-	10	-	40	-	-	-	50	0.4	10
SST512	-	15	-	40	-	-	-	45	0.4	3
SST601	-	5	-	12.5	12.5	-	-	70	0.4	12
SST602	-	10	-	12.5	12.5	-	-	65	0.4	3.5
SST603	-	15	-	12.5	12.5	-	-	60	0.4	16
SST604	-	5	-	15	15	-	-	65	0.4	>24
SST605	-	10	-	15	15	-	-	60	0.4	6.0
SST606	-	15	-	15	15	-	-	55	0.4	12
SST607	-	5	-	17.5	17.5	-	-	60	0.4	15
SST608	-	10	-	17.5	17.5	-	-	55	0.4	12
SST609	-	15	-	17.5	17.5	-	-	50	0.4	12
SST610	-	5	-	20	20	-	-	55	0.4	12
SST611	-	10	-	20	20	-	-	50	0.4	9
SST612	-	15	-	20	20	-	-	45	0.4	3

As has been shown in Table B1, it was not possible to generalise the effect of percentage composition of each ME component on the stability of TCPL4-based CER [AP] MEs. However, interestingly, a trend was observed and in general O/W MEs that are at the close proximity of the O/W-BC MEs border were the most stable.

Given appropriate percentages of the ME components are chosen, Lin A has significantly increased the stability of TCPL4-based CER [AP] MEs. None of the MEs obtained without Lin A were sufficiently stable (≤ 5 Mons). Nevertheless, several MEs that contain Lin A were sufficiently stable, some of which were stable for more than 2 years. As can be referred in Fig 2.1 it had also enormously increased the ME region within the PT-PD. Thus Lin A played a major role in obtaining clear and stable TCPL4-based CER [AP] MEs, suggesting that it possibly acts as a co-SAA.

In the absence of Lin A, the percentage PeG in the hydrophilic component showed no significant effect on stability at the ratios investigated. However, in those MEs that contain Lin A, higher proportion of PeG in the hydrophilic phase (lower proportion of water) has significantly increased stability. As has been shown in Fig 2.1 higher percentage of PeG in the hydrophilic component tremendously expanded the ME region within the PT-PD minimising both the two-phase as well as the LC regions.

Using HPGMO4/TCPL4 (1:1) rather than TCPL4 alone has increased the stability of the MEs extensively. The results in Fig 2.1 also showed that combination of the SAAs has enormously expanded the ME region.

Therefore, the effect of each ME component on stability of TCPL4-based MEs cannot be generalised and the right composition that gives stable CER [AP] ME should be chosen. However, generally, stable MEs were obtained at OW-BC MEs border. Given the right percentage of the ME components are chosen, Lin A, HPGMO4 and high percentage of PeG in the hydrophilic phase have tremendously increased stability of CER [AP] MEs, with MEs that stable for more than 2 years were obtained. Hence, 10 stable TCPL4-based CER [AP] MEs were chosen for further characterisation, Table 2.2.

II-Development of Lecithin-based CER [AP] MEs

Miglyol, phosal and water-PeG mixture were selected as oily, amphiphilic and hydrophilic components, respectively, for the preparation of lecithin-based CER [AP] MEs (see Appendix A). Using the components selected, the effect of the percent ME component on the stability of lecithin-based CER [NP] MEs was thoroughly investigated, Table B2. Since O/W MEs were envisaged the oil level was maintained low, (5-15) %. Due to stability and safety concerns the minimum and maximum SAA limits were maintained at 30 and 45 %, respectively. After a week of preparation the formulations were further challenged for thermodynamic stability

Appendixes

through centrifugation at 3500 rpm for 30 min. The formulations were kept at ambient conditions and were observed for physical stability over a period of time.

Table B2: Effect of percent oily phase, percent SAA and the percentage of PeG in the hydrophilic phase on the stability lecithin-based CER [AP] MEs.

Formulation	Miglyol %	Phosol %	Water-PeG (1:9) %	Water-PeG (1.5:8.5) %	Water-PeG (1:3) %	CER [AP] %	Stability (Mon)
SSP101	5	30	-	-	65	0.3	2 phase
SSP102	10	30	-	-	60	0.3	2 phase
SSP103	15	30	-	-	55	0.3	2 phase
SSP104	5	35	-	-	60	0.3	0.7
SSP105	10	35	-	-	55	0.3	0.7
SSP106	15	35	-	-	50	0.3	2.3
SSP107	5	40	-	-	55	0.3	1.3
SSP108	10	40	-	-	50	0.3	>27
SSP109	15	40	-	-	45	0.3	>27
SSP110	5	45	-	-	50	0.3	1.3
SSP111	10	45	-	-	45	0.3	26
SSP112	15	45	-	-	40	0.3	26
SSP201	5	30	-	65	-	0.5	0.3
SSP202	10	30	-	60	-	0.5	3.5
SSP203	15	30	-	55	-	0.5	0.8
SSP204	5	35	-	60	-	0.5	>27
SSP205	10	35	-	55	-	0.5	5
SSP206	15	35	-	50	-	0.5	1
SSP207	5	40	-	55	-	0.5	1.8
SSP208	10	40	-	50	-	0.5	5
SSP209	15	40	-	45	-	0.5	4
SSP210	5	45	-	50	-	0.5	1.8
SSP211	10	45	-	45	-	0.5	>27
SSP212	15	45	-	40	-	0.5	16
SSP301	5	30	65	-	-	0.5	13
SSP302	10	30	60	-	-	0.5	15
SSP303	15	30	55	-	-	0.5	15
SSP304	5	35	60	-	-	0.5	15
SSP305	10	35	55	-	-	0.5	6
SSP306	15	35	50	-	-	0.5	>27
SSP307	5	40	55	-	-	0.5	>27
SSP308	10	40	50	-	-	0.5	>27
SSP309	15	40	45	-	-	0.5	>27
SSP310	5	45	50	-	-	0.5	>27
SSP311	10	45	45	-	-	0.5	>27
SSP312	15	45	40	-	-	0.5	>27

As can be seen in Table B2, stability of lecithin-based MEs increased significantly as the percentage of PeG in the hydrophilic phase increases. Fig 2.9 showed that as the percentage of PeG in the hydrophilic phase increases the ME region expanded tremendously. In accordance with the results of the PT-PD, as the percentage of water in the hydrophilic phase increases, higher percentages of oil and SAA were necessary to obtain stable CER [AP] MEs. Stable ME

regions were shown in Fig 2.9 (a-c). Thus, 10 of the stable formulations were chosen for further characterisation, Table 2.6.

Appendix C: Development of CER [EOS] MEs containing other SC lipids

Since CERs have structural similarities and share some physicochemical characteristics in common the same ME components, used for the preparation of CER [AP] MEs, were used for the development of CER [EOS] MEs. Hence, like the CER [AP] MEs, two classes of CER [EOS] MEs were envisaged. During development of CER [EOS] MEs instability was expressed as formation a cloudy system that subsequently resulted in very loose and fluffy aggregates of the CER that remained suspended within the ME.

I-Development of TCPL4-based CER [EOS] MEs

Despite structural similarities between CERs the results of preliminary experiments revealed that CER [EOS] needs a different microenvironment than CER [AP], which is attributed to the bigger diameter and reduced polarity of CER [EOS], Fig 1.2. Hence the effect of type and percent ME component on the stability of CER [EOS] MEs was thoroughly investigated as has been shown in Table C1. In addition, the results have designated the effects of the level of PeG in the hydrophilic phase and CER [AP] on the stability of CER [EOS] MEs.

Table C1: Effect of percentage of ME components, percentage of PeG in the hydrophilic component and CER [AP] on the stability of TCPL4-based CER [EOS] MEs.

ME	IPP-Lin A (4:1) %	TCPL 4 %	Water- PeG (1:9) %	Water-PeG (1.5:8.5) %	CER [AP] %	CER [EOS] %	Stability (Days)
TAPEOS1	5	30		65	0.4	0.1	ON
TAPEOS2	5	35		60	0.4	0.1	ON
TAPEOS3	5	40		55	0.4	0.1	ON
TAPEOS4	5	45		50	0.4	0.1	ON
TAPEOS5	10	30		60	0.4	0.1	ON
TAPEOS6	10	35		55	0.4	0.1	ON
TAPEOS7	10	40		50	0.4	0.1	ON
TAPEOS8	10	45		45	0.4	0.1	ON
TAPEOS9	15	30		55	0.4	0.1	7
TAPEOS10	15	35		50	0.4	0.1	10
TAPEOS11	15	40		45	0.4	0.1	10
TAPEOS12	15	45		40	0.4	0.1	10
TEOS1	5	30		65	-	0.1	ON
TEOS2	5	35		60	-	0.1	ON
TEOS3	5	40		55	-	0.1	ON
TEOS4	5	45		50	-	0.1	ON
TEOS5	10	30		60	-	0.1	ON
TEOS6	10	35		55	-	0.1	ON
TEOS7	10	40		50	-	0.1	ON
TEOS8	10	45		45	-	0.1	ON
TEOS9	15	30		55	-	0.1	7

TEOS10	15	35		50	-	0.1	7
TEOS11	15	40		45	-	0.1	10
TEOS12	15	45		40	-	0.1	7
TAPEOS25	5	30	65		0.4	0.1	ON
TAPEOS26	5	35	60		0.4	0.1	ON
TAPEOS27	5	40	55		0.4	0.1	ON
TAPEOS28	5	45	50		0.4	0.1	ON
TAPEOS29	10	30	60		0.4	0.1	2
TAPEOS30	10	35	55		0.4	0.1	2
TAPEOS31	10	40	50		0.4	0.1	2
TAPEOS32	10	45	45		0.4	0.1	7
TAPEOS33	15	30	55		0.4	0.1	2
TAPEOS34	15	35	50		0.4	0.1	7
TAPEOS35	15	40	45		0.4	0.1	10
TAPEOS36	15	45	40		0.4	0.1	15
TEOS25	5	30	65		-	0.1	ON
TEOS26	5	35	60		-	0.1	ON
TEOS27	5	40	55		-	0.1	ON
TEOS28	5	45	50		-	0.1	ON
TEOS29	10	30	60		-	0.1	ON
TEOS30	10	35	55		-	0.1	1
TEOS31	10	40	50		-	0.1	1
TEOS32	10	45	45		-	0.1	1
TEOS33	15	30	55		-	0.1	2
TEOS34	15	35	50		-	0.1	2
TEOS35	15	40	45		-	0.1	2
TEOS36	15	45	40		-	0.1	2

The results in Table C1 showed that CER [AP] contributed positively to the stability of CER [EOS] MEs. However, unlike CER [AP] MEs, relatively stable CER [EOS] MEs could only be obtained at relatively higher percentages of oil and, despite very slightly positive effect, the effect of PeG percent in the hydrophilic component on the stability CER [EOS] MEs was not too significant. Moreover, the formulations obtained were too unstable and hence further optimisation was carried out.

▪ **Effect of CER [AP] and Lin A on Stability of CER [EOS] MEs**

As has been depicted in Table C2 the combined effect of Lin A and CER [AP] on the stability of CER [EOS] MEs was investigated.

The results in Table C2 clearly indicated the enormous stability enhancing effect of CER [AP] on CER [EOS] MEs. Interestingly, in the presence of CER [AP] Lin A enhanced stability significantly while in the absence of CER [AP] it had a negative influence on the stability of CER [EOS] MEs. Besides, fairly stable TCPL4-based CER [EOS] MEs could only be obtained at higher percentage of oil and hence to further investigate the possibility of formulating stable CER [EOS] MEs at lower oil percent, which potentially form an O/W ME, some MEs were prepared, Table C3. As can be seen in the table, all the MEs were not sufficiently stable and the

results clearly indicated that it is not possible to obtain stable TCPL4-based CER [EOS] MEs at low oil percent.

Table C2: effect of CER [AP] and Lin A on stability of TCPL4-based CER [EOS] MEs.

ME	IPP-Lin A (4:1) %	IPP %	TCPL 4 %	Water-PeG (1.5:8.5) %	CER [AP] %	CER [EOS] %	Stability (Mon)
TEOS19	15		30	55	-	0.05	1
TEOS20	15		35	50	-	0.05	2.5
TEOS21	15		40	45	-	0.05	1
TEOS22		15	30	55	-	0.05	1
TEOS23		15	35	50	-	0.05	>28
TEOS24		15	40	45	-	0.05	2
TAPEOS19	15		30	55	0.4	0.05	15
TAPEOS20	15		35	50	0.4	0.05	>28
TAPEOS21	15		40	45	0.4	0.05	3.5
TAPEOS22		15	30	55	0.4	0.05	3.5
TAPEOS23		15	35	50	0.4	0.05	3.5
TAPEOS24		15	40	45	0.4	0.05	3.5

Table C3: Stability profiles of CER [EOS] MEs at lower percentage of oils.

ME	IPP-Lin A (9:1) %	IPP %	TCPL 4 %	Water-PeG (1:9) %	CER [AP] %	CER [EOS] %	Stability (Days)
TAPEOS37	5		30	65	0.4	0.05	ON
TAPEOS38	5		35	60	0.4	0.05	1
TAPEOS39	5		40	55	0.4	0.05	1
TAPEOS40		5	30	65	0.4	0.05	ON
TAPEOS41		5	35	60	0.4	0.05	1
TAPEOS42		5	40	55	0.4	0.05	2
TAPEOS43	10		30	60	0.4	0.05	2
TAPEOS44	10		35	55	0.4	0.05	15
TAPEOS45	10		40	50	0.4	0.05	15
TAPEOS46		10	30	60	0.4	0.05	7
TAPEOS47		10	35	55	0.4	0.05	7
TAPEOS48		10	40	50	0.4	0.05	15

▪ **Effect of HPGMO4**

Studies with CER [AP] (see Appendix B) showed that HPGMO4 improved the stability and other characteristics of the MEs. The effect of HPGMO4 as a co-SAA on the stability of CER [EOS] MEs was also investigated, Table C4. As can be shown in the table, using HPGMO4 as a co-SAA has improved the stability CER [EOS] considerably.

Table C4: Effect of HPGMO4 as a co-SAA on stability of CER [EOS] MEs.

Formulation	IPP-Lin A 14:1) %	TCP L4 %	TCPL4- HPGMO4 (1:1) %	Water- PeG (1:9) %	Water- PeG (1:4) %	CER [AP] %	CER EOS] %	Stability (Days)
TAPEOS49	15	30	-	55		0.4	0.1	Cloudy
TAPEOS50	15	35	-	50		0.4	0.1	4
TAPEOS51	15	40	-	45		0.4	0.1	12
TAPEOS52	15	-	30	55		0.4	0.1	7
TAPEOS53	15	-	35	50		0.4	0.1	13
TAPEOS54	15	-	40	45		0.4	0.1	90
TAPEOS55	15	30	-		55	0.4	0.1	Cloudy
TAPEOS56	15	35	-		50	0.4	0.1	4
TAPEOS57	15	40	-		45	0.4	0.1	16
TAPEOS58	15	-	30		55	0.4	0.1	7
TAPEOS59	15	-	35		50	0.4	0.1	16
TAPEOS60	15	-	40		45	0.4	0.1	19

▪ Effect of FFAs and CHOL

Alongside CERs FFAs and CHOL constitute the major classes of SC lipids [4, 17, 27] and several skin disease conditions are associated with impairment of either one or a combination of these SC lipids, Table 1.1. Hence, formulation of stable MEs that contain these SC lipids combined can help tackle those skin disease conditions, which are caused by depletion of total SC lipids.

CERs are compounds, which are both hydrophobic and lipophobic in nature that exhibit a limited degree of solubility in most pharmaceutical solvents. Table 2.1 represented solubility of CER [AP] in some of commonly used ME components. Consequently, formulation of stable CER MEs was a challenge, which demanded intensive optimisation steps. In contrast, FFAs and CHOL are lipid soluble compounds that may easily be incorporated into any of the skin compatible pharmaceutical oils. Therefore, the effects of FFAs and CHOL on the stability of the CER [EOS] MEs were investigated.

Effect of FFAs

As has been shown in Table C5 various FFAs, namely PA, SA, BA and LA, were separately incorporated into selective CER [EOS] MEs and the effect of the FFAs was investigated. The results in the table indicated that addition of FFAs, generally, affected stability of CER [EOS] MEs. However, the effect of BA was not as significant as the other three FFAs and hence its effect was further assessed in combination with the other FFAs.

Table C5: Effect of FFA on stabilities of TCPL4-based CER [EOS] MEs.

ME	IPP-Lin A (9:1) %	TCP L4 %	HPG MO4 %	Water-PeG (1:9) %	Water-PeG (1:4) %	CER [AP] %	CER [EOS] %	PA %	SA %	BA %	LA %	Stability (days)
TAPCOM 1	15	40	-	45		0.4	0.05	-	-	-	-	10
TAPCOM 2	15	17.5	17.5	50		0.4	0.05	-	-	-	-	22
TAPEOSME1	15	20	20	45		0.4	0.05	-	-	-	-	365
TAPCOM 4	15	40	-		45	0.4	0.05	-	-	-	-	10
TAPCOM 5	15	20	20		45	0.4	0.05	-	-	-	-	17
TAPCOM 6	15	40	-	45		0.4	0.1	-	-	-	-	2
TAPCOM 7	15	17.5	17.5	50		0.4	0.1	-	-	-	-	2
TAPCOM 8	15	20	20	45		0.4	0.1	-	-	-	-	2
TAPCOM 9	15	40	-		45	0.4	0.1	-	-	-	-	ON
TAPCOM 10	15	20	20		45	0.4	0.1	-	-	-	-	2
TAPCOM 11	15	40	-	45		0.4	0.05	0.3	-	-	-	2
TAPCOM 12	15	17.5	17.5	50		0.4	0.05	0.3	-	-	-	13
TAPCOM 13	15	20	20	45		0.4	0.05	0.3	-	-	-	3
TAPCOM 14	15	40	-		45	0.4	0.05	0.3	-	-	-	3
TAPCOM 15	15	20	20		45	0.4	0.05	0.3	-	-	-	3
TAPCOM 16	15	40	-	45		0.4	0.1	0.3	-	-	-	2
TAPCOM 17	15	17.5	17.5	50		0.4	0.1	0.3	-	-	-	2
TAPCOM 18	15	20	20	45		0.4	0.1	0.3	-	-	-	ON
TAPCOM 19	15	40	-		45	0.4	0.1	0.3	-	-	-	ON
TAPCOM 20	15	20	20		45	0.4	0.1	0.3	-	-	-	4
TAPCOM 21	15	40	-	45		0.4	0.05	-	0.3	-	-	2
TAPCOM 22	15	17.5	17.5	50		0.4	0.05	-	0.3	-	-	3
TAPCOM 23	15	20	20	45		0.4	0.05	-	0.3	-	-	3
TAPCOM 24	15	40	-		45	0.4	0.05	-	0.3	-	-	3
TAPCOM 25	15	20	20		45	0.4	0.05	-	0.3	-	-	3
TAPCOM 26	15	40	-	45		0.4	0.1	-	0.3	-	-	2
TAPCOM 27	15	17.5	17.5	50		0.4	0.1	-	0.3	-	-	3
TAPCOM 28	15	20	20	45		0.4	0.1	-	0.3	-	-	ON
TAPCOM 29	15	40	-		45	0.4	0.1	-	0.3	-	-	ON
TAPCOM 30	15	20	20		45	0.4	0.1	-	0.3	-	-	ON
TAPCOM 31	15	40	-	45		0.4	0.05	-	-	0.3	-	3
TAPCOM 32	15	17.5	17.5	50		0.4	0.05	-	-	0.3	-	22
TAPCOM 33	15	20	20	45		0.4	0.05	-	-	0.3	-	10
TAPCOM 34	15	40	-		45	0.4	0.05	-	-	0.3	-	2
TAPCOM 35	15	20	20		45	0.4	0.05	-	-	0.3	-	13
TAPCOM 36	15	40	-	45		0.4	0.1	-	-	0.3	-	ON
TAPCOM 37	15	17.5	17.5	50		0.4	0.1	-	-	0.3	-	2
TAPCOM 38	15	20	20	45		0.4	0.1	-	-	0.3	-	ON
TAPCOM 39	15	40	-		45	0.4	0.1	-	-	0.3	-	ON
TAPCOM 40	15	20	20		45	0.4	0.1	-	-	0.3	-	2
TAPCOM 41	15	40	-	45		0.4	0.05	-	-	-	0.3	2
TAPCOM 42	15	17.5	17.5	50		0.4	0.05	-	-	-	0.3	7
TAPCOM 43	15	20	20	45		0.4	0.05	-	-	-	0.3	7
TAPCOM 44	15	40	-		45	0.4	0.05	-	-	-	0.3	3
TAPCOM 45	15	20	20		45	0.4	0.05	-	-	-	0.3	7
TAPCOM 46	15	40	-	45		0.4	0.1	-	-	-	0.3	ON
TAPCOM 47	15	17.5	17.5	50		0.4	0.1	-	-	-	0.3	ON
TAPCOM 48	15	20	20	45		0.4	0.1	-	-	-	0.3	ON
TAPCOM 49	15	40	-		45	0.4	0.1	-	-	-	0.3	ON
TAPCOM 50	15	20	20		45	0.4	0.1	-	-	-	0.3	ON

Effect of BA in combination with PA or LA

The effect of BA in combination with either PA or LA was investigated as has been shown in Table C6. In addition, since most of the above MEs were not sufficiently stable, to better assess the effect of combined FFAs on stability of CER MEs stable CER [EOS] MEs were employed.

Table C6: Effect of combined FFA on stabilities of TCPL4-based CER [EOS] MEs.

ME	IP P %	IPP- Lin A (9:1) %	TCP L4 %	HP GM O4 %	Water -PeG (1:9) %	Water -PeG (1.5:8 5) %	CER [AP] %	CER [EOS] %	PA %	BA %	LA %	Stabil ity (Day s)
TAPEOSME1		15	20	20	45		0.4	0.05	-	-	-	365
TAPEOSME2		15	22.5	22.5	40		0.4	0.05	-	-	-	480
TAPEOSME3		15	35	-		50	0.4	0.05	-	-	-	330
TAPEOSME4		15	17.5	17.5		50	0.4	0.05	-	-	-	330
TAPEOSME5	15		35	-		50	-	0.05	-	-	-	>570
TAPEOSME6	15		17.5	17.5		50	-	0.05	-	-	-	>570
TAPCOM67		15	20	20	45		0.4	0.1	-	-	-	3
TAPCOM68		15	22.5	22.5	40		0.4	0.1	-	-	-	20
TAPCOM69		15	35	-		50	0.4	0.1	-	-	-	ON
TAPCOM70		15	17.5	17.5		50	0.4	0.1	-	-	-	2
TAPCOM71	15		35	-		50	-	0.1	-	-	-	ON
TAPCOM72	15		17.5	17.5		50	-	0.1	-	-	-	4
TAPCOM73		15	20	20	45		0.4	0.05	-	0.3	-	45
TAPCOM74		15	22.5	22.5	40		0.4	0.05	-	0.3	-	7
TAPCOM75		15	35	-		50	0.4	0.05	-	0.3	-	35
TAPCOM76		15	17.5	17.5		50	0.4	0.05	-	0.3	-	35
TAPCOM77	15		35	-		50	-	0.05	-	0.3	-	17
TAPCOM78	15		17.5	17.5		50	-	0.05	-	0.3	-	>570
TAPCOM79		15	20	20	45		0.4	0.1	-	0.3	-	17
TAPCOM80		15	22.5	22.5	40		0.4	0.1	-	0.3	-	17
TAPCOM81		15	35	-		50	0.4	0.1	-	0.3	-	ON
TAPCOM82		15	17.5	17.5		50	0.4	0.1	-	0.3	-	3
TAPCOM83	15		35	-		50	-	0.1	-	0.3	-	ON
TAPCOM84	15		17.5	17.5		50	-	0.1	-	0.3	-	3
TAPCOM85		15	20	20	45		0.4	0.05	-	0.15	0.15	25
TAPCOM86		15	22.5	22.5	40		0.4	0.05	-	0.15	0.15	330
TAPCOM87		15	35	-		50	0.4	0.05	-	0.15	0.15	20
TAPCOM88		15	17.5	17.5		50	0.4	0.05	-	0.15	0.15	17
TAPCOM89	15		35	-		50	-	0.05	-	0.15	0.15	ON
TAPCOM90	15		17.5	17.5		50	-	0.05	-	0.15	0.15	17
TAPCOM91		15	20	20	45		0.4	0.1	-	0.15	0.15	5
TAPCOM92		15	22.5	22.5	40		0.4	0.1	-	0.15	0.15	5
TAPCOM93		15	35	-		50	0.4	0.1	-	0.15	0.15	ON
TAPCOM94		15	17.5	17.5		50	0.4	0.1	-	0.15	0.15	5
TAPCOM95	15		35	-		50	-	0.1	-	0.15	0.15	ON
TAPCOM96	15		17.5	17.5		50	-	0.1	-	0.15	0.15	ON
TAPCOM97		15	20	20	45		0.4	0.05	0.15	0.15	-	330
TAPCOM98		15	22.5	22.5	40		0.4	0.05	0.15	0.15	-	330
TAPCOM99		15	35	-		50	0.4	0.05	0.15	0.15	-	180
TAPCOM100		15	17.5	17.5		50	0.4	0.05	0.15	0.15	-	330
TAPCOM101	15		35	-		50	-	0.05	0.15	0.15	-	17
TAPCOM102	15		17.5	17.5		50	-	0.05	0.15	0.15	-	17
TAPCOM103		15	20	20	45		0.4	0.1	0.15	0.15	-	17
TAPCOM104		15	22.5	22.5	40		0.4	0.1	0.15	0.15	-	30
TAPCOM105		15	35	-		50	0.4	0.1	0.15	0.15	-	ON
TAPCOM106		15	17.5	17.5		50	0.4	0.1	0.15	0.15	-	2
TAPCOM107	15		35	-		50	-	0.1	0.15	0.15	-	ON
TAPCOM108	15		17.5	17.5		50	-	0.1	0.15	0.15	-	2

The results in Table C6 showed that, in agreement with the above results, formulations without FFAs had better thermodynamic stability. Unlike combination of BA with LA, combination of BA with PA had better stability than BA alone.

Effect of CHOL

Comparing the stabilities of MEs containing CHOL, Table C7, with those MEs, which are devoid of CHOL (given in Table C5), CHOL has, in general, a very slight negative effect on stability on CER [EOS] MEs investigated.

Table C7: Effect of CHOL on stabilities of TCPL4-based CER [EOS] MEs.

ME	IPP-Lin A (9:1) %	TCP L4 %	HPG MO4 %	Water-PeG (1:9) %	Water-PeG (1:4) %	CER [AP] %	CER [EOS] %	CH OL %	Stability (days)
TAPCOM 51	15	40	-	45		0.4	0.05	0.3	60
TAPCOM 52	15	17.5	17.5	50		0.4	0.05	0.3	7
TAPCOM 53	15	20	20	45		0.4	0.05	0.3	13M
TAPCOM 54	15	40	-		45	0.4	0.05	0.3	3
TAPCOM 55	15	20	20		45	0.4	0.05	0.3	6
TAPCOM 56	15	40	-	45		0.4	0.1	0.3	ON
TAPCOM 57	15	17.5	17.5	50		0.4	0.1	0.3	3
TAPCOM 58	15	20	20	45		0.4	0.1	0.3	4
TAPCOM 59	15	40	-		45	0.4	0.1	0.3	ON
TAPCOM 60	15	20	20		45	0.4	0.1	0.3	2

Combined Effect of FFAs and CHOL

The combined effect of FFAs and CHOL on stabilities of TCPL4-based CER [EOS] MEs was investigated, using ME systems whose stability was less affected by FFAs or CHOL, Table C8. The results showed that it is difficult to obtain stable TCPL4-based CER MEs that contain FFAs and CHOL combined.

Table C8: Combined effect of FFAs and CHOL on stabilities of TCPL4-based CER [EOS] MEs.

ME	IPP-Lin A (9:1) %	TCP L4 %	HPG MO4 %	Water-PeG (1:9) %	Water-PeG (1.5:8.5) %	CER [AP] %	CER [EOS] %	PA %	BA %	LA %	CH OL %	Stability (Months)
TAPCOM61	15	20	20	45		0.4	0.05	-	-	-	-	6
TAPCOM62	15	22.5	22.5	40		0.4	0.05	-	-	-	-	6
TAPCOM64	15	17.5	17.5		50	0.4	0.05	-	-	-	-	7
TAPCOM85	15	20	20	45		0.4	0.05	-	0.15	0.15	-	2.2
TAPCOM86	15	22.5	22.5	40		0.4	0.05	-	0.15	0.15	-	1.7
TAPCOM88	15	17.5	17.5		50	0.4	0.05	-	0.15	0.15	-	1

TAPCOM97	15	20	20	45		0.4	0.05	0.15	0.15	-	-	4
TAPCOM98	15	22.5	22.5	40		0.4	0.05	0.15	0.15	-	-	4
TAPCOM100	15	17.5	17.5		50	0.4	0.05	0.15	0.15	-	-	7
TAPCOM 53	15	20	20	45		0.4	0.05	-	-	-	0.3	10
TAPCOM110	15	22.5	22.5	40		0.4	0.05	-	-	-	0.3	5
TAPCOM111	15	17.5	17.5		50	0.4	0.05	-	-	-	0.3	7
TAPCOM112	15	20	20	45		0.4	0.1	-	-	-	0.3	ON
TAPCOM113	15	22.5	22.5	40		0.4	0.1	-	-	-	0.3	1
TAPCOM114	15	17.5	17.5		50	0.4	0.1	-	-	-	0.3	0.4
TAPCOM115	15	20	20	45		0.4	0.05	-	0.15	0.15	0.3	0.8
TAPCOM116	15	22.5	22.5	40		0.4	0.05	-	0.15	0.15	0.3	0.8
TAPCOM117	15	17.5	17.5		50	0.4	0.05	-	0.15	0.15	0.3	0.7
TAPCOM118	15	20	20	45		0.4	0.1	-	0.15	0.15	0.3	0.2
TAPCOM119	15	22.5	22.5	40		0.4	0.1	-	0.15	0.15	0.3	0.03
TAPCOM120	15	17.5	17.5		50	0.4	0.1	-	0.15	0.15	0.3	0.13
TAPCOM121	15	20	20	45		0.4	0.05	0.15	0.15	-	0.3	5
TAPCOM122	15	22.5	22.5	40		0.4	0.05	0.15	0.15	-	0.3	1.7
TAPCOM123	15	17.5	17.5		50	0.4	0.05	0.15	0.15	-	0.3	1.3
TAPCOM124	15	20	20	45		0.4	0.1	0.15	0.15	-	0.3	0.3
TAPCOM125	15	22.5	22.5	40		0.4	0.1	0.15	0.15	-	0.3	0.2
TAPCOM126	15	17.5	17.5		50	0.4	0.1	0.15	0.15	-	0.3	0.1

Concluding, the above results showed that, if not used along with CER [AP], Lin A has a negative effect on the stability of CER [EOS] MEs. CER [AP] played a profound role in stabilising CER [ESO] MEs. Thus, the combined use of CER [AP] along with Lin A enhanced the stability of CER [EOS] MEs. In addition, higher percentage of oil was required to obtain stable TCPL4-based CER [EOS] MEs, where the most stable MEs were found to be in the BC region. The percentage of SAA to be used was highly dependent on the percentage of water in the hydrophilic phase. HPGMO significantly improved stability. Both FFAs and CHOL affected the stability of lecithin-based CER [EOS] MEs. Therefore, 9 CER [EOS] MEs with optimum stability were chosen for further characterisation, Table 2.9.

II-Development of Lecithin-based CER [EOS] MEs

As has been mentioned under Appendix C, despite structural similarities between CERs, the results of preliminary studies showed that CER [EOS] needs a different microenvironment than CER [AP]. Hence, the effect of Percent ME component on the stability of CER [EOS] MEs was investigated, Table C9. In addition, the effect of CER [AP] on the stability of CER [EOS] was studied. The results showed that relatively stable CER [EOS] could only be obtained at higher percentages of the SAA and oil: all stable MEs were BC type. CER [AP] had a positive influence on the stability of CER [EOS] MEs.

Table C9: Effect of levels of the oily phase, SAA and CER [AP] on stability of lecithin-based CER [EOS] MEs.

ME	Miglyol %	Phosal %	Water-PeG (1.5:8.5) %	CER [AP] %	CER [EOS] %	Stability (Days)
PAPEOS1	5	30	65	0.4	0.1	ON
PAPEOS2	5	35	60	0.4	0.1	ON
PAPEOS3	5	40	55	0.4	0.1	ON
PAPEOS4	5	45	50	0.4	0.1	ON
PAPEOS5	10	30	60	0.4	0.1	ON
PAPEOS6	10	35	55	0.4	0.1	30
PAPEOS7	10	40	50	0.4	0.1	7
PAPEOS8	10	45	45	0.4	0.1	120
PAPEOS9	15	30	55	0.4	0.1	1
PAPEOS10	15	35	50	0.4	0.1	90
PAPEOS11	15	40	45	0.4	0.1	30
PAPEOS12	15	45	40	0.4	0.1	120
PEOS1	5	30	65	-	0.1	ON
PEOS2	5	35	60	-	0.1	ON
PEOS3	5	40	55	-	0.1	ON
PEOS4	5	45	50	-	0.1	ON
PEOS5	10	30	60	-	0.1	ON
PEOS6	10	35	55	-	0.1	30
PEOS7	10	40	50	-	0.1	7
PEOS8	10	45	45	-	0.1	7
PEOS9	15	30	55	-	0.1	1
PEOS10	15	35	50	-	0.1	30
PEOS11	15	40	45	-	0.1	60
PEOS12	15	45	40	-	0.1	150

▪ **Effect of Level of Co-solvent**

In order to see the effect of the ration of PeG in the hydrophilic phase on the stability of CER [EOS] MEs, varying Water-PeG mixtures were used as a hydrophilic component, Table C10. The results in the table showed that as the proportion of PeG in the hydrophilic phase increases the stability of the MEs increased.

Table C10: Effect of proportion of PeG in hydrophilic component on stability of lecithin-based CER [EOS] MEs.

ME	Miglyol %	Phosal %	Water-PeG (1:9) %	Water-PeG (1:3) %	CER [AP] %	CER [EOS] %	Stability (Days)
PAPEOS25	5	30	65	-	0.5	0.15	ON
PAPEOS26	5	35	60	-	0.5	0.15	2
PAPEOS27	5	40	55	-	0.5	0.15	30
PAPEOS28	5	45	50	-	0.5	0.15	30
PAPEOS29	10	30	60	-	0.5	0.15	7
PAPEOS30	10	35	55	-	0.5	0.15	60
PAPEOS31	10	40	50	-	0.5	0.15	60
PAPEOS32	10	45	45	-	0.5	0.15	60

PAPEOS33	15	30	55	-	0.5	0.15	30
PAPEOS34	15	35	50	-	0.5	0.15	60
PAPEOS35	15	40	45	-	0.5	0.15	75
PAPEOS36	15	45	40	-	0.5	0.15	75
PAPEOS37	5	30	-	65	0.5	0.15	ON
PAPEOS38	5	35	-	60	0.5	0.15	ON
PAPEOS39	5	40	-	55	0.5	0.15	2
PAPEOS40	5	45	-	50	0.5	0.15	2
PAPEOS41	10	30	-	60	0.5	0.15	ON
PAPEOS42	10	35	-	55	0.5	0.15	7
PAPEOS43	10	40	-	50	0.5	0.15	30
PAPEOS44	10	45	-	45	0.5	0.15	30
PAPEOS45	15	30	-	55	0.5	0.15	ON
PAPEOS46	15	35	-	50	0.5	0.15	30
PAPEOS47	15	40	-	45	0.5	0.15	30
PAPEOS48	15	45	-	40	0.5	0.15	60

Effect of other SC lipids

Like TCPL4-based lecithin MEs, with the idea of incorporation other SC lipids into the MEs their effect on the stability of the MEs was assessed in detail.

Effect of FFAs

As can be seen in Table C11, the effects of four FFAs, namely PA, SA, BA and LA, on the stability of selected CER [EOS] MEs were investigated. As can be seen in the table, like TCPL4 base MEs, the effect of the added FFA was dependent on the chain length of the FFA. SA and PA improved stability significantly followed BA, where as LA has a negative effect on stability.

Table C11: Effect of FFAs on stabilities of lecithin-based CER [EOS] MEs.

ME	Miglyol %	Phosal %	Water-PeG (1:9) %	Water-PeG (1.5:8.5) %	CER [AP] %	CER [EOS] %	PA %	SA %	BA %	LA %	Stability (Days)
PAPCOM1	10	45	45	-	0.5	0.1	-	-	-	-	7
PAPCOM2	15	35	50	-	0.5	0.1	-	-	-	-	6
PAPCOM3	15	40	45	-	0.5	0.1	-	-	-	-	15
PAPCOM4	15	45	40	-	0.5	0.1	-	-	-	-	70
PAPCOM5	15	45	-	40	0.5	0.1	-	-	-	-	30
PAPCOM6	10	45	45	-	0.5	0.2	-	-	-	-	ON
PAPCOM7	15	35	50	-	0.5	0.2	-	-	-	-	ON
PAPCOM8	15	40	45	-	0.5	0.2	-	-	-	-	3
PAPCOM9	15	45	40	-	0.5	0.2	-	-	-	-	ON
PAPCOM10	15	45	-	40	0.5	0.2	-	-	-	-	3
PAPCOM11	10	45	45	-	0.5	0.1	0.3	-	-	-	10
PAPCOM12	15	35	50	-	0.5	0.1	0.3	-	-	-	30
PAPCOM13	15	40	45	-	0.5	0.1	0.3	-	-	-	30
PAPCOM14	15	45	40	-	0.5	0.1	0.3	-	-	-	365
PAPCOM15	15	45	-	40	0.5	0.1	0.3	-	-	-	10
PAPCOM16	10	45	45	-	0.5	0.2	0.3	-	-	-	ON

Appendixes

PAPCOM17	15	35	50	-	0.5	0.2	0.3	-	-	-	ON
PAPCOM18	15	40	45	-	0.5	0.2	0.3	-	-	-	ON
PAPCOM19	15	45	40	-	0.5	0.2	0.3	-	-	-	3
PAPCOM20	15	45	-	40	0.5	0.2	0.3	-	-	-	3
PAPCOM21	10	45	45	-	0.5	0.1	-	0.3	-	-	70
PAPCOM22	15	35	50	-	0.5	0.1	-	0.3	-	-	50
PAPCOM23	15	40	45	-	0.5	0.1	-	0.3	-	-	115
PAPCOM24	15	45	40	-	0.5	0.1	-	0.3	-	-	115
PAPCOM25	15	45	-	40	0.5	0.1	-	0.3	-	-	50
PAPCOM26	10	45	45	-	0.5	0.2	-	0.3	-	-	3
PAPCOM27	15	35	50	-	0.5	0.2	-	0.3	-	-	ON
PAPCOM28	15	40	45	-	0.5	0.2	-	0.3	-	-	3
PAPCOM29	15	45	40	-	0.5	0.2	-	0.3	-	-	3
PAPCOM30	15	45	-	40	0.5	0.2	-	0.3	-	-	3
PAPCOM31	10	45	45	-	0.5	0.1	-	-	0.3	-	10
PAPCOM32	15	35	50	-	0.5	0.1	-	-	0.3	-	7
PAPCOM33	15	40	45	-	0.5	0.1	-	-	0.3	-	6
PAPCOM34	15	45	40	-	0.5	0.1	-	-	0.3	-	45
PAPCOM35	15	45	-	40	0.5	0.1	-	-	0.3	-	30
PAPCOM36	10	45	45	-	0.5	0.2	-	-	0.3	-	ON
PAPCOM37	15	35	50	-	0.5	0.2	-	-	0.3	-	ON
PAPCOM38	15	40	45	-	0.5	0.2	-	-	0.3	-	3
PAPCOM39	15	45	40	-	0.5	0.2	-	-	0.3	-	3
PAPCOM40	15	45	-	40	0.5	0.2	-	-	0.3	-	3
PAPCOM41	10	45	45	-	0.5	0.1	-	-	-	0.3	3
PAPCOM42	15	35	50	-	0.5	0.1	-	-	-	0.3	3
PAPCOM43	15	40	45	-	0.5	0.1	-	-	-	0.3	3
PAPCOM44	15	45	40	-	0.5	0.1	-	-	-	0.3	9
PAPCOM45	15	45	-	40	0.5	0.1	-	-	-	0.3	4
PAPCOM46	10	45	45	-	0.5	0.2	-	-	-	0.3	ON
PAPCOM47	15	35	50	-	0.5	0.2	-	-	-	0.3	ON
PAPCOM48	15	40	45	-	0.5	0.2	-	-	-	0.3	ON
PAPCOM49	15	45	40	-	0.5	0.2	-	-	-	0.3	ON
PAPCOM50	15	45	-	40	0.5	0.2	-	-	-	0.3	ON

However, since BA is one of the major long chain FFAs in the SC, its effect in combination with the other FFAs was further investigated using stable CER [EOS] MEs obtained above, Table C12.

The results in Table C12 showed that addition of FFAs, except LA, has slightly improved stability of CER [EOS] MEs, which was statistically insignificant, provided that a higher percent of the oil is used. In those MEs that contain reduced oil percent or increased proportion of water in the hydrophilic component, FFAs had negative effect on stability. In addition, combination of BA with the other FFAs resulted in better stability than using BA alone. In terms of stability enhancing effect, BA/PA was the best.

Table C12: Effect of combined FFAs on stabilities of lecithin-based CER [EOS] MEs.

ME	Miglyol %	Phosol %	Water-PeG (1:9) %	Water-PeG (1.5:8.5) %	CER [AP] %	CER [EOS] %	PA %	SA %	BA %	LA %	Stability (Mon)
PAPCOM61	15	45	40	-	0.5	0.05	-	-	-	-	>21
PAPCOM62	15	45	40	-	0.5	0.1	-	-	-	-	11
PAPCOM63	20	45	35	-	0.5	0.1	-	-	-	-	>21
PAPCOM64	15	45	-	40	0.5	0.1	-	-	-	-	>21
PAPCOM65	20	45	-	35	0.5	0.1	-	-	-	-	>21
PAPCOM66	10	45	40	-	0.5	0.1	-	-	-	-	>21
PAPCOM67	15	45	40	-	0.5	0.2	-	-	-	-	0.1
PAPCOM68	20	45	35	-	0.5	0.2	-	-	-	-	0.2
PAPCOM69	15	45	-	40	0.5	0.2	-	-	-	-	0.1
PAPCOM70	20	45	-	35	0.5	0.2	-	-	-	-	0.2
PAPCOM71	15	45	40	-	0.5	0.05	-	-	0.3	-	>21
PAPCOM72	15	45	40	-	0.5	0.1	-	-	0.3	-	>21
PAPCOM73	20	45	35	-	0.5	0.1	-	-	0.3	-	>21
PAPCOM74	15	45	-	40	0.5	0.1	-	-	0.3	-	9
PAPCOM75	20	45	-	35	0.5	0.1	-	-	0.3	-	>21
PAPCOM76	10	45	40	-	0.5	0.1	-	-	0.3	-	1.5
PAPCOM77	15	45	40	-	0.5	0.2	-	-	0.3	-	0.1
PAPCOM78	20	45	35	-	0.5	0.2	-	-	0.3	-	0.1
PAPCOM79	15	45	-	40	0.5	0.2	-	-	0.3	-	0.07
PAPCOM80	20	45	-	35	0.5	0.2	-	-	0.3	-	0.1
PAPCOM81	15	45	40	-	0.5	0.05	0.15	-	0.15	-	11
PAPCOM82	15	45	40	-	0.5	0.1	0.15	-	0.15	-	>21
PAPCOM83	20	45	35	-	0.5	0.1	0.15	-	0.15	-	>21
PAPCOM84	15	45	-	40	0.5	0.1	0.15	-	0.15	-	>21
PAPCOM85	20	45	-	35	0.5	0.1	0.15	-	0.15	-	>21
PAPCOM86	10	45	40	-	0.5	0.1	0.15	-	0.15	-	>21
PAPCOM87	15	45	40	-	0.5	0.2	0.15	-	0.15	-	0.1
PAPCOM88	20	45	35	-	0.5	0.2	0.15	-	0.15	-	0.2
PAPCOM89	15	45	-	40	0.5	0.2	0.15	-	0.15	-	0.07
PAPCOM90	20	45	-	35	0.5	0.2	0.15	-	0.15	-	0.2
PAPCOM91	15	45	40	-	0.5	0.05	-	-	0.15	0.15	11
PAPCOM92	15	45	40	-	0.5	0.1	-	-	0.15	0.15	2.3
PAPCOM93	20	45	35	-	0.5	0.1	-	-	0.15	0.15	16
PAPCOM94	15	45	-	40	0.5	0.1	-	-	0.15	0.15	12
PAPCOM95	20	45	-	35	0.5	0.1	-	-	0.15	0.15	>21
PAPCOM96	10	45	40	-	0.5	0.1	-	-	0.15	0.15	2.3
PAPCOM97	15	45	40	-	0.5	0.2	-	-	0.15	0.15	0.1
PAPCOM98	20	45	35	-	0.5	0.2	-	-	0.15	0.15	0.1
PAPCOM99	15	45	-	40	0.5	0.2	-	-	0.15	0.15	0.07
PAPCOM100	20	45	-	35	0.5	0.2	-	-	0.15	0.15	0.1
PAPCOM101	15	45	40	-	0.5	0.05	-	0.15	0.15	-	16
PAPCOM102	15	45	40	-	0.5	0.1	-	0.15	0.15	-	>21
PAPCOM103	20	45	35	-	0.5	0.1	-	0.15	0.15	-	>21
PAPCOM104	15	45	-	40	0.5	0.1	-	0.15	0.15	-	21
PAPCOM105	20	45	-	35	0.5	0.1	-	0.15	0.15	-	21
PAPCOM106	10	45	40	-	0.5	0.1	-	0.15	0.15	-	2
PAPCOM107	15	45	40	-	0.5	0.2	-	0.15	0.15	-	0.2
PAPCOM108	20	45	35	-	0.5	0.2	-	0.15	0.15	-	0.3
PAPCOM109	15	45	-	40	0.5	0.2	-	0.15	0.15	-	0.1
PAPCOM110	20	45	-	35	0.5	0.2	-	0.15	0.15	-	0.2

Effect of CHOL

As has been shown in Table C13, the effect of CHOL on the stability of CER [EOS] MEs was studied. Comparison of the results in the table with those MEs, which are devoid of CHOL (PAPCOM1- PAPCOM10, Table C11), CHOL significantly enhanced the stability of all the MEs, except those MEs that contain higher percentage of SAA.

Table C13: Effect of CHOL on stabilities of lecithin-based CER [EOS] MEs.

ME	Miglyol %	Phosal %	Water-PeG (1:9) %	Water-PeG (1.5:8.5) %	CER [AP] %	CER [EOS] %	CHOL %	Stability (Days)
PAPCOM51	10	45	45	-	0.5	0.1	0.3	70
PAPCOM52	15	35	50	-	0.5	0.1	0.3	45
PAPCOM53	15	40	45	-	0.5	0.1	0.3	30
PAPCOM54	15	45	40	-	0.5	0.1	0.3	30
PAPCOM55	15	45	-	40	0.5	0.1	0.3	10
PAPCOM56	10	45	45	-	0.5	0.2	0.3	3
PAPCOM57	15	35	50	-	0.5	0.2	0.3	ON
PAPCOM58	15	40	45	-	0.5	0.2	0.3	3
PAPCOM59	15	45	40	-	0.5	0.2	0.3	3
PAPCOM60	15	45	-	40	0.5	0.2	0.3	3

Effect of FFAs and CHOL combined

The effect of FFAs combined with CHOL on CER [EOS] MEs was assessed as has been shown in Table C14. The results in the table showed that, although MEs with sufficient stability could be obtained, LA has a negative effect on stability. Since CHOL was added to those MEs with higher concentration of the SAA, it has slight negative effect on stability, which was not statistically significant. However, the results, in general, showed that incorporation of FFAs and CHOL combined than either of the SC lipids alone had a positive impact on the stability of CER [EOS] MEs.

Table C14: Combined effects of FFAs and CHOL on stabilities of lecithin-based CER [EOS] MEs.

ME	Miglyol %	Phosal %	Water-PeG (1:9) %	Water-PeG (1.5:8.5) %	CER [AP] %	CER [EOS] %	SA %	BA %	LA %	CHOL %	Stability (Months)
PAPCOM61	15	45	40	-	0.5	0.05	-	-	-	-	10
PAPCOM62	15	45	40	-	0.5	0.1	-	-	-	-	10
PAPCOM63	20	45	35	-	0.5	0.1	-	-	-	-	>20
PAPCOM64	15	45	-	40	0.5	0.1	-	-	-	-	11
PAPCOM65	20	45	-	35	0.5	0.1	-	-	-	-	>20
PAPCOM66	10	45	40	-	0.5	0.1	-	-	-	-	10
PAPCOM91	15	45	40	-	0.5	0.05	-	0.15	0.15	-	10
PAPCOM92	15	45	40	-	0.5	0.1	-	0.15	0.15	-	1.5

Appendixes

PAPCOM93	20	45	35	-	0.5	0.1	-	0.15	0.15	-	7
PAPCOM94	15	45	-	40	0.5	0.1	-	0.15	0.15	-	1.5
PAPCOM95	20	45	-	35	0.5	0.1	-	0.15	0.15	-	8
PAPCOM96	10	45	40	-	0.5	0.1	-	0.15	0.15	-	0.8
PAPCOM101	15	45	40	-	0.5	0.05	0.15	0.15		-	8
PAPCOM102	15	45	40	-	0.5	0.1	0.15	0.15		-	8
PAPCOM103	20	45	35	-	0.5	0.1	0.15	0.15		-	>20
PAPCOM104	15	45	-	40	0.5	0.1	0.15	0.15		-	10
PAPCOM105	20	45	-	35	0.5	0.1	0.15	0.15		-	10
PAPCOM106	10	45	40	-	0.5	0.1	0.15	0.15		-	7
PAPCOM111	15	45	40	-	0.5	0.05	-	-	-	0.3	>20
PAPCOM112	15	45	40	-	0.5	0.1	-	-	-	0.3	7
PAPCOM113	20	45	35	-	0.5	0.1	-	-	-	0.3	10
PAPCOM114	15	45	-	40	0.5	0.1	-	-	-	0.3	>20
PAPCOM115	20	45	-	35	0.5	0.1	-	-	-	0.3	16
PAPCOM116	10	45	40	-	0.5	0.1	-	-	-	0.3	7
PAPCOM117	15	45	40	-	0.5	0.2	-	-	-	0.3	0.2
PAPCOM118	20	45	35	-	0.5	0.2	-	-	-	0.3	0.4
PAPCOM119	15	45	-	40	0.5	0.2	-	-	-	0.3	0.1
PAPCOM120	20	45	-	35	0.5	0.2	-	-	-	0.3	0.2
PAPCOM121	10	45	40	-	0.5	0.2	-	-	-	0.3	0.07
PAPCOM122	15	45	40	-	0.5	0.05	-	0.15	0.15	0.3	>20
PAPCOM123	15	45	40	-	0.5	0.1	-	0.15	0.15	0.3	7
PAPCOM124	20	45	35	-	0.5	0.1	-	0.15	0.15	0.3	7
PAPCOM125	15	45	-	40	0.5	0.1	-	0.15	0.15	0.3	>20
PAPCOM126	20	45	-	35	0.5	0.1	-	0.15	0.15	0.3	8
PAPCOM127	10	45	40	-	0.5	0.1	-	0.15	0.15	0.3	1.5
PAPCOM128	15	45	40	-	0.5	0.2	-	0.15	0.15	0.3	0.1
PAPCOM129	20	45	35	-	0.5	0.2	-	0.15	0.15	0.3	0.3
PAPCOM130	15	45	-	40	0.5	0.2	-	0.15	0.15	0.3	0.1
PAPCOM131	20	45	-	35	0.5	0.2	-	0.15	0.15	0.3	0.1
PAPCOM132	10	45	40	-	0.5	0.2	-	0.15	0.15	0.3	ON
PAPCOM133	15	45	40	-	0.5	0.05	0.15	0.15	-	0.3	16
PAPCOM134	15	45	40	-	0.5	0.1	0.15	0.15	-	0.3	8
PAPCOM135	20	45	35	-	0.5	0.1	0.15	0.15	-	0.3	>20
PAPCOM136	15	45	-	40	0.5	0.1	0.15	0.15	-	0.3	>20
PAPCOM137	20	45	-	35	0.5	0.1	0.15	0.15	-	0.3	16
PAPCOM138	10	45	40	-	0.5	0.1	0.15	0.15	-	0.3	8
PAPCOM139	15	45	40	-	0.5	0.2	0.15	0.15	-	0.3	0.1
PAPCOM140	20	45	35	-	0.5	0.2	0.15	0.15	-	0.3	0.3
PAPCOM141	15	45	-	40	0.5	0.2	0.15	0.15	-	0.3	0.1
PAPCOM142	20	45	-	35	0.5	0.2	0.15	0.15	-	0.3	0.2
PAPCOM143	10	45	40	-	0.5	0.2	0.15	0.15	-	0.3	0.07

Generalising, the results showed that higher percentages of oil and the SAA, which can give BC type MEs, was necessary to develop stable lecithin-based CER [EOS] MEs. CER [AP] and higher proportion of PeG in the hydrophilic component improved stability considerably. PA, SA and BA, alone or in combination, had a slight positive effect on the stability of the MEs especially at higher oil percent. The smaller the FFA chain the better was the stabilising effect. However, LA had a slight negative effect on the stability of the MEs although it could be incorporated in those MEs containing lower percentage of CER [EOS]. CHOL improved the

stability of CER [EOS] at lower concentration of the SAA. CHOL combined with the FFAs had positive influence on the stability than using either FFA or CHOL alone. Therefore, twelve stable lecithin-based CER [EOS] MEs were obtained for further characterisation, Table 2.11.

Appendix D: Development of CER [NP] MEs containing other SC Lipids

Like CER [AP] and CER [EOS] MEs, both TCPL4 and lecithin-based CER [NP] MEs were formulated as has been shown bellow. Attempt was made to incorporate the other SC components incorporated n CER [EOS]. In case of CER [NP] MEs instability was expressed by formation of star like crystalline aggregates, which are formed from needle shaped crystals, and remained suspended within the MEs.

I-Development of TCPL4-based CER [NP] MEs

During the preparation of CER [AP] and CER [EOS] MEs it was revealed that combining TCPL4 with HPGMO4, rather than using TCPL4 alone SAA, gave MEs with better stability and psychochemical characteristics. Hence, for the preparation of CER [NP] MEs the mixture, mostly, TCPL4/HPGMO4 (1:1) was used as a SAA. In addition, the same oily (IPP alone or in combination with small percentage of Lin A) and hydrophilic (water-PeG mixture) components were used for the preparation of TCPL4-based CER [NP] MEs. As can be seen in Table D1, optimisation of the MEs was started by assessing the effect of percent ME component on the stability of CER [NP] MEs. The compositions selected were, as far as possible, limited to the ME region that can possibly give O/W MEs (Fig 2.1).

Table D1: Effect of percent ME component on stability of TCPL4-based CER [NP] MEs.

ME	IPP %	TCPL4-HPGMO4 (1:1) %	Water-PeG (1.5:8.5) %	CER [NP] %	Stability (Days)
TNPME1	5	25	70	0.2	ON
TNPME2	10	25	65	0.2	2
TNPME3	15	25	60	0.2	3
TNPME4	20	25	55	0.2	4
TNPME5	5	30	65	0.2	ON
TNPME6	10	30	60	0.2	2
TNPME7	15	30	55	0.2	4
TNPME8	20	30	50	0.2	4
TNPME9	5	35	60	0.2	ON
TNPME10	10	35	55	0.2	2
TNPME11	15	35	50	0.2	3
TNPME12	20	35	45	0.2	4
TNPME13	5	40	55	0.2	ON
TNPME14	10	40	50	0.2	2
TNPME15	15	40	45	0.2	3
TNPME16	20	40	40	0.2	3

As can clearly be seen in Table D1, the MEs obtained were too unstable, calling for further optimisation. However, the results showed that stability increased as the percentage of oil increases and was almost independent of the level of SAA.

▪ **Effect of Lin A on Stability of TCPL4-based CER [NP] MEs**

As the MEs were too unstable at a very low oil percentage, in this case the level of oil was maintained at or above 10 %. The effect of Lin A on the stability of CER [NP] MEs was investigated at two different levels, Table D2.

Table D2: Effect of Lin A on stability of TCPL4-based CER [NP] MEs.

ME	IPP-Lin A (4:1) %	IPP-Lin A (5:2) %	TCPL4-HPGMO4 (1:1) %	Water-PeG (1.5:8.5) %	CER [NP] %	Stability (Days)
TNPME17	10	-	25	65	0.2	ON
TNPME18	15	-	25	60	0.2	2
TNPME19	20	-	25	55	0.2	3
TNPME20	10	-	30	60	0.2	ON
TNPME21	15	-	30	55	0.2	2
TNPME22	20	-	30	50	0.2	3
TNPME23	10	-	35	55	0.2	ON
TNPME24	15	-	35	50	0.2	2
TNPME25	20	-	35	45	0.2	3
TNPME26	10	-	40	50	0.2	ON
TNPME27	15	-	40	45	0.2	2
TNPME28	20	-	40	40	0.2	2
TNPME29	-	10	25	65	0.2	2
TNPME30	-	15	25	60	0.2	3
TNPME31	-	20	25	55	0.2	5
TNPME32	-	10	30	60	0.2	2
TNPME33	-	15	30	55	0.2	4
TNPME34	-	20	30	50	0.2	6
TNPME35	-	10	35	55	0.2	ON
TNPME36	-	15	35	50	0.2	2
TNPME37	-	20	35	45	0.2	4
TNPME38	-	10	40	50	0.2	ON
TNPME39	-	15	40	45	0.2	4
TNPME40	-	20	40	40	0.2	4

Lin A did not show significant effect on the stability of TCPL4-based MEs, although at high percent a slight improvement in stability was observed. Nonetheless, in line with the above finding, stability of CER [NP] MEs increased with oil percentage, whereas, the level of SAA showed no significant effect.

▪ **Effect of PeG level on Stability of TCPL4-based CER [NP] MEs**

As has been depicted in Table D3, the effect of the ration of PeG in the hydrophilic phase on the stability of TCPL4-based CER [NP] MEs was assessed at two levels.

Table D3: Effect of ratio of PeG in the hydrophilic phase on stability of TCPL4-based CER [NP] MEs.

ME	IPP %	TCPL4-HPGMO4 (1:1) %	Water-PeG (1:9) %	Water-PeG (1:4) %	CER [NP] %	Stability (Days)
TNPME41	10	25	65	-	0.2	2
TNPME42	15	25	60	-	0.2	2
TNPME43	20	25	55	-	0.2	3
TNPME44	10	30	60	-	0.2	2
TNPME45	15	30	55	-	0.2	4
TNPME46	20	30	50	-	0.2	3
TNPME47	10	35	55	-	0.2	3
TNPME48	15	35	50	-	0.2	3
TNPME49	20	35	45	-	0.2	4
TNPME50	10	40	50	-	0.2	2
TNPME51	15	40	45	-	0.2	3
TNPME52	20	40	40	-	0.2	3
TNPME53	10	25	-	65	0.2	3
TNPME54	15	25	-	60	0.2	ON
TNPME55	20	25	-	55	0.2	3
TNPME56	10	30	-	60	0.2	4
TNPME57	15	30	-	55	0.2	3
TNPME58	20	30	-	50	0.2	2
TNPME59	10	35	-	55	0.2	2
TNPME60	15	35	-	50	0.2	5
TNPME61	20	35	-	45	0.2	ON
TNPME62	10	40	-	50	0.2	2
TNPME63	15	40	-	45	0.2	3
TNPME64	20	40	-	40	0.2	8

As has been shown in Table D3, increasing the ratio of PeG in the hydrophilic phase showed no significant effect on stability of TCPL4-based MEs, except the slight improvement observed by TNPME64.

Therefore, unlike CER [AP] and CER [EOS] MEs, Lin A and a high ratio of PeG in the hydrophilic phase showed no significant effect on the stability of TCPL4-based CER [NP] MEs. However, like CER [EOS] MEs, relatively stable CER [NP] MEs were obtained at higher percentages of oil. Hence, the stability of CER [NP] in those systems, which gave stable CER [EOS] MEs was investigated as has been depicted in Table D4. In addition, to investigate the effect of other CERs on the stability of CER [NP] MEs, the formulations were prepared with and without CER [AP] and CER [EOS].

Strikingly, the results in Table D4 showed the tremendous stability enhancing effect of other CERs, especially CER [AP], on the stability of CER [NP] MEs. During the preparation of CER [EOS] MEs CER [AP] enhanced the stability of CER [EOS] MEs. Thus, these findings support the conclusion that appropriate combination of CERs helps stabilizing each other in the resulting MEs. Furthermore, like the case of CER [AP] MEs, too high concentration of SAA

decreased stability while combination of SAAs enhanced stability. But Lin A had slightly decreased stability, which was not statistically significant.

Table D4: Effect of CER [AP] and CER [EOS] on stabilities of CER [NP] MEs prepared in ME systems that gave stable CER [EOS] MEs.

ME	IPP %	IPP-Lin A (9:1) %	TCP L4 %	HPG MO4 %	Water-PeG (1:9) %	Water-PeG (1.5:8.5) %	CER [AP] %	CER [EOS] %	CER [NP] %	Stability (Days)
TNAEOSME1		15	20	20	45		0.2	0.05	0.2	17
TNAEOSME2		15	22.5	22.5	40		0.2	0.05	0.2	12
TNAEOSME3		15	35	-		50	0.2	0.05	0.2	34
TNAEOSME4		15	17.5	17.5		50	0.2	0.05	0.2	54
TNAEOSME5	15		35	-		50	-	0.05	0.2	3
TNAEOSME6	15		17.5	17.5		50	-	0.05	0.2	4
TNPTME1		15	20	20	45		-	-	0.2	2
TNPTME2		15	22.5	22.5	40		-	-	0.2	ON
TNPTME3		15	35	-		50	-	-	0.2	2
TNPTME4		15	17.5	17.5		50	-	-	0.2	2
TNPTME5	15		35	-		50	-	-	0.2	2
TNPME11	15		17.5	17.5		50	-	-	0.2	3

Therefore, incorporation of small percentages of CER [AP] and CER [EOS] and employing HPGMO4 as a co-SAA at (1:1) has increased stability of TCPL4-based CER [NP] MEs by several factors. However, Lin A had a very slight negative effect on the stability and the effect of the ratio of PeG to water in the hydrophilic phase, with the ratios investigated (water-PeG; 1:9-1:4), was insignificant. TNAEOSME4, which fulfill the above criteria, was hence the most stable of all CER [NP] MEs formulated so far.

Effect of CER [AP] and CER [EOS] on Stability of TCPL4-based CER [NP] MEs at large

Results in Table D4 showed that CER [AP] and CER [EOS] MEs increased stability of CER [NP] MEs. However, the effects were observed on limited number of MEs, which have relatively higher percentages of oil(s) and SAA(s). Below the effect of these CERs on the stability CER [NP] MEs was investigated at large.

a) Effect of CER [AP] on the Stability of TCPL4-based CER [NP] MEs

To investigate the effect of CER [AP] on the stability of CER [NP] MEs at large, MEs which showed better stability, when prepared in the absence of CER [AP], were taken and the effect of CER [AP] on the stability of these MEs was assessed, Table D5. The level of Lin A in the oily phase was maintained constant (IPP-Lin A, 9:1). In addition, stability was investigated at reduced percentage of CER [NP], 0.1 %.

Table D5: Effect of CER [AP] on the stability of TCPL4-based CER [NP] MEs at large.

ME	IPP-Lin A (9:1) %	TCPL4- HPGM O4 (1:1) %	Water- PeG (1:9) %	Water- PeG (1.5:8. 5) %	Water- PeG (1:4) %	CER [AP] %	CER [NP] %	Stability (Mon)
TNPME65	15	30	55	-	-	-	0.2	0.07
TNPME66	20	35	45	-	-	-	0.2	ON
TNPME67	20	25	-	55	-	-	0.2	0.1
TNPME68	15	30	-	55	-	-	0.2	0.1
TNPME69	20	30	-	50	-	-	0.2	0.2
TNPME70	15	35	-	50	-	-	0.2	0.07
TNPME71	20	35	-	45	-	-	0.2	0.2
TNPME72	15	40	-	45	-	-	0.2	ON
TNPME73	20	40	-	40	-	-	0.2	0.07
TNPME74	10	30	-	-	60	-	0.2	ON
TNPME75	15	35	-	-	50	-	0.2	0.07
TNPME76	20	40	-	-	40	-	0.2	0.07
TNAPME1	15	30	55	-	-	0.2	0.2	0.3
TNAPME2	20	35	45	-	-	0.2	0.2	0.3
TNAPME3	20	25	-	55	-	0.2	0.2	0.3
TNAPME4	15	30	-	55	-	0.2	0.2	0.3
TNAPME5	20	30	-	50	-	0.2	0.2	0.3
TNAPME6	15	35	-	50	-	0.2	0.2	0.5
TNAPME7	20	35	-	45	-	0.2	0.2	0.4
TNAPME8	15	40	-	45	-	0.2	0.2	0.3
TNAPME9	20	40	-	40	-	0.2	0.2	0.4
TNAPME10	10	30	-	-	60	0.2	0.2	0.1
TNAPME11	15	35	-	-	50	0.2	0.2	0.3
TNAPME12	20	40	-	-	40	0.2	0.2	0.2
TNAPME13	15	30	55	-	-	0.2	0.1	>12
TNAPME14	20	35	45	-	-	0.2	0.1	>12
TNAPME15	20	25	-	55	-	0.2	0.1	>12
TNAPME16	15	30	-	55	-	0.2	0.1	>12
TNAPME17	20	30	-	50	-	0.2	0.1	>12
TNAPME18	15	35	-	50	-	0.2	0.1	>12
TNAPME19	20	35	-	45	-	0.2	0.1	>12
TNAPME20	15	40	-	45	-	0.2	0.1	>12
TNAPME21	20	40	-	40	-	0.2	0.1	>12
TNAPME22	10	30	-	-	60	0.2	0.1	3.7
TNAPME23	15	35	-	-	50	0.2	0.1	>12
TNAPME24	20	40	-	-	40	0.2	0.1	>12

The results in Table D5 confirmed that CER [AP] enhanced the stability of CER [NP] MEs by several times. In addition, the increase in stability was many folds when the level of CER [NP] was reduced to 0.1 %.

b) Effect of CER [EOS] on Stability of TCPL4-based CER [NP] MEs

As can be seen in Table D6, further investigation of the effect of CER [EOS] on the stability of CER [NP] MEs was made and the results showed that, like CER [AP], CER [EOS] has significantly improved the stability of TCPL4-based CER [NP] MEs.

Table D6: Effect of CER [EOS] on the stability of TCPL4-based CER [NP] MEs at large.

ME	IPP-Lin A (9:1) %	TCPL4-HPGM O4(1:1) %	Water-PeG (1:9) %	Water-PeG (1.5:8.5) %	Water-PeG (1:4) %	CER [AP] %	CER [EOS] %	CER [NP] %	Stability (Days)
TNAPME1	15	30	55	-	-	0.2	-	0.2	3
TNAPME2	20	35	45	-	-	0.2	-	0.2	11
TNAPME3	20	25	-	55	-	0.2	-	0.2	7
TNAPME4	15	30	-	55	-	0.2	-	0.2	7
TNAPME5	20	30	-	50	-	0.2	-	0.2	23
TNAPME6	15	35	-	50	-	0.2	-	0.2	21
TNAPME7	20	35	-	45	-	0.2	-	0.2	11
TNAPME8	15	40	-	45	-	0.2	-	0.2	12
TNAPME9	20	40	-	40	-	0.2	-	0.2	13
TNAPME10	10	30	-	-	60	0.2	-	0.2	2
TNAPME11	15	35	-	-	50	0.2	-	0.2	7
TNAPME12	20	40	-	-	40	0.2	-	0.2	2
TNAEOSME27	15	30	55	-	-	0.2	0.05	0.2	>330
TNAEOSME28	20	35	45	-	-	0.2	0.05	0.2	37
TNAEOSME29	20	25	-	55	-	0.2	0.05	0.2	23
TNAEOSME30	15	30	-	55	-	0.2	0.05	0.2	23
TNAEOSME31	20	30	-	50	-	0.2	0.05	0.2	23
TNAEOSME4	15	35	-	50	-	0.2	0.05	0.2	23
TNAEOSME32	20	35	-	45	-	0.2	0.05	0.2	23
TNAEOSME33	15	40	-	45	-	0.2	0.05	0.2	23
TNAEOSME34	20	40	-	40	-	0.2	0.05	0.2	20
TNAEOSME35	10	30	-	-	60	0.2	0.05	0.2	16
TNAEOSME36	15	35	-	-	50	0.2	0.05	0.2	23
TNAEOSME37	20	40	-	-	40	0.2	0.05	0.2	20

Effects of FFAs and CHOL on Stability of TCPL4-Based CER [NP] MEs

So far, it was possible to incorporate three important CERs, CER [AP], CER [EOS] and CER [NP] in one ME. Apart from the CERs, it is also advantageous to incorporate the other two important SC lipids, FFAs and CHOL, to the MEs. Hence, the effect of these lipids on the stability of CER [NP] MEs was assessed as has been shown in Tables D7 and D8.

Table D7 shows the effect of individual FFAs and CHOL on stability of selected CER [NP] MEs. As can be seen in the table, CHOL has significantly improved the stability of TCPL4-based CER [NP] MEs, which might be attributed to its amphiphilic structure. However, the effect of FFAs was dependent on the level of SAA added and the chain length of the FFA incorporated. PA and SA decreased stability of the MEs at higher concentration of SAA(s) and vice-versa, whereas, BA and LA decreased stability at lower levels of the SAA(s). Since stable TCPL4-based CER [NP] MEs can be obtained at medium levels of the SAA (s), incorporation of longer chain FFAs, especially BA, is possible slightly compromising the stability. Thus, the effect of combined FFAs on the stability of stable CER [NP] MEs was investigated, Table D8.

Table D7: Effect of FFAs and CHOL on stability of selected CER [NP] MEs.

ME	IPP-Lin A (9:1) %	TC PL4 %	HP GM O4 %	Water-PeG (1:9) %	Water-PeG (1.5:8.5) %	CER [AP] %	CER [EOS] %	CER [NP] %	PA %	SA %	BA %	LA %	CHOL %	Stability (Days)
TNAEOSME1	15	20	20	45		0.2	0.05	0.2	-	-	-	-	-	0.5
TNAEOSME2	15	22.5	22.5	40		0.2	0.05	0.2	-	-	-	-	-	0.5
TNAEOSME3	15	35	-		50	0.2	0.05	0.2	-	-	-	-	-	0.8
TNAEOSME4	15	17.5	17.5		50	0.2	0.05	0.2	-	-	-	-	-	2
TNAEOSME7	15	20	20	45		0.2	0.05	0.2	0.1	-	-	-	-	0.2
TNAEOSME8	15	22.5	22.5	40		0.2	0.05	0.2	0.1	-	-	-	-	0.3
TNAEOSME9	15	35	-		50	0.2	0.05	0.2	0.1	-	-	-	-	1.2
TNAEOSME10	15	17.5	17.5		50	0.2	0.05	0.2	0.1	-	-	-	-	>12
TNAEOSME11	15	20	20	45		0.2	0.05	0.2	-	0.1	-	-	-	0.5
TNAEOSME12	15	22.5	22.5	40		0.2	0.05	0.2	-	0.1	-	-	-	0.4
TNAEOSME13	15	35	-		50	0.2	0.05	0.2	-	0.1	-	-	-	0.5
TNAEOSME14	15	17.5	17.5		50	0.2	0.05	0.2	-	0.1	-	-	-	>12
TNAEOSME15	15	20	20	45		0.2	0.05	0.2	-	-	0.1	-	-	0.7
TNAEOSME16	15	22.5	22.5	40		0.2	0.05	0.2	-	-	0.1	-	-	0.7
TNAEOSME17	15	35	-		50	0.2	0.05	0.2	-	-	0.1	-	-	0.2
TNAEOSME18	15	17.5	17.5		50	0.2	0.05	0.2	-	-	0.1	-	-	0.8
TNAEOSME19	15	20	20	45		0.2	0.05	0.2	-	-	-	0.1	-	0.7
TNAEOSME20	15	22.5	22.5	40		0.2	0.05	0.2	-	-	-	0.1	-	0.5
TNAEOSME21	15	35	-		50	0.2	0.05	0.2	-	-	-	0.1	-	0.1
TNAEOSME22	15	17.5	17.5		50	0.2	0.05	0.2	-	-	-	0.1	-	2
TNAEOSME23	15	20	20	45		0.2	0.05	0.2	-	-	-	-	0.1	>12
TNAEOSME24	15	22.5	22.5	40		0.2	0.05	0.2	-	-	-	-	0.1	0.7
TNAEOSME25	15	35	-		50	0.2	0.05	0.2	-	-	-	-	0.1	1.4
TNAEOSME26	15	17.5	17.5		50	0.2	0.05	0.2	-	-	-	-	0.1	>12

The results in Table D8 showed that the FFA mixture on the stability of the MEs was slight and statistically insignificant and can be incorporated into the MEs at lower levels together with CHOL.

Table D8: Effect of a FFA mixture on the stability of TCPL4-based CER [NP] MEs.

ME	IPP-Lin A (9:1) %	TCPL 4-HPG MO4 (1:1) %	Water-PeG (1:9) %	Water-PeG (1.5:8.5) %	Water-PeG (1:4) %	CER [AP] %	CER [EOS] %	CER [NP] %	PA-SA-BA-LA (1:1:2:2) %	CHOL %	Stability (Month)
TNAEOSME38	20	35	45	-	-	0.2	0.05	0.1	-	-	>10
TNAEOSME39	20	25	-	55	-	0.2	0.05	0.1	-	-	>10
TNAEOSME40	20	30	-	50	-	0.2	0.05	0.1	-	-	>10
TNAEOSME41	15	35	-	50	-	0.2	0.05	0.1	-	-	>10
TNAEOSME42	15	40	-	45	-	0.2	0.05	0.1	-	-	>10
TNAEOSME43	15	35	-	-	50	0.2	0.05	0.1	-	-	>10
TNAEOSME28	20	35	45	-	-	0.2	0.05	0.2	-	-	>10
TNAEOSME29	20	25	-	55	-	0.2	0.05	0.2	-	-	2.3
TNAEOSME31	20	30	-	50	-	0.2	0.05	0.2	-	-	>10
TNAEOSME4	15	35	-	50	-	0.2	0.05	0.2	-	-	0.7
TNAEOSME33	15	40	-	45	-	0.2	0.05	0.2	-	-	0.7
TNAEOSME36	15	35	-	-	50	0.2	0.05	0.2	-	-	0.5
TNAEOSME44	20	35	45	-	-	0.2	0.05	0.1	-	0.15	>10
TNAEOSME45	20	25	-	55	-	0.2	0.05	0.1	-	0.15	>10
TNAEOSME46	20	30	-	50	-	0.2	0.05	0.1	-	0.15	>10
TNAEOSME47	15	35	-	50	-	0.2	0.05	0.1	-	0.15	>10

TNAEOSME48	15	40	-	45	-	0.2	0.05	0.1	-	0.15	>10
TNAEOSME49	15	35	-	-	50	0.2	0.05	0.1	-	0.15	>10
TNAEOSME50	20	35	45	-	-	0.2	0.05	0.2	-	0.15	>10
TNAEOSME51	20	25	-	55	-	0.2	0.05	0.2	-	0.15	2.3
TNAEOSME52	20	30	-	50	-	0.2	0.05	0.2	-	0.15	2.3
TNAEOSME53	15	35	-	50	-	0.2	0.05	0.2	-	0.15	0.7
TNAEOSME54	15	40	-	45	-	0.2	0.05	0.2	-	0.15	2.3
TNAEOSME55	15	35	-	-	50	0.2	0.05	0.2	-	0.15	0.5
TNAEOSME56	20	35	45	-	-	0.2	0.05	0.1	0.1	0.15	>10
TNAEOSME57	20	25	-	55	-	0.2	0.05	0.1	0.1	0.15	>10
TNAEOSME58	20	30	-	50	-	0.2	0.05	0.1	0.1	0.15	>10
TNAEOSME59	15	35	-	50	-	0.2	0.05	0.1	0.1	0.15	12
TNAEOSME60	15	40	-	45	-	0.2	0.05	0.1	0.1	0.15	>10
TNAEOSME61	15	35	-	-	50	0.2	0.05	0.1	0.1	0.15	22
TNAEOSME62	20	35	45	-	-	0.2	0.05	0.2	0.1	0.15	>10
TNAEOSME63	20	25	-	55	-	0.2	0.05	0.2	0.1	0.15	2.8
TNAEOSME64	20	30	-	50	-	0.2	0.05	0.2	0.1	0.15	>10
TNAEOSME65	15	35	-	50	-	0.2	0.05	0.2	0.1	0.15	>10
TNAEOSME66	15	40	-	45	-	0.2	0.05	0.2	0.1	0.15	0.4
TNAEOSME67	15	35	-	-	50	0.2	0.05	0.2	0.1	0.15	>10

Therefore, the above findings indicated that CER [AP] and CER [EOS] have tremendously enhanced the stability of TCPL4-based CER [NP] MEs. In addition, combination of TCPL4 with HPGMO4 and CHOL enhanced stability. However, Lin A and other saturated FFAs, especially BA, and a high level of SAA slightly decreased stability, which was found to be statistically insignificant. Therefore, ten TCPL4-based CER [NP] MEs, with optimum stabilities, were chosen for further characterisation, Table 2.13.

II-Development of Lecithin-based CER [NP] MEs

Like the case of lecithin-based CER [AP] and CER [EOS] MEs, attempt was made to formulate lecithin-based CER [NP] MEs using miglyol, phosal and Water-PeG mixture as oil, SAA and hydrophilic components, respectively. Despite the structural similarities CERs share, they differ in their physicochemical characteristics hence should demand different microenvironments. Subsequently, the effect of percent ME components on the stability of lecithin-based CER [NP] MEs was investigated as has been outlined in Table D9. Like the previous cases, the percentage of oil was maintained low with the intention of preferentially obtaining O/W type MEs.

Table D9: The effects of levels of SAA and oily components on the stability of lecithin-based CER [NP] MEs.

Formulation	Miglyol %	Phosal %	Water-PeG (1.5:8.5) %	CER [NP] %	Stability (Days)
PNPME1	5	25	70	0.2	Turbid
PNPME2	10	25	65	0.2	ON
PNPME3	15	25	60	0.2	ON
PNPME4	20	25	55	0.2	ON
PNPME5	5	30	65	0.2	10
PNPME6	10	30	60	0.2	3
PNPME7	15	30	55	0.2	2
PNPME8	20	30	50	0.2	2
PNPME9	5	35	60	0.2	2
PNPME10	10	35	55	0.2	2

PNPME11	15	35	50	0.2	17
PNPME12	20	35	45	0.2	15
PNPME13	5	40	55	0.2	2
PNPME14	10	40	50	0.2	15
PNPME15	15	40	45	0.2	7
PNPME16	20	40	40	0.2	3

Generally, like lecithin-based CER EOS MEs, the results in Table D9 showed that relatively higher percentage of the SAA was necessary to obtain comparably stable CER [NP] MEs. The effect of the level of oil component was dependent on the level of SAA used, which together govern the nanostructure of the resulting ME. However, all the MEs obtained were not sufficiently stable and further optimisation was carried out.

▪ **Effect of PeG level**

The level of SAA was maintained at $\geq 30\%$ as it is less likely to obtain stable lecithin-based CER [NP] MEs at lower concentrations. Table D10 represents the effect of the ratio of PeG in the hydrophilic phase on the stability of the MEs.

Table D10: Effect of ratio of PeG in the hydrophilic phase on stability of lecithin-based CER [NP] MEs.

Formulation	Migly ol %	Phosal %	Water-PeG (1:9) %	Water-PeG (1:4) %	CER [NP] %	Stability (Days)
PNPME17	5	30	65	-	0.2	4
PNPME18	10	30	60	-	0.2	5
PNPME19	15	30	55	-	0.2	10
PNPME20	20	30	50	-	0.2	12
PNPME21	5	35	60	-	0.2	60
PNPME22	10	35	55	-	0.2	5
PNPME23	15	35	50	-	0.2	13
PNPME24	20	35	45	-	0.2	5
PNPME25	5	40	55	-	0.2	10
PNPME26	10	40	50	-	0.2	10
PNPME27	15	40	45	-	0.2	12
PNPME28	20	40	40	-	0.2	10
PNPME29	5	30	-	65	0.2	Turbid
PNPME30	10	30	-	60	0.2	Turbid
PNPME31	15	30	-	55	0.2	Turbid
PNPME32	20	30	-	50	0.2	Turbid
PNPME33	5	35	-	60	0.2	3
PNPME34	10	35	-	55	0.2	17
PNPME35	15	35	-	50	0.2	5
PNPME36	20	35	-	45	0.2	4
PNPME37	5	40	-	55	0.2	60
PNPME38	10	40	-	50	0.2	3
PNPME39	15	40	-	45	0.2	12
PNPME40	20	40	-	40	0.2	15

As can be seen in the table, unlike CER [AP] and CER [EOS] MEs, the effect of PeG on the stability of CER [NP] MEs was insignificant. The observed trend rather showed that high level of SAA was needed when the level of PeG was reduced and vice-versa. However, in agreement with the above findings and irrespective of the level of PeG, relatively stable MEs were obtained at high SAA concentration. Formation of stable lecithin-based CER [EOS] MEs demanded higher concentration of phosal and oil. Therefore, the stability of CER [NP] in systems that gave stable CER [EOS] MEs was investigated, Table D11. To effects of CER [AP] and CER [EOS] on the stability of lecithin-based CER [NP] MEs was investigated.

Table D11: Effect of CER [AP] and CER [EOS] on the stability of lecithin-based CER [NP] MEs, which are prepared in systems that gave stable CER [EOS] MEs.

ME	Migl yol %	Pho sal %	Water- PeG (1:9) %	Water-PeG (1.5:8.5) %	CER [AP] %	CER [EOS] %	CER [NP] %	Stability (Days)
PNAEOSME1	15	45	40	-	0.3	0.05	0.2	>13
PNAEOSME2	15	45	40	-	0.3	0.1	0.2	2.3
PNAEOSME3	20	45	35	-	0.3	0.1	0.2	>13
PNAEOSME4	15	45	-	40	0.3	0.1	0.2	>13
PNAEOSME5	20	45	-	35	0.3	0.1	0.2	>13
PNAEOSME6	10	45	45	-	0.3	0.1	0.2	0.8
PNPTME1	15	45	40	-	-	-	0.2	0.5
PNPTME3	20	45	35	-	-	-	0.2	0.3
PNPME42	15	45	-	40	-	-	0.2	0.4
PNPME43	20	45	-	35	-	-	0.2	0.4
PNPTME6	10	45	45	-	-	-	0.2	0.3

As can be seen in the table, strikingly, like TCPL4-based CER [NP] MEs, inclusion of CER [AP] and CER [EOS] has tremendously enhanced the stability of lecithin-based CER [NP] MEs. In addition, high percentage of oil was necessary to obtain stable MEs, which might be explained by the fact that stable CER [EOS] MEs can only be obtained as BC MEs. Therefore, the stability enhancing effect of CER [AP] alone and in combination with CER [EOS] was further investigated at large.

▪ **Effect of CER [AP] on Stability of Lecithin-based CER [NP] MEs at large**

The above stable MEs were obtained only at higher percentages of SAA and oil. To investigate the possibility of obtaining stable lecithin-based CER [NP] MEs at lower percentage of SAA and oil, the relatively stable MEs obtained without addition of CER [AP] were prepared with CER [AP] included, Table D12.

The results in Table D12 showed that CER [AP] increased stability of CER [NP] MEs by several factors especially in those MEs that contain higher ratio of PeG in the hydrophilic phase. Even with the other MEs that contain lower percentage of PeG/higher percentage of water in the hydrophilic phase the type of instability observed was the one which was displayed by CER

[AP] MEs, which demanded a relatively higher percentage of PeG to remain stable within the MEs. In addition, the results showed the possibility of obtaining stable lecithin-based O/W CER [NP] MEs.

Table D12: Effect of CER [AP] on the stability of selected lecithin-based CER [NP] MEs.

ME	Migly ol %	Phos al %	Water- PeG (1:9) %	Water-PeG (1.5:8.5) %	Water- PeG (1:4) %	CER [AP] %	CER [NP] %	Stability (Mon)
PNPME89	15	30	55	-	-	0.3	0.2	3.0
PNPME90	20	30	50	-	-	0.3	0.2	1.5
PNPME91	5	35	60	-	-	0.3	0.2	10
PNPME92	15	35	50	-	-	0.3	0.2	11
PNPME93	5	40	55	-	-	0.3	0.2	1.5
PNPME94	10	40	50	-	-	0.3	0.2	>12
PNPME95	15	40	45	-	-	0.3	0.2	>12
PNPME96	20	40	40	-	-	0.3	0.2	>12
PNPME97	10	45	45	-	-	0.3	0.2	>12
PNPME98	15	45	40	-	-	0.3	0.2	>12
PNPME99	20	45	35	-	-	0.3	0.2	>12
PNPME100	5	30	-	65	-	0.3	0.2	1.3
PNPME101	15	35	-	50	-	0.3	0.2	0.4
PNPME102	20	35	-	45	-	0.3	0.2	3.7
PNPME103	10	40	-	50	-	0.3	0.2	0.7
PNPME104	15	40	-	45	-	0.3	0.2	0.6
PNPME105	20	40	-	40	-	0.3	0.2	2.0
PNPME106	10	45	-	45	-	0.3	0.2	3.0
PNPME107	15	45	-	40	-	0.3	0.2	1.5
PNPME108	20	45	-	35	-	0.3	0.2	3.0
PNPME109	10	35	-	-	55	0.3	0.2	1.0
PNPME110	5	40	-	-	55	0.3	0.2	0.5
PNPME111	10	40	-	-	50	0.3	0.2	1.3
PNPME112	15	40	-	-	45	0.3	0.2	1.3
PNPME113	20	40	-	-	40	0.3	0.2	0.4
PNPME114	10	45	-	-	45	0.3	0.2	1.0
PNPME115	15	45	-	-	40	0.3	0.2	1.3
PNPME116	20	45	-	-	35	0.3	0.2	0.4

▪ **Effect of CER [EOS] on Stability of Lecithin-based CER [NP] MEs**

The impact of CER [EOS] on the stabilities of CER [NP] MEs was assessed separately as has been shown in Table D13. The level of SAA was maintained high because preparation of CER [EOS] ME can only be attained at higher percentage of the SAA, which can form BC ME. The results indicated that CER [EOS] increased stability of CER [NP] MEs significantly.

Hence, as has been observed from TCPL4-based CER [NP], TCPL4-based CER [EOS] and lecithin-based CER [EOS] MEs incorporation of other CERs to MEs of one CER significantly enhances stability.

Table D13: Effect of CER [EOS] on the stabilities of selected lecithin-based CER [NP] MEs.

ME	Migl yol %	Pho sal %	Water- PeG (1:9) %	Water-PeG (1.5:8.5) %	CER [AP] %	CER [EOS] %	CER [NP] %	Stability (Days)
PNPME97	10	45	45	-	0.3	-	0.2	7
PNPME98	15	45	40	-	0.3	-	0.2	7
PNPME99	20	45	35	-	0.3	-	0.2	13
PNPME107	15	45	-	40	0.3	-	0.2	60
PNPME108	20	45	-	35	0.3	-	0.2	6
PNAEOSME6	10	45	45	-	0.3	0.1	0.2	25
PNAEOSME2	15	45	40	-	0.3	0.1	0.2	70
PNAEOSME3	20	45	35	-	0.3	0.1	0.2	55
PNAEOSME4	15	45	-	40	0.3	0.1	0.2	30
PNAEOSME5	20	45	-	35	0.3	0.1	0.2	300

▪ **Effect of FFAs and CHOL on Stability of Lecithin-based CER [NP] MEs**

As has been mentioned previously, besides CERs, it is advantageous to incorporate other SC lipids into CER MEs. Therefore, attempt was made to incorporate FFAs and CHOL into lecithin-based CER [NP] MEs, Table D14.

Table D14: Effect of FFAs and CHOL on stability of lecithin-based CER [NP] MEs.

ME	Migl yol %	Phos al %	Water-PeG (1.5:8.5) %	CER [NP] %	PA %	SA %	BA %	LA %	CH OL %	Stability (Days)
PNPME10	10	35	55	0.2	-	-	-	-	-	6
PNPME11	15	35	50	0.2	-	-	-	-	-	9
PNPME12	20	35	45	0.2	-	-	-	-	-	2
PNPME14	10	40	50	0.2	-	-	-	-	-	60
PNPME15	15	40	45	0.2	-	-	-	-	-	10
PNPME16	20	40	40	0.2	-	-	-	-	-	2
PNPME41	10	45	45	0.2	-	-	-	-	-	6
PNPME42	15	45	40	0.2	-	-	-	-	-	16
PNPME43	20	45	35	0.2	-	-	-	-	-	10
PNPME44	10	35	55	0.2	0.1	-	-	-	-	8
PNPME45	15	35	50	0.2	0.1	-	-	-	-	3
PNPME46	20	35	45	0.2	0.1	-	-	-	-	3
PNPME47	10	40	50	0.2	0.1	-	-	-	-	2
PNPME48	15	40	45	0.2	0.1	-	-	-	-	8
PNPME49	20	40	40	0.2	0.1	-	-	-	-	3
PNPME50	10	45	45	0.2	0.1	-	-	-	-	12
PNPME51	15	45	40	0.2	0.1	-	-	-	-	3
PNPME52	20	45	35	0.2	0.1	-	-	-	-	3
PNPME53	10	35	55	0.2	-	0.1	-	-	-	3
PNPME54	15	35	50	0.2	-	0.1	-	-	-	4
PNPME55	20	35	45	0.2	-	0.1	-	-	-	3
PNPME56	10	40	50	0.2	-	0.1	-	-	-	4
PNPME57	15	40	45	0.2	-	0.1	-	-	-	6
PNPME58	20	40	40	0.2	-	0.1	-	-	-	3

Appendixes

PNPME59	10	45	45	0.2	-	0.1	-	-	-	3
PNPME60	15	45	40	0.2	-	0.1	-	-	-	3
PNPME61	20	45	35	0.2	-	0.1	-	-	-	60
PNPME62	10	35	55	0.2	-	-	0.1	-	-	7
PNPME63	15	35	50	0.2	-	-	0.1	-	-	5
PNPME64	20	35	45	0.2	-	-	0.1	-	-	2
PNPME65	10	40	50	0.2	-	-	0.1	-	-	4
PNPME66	15	40	45	0.2	-	-	0.1	-	-	2
PNPME67	20	40	40	0.2	-	-	0.1	-	-	4
PNPME68	10	45	45	0.2	-	-	0.1	-	-	3
PNPME69	15	45	40	0.2	-	-	0.1	-	-	8
PNPME70	20	45	35	0.2	-	-	0.1	-	-	5
PNPME71	10	35	55	0.2	-	-	-	0.1		3
PNPME72	15	35	50	0.2	-	-	-	0.1		3
PNPME73	20	35	45	0.2	-	-	-	0.1		3
PNPME74	10	40	50	0.2	-	-	-	0.1		8
PNPME75	15	40	45	0.2	-	-	-	0.1		60
PNPME76	20	40	40	0.2	-	-	-	0.1		3
PNPME77	10	45	45	0.2	-	-	-	0.1		75
PNPME78	15	45	40	0.2	-	-	-	0.1		3
PNPME79	20	45	35	0.2	-	-	-	0.1		3
PNPME80	10	35	55	0.2	-	-	-	-	0.1	3
PNPME81	15	35	50	0.2	-	-	-	-	0.1	9
PNPME82	20	35	45	0.2	-	-	-	-	0.1	3
PNPME83	10	40	50	0.2	-	-	-	-	0.1	3
PNPME84	15	40	45	0.2	-	-	-	-	0.1	9
PNPME85	20	40	40	0.2	-	-	-	-	0.1	15
PNPME86	10	45	45	0.2	-	-	-	-	0.1	10
PNPME87	15	45	40	0.2	-	-	-	-	0.1	12
PNPME88	20	45	35	0.2	-	-	-	-	0.1	13

As has been depicted in the table, generally, FFAs slightly decreased the stability of CER [NP] MEs, especially at lower levels of the SAA and oil. BA gave the least stable MEs followed by PA, SA and LA. Unlike FFAs, CHOL improved stability slightly. However, the investigation was made in the absence of other stabilising CERs, CER [AP] and CER [EOS] in this case, and hence the effects of the lipids on stability of the MEs was investigated in the presence of the CERs.

- **Effect of FFAs and CHOL on Stability of Lecithin-based CER [NP] MEs Stabilised by CER [AP] and CER [EOS]**

Table D15 represents the effect FFAs and CHOL on the stability of CER [NP] MEs in the presence of other stabilising CERs. As can clearly be seen in the table all the FFAs and CHOL significantly increased stability of lecithin-based CER [NP] MEs. A higher percent of CHOL had better stabilising effect, especially at higher oil percent.

Table D15: Effect of FFAs and CHOL on stability of lecithin-based CER [NP] MEs stabilised by CER [AP] and CER [EOS].

ME	M igl yo l %	P ho sa l %	Wat er- PeG (1:9) %	Water -PeG (1.5:8 .5) %	CER [AP] %	CER [EO S] %	CER [NP] %	PA %	SA %	BA %	LA %	CH OL %	Stabil ity (Mon)
PNAEOSME6	10	45	45	-	0.3	0.1	0.2	-	-	-	-	-	0.5
PNAEOSME2	15	45	40	-	0.3	0.1	0.2	-	-	-	-	-	0.6
PNAEOSME3	20	45	35	-	0.3	0.1	0.2	-	-	-	-	-	1.8
PNAEOSME4	15	45	-	40	0.3	0.1	0.2	-	-	-	-	-	1
PNAEOSME5	20	45	-	35	0.3	0.1	0.2	-	-	-	-	-	10
PNAEOSME7	10	45	45	-	0.3	0.1	0.2	0.1	-	-	-	-	0.4
PNAEOSME8	15	45	40	-	0.3	0.1	0.2	0.1	-	-	-	-	>11
PNAEOSME9	20	45	35	-	0.3	0.1	0.2	0.1	-	-	-	-	10
PNAEOSME10	15	45	-	40	0.3	0.1	0.2	0.1	-	-	-	-	1.8
PNAEOSME11	20	45	-	35	0.3	0.1	0.2	0.1	-	-	-	-	>11
PNAEOSME12	10	45	45	-	0.3	0.1	0.2	-	0.1	-	-	-	1
PNAEOSME13	15	45	40	-	0.3	0.1	0.2	-	0.1	-	-	-	10
PNAEOSME14	20	45	35	-	0.3	0.1	0.2	-	0.1	-	-	-	>11
PNAEOSME15	15	45	-	40	0.3	0.1	0.2	-	0.1	-	-	-	1.5
PNAEOSME16	20	45	-	35	0.3	0.1	0.2	-	0.1	-	-	-	>4
PNAEOSME17	10	45	45	-	0.3	0.1	0.2	-	-	0.1	-	-	0.7
PNAEOSME18	15	45	40	-	0.3	0.1	0.2	-	-	0.1	-	-	10
PNAEOSME19	20	45	35	-	0.3	0.1	0.2	-	-	0.1	-	-	>11
PNAEOSME20	15	45	-	40	0.3	0.1	0.2	-	-	0.1	-	-	1.8
PNAEOSME21	20	45	-	35	0.3	0.1	0.2	-	-	0.1	-	-	>11
PNAEOSME22	10	45	45	-	0.3	0.1	0.2	-	-	-	0.1	-	23
PNAEOSME23	15	45	40	-	0.3	0.1	0.2	-	-	-	0.1	-	10
PNAEOSME24	20	45	35	-	0.3	0.1	0.2	-	-	-	0.1	-	10
PNAEOSME25	15	45	-	40	0.3	0.1	0.2	-	-	-	0.1	-	10
PNAEOSME26	20	45	-	35	0.3	0.1	0.2	-	-	-	0.1	-	>11
PNAEOSME27	10	45	45	-	0.3	0.1	0.2	-	-	-	-	0.1	0.8
PNAEOSME28	15	45	40	-	0.3	0.1	0.2	-	-	-	-	0.1	1.0
PNAEOSME29	20	45	35	-	0.3	0.1	0.2	-	-	-	-	0.1	>11
PNAEOSME30	15	45	-	40	0.3	0.1	0.2	-	-	-	-	0.1	>11
PNAEOSME31	20	45	-	35	0.3	0.1	0.2	-	-	-	-	0.1	>11
PNAEOSME32	10	45	45	-	0.3	0.1	0.2	-	-	-	-	0.3	1.8
PNAEOSME33	15	45	40	-	0.3	0.1	0.2	-	-	-	-	0.3	>11
PNAEOSME34	20	45	35	-	0.3	0.1	0.2	-	-	-	-	0.3	>11
PNAEOSME35	15	45	-	40	0.3	0.1	0.2	-	-	-	-	0.3	1.1
PNAEOSME36	20	45	-	35	0.3	0.1	0.2	-	-	-	-	0.3	>11

All the above MEs, however, were obtained at higher concentrations of the oily phase and the SAA, which particularly favours stabilisation of CER [EOS]. To investigate the possibility of obtaining MEs at reduced percentages of the oil and the SAA, some MEs were formulated based on those MEs that were stabilised by CER [AP] and CER [EOS], Table D16.

Comparison of the results of Table D16 with that of Table D12 showed that CER [EOS] significantly decreased the stability of those MEs that contain low percentages of the oil and the SAA. Therefore, the results clearly indicated that any addition of CER [EOS], which has stabilizing effect on other CER MEs, is possible at higher percentage of the SAA and oil, which can give BC MEs. Accordingly, it was possible to obtain stable MEs at higher concentrations of the oily and SAA components.

Table D16: Effect of CER [EOS], CHOL and FFAs on stability of CER [NP] MEs at large.

ME	Miglyol %	Phosal %	Water-PeG (1:9) %	Water-PeG (1.5:8.5) %	Water-PeG (1:4) %	CER [AP] %	CER [EOS] %	CER [NP] %	PA-SA-BA-LA (1:1:2:2) %	CHOL %	Stability (Mon)
PNPCOMME1	15	30	55	-	-	0.3	0.1	0.2	0.15	0.2	0.1
PNPCOMME2	20	30	50	-	-	0.3	0.1	0.2	0.15	0.2	0.2
PNPCOMME3	5	35	60	-	-	0.3	0.1	0.2	0.15	0.2	0.1
PNPCOMME4	15	35	50	-	-	0.3	0.1	0.2	0.15	0.2	0.4
PNPCOMME5	5	40	55	-	-	0.3	0.1	0.2	0.15	0.2	ON
PNPCOMME6	10	40	50	-	-	0.3	0.1	0.2	0.15	0.2	0.7
PNPCOMME7	15	40	45	-	-	0.3	0.1	0.2	0.15	0.2	0.4
PNPCOMME8	20	40	40	-	-	0.3	0.1	0.2	0.15	0.2	2.8
PNPCOMME9	10	45	45	-	-	0.3	0.1	0.2	0.15	0.2	0.7
PNPCOMME10	15	45	40	-	-	0.3	0.1	0.2	0.15	0.2	9
PNPCOMME11	20	45	35	-	-	0.3	0.1	0.2	0.15	0.2	0.9
PNPCOMME12	5	30	-	65	-	0.2	0.1	0.2	0.15	0.2	Turbid
PNPCOMME13	15	35	-	50	-	0.2	0.1	0.2	0.15	0.2	0.2
PNPCOMME14	20	35	-	45	-	0.2	0.1	0.2	0.15	0.2	0.3
PNPCOMME15	10	40	-	50	-	0.2	0.1	0.2	0.15	0.2	0.2
PNPCOMME16	15	40	-	45	-	0.2	0.1	0.2	0.15	0.2	0.4
PNPCOMME17	20	40	-	40	-	0.2	0.1	0.2	0.15	0.2	1.4
PNPCOMME18	10	45	-	45	-	0.2	0.1	0.2	0.15	0.2	0.3
PNPCOMME19	15	45	-	40	-	0.2	0.1	0.2	0.15	0.2	0.9
PNPCOMME20	20	45	-	35	-	0.2	0.1	0.2	0.15	0.2	>9.5
PNPCOMME21	10	35	-	-	55	0.2	0.1	0.2	0.15	0.2	0.1
PNPCOMME22	5	40	-	-	55	0.2	0.1	0.2	0.15	0.2	ON
PNPCOMME23	10	40	-	-	50	0.2	0.1	0.2	0.15	0.2	0.2
PNPCOMME24	15	40	-	-	45	0.2	0.1	0.2	0.15	0.2	0.4
PNPCOMME25	20	40	-	-	40	0.2	0.1	0.2	0.15	0.2	>9.5
PNPCOMME26	10	45	-	-	45	0.2	0.1	0.2	0.15	0.2	0.1
PNPCOMME27	15	45	-	-	40	0.2	0.1	0.2	0.15	0.2	0.9
PNPCOMME28	20	45	-	-	35	0.2	0.1	0.2	0.15	0.2	0.7

Therefore, CER [AP] and CER [EOS] increased the stability of lecithin-based CER [NP] MEs by several factors. However, in all cases incorporation of CER [EOS] was possible only at higher percentages of the SAA and the oil, which can give BC type MEs. The ratio of PeG in the hydrophilic phase and FFAs showed no significant effect on stability of CER [NP] MEs, which were devoid of other CERs, whereas, both PeG and FFAs increased stability of lecithin-based CER [NP] MEs, which were stabilised by CER [AP] and CER [EOS]. In all cases CHOL enhanced stability of lecithin-based CER [NP] MEs. Hence, 6 stable lecithin-based CER [NP] MEs were selected for further characterizations, Table 2.15.

Appendix E: Investigation the Partitioning behaviour of HD-PMI in ME phases

HD-PMI is a lipophilic spin probe that partitions exclusively in oily phases [193]. However, due to the inclusion of PeG within the MEs, which partitioned between the oily and aqueous phases, the partitioning behaviour of the spin probe might be altered and hence it was investigated.

Interpretation of EPR spectra of HD-PMI in ME components

For better understanding of the system, before determining the EPR parameters of HD-PMI in MEs, the EPR spectra of the pure ME components as a function of PeG percent (Table E1) and temperature were obtained, Fig E1. Because HD-PMI is insoluble in water its EPR data in pure water could not be obtained. 50 % PeG in miglyol gave a turbid mixture (two-phase system) at RT and some irregularities were observed on the EPR parameters obtained, Fig E1.

Table E1: Compositions of various ME components obtained for EPR analysis using HD-PMI as a spin probe.

No.	Hydrophilic phase	Oily phase I	Oily phase II
1	Water ^a	Miglyol	IPP
2	25 % PeG in water	25 % PeG in miglyol	25 % PeG in IPP
3	50 % PeG in water	50 % PeG in miglyol ^b	50 % PeG in IPP
4	75 % PeG in water	75 % PeG in miglyol	75 % PeG in IPP
5	90 % PeG in water	90 % PeG in miglyol	90 % PeG in IPP
6	PeG	PeG	PeG

^aHD-PMI is insoluble; ^bTurbid mixture at RT

As can be seen in Fig E1, as the percentage of PeG increases τ_c increased attributing to the high viscosity of PeG when compared with the other vehicles, Table E2. In addition, τ_c decreased with temperature. Since 50 % PeG in miglyol doesn't give a clear solution, the value of τ_c obtained was out of trend.

Table E2: Viscosities of pure vehicles used as ME components at 25°C.

No.	Component	Viscosity (mPa.s)
1	PeG	45.99
2	IPP	7
3	Miglyol	30 (at 20°C)
4	Water	0.91

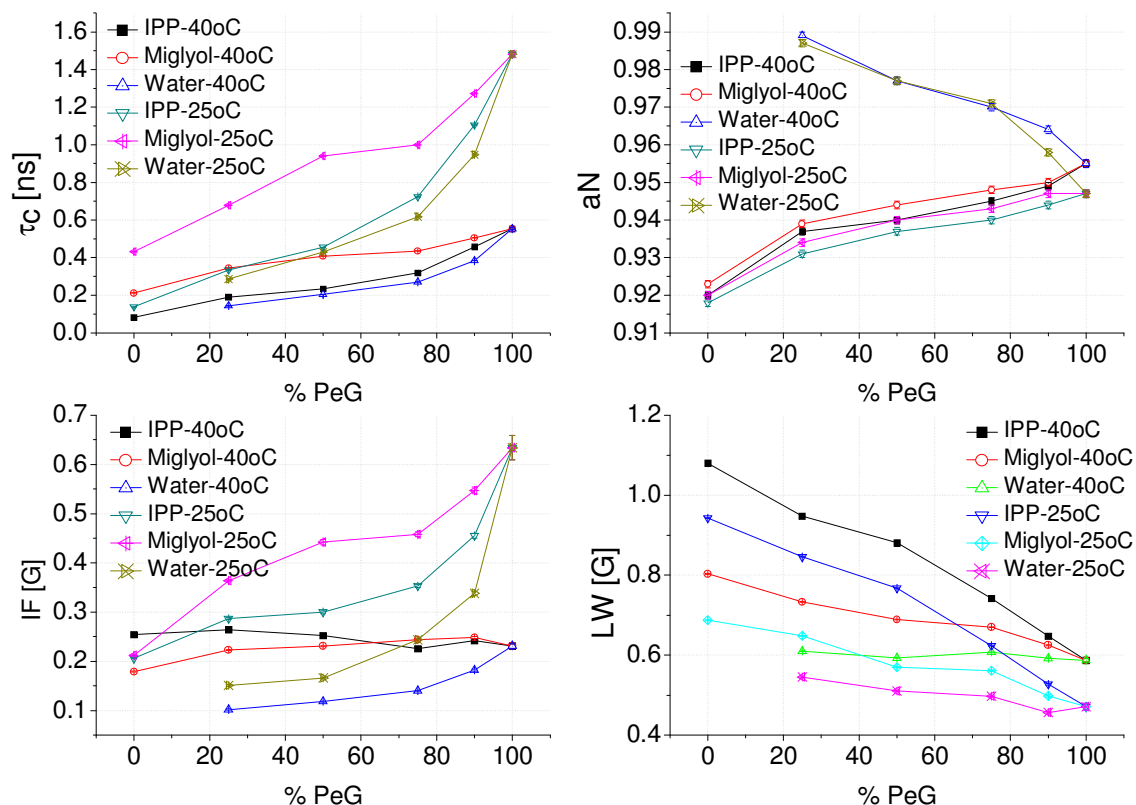


Figure E1: Effects of PeG percent and temperature on τ_c (top-left), a_N (top-right), IF (bottom-left) and LW (bottom-right) of HD-PMI in oils and water at 25 and 40°C.

a_N is a parameter sensitive to the polarity of the environment surrounding the spin probe [159, 163]. It is proportional to the spin density at the nitrogen atom of the probe molecule, which further depends on polarity of the surrounding medium: lowering of a_N is expected when the probe transfers from the aqueous phase to a less polar phase [158]. In non polar solvents, the unpaired electron largely resides on oxygen atom weakening the magnetic interactions between the unpaired electron and the nitrogen nucleus thereby reducing a_N [159]. When it is properly calibrated it can be used as a measure of local polarity [194]. Thus, as can be seen in Fig E1, water gave the highest a_N followed by PeG. As expected the oils have lower a_N values with miglyol slightly greater than IPP. However, calculation of log P values showed that IPP is more polar than miglyol (IPP=6.066; miglyol=7.648). Accordingly, a_N decreased with PeG percent for water and increased for the oils. Temperature increased a_N values very slightly and its effect on water was insignificant. A study by [194] showed that temperature has no significant effect on a_N values.

LW is a measure of spin-spin interaction as well as rotational motion of a probe. It is broadened with an increase in spin probe concentration through either spin-spin exchange or magnetic dipole interactions [166]. However, given the same concentration of HD-PMI added, addition of PeG resulted in LW reduction. In addition IPP displayed the highest LW. Moreover, LW increased significantly as a function of temperature.

The IF of EPR spectrum shows interactions of spin probes among themselves and with the surrounding molecules [159]. Higher interaction leads to higher IF. As can be seen in Fig E1 IF increased as the level of PeG increases. IF factor of miglyol was greater than IPP and water has the list. IF also decreased with temperature. The IF trend followed by the probe was more or less like that of T_c .

Investigation of the Partitioning Behaviour of HD-PMI in the MEs

Before characterisation of MEs using EPR, it was necessary to understand the distribution behaviour of the spin probe within the phases of the MEs. IN most cases, a_N values and other EPR parameters give information about the environment in which the spin probe is located [163].

HD-PMI, Fig 2.4, is a lipophilic spin probe with a very high partitioning coefficient [165]. In two-phase systems containing oil and water its distribution to the water phase might be disregarded [193]. However, the MEs under investigation contain PeG as a co-solvent that modifies the polarities of both aqueous and oily phases, which might alter the distribution pattern of the spin probe. Hence, the distribution pattern of HD-PMI in the MEs phases were investigated by taking MEs, which have the same proportion of water, oil and SAA, but increasing percentage of PeG, Table E3.

Table E3: Compositions and EPR parameters of selected TCPL4 and lecithin-based MEs investigated to determine the distribution pattern of HD-PMI in the MEs.

No.	Miglyol (g)	IPP (g)	Water (g)	Phosal (g)	TCPL4 (g)	PeG (g)	T_c [ns]	a_N [G]	LW [G]
EPRL1	0.25	-	0.25	0.8	-	0.3	0.451	0.946	0.593
EPRL2	0.25	-	0.25	0.8	-	0.6	0.528	0.949	0.591
EPRL3	0.25	-	0.25	0.8	-	0.9	0.587	0.950	0.579
EPRT1	-	0.25	0.25	-	0.8	0.2	0.627	0.938	0.587
EPRT2	-	0.25	0.25	-	0.8	0.4	0.678	0.944	0.567
EPRT3	-	0.25	0.25	-	0.8	0.8	0.736	0.947	0.543

The polarity factor, a_N , of a spin probe is capable of predicting the polarity of the environment in which the spin probe is located [160, 163-164]. Investigation of the EPR parameters in pure components showed that a_N values of systems that contain water is higher, Fig E1. Quantitatively, a_N value of a system that contains 10 % water has a_N value above 0.96 G, which is slightly affected by temperature. However, as has been depicted in Table E3, for the MEs investigated the a_N values were bellow 0.96 and was closer to the values obtained for the pure oils, suggesting that HD-PMI is almost completely partitioned in the oily phases. In addition, a_N values of the MEs increased as the percentage of PeG increases. This strongly supports that PeG has also partitioned in the oily phases and HD-PMI is almost completely partitioned in the oily phases, had the spin probe portioned in the aqueous phase there might be a decrease in a_N as percent PeG increases.

T_c increased as the percentage of PeG increased further suggesting the partitioning of PeG in the oily phases. Despite IPP has the lowest T_c values, TCPL4-based MEs showed higher T_c values suggesting a high degree of partitioning of PeG into IPP as compared to miglyol. This would further be substantiated by the fact that PeG is more soluble in IPP than in miglyol. In addition, as can be referred in Fig E1 the increase in viscosity was too big for the amount of PeG incorporated, which attributes to the entrapment of the oily phase in droplets or between SAA films [171].

Thus, the EPR investigation showed that PeG partitioned between the aqueous and oily phases, where there is a high degree of partitioning into IPP than miglyol. The HD-PMI distributed solely in the oily (oil rich) layer.

However a_N and T_c values of MEs may not reflect the proportion of PeG in the oily phase, one reason being the partitioning of other ME components like SAAs into the oily phases. Furthermore, [160] find out that for an W/O kind of ME, the micropolarity of the ME interior for all examined systems was higher than that of micelles in pure SAA solution, but it remained far below that in pure water. As has been mentioned above, T_c values of the MEs increases due to entrapment of the spin probe within the oil.

List of Publications:

Research articles:

- F. F. Sahle, S. Lange, B. Dobner, J. Wohlrab, R.H.H. Neubert, Development and validation of LC/ESI-MS method for the detection and quantification of exogenous ceramide NP in stratum corneum and other layers of the skin. *Journal of Pharmaceutical and Biomedical Analysis* 60 (2012) 7– 13.
- B.S. Zewde, F.F. Sahle, T. Gebre-Mariam, K. Asres, R.H.H. Neubert, Microencapsulation of citronella oil for mosquito repellent application: Formulation and In Vitro Permeation Studies: *European Journal of Pharmaceutics and Biopharmaceutics* 80 (2012) 61–66

Poster presentations:

- Fitsum F. Sahle , Johannes Wohlrab, Reinhard H.H. Neubert, Comparative In Vitro Release and Skin Penetration Study of Ceramide AP from Microemulsions and a Hydrophilic Cream. GRC Conference on Barrier Function of Mammalian Skin 08/07/2011 - 08/12/2011, Waterville Valley Resort in Waterville Valley, NH, USA
- B.S. Zewde, F.F. Sahle, T. Gebre-Mariam, K. Asres, R.H.H. Neubert, In Vitro Membrane Permeability Study from Microencapsulated Volatile Oil Extracts of *Cymbopogon Nardus* Incorporated in Various Ointment Bases for Mosquito Repellant Action. Poster presented on the 7th PBP World Meeting, 8-11 March 2010 Malta-valletta.

Acknowledgements:

First and for most I would like to express my deepest gratitude and appreciation to my supervisor Prof. Dr. Dr. h.c. Reinhard Neubert for the continuous and unreserved advice and support he provided me throughout my stay.

I am also thankful to Prof. Dr. Johannes Wohlrab for sharing me his invaluable experience and advising me on some key scientific aspects of my work.

I am grateful to Dr. Hendrik Metz, Prof. Bodo Dobner and Dr. Karsten Busse for their extended, fruitful and insightful discussions and sharing their precious time with me.

Many thanks go to Dr. Klaus Schröter for being more than willing and allowed me to use the viscometer at their facility.

I am very much grateful to Mrs. Adelheid Pöttsch, Mrs. Manuela Woigk, Mrs. Kerstin Schwartz, Mrs. Ursula Schramm and Mrs. Anke Niece for the technical support that they provided me throughout my stay.

Heartfelt thanks to DAAD for the financial support and sharing me the burden by doing things in my behalf. It made my start and stay much easier and enjoyable. Likewise I thank KAAD who gave me the opportunity to be a non-paid KAAD scholar.

I would like to thank Dr. Christian Schmelzer and Dr. Yahya Mrestani who were more than willing to help me whenever I needed help of any kind as well as Dr. Alexandra Göbel for sharing her resources and time to help me start my study.

Many thanks to my great friends and colleagues in “AG Neubert” and friends in Halle for making my stay lively and enjoyable.

I am indebted to Prof. Tsige Gebre-Mariam for being such a positive influence in my life.

Special thanks to my late father Feleke Sahle, who believed in me and made me the man who I am today and for my late mother Tsedale Gebre-Giorgis, who made me realize the values of giving, sharing, loving and living for others.

Finally, I remain indebted to my dear Fiancée Ruth W. Tadesse, my family and my amazing friends for their understanding and the moral support that they provide me. Special thanks to Joseph F. Sahle and Ruth W. Tadesse for sharing my thoughts and feelings.

Curriculum Vitae:

Personal details:

Name: Fitsum Feleke Sahle
Born: August 30, 1980 in Wolliso, Ethiopia
Nationality: Ethiopian
Sex: Male

Education:

09/1995 - 06/1998 Dejazmach Geresu Duki Comp. Sec. School, Wolliso, Ethiopia
(High School)
09/1998 - 07/2003 First degree in pharmacy (BPharm.), School of Pharmacy, Addis
Ababa University, Addis Ababa, Ethiopia
09/ 2004 - 08/ 2006 MSc. in Pharmaceutics (MSc.), School of Pharmacy, Addis
Ababa University, Addis Ababa, Ethiopia
10/2008 - to date PhD student at the Department of Pharmaceutical Technology and
Biopharmaceutics, Institute of Pharmacy, Martin Luther
University Halle-Wittenberg, Halle, Germany

Work Experience:

08/2003 - 08/2004 Graduate Assistant II, Department of Pharmaceutics, School of
Pharmacy, Addis Ababa University, Addis Ababa, Ethiopia
08/2004 - 08/2006 Assistant Lecturer, Department of Pharmaceutics, School of
Pharmacy, Addis Ababa University, Addis Ababa, Ethiopia
08/2006 - 05/2008 Lecturer, Department of Pharmaceutics, School of Pharmacy,
Addis Ababa University, Addis Ababa, Ethiopia
09/2005 - 12/2006 Department Secretary, Department of Pharmaceutics, School of
Pharmacy, Addis Ababa University, Addis Ababa, Ethiopia
09/2005 - 07/2007 Coordinator for the Extension Program, School of Pharmacy,
Addis Ababa University, Addis Ababa, Ethiopia

-
- 08/2007 - 05/2008 Assistant Dean for the Extension Program, School of Pharmacy, Addis Ababa University, Addis Ababa, Ethiopia
- 09/2005 - 05/2008 Member of the academic sub affair committee, School of Pharmacy, Addis Ababa University, Addis Ababa, Ethiopia
- 07/2007 - 05/2008 Member of the Academic Commission, School of Pharmacy, Addis Ababa University, Addis Ababa, Ethiopia
- 09/2006 - 05/2008 Vice Chairman of the Editorial Committee (Pharma Forum), the Ethiopian Pharmaceutical Association

Selbständigkeitserklärung

Hiermit erkläre ich gemas § 5 Absatz 2b der Promotionsordnung der Naturwissenschaftliche Fakultät I (Biowissenschaften) der Martin-Luther-Universität Halle-Wittenberg, dass ich die Ergebnisse der vorliegenden Dissertationsarbeit

„Development and Biopharmaceutical Evaluation of Microemulsions for Targeted Delivery of Ceramides and other Stratum Corneum Lipids into the Stratum Corneum“

am Institut für Pharmazeutische Technologie und Biopharmazie der Martin-Luther-Universität Halle-Wittenberg selbständig und ohne fremde Hilfe erarbeitet und verfasst habe. Ferner habe ich nur die in der Dissertation angegebenen Literaturstellen und Hilfsmittel verwendet und die entnommenen und benutzten Literaturstellen auch als solche kenntlich gemacht. Weiterhin habe ich die vorliegende Arbeit bisher keiner anderen Prüfungsbehörde vorgelegt.

Halle (Saale), 09. 03. 2012

Fitsum Feleke Sahle